OSCILLATORY AND EPILEPTIFORM ACTIVITY IN HUMAN AND RODENT CORTICAL REGIONS *IN VITRO*

Jane Pennifold

Doctor of Philosophy

Aston University

October 2016

Aston University

OSCILLATORY AND EPILEPTIFORM ACTIVITY IN HUMAN AND RODENT CORTICAL REGIONS *IN VITRO*

Jane Pennifold

Doctor of Philosophy 2016

Epilepsy is a chronic neurological disorder in which patients have spontaneous recurrent seizures. Approximately 50 million people worldwide live with epilepsy and of those ~30% fail to adequately respond to anti-epileptic drugs (AEDs), indicating a need for further research. In this study oscillatory and epileptiform activity was explored in the rodent piriform cortex (PC) *in vitro,* an underexplored brain region implicated in the development of epilepsy.

PC gamma oscillations have been studied in both anaesthetised and awake rodents *in vivo*; however, to date they have not been reported *in vitro*. Extracellular field potential recordings were made in rodent PC brain slices prepared from 70-100g male Wistar rats *in vitro*. Application of kainic acid and carbachol reliably induced persistent gamma oscillations (30 – 40 Hz) in layer II of the PC. These oscillations were found to be pharmacologically similar to gamma oscillations previously found in other rodent brain regions *in vitro,* as they were dependent on $GABA_A$ receptors, AMPA receptors and gap junctions.

Persistent oscillations were also induced and characterised for the first time in human neuronal tissue *in vitro*. Human brain slices were prepared from excised tissue from various brain regions (primarily temporal) from paediatric patients undergoing surgery to alleviate the symptoms of drug resistant epilepsy. As in the rodent PC, oscillations were induced by application of kainic acid and carbachol, however, these oscillations were found to be within the beta frequency range (12 – 30 Hz). Despite this difference in frequency band, these beta oscillations were pharmacologically similar to gamma oscillations found in the rodent PC.

Seizure-like events (SLEs) were induced in brain slices prepared from 70-100g male Wistar rats via application of zero Mg^{2+} artificial cerebral spinal fluid (0$[Mg]^{2+}$ aCSF). The properties of these SLEs were found to be similar between brain regions when recordings were performed in layer II of the anterior and posterior PC and lateral entorhinal cortex (LEC) and the stratum pyramidale of CA1. In the majority of recordings SLEs occurred in the PC before the LEC or CA1 and SLEs were displayed in the PC in a higher proportion of slices than the LEC. The sensitivity of these PC slices to 0$[Mg]^{2+}$ aCSF was assessed at several stages (24 hours and 1 week (early latent), 4 weeks (mid latent) and 3 months+ (chronic period)) following the reduced intensity status epilepticus (SE) protocol for epilepsy induction compared to age-matched controls (AMCs). A decrease in excitability of the slices was observed in slices prepared from AMC animals with age, as the inter-event interval and latency to first SLE was observed to be longer in slices prepared from aged compared to young AMC animals. Slices prepared from SE animals maintained their youthful hyperexcitability with no difference in IEI or latency to first SLE observed in the early latent period compared to the chronic period.

The pharmacoresistance (or sensitivity) of these SLEs to single and double AED challenge was evaluated. Differences in efficacy of the AEDs were found between SE and AMC in the mid-latent period; increased efficacy of Na^+ channel modulating AEDs were found in slices prepared from SE compared to AMC animals. The proportion of slices that displayed pharmacoresistance of these SLEs to AEDs was found to be higher in slices prepared from young animals (early latent period and AMCs), and was similar to that found clinically in human patients. The pharmacoresistance of the SLEs to AEDs was lower in slices prepared from older animals (mid latent, chronic and AMCs) compared to young animals (early latent and AMCs). This age-dependent reduction in resistance likely reflects normal alterations in neuronal networks with ageing. SLEs induced in young control PC slices could be exploited as a new *in vitro* model of drug resistant epilepsy.

Overall, oscillatory and epileptiform activity in the PC and human cortex *in vitro* could be further explored as tools to evaluate the efficacy and mechanism of action of newly developed AEDs, as well as to explore the networks involved in drug resistant epilepsy.

Acknowledgements

I would first like to express my gratitude to my supervisors Prof. Gavin Woodhall and Prof. Stefano Seri. I would particularly like to thank Prof. Woodhall for his help, guidance and support throughout my PhD and for creating such a wonderful working environment. I would also like to thank Prof. Ian Stanford for his advice particularly in the later stages of my PhD. Although you are still not forgiven for that April fools prank!

I also wish to thank the Biomed facility, particularly Matt and Wayne for all your help over the three years. Equally, I am grateful to Birmingham Children's Hospital, members of staff and patients for supporting this research.

Thank you to current and past laboratory members Tamara, Emma, Nick, Darshna, Swetha, Ben, Serena, Katy, Mazhar and Becky. Thanks for making the last three years so enjoyable. I am particularly grateful to Tamara and Nick for training me, to Katy for help with data collection in my final year and Serena and Tamara for all the tea.

I would also like to thank my family and friends for providing entertainment, beer and fun throughout my education. I particularly want to acknowledge my brother Mike and mum Sue for your support, encouragement and understanding.

Finally, my most important acknowledgment goes to Nick, without whom I wouldn't be where I am today. Thank you for sharing this journey.

Table of Contents

Table of Figures

Table of Tables

Abbreviations

aCSF – artificial cerebral spinal fluid

AD – afterdischarge

AMC – age-matched control

AMPA - α-amino-3-hydroxy-5-methyl-4-isoxazolepropionic acid

aPC – anterior piriform cortex

ATP – adenosine triphosphate

BBB – blood brain barrier

BOLD – blood-oxygen-level dependent

CA1/3 - cornu ammonis 1 or 3

Ca^{2+} - calcium ion

CBD – cannabidiol

CBZ – carbamazepine

CNS – central nervous system

DMSO - dimethyl sulfoxide

EEG - electroencephalogram

EPSCs – excitatory postsynaptic currents

EPSPs – excitatory postsynaptic potentials

FCD – focal cortical dysplasia

FFT – fast Fourier transform

fMRI – functional magnetic resonance imaging

g - grams

GABA - γ-aminobutyric acid

GBP – gabapentin

GPCR – G-protein coupled receptor

h - hours

HFO – high frequency oscillations

i/m – intramuscular

I_{cat} – Ca^{2+}-dependent nonspecific cation current

IEI – inter-event interval

I_h – hyperpolarisation-activated cyclic nucleotide-gated channel

IIB – inter-ictal burst

IIE – inter-ictal event

I_M – M current

IN – interneuron

ING – interneuron-network gamma

IPSCs – inhibitory postsynaptic currents

IPSPs – inhibitory postsynaptic potentials

K^+ - potassium ion

KA – kainic acid

KO – knock-out (mouse)

LEC – lateral entorhinal cortex

LFP – local field potential

LiCl – lithium chloride

M1 – muscarinic acetylcholine receptor subtype 1

mACh – muscarinic acetylcholine

MEA – multielectrode array

MEG - magnetoencephalogram

Mg^{2+} - magnesium ion

mGluR – metabotropic glutamate receptor

min - minutes

mM – millimolar

mnths - months

MR – magnetic resonance

MRI – magnetic resonance imaging

ms - milliseconds

MΩ - megohm

Na^+ - sodium ion

NC3R – national centre for replacement, reduction and refinement

NMDA - N-methyl-D-aspartate receptor

PDS – paroxysmal depolarising shift

PET - positron emission tomography

PING – pyramidal-cell interneuron-network gamma

pPC – posterior piriform cortex

PSBB – post status behavioural battery

RISE – reduced intensity status epilepticus (model)

s - seconds

s/c – subcutaneous

SE – status epilepticus

SEM – standard error of the mean

SLE – seizure-like events

SRS – spontaneous recurrent seizures

TGB - tiagabine

TLE – temporal lobe epilepsy

VFO – very fast oscillations

VPA – valproic acid

wks - weeks

ZNS – zonisamide

μM – micromolar

Chapter 1 Introduction

1 Introduction

50 million people worldwide have epilepsy, a serious neurological disorder in which patients experience spontaneous repetitive seizures. Despite significant research into epileptic disorders, up to 30 % of patients will not gain adequate control over their seizures with antiepileptic drug (AED) treatment, indicating a need for further research (WHO, 2012). Electrophysiological recordings of neuronal network oscillations are used as a tool by researchers to investigate alterations in network activity in epilepsy both *in vivo* and *in vitro*. *In vitro* investigations in brain slices of the hippocampus and entorhinal cortex have dominated this field of epilepsy research, and this probably reflects the relative dominance of temporal lobe epilepsy (TLE) in the historical development of animal models. However, as early as 1985, the piriform cortex (PC) was identified as being more sensitive to seizure induction than hippocampal and parahippocampal regions (Piredda and Gale, 1985a). This study comprises of an investigation into the physiology and pathology of neuronal networks in the PC.

1.1 The temporal lobe

The temporal lobe (TL) is one of four lobes in in the cerebral hemisphere, the others being the parietal, frontal and occipital lobes. TLE is one of the most common types of epilepsy and patients with TLE are the most frequent group to be referred for surgical assessment due to inadequate seizure control with AEDs (Semah et al., 1998). Animal models of TLE have identified a number of structures which are thought to be involved in seizure manifestation and generation, including the entorhinal cortex, hippocampus and PC (Piredda and Gale, 1985a; Mathern et al., 2002).

1.2 The piriform cortex

The PC is a phylogenetically old brain region with a trilaminate structure. Its functions include olfactory processing and memory consolidation. In the rodent brain, the PC is located along the ventral surface on the rostral-caudal axis and can be divided into the anterior PC (aPC) and the posterior PC (pPC) (figure 1.1 A). The aPC runs parallel to the lateral olfactory tract (LOT), while the pPC runs along the ventral surface of the brain beyond the most dorsal extent of the LOT (Neville and Haberly, 2004). Each layer of the PC consists of distinct distributions of principal and inhibitory neuronal somata. In brief, layer I is separated into layers Ia and Ib based on fibre pathways and both consist primarily of dendrites, fibres and very few (mostly inhibitory) neurons. Layer II is the most densely populated, containing both pyramidal cells and interneurons (Price, 1973). Layer III is less densely populated with the most superficial section containing proportionally more pyramidal cells than deeper sections which contain more inhibitory neurons (figure 1.1 B) (Neville and Haberly, 2004; Bekkers and Suzuki, 2013). The endopiriform nucleus is sometimes referred to as layer IV and is more densely populated than layer III but not as well populated as layer II (Tseng and Haberly, 1989b, a; Behan and Haberly, 1999).

In contrast to the processing of most other sensory information, the olfactory information processed by the PC bypasses the thalamic-relay and is only two synapses removed from the environment.

In terms of function, olfactory receptor neurons in the olfactory epithelium sample odour during inhalation and pass this sensory information to the glutamatergic mitral/tufted cells in the olfactory bulb (OB). The mitral/tufted cells project to the PC via the LOT (Wilson, 2001; Neville and Haberly, 2004). This afferent input to pyramidal cells and interneurons terminates in layer Ia only in the PC and is more dense in the aPC than the pPC (Devor, 1976; Luna and Pettit, 2010). The associational input from both pyramidal cells and interneurons extends throughout layers Ib-III. This clear division of pathway termination has allowed researchers to differentiate experimentally between the afferent and associational inputs (Neville and Haberly, 2004).

Return projections to the OB pass via the olfactory peduncle and are denser than the afferent connections from the OB (De Olmos et al., 1978; Haberly and Price, 1978a; Luskin and Price, 1983). Pyramidal cells synapse onto OB granule cells which provide inhibitory inputs to mitral cells. This back-projection is not uniform throughout the PC as return projections from pPC are weaker than those from the aPC (Haberly and Price, 1978a). The differences between the aPC and pPC regions are thought to underlie slight differences in function, with the aPC receiving stronger input from the OB and is therefore believed to play a greater role in odour identification. Conversely, the pPC receives more input from other areas in the brain and is thought to process odour similarity (Gottfried et al., 2006; Kadohisa and Wilson, 2006; Barnes et al., 2008; Zelano et al., 2011). Pyramidal neuron output to other cortical areas include the lateral entorhinal cortex, subiculum, perirhinal cortex, amygdala, prefrontal cortex and the hypothalamus (Tanabe et al., 1975; Veening, 1978; Luskin and Price, 1983; Price, 1985; Takagi, 1986).

Figure 1.1 The piriform cortex; location, structure and circuitry.
A) The PC is located along the ventral surface of the rat brain, running from the olfactory bulb (OB) to the lateral entorhinal cortex. The PC can be broken into the anterior PC (aPC) which runs parallel with the lateral olfactory tract (LOT) until the LOT disappears and the aPC becomes the posterior PC (pPC). B) The cell body density per layer. The most densely populated is layer II, layer I is the least densely populated and layer III is intermediate. C) The glutamatergic system in the PC. Layer II contains cell bodies of semilunar (SL) and superficial (SP) pyramidal cells which receive afferent input from the LOT and associational input from other neurons within the PC. Deep pyramidal (DP) are found in layer III and receive both association and afferent input as well. D) The GABAergic system in the PC. Feedforward inhibition to SL and SP neurons from the LOT is provided by the neuroglia (NG) and horizontal (HZ) interneurons. Fast spiking multipolar (fMP) cells are thought to provide most of the feedback inhibition. The other interneurons are bitufted (BT), regular spiking multipolar (rMP) and deep NG neurons. Adapted from (Bekkers and Suzuki, 2013).

1.2.1 Neurotransmitters and receptors

1.2.1.1 Glutamate

Both the associational and afferent pathways within the PC use glutamate as the primary neurotransmitter. Pharmacological experiments have identified the ionotropic receptors AMPA, kainate and NMDA and metabotropic receptors in the PC (Jung et al., 1990).

AMPA receptors comprise of a tetramer of subunits ($GluR_{1-4}$) with a reversal potential of approximately 0 mV. Two glutamate molecules (L-glutamate) bind to generate the conformational change required to open the central pore allowing cation (Na^+, K^+) transport into the cell. This generates a fast excitatory postsynaptic current (EPSC) as the receptor is rapidly activated then deactivated (Tzschentke, 2002; Platt, 2007). Most AMPA receptors are

not permeable to Ca^{2+}; however, exclusion of the $GluR_2$ subunit via post-transcriptional modification allows Ca^{2+} entry through the receptor ionophore (Hollmann et al., 1991; Sommer et al., 1991). Downregulation of the $GluR_2$ subunit in pyramidal cells has been noted in the PC following electrical kindling (a model of epilepsy, see 1.5.1). Increased Ca^{2+} entry into pyramidal cells could contribute to increased neuronal excitability, seizure spread and excitotoxicity (DeLorenzo et al., 2005).

NMDA receptor activation also generates EPSCs, although with a much slower time course than AMPA receptor activation. NMDA receptor activation occurs following the binding of two molecules of glutamate and a glycine/D-serine molecule as well as depolarisation of the membrane potential to remove the Mg^{2+} block of the ion channel pore (Mayer et al., 1984; Qian and Johnson, 2002). NMDA receptors are expressed both presynaptically (Berretta and Jones, 1996; Woodhall et al., 2001; Chamberlain et al., 2008) and postsynaptically (McLennan and Lodge, 1979). They are permeable to Na^+, K^+ and Ca^{2+}. NMDA receptor-dependent long term potentiation (LTP) in the PC is thought to play a role in odour discrimination (Roman et al., 1987; Staubli et al., 1989; Jung et al., 1990; Kanter and Haberly, 1990). They have also been implicated in the induction of epilepsy and subsequent brain damage, as infusion of an NMDA receptor antagonist into the PC reduced susceptibility to kindling induction and reduced brain damage in the kainate model of epilepsy (Holmes et al., 1992; Brandt et al., 2003).

Kainate receptors are expressed both pre- and postsynaptically in the brain and are permeable to Na^+, K^+ and Ca^{2+}. Postsynaptic receptors are thought to regulate neuronal excitability whilst presynaptic receptors regulate excitatory and inhibitory neurotransmitter release (Chittajallu et al., 1996; Castillo et al., 1997; Clarke et al., 1997; Rodriguez-Moreno et al., 1997; Vignes and Collingridge, 1997; Jiang et al., 2001; Frerking and Ohligre-Frerking, 2002; Goldin et al., 2007; Sachidhanandam et al., 2009). Kainate receptors, like NMDA and AMPA receptors are comprised of a tetramer of different receptor subunits ($GluK_{1-5}$). $GluK_2$ subunits are thought to be involved in oscillation generation whilst the $GluK_1$ subtype is thought to be protective against over-excitability and seizure activity (Fisahn et al., 2004). All five subunits are expressed across the PC, although $GluK_3$ and $GluK_4$ are expressed at low levels (Wisden and Seeburg, 1993).

Metabotropic glutamate receptors (mGluRs) are G protein coupled receptors (GPCRs) which exert their effect via second messenger cascades. The receptor subtypes ($mGluR_{1-8}$) are classified into groups I-III based on their sequence homology. Group I are primarily located postsynaptically and are positively coupled to adenylate cyclase and phospholipase C. Groups II and III are located on presynaptic receptors and are negatively coupled to adenylate cyclase and activate K^+ and Ca^{2+} channels (Niswender and Conn, 2010). In the PC, mGluR activation has been found to potentiate afferent NMDA receptor mediated

EPSCs (Collins, 1993). This effect on NMDA receptors might influence the cells' susceptibility to NMDA receptor mediated excitotoxicity (Adamchik and Baskys, 2000; Blaabjerg et al., 2003; Baskys et al., 2005).

1.2.1.2 GABA

Inhibition in the brain is important in regulating neuronal excitability and network synchrony; in the PC the primary inhibitory neurotransmitter is GABA which acts through $GABA_A$ and $GABA_B$ receptors (Neville and Haberly, 2004).

The $GABA_A$ receptor has at least 18 different subunits of which five form a pentameric receptor with a Cl^- channel in the centre. The most common form of the $GABA_A$ receptor is comprised of $2\alpha_1 2\beta_2\gamma_2$, see figure 1.2 (Farrar et al., 1999). The combination of subunits affects channel behaviour and GABA binding affinity as well as binding properties of various pharmacological agents. Binding of two GABA molecules opens the central pore which allows both Cl^- and HCO_3^- movement across the membrane. When the membrane potential is depolarised, $GABA_A$ receptor mediated Cl^- entry hyperpolarises the cell and brings it closer to resting membrane potential (Olsen and Sieghart, 2009).

$GABA_A$ receptor activation occurs in two forms; fast phasic and slow tonic inhibition. Phasic, often referred to as synaptic, mediates inhibitory postsynaptic currents (IPSCs). GABA left in the terminal following phasic transmission can diffuse to extrasynaptic receptors and generate tonic inhibition. Extrasynaptic $GABA_A$ receptors have a high affinity for GABA therefore allowing activation at very low concentrations (Farrant and Nusser, 2005). Tonic currents are recorded in *in vitro* brain slices as alterations in the baseline of the holding current (Kaneda et al., 1995).

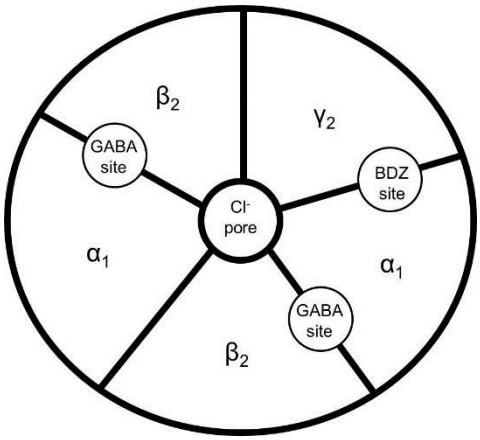

Figure 1.2 Typical $GABA_A$ receptor subunit composition.
Two GABA molecules bind to the GABA binding sites between the β and α subunits. The benzodiazepine modulatory site is situated between α1 and γ2 receptor subunits. Adapted from (Farrar et al., 1999).

Benzodiazepine and non-benzodiazepine modulators bind to the benzodiazepine site, which is located between the γ and α subunits. The benzodiazepine site is the locus of action for many sedative and hypnotic drugs and agonists at the site are used in a medical emergency to treat status epilepticus (SE - continual seizures lasting >5 minutes) (Isojarvi and Tokola, 1998; Rudolph et al., 1999).

$GABA_B$ receptors are metabotropic GPCRs linked to K^+ channels with a reversal potential close to -100 mV. $GABA_B$ receptor activation initiates a cascade of events including K^+ exit from the cell which hyperpolarises the cellular membrane (Kerr and Ong, 1995). In the PC, $GABA_B$ receptors are found both pre- and postsynaptically and are thought to regulate neuronal excitability (Tang and Hasselmo, 1994; Kapur et al., 1997). As this effect is larger on associational than afferent input, $GABA_B$ receptor agonists such as baclofen are often used to isolate the afferent input to the PC (Tang and Hasselmo, 1994; Franks and Isaacson, 2005; Suzuki and Bekkers, 2011).

1.2.2 Neurons

1.2.2.1 Principal neurons

Three distinct classes of principal neurons exist in the PC. Semilunar (SL), superficial (SP) and deep (DP) pyramidal cells, which are primarily located in layer IIa, IIb and III respectively. The more primitive SL cells lack basal dendrites and were first observed in 1978 as a distinct third population of principal neurons (Haberly and Price, 1978b; Haberly and Feig, 1983). In the past, researchers have largely grouped SL and SP cells together, however, recent evidence suggests they possess distinct morphological and electrical properties and should therefore be considered independently (Suzuki and Bekkers, 2006). SL cells, found primarily in layer IIa, resemble dentate granule cells whilst SP and DP cells are morphologically similar to hippocampal pyramidal cells (figure 1.1 and table 1.1). The clear division of the PC layers into layer Ia, afferent input and layer Ib-III associational input has allowed researchers to dissect the properties of these inputs in different cell types. All three cell types receive afferent and associational input, however, the strength of these inputs is variable. When a direct comparison was made, SL cells received stronger afferent input from the LOT and weaker associational input compared to SP cells (Suzuki and Bekkers, 2006, 2011). The difference in synaptic strength from afferent stimulation is likely due to variations in the number of synaptic contacts (Haberly and Behan, 1983; Haberly and Feig, 1983; Choy et al., 2015). SP cells have extensive apical and basal dendrites that extend across all cortical layers whereas the dendritic tree of SL cells is mostly restricted to the more superficial layers, meaning SP cells are more likely to make synaptic contacts in the associational layers than SL cells (Ib-III) (see figure 1.1). All three cell types have a non-facilitating associational input, however, both SP and DP but not SL cells respond to afferent input with facilitation (Tseng and Haberly, 1989b, a; Suzuki and Bekkers, 2006, 2011). This

specialisation allows for differential synaptic processing of incoming information and likely underlies processing of mnemonic information (Bekkers and Suzuki, 2013).

Name	Morphology	Layer	Response to depolarising current step	Afferent / associational facilitation?
Semilunar (SL)	Small basal and extensive apical dendrites. Apical dendrites extend to layer Ia.	Primarily IIa	Regularly spaced action potentials	Afferent – non facilitating Associational – non facilitating
Superficial pyramidal (SP)	Extensive basal and apical dendrites. Apical dendrites extend to layer Ia.	Primarily IIb	Bursts of action potentials	Afferent – facilitating Associational – non facilitating
Deep pyramidal (DP)	Extensive basal and apical dendrites. Longer apical dendrites extending to layer Ia.	Primarily III	Bursting at beginning of step	Afferent – facilitating Associational – non facilitating

Table 1.1 Morphological and electrophysiological properties of principal cells in the piriform cortex. (Tseng and Haberly, 1989b, a; Suzuki and Bekkers, 2006, 2011).

1.2.2.2 Inhibitory neurons

Interneurons (IN) are expressed more uniformly across the PC than pyramidal cells. Proportionally, INs represent 80%, 7% and 20-30% of all neurons found in layers I, II and III respectively (Suzuki and Bekkers, 2010a, b). Early studies to identify subdivisions of INs based on both morphological and electrophysiological characteristics within the PC were largely unsuccessful; with no clear association found. Morphological description identified five major subtypes of IN: multipolar which was split into larger sparsely spiny (dendrites) and smaller multipolar with thin dendrites, bitufted cells (BT), neuroglial and horizontal cells (HZ) (Neville and Haberly, 2004). This was further expanded by the Bekkers' group who used cluster analysis and identified an association between both the morphological and electrophysiological properties for the first time (Suzuki and Bekkers, 2010a, b). HZ and BT cells were found to be restricted to layers Ia and II respectively. Multipolar cells were separated into fast spiking (fMP) (layer III) and regular spiking (rMP) (layers II and III) based on their firing pattern in response to a depolarising current step. Neuroglial (NG) cells' electrophysiological properties varied between layers but all had the same morphological features (figures 1.1 and table 1.2). Feedforward inhibition was found to be provided by NG and HZ cells in layers Ia which are activated by the same LOT afferent input as pyramidal cells. The resulting inhibitory output can have a significant impact on the output of connected principal cells. Feedback inhibition is largely provided by perisomatic targeting fMP cells which receive no afferent input and are only indirectly activated by the associational input

from SL cells (Suzuki and Bekkers, 2012). Within each layer a phase lag in response to excitatory postsynaptic potentials (EPSPs) exists between the two main INs expressed, a common feature found in circuits that oscillate (Suzuki and Bekkers, 2010a, b)

Name	Morphology	Layer	Response to depolarising current step	Afferent / associational facilitation?
Neuroglial (NG)	Small soma, short aspiny dendrites restricted to single layer.	all	Different depending on layer (layer I erratic firing, layer II more regular)	Afferent – facilitation in layer Ia cells only Associational – non facilitating
Horizontal (HZ)	Elongated soma, long dendrites extend throughout the layers.	Ia	Accommodating action potentials (more at beginning of step than end)	Afferent – depressive Associational – weak and depressive
Bitufted (BT)	Small bipolar soma and long aspiny dendrites extending into all layers except Ia.	II	Initial burst then accommodation	Afferent – minimal input (facilitating) Associational - facilitating
Fast spiking multipolar (fMP)	Multipolar sparsely spiny dendrites extend into layer Ia, axon concentrated in layer II.	II and III	Fast, regular action potentials	Afferent – non facilitating Associational – depressive in layer III cells, facilitating in layer II cells
Regular spiking multipolar (rMP)	Spiny dendrites, diffuse axonal projections.	III	Weakly accommodating and at a lower frequency and larger hyperpolarisation than fMP	Afferent – minimal Associational - facilitating

Table 1.2 Morphological and electrophysiological properties of interneurons in the piriform cortex.
(Suzuki and Bekkers, 2010a, b, 2012)

The diversity in physiology of these five inhibitory cell types combined with the cortical location and synaptic connections is likely to be finely tuned to process odour information. Neuronal network oscillations were first identified in the PC in 1942 in response to inhalation of a strong odour (Adrian, 1942, 1950). These bursts of oscillatory activity are thought to be initiated by OB input via the LOT but local circuits within the PC maintain them (Freeman, 1968a, b; Kay, 2014). In other brain regions, extensive *in vivo* and *in vitro* electrophysiological studies have identified interneurons as playing a critical role in the generation of oscillations such as beta (12 – 30 Hz) and gamma (30 – 70 Hz) (Buzsaki, 2006; Traub and Whittington, 2010). Despite significant research *in vivo*, PC persistent

gamma oscillations have not been found *in vitro* and as such the synaptic mechanisms that underlie oscillatory activity in the PC are not well understood.

1.3 Neuronal network oscillations

Neuronal network oscillations, which are defined as rhythmic fluctuations in the local field potential (LFP), were first recorded in the human cortex by German psychiatrist Hans Berger (1929) using an electroencephalogram (EEG), which he invented and later named (Berger, 1929). An EEG recording measures extracellular voltage change (potential difference) in the brain and is thought to be the summation of repetitive neuronal activity close to the recording electrode. Since the EEG was invented, further techniques have been developed to detect extracellular field potentials including the electrocorticogram (ECoG) and magnetoencephalography (MEG). These tools are now routinely used in clinical diagnostics for epilepsy, Parkinson's disease, sleep disorders and other neurological conditions (Traub and Whittington, 2010).

Extracellular field potentials are generated by the summation of current loops within an area and comprise of sources and sinks which together maintain electroneutrality. For example, if an active sink develops in the extracellular space when positive ions travel from the extracellular space into a neuron (e.g Na^+ entry following AMPA receptor activation), this must be balanced by a return current (passive source), creating a dipole (figure 1.3) (Leung, 2010). The opposite is true for Cl^- entry following $GABA_A$ receptor activation, as an active source develops in the extracellular space which is balanced by a passive sink. Determining if an identified source is active or passive is more difficult, and would require identification of the type of synapse (Buzsaki et al., 2003; Buzsaki, 2006; Buzsaki et al., 2012). Cellular geometrical arrangement and properties are important factors in determining frequency and amplitude of oscillations. Two types of dipoles can develop depending on the cellular geometry; open fields which are found in brain areas densely populated with closely aligned asymmetrical neurons such as pyramidal cells, and closed fields which are more common in areas with small, round symmetrical cells. High oscillatory power is found in an open field owing to the large spatial separation between the current sink and source whereas closed fields generate lower oscillatory power due to the sink and source being closer together. It should be noted however, that closed fields are rare; the dendrites of even the most symmetrical of cells will not all be simultaneously activated, instead, most spherical symmetrical cells generate small dipoles (Linden et al., 2010). Brain areas with distinct layers in which dendrites of individual pyramidal cells are closely packed and run parallel to each other, such as in the hippocampus and PC, tend to generate higher amplitude oscillations than less dense regions (Buzsaki et al., 2012).

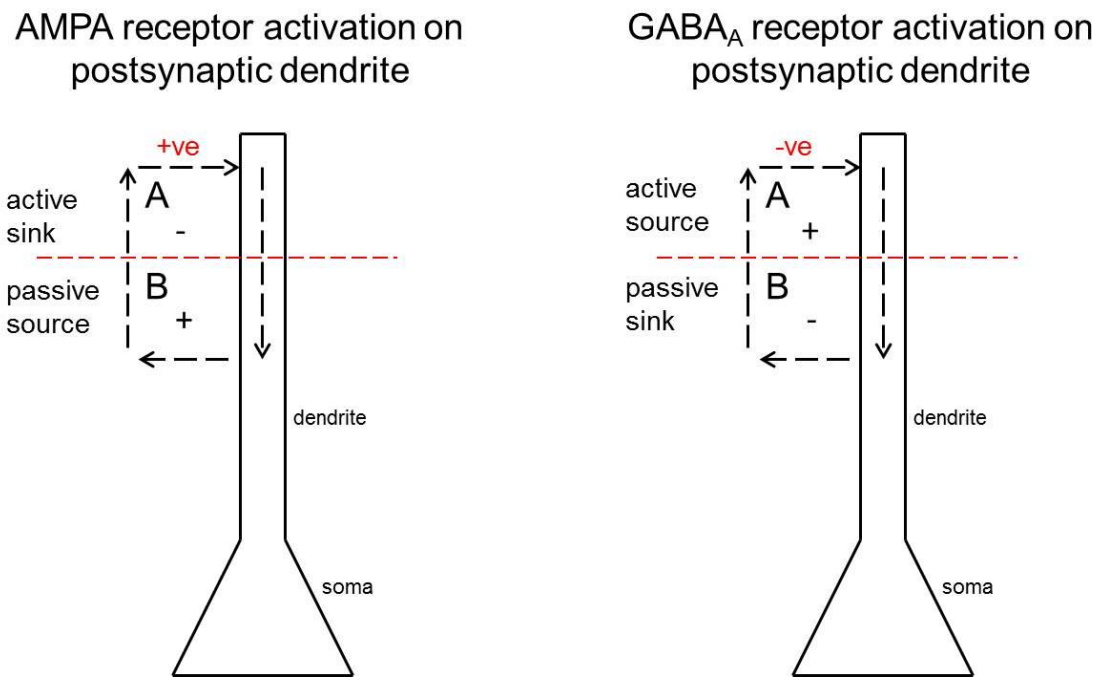

Figure 1.3 Extracellular recording during synaptic activity.
Left, the AMPA receptor is activated on the postsynaptic membrane; this generates an inward flux of Na^+ ions into the intracellular space and an active sink in the extracellular space. The charge flowing across a membrane at any given time must summate to zero, to balance. Further down the dendrite there is a passive return current in which positive ions flow out of the cell, creating a dipole. The dipole can be recorded when extracellular electrodes are simultaneously inserted into area A and B. At the same time area A would present a negative voltage compared to area B which would be positive. Right, when a $GABA_A$ receptor is activated on the postsynaptic membrane it generates an inward flux of Cl^- into the intracellular space and an active source in the extracellular space. Again, the charge flowing across a membrane at any given time must summate to zero. Further down the dendrite there is a passive return current in which negative ions flow out of the cell creating a dipole. The dipole can be recorded when extracellular electrodes are simultaneously inserted into area A and B. At the same time area A would show a positive voltage compared to area B which would be negative. Adapted from (Leung, 2010).

The majority of the potential difference recorded with an extracellular electrode is the summation of synaptic activity. The contribution of action potentials to the extracellular signal is believed to be minimal, as neurons do not often spike at the same time and the signal is attenuated by distance. This is largely due to event duration; although excitatory/inhibitory postsynaptic potentials (E/IPSPs) generate a much lower change in transmembrane potential, they have a much longer duration than action potentials. The extracellular fluid acts as a low pass filter, attenuating the signal generated by events with fast kinetics. However, it should be noted that although action potentials are usually only recorded when the electrode is very close to a cell, it is these action potentials that generate the synaptic activity that is recorded, therefore, action potentials do contribute indirectly to the LFP (Einevoll et al., 2007;

Pettersen et al., 2008). Other, non-synaptic activity that contributes to the signal includes spike after-hyperpolarisations, Ca^{2+} spikes, voltage-dependent intrinsic oscillations and gap junctions (Buzsaki et al., 2003; Buzsaki, 2006; Buzsaki et al., 2012).

The development of the brain slice technique in the 1950s allowed for the maintenance of living tissue *in vitro* for electrophysiological recording. The use of brain slices and *in vitro* LFP recordings in animal and human neuronal tissue has vastly improved our knowledge of the mechanisms that underlie oscillatory activity in the brain (Traub and Whittington, 2010). The size of area in which the LFP electrode is recording from has been reported to be anywhere from hundreds of µm (Katzner et al., 2009; Xing et al., 2009; Leski et al., 2013) to mm (Kreiman et al., 2006). This is likely to depend on the size of the animal, species, brain region, frequency and coherence of the signal and the specific neuronal properties (Linden et al., 2011; Leski et al., 2013). Oscillations can occur at different frequencies with individual bands associated with different functions and behaviours (see table 1.3) (Traub and Whittington, 2010). The most well studied of these is gamma frequency oscillations.

Name	Frequency band (Hz)
slow	<1
delta	2 - 4
theta	4 - 12
alpha	8 - 13
spindle	10 - 15
beta	12 - 30
gamma	30 - 70
fast oscillations	70 +

Table 1.3 Frequency bands of neuronal network oscillations

1.3.1 Gamma

Neuronal rhythms, particularly gamma oscillations (30 - 70 Hz) are thought to play a key role in the coordination of a response to a stimulus. This “binding by synchrony” theory postulates that coordinating rhythmic activity between brain regions leads to the effective combining and processing of this incoming sensory information leading to an appropriate output or response. The earliest example of sensory induced rhythmic activity was found in the OB and PC in an anesthetised hedgehog (Adrian, 1942, 1950). Gamma oscillations were observed following a natural stimulus, in this case a strong odour, linking neurophysiology with complex behaviour for the first time. However, it was not until the late 1980s that the binding by synchrony theory was more rigorously explored. Gamma oscillations *in vivo* were

reported to be induced by visual stimulation in anesthetised cats (Eckhorn et al., 1988; Gray and Singer, 1989) and later in awake cats (Gray and DiPrisco, 1997), non-human primates (Kreiter et al., 1992; Frien and Eckhorn, 2000) and humans (Lachaux *et al.,* 2000). Sensory induced gamma oscillations have since been reported in response to auditory and somatosensory stimulation (Pantev et al., 1991; Barth and MacDonald, 1996; Chen and Herrmann, 2001; Sukov and Barth, 2001). Gamma oscillations have also been implicated in object recognition (Keil et al., 1999), arousal (Struber et al., 2000), attention (Tiitinen et al., 1993) and language perception (Pulvermuller et al., 1995; Eulitz et al., 1996). Pathologically, gamma rhythms are thought to play a key role in a number of neurological disorders including schizophrenia (Clementz et al., 1997), Alzheimer's disease (Stam et al., 2002), migraine (Hall et al., 2004), stroke (Molnar et al., 1997), epilepsy (Willoughby et al., 2003) and attention deficit disorder (Yordanova et al., 2001).

Our understanding of the cellular and synaptic mechanisms that underlie these oscillations is largely based on experimental work performed *in vitro*, primarily in rodent brain slices. Initially, gamma oscillations were reported to be transiently evoked for a few seconds via tetanic stimulation (Whittington et al., 1995; Whittington et al., 1997). Later, persistent gamma oscillations were reported to be induced by bath application of agonists of metabotropic glutamate, kainate or muscarinic acetylcholine (mACh) receptors (Whittington et al., 1995; Fisahn et al., 1998; Hormuzdi et al., 2001). Persistent gamma has been investigated in a number of brain regions *in vitro*, of which, those found in the CA3 region have been most closely studied due to its clear profile, similarity to *in vivo* CA3 gamma and ease of induction (Whittington et al., 1995; Fisahn et al., 1998; Fisahn et al., 2004; Hajos et al., 2004). Mathematical modelling of both the network rhythm and the individual cellular behaviour has been crucial in understanding the underlying mechanisms (Cobb et al., 1995). The method of induction has been demonstrated to determine the cellular-synaptic mechanism of the oscillations, particularly whether or not pyramidal cells contribute to the rhythm (Whittington et al., 1995; Buhl et al., 1998; Fisahn et al., 2002; Fisahn, 2005; Bartos et al., 2007). There are two commonly used models of gamma oscillations, those that occur in the absence of pyramidal cell input; interneuron network gamma (ING) and those that require phasic excitation from pyramidal cells; pyramidal cell interneuron network gamma (PING) (Cobb et al., 1995; Traub et al., 1996a). Both models depend on a highly connected interneuron network with the frequency of the oscillations determined by the kinetics of IPSCs (Bartos et al., 2007). Tonic or stochastic excitation of the inhibitory interneurons initiates oscillations in the ING model (Whittington et al., 1995; Traub et al., 1996b; Fisahn et al., 2004), whereas interneurons are excited indirectly via pyramidal cells in the PING model (figure 1.4) (Cobb et al., 1995; Traub et al., 1996b).

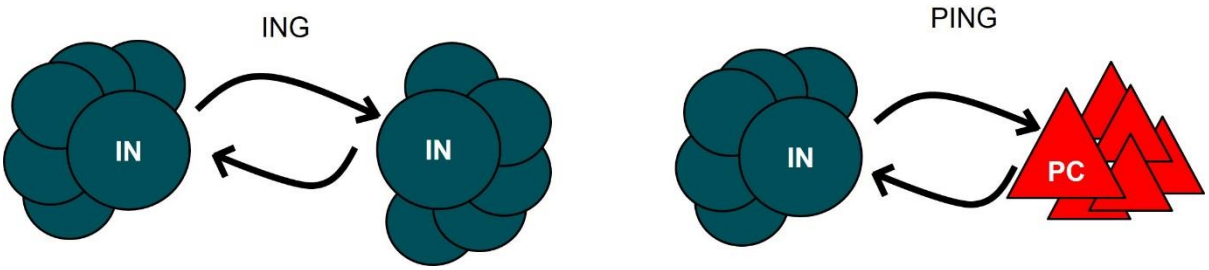

Figure 1.4 Interneuron network gamma (ING) and pyramidal-interneuron network gamma (PING).

1.3.1.1 Interneuron network gamma (ING)

Pharmacological isolation of the IN network allows researchers to study the network model ING (figure 1.4). ING can be induced experimentally in CA1 via bath application of the group I mGluR agonist dihydroxyphenylglycine (DHPG) or pressure injection of glutamate or in CA3 by pressure injection of 1.5 M potassium, with all experiments performed in the presence of ionotropic glutamate receptor blockade (Whittington et al., 1995; Traub et al., 1996a; Whittington et al., 2000; LeBeau et al., 2002). Kainic acid induced oscillations in CA3 have been reported to be both ING- (Fisahn et al., 2004) and PING-like (Traub and Whittington, 2010; Modebadze, 2014). The ING model stipulates that in the absence of a fast phasic excitatory drive, tonic/stochastic excitation initiates oscillatory activity in networks of mutually connected INs (Whittington et al., 1995; Traub et al., 1996b). During ING type oscillations, a population of INs (population one) fires action potentials, generating an IPSC in a connected population of INs (population two). If sufficient tonic/stochastic excitation of the INs is present, following the IPSC, population two responds by generating rebound spiking recorded as IPSCs in population one and the cycle repeats (figure 1.7). This generates a rhythm with the frequency-dependent on IPSC decay kinetics and the cells refractory period, the slower these events, the slower the frequency of the rhythm (Buzsaki and Wang, 2012).

When $GABA_A$ receptor antagonists were applied to kainic acid induced gamma oscillations in CA3, it abolished oscillatory activity whilst AMPA receptor blockade has no impact (Fisahn et al., 2004). Pharmacological manipulation of IPSC kinetics demonstrated agents that increase IPSC decay, such the $GABA_A$ receptor positive modulator, pentobarbital, are associated with decreased frequency of the oscillations (Segal and Barker, 1984; Traub et al., 1996b; Fisahn et al., 2004). If the IPSC decay kinetics were not setting the frequency of the rhythm, increasing the decay phase would be expected to increase the amplitude of the oscillations without altering the frequency. The preferential expression of kainate receptors and mGluRs on INs in CA3 and CA1 respectively, likely underlies the exclusion of phasic excitation in the rhythm (McBain et al., 1994; Van Hooft et al., 2000; Fisahn et al., 2004). Although pyramidal cells do not contribute to the network rhythm, those that are connected to the populations of INs still record gamma in the form of rhythmic IPSPs. It's thought to be unlikely that ING occurs *in vivo*, either in the hippocampus or cortex, owing to the strength of the excitatory

circuit. However, some areas of the brain such as the cerebellum have extensive interneuronal networks with little contribution from excitatory neurons and in these regions ING *in vivo* is more likely (Traub et al., 1996a; Middleton et al., 2008; Traub and Whittington, 2010). Many of the lessons learnt when investigating ING can be applied when pyramidal cells are added to the network.

1.3.1.2 Pyramidal-interneuron network gamma (PING)

The gamma oscillation model, PING, includes carbachol induced oscillations in CA3, and kainic acid/carbachol induced gamma in the entorhinal cortex, somatosensory cortex and motor cortex. These rhythms are dependent on phasic excitation as well as inhibition to drive the oscillatory activity (Fisahn et al., 1998; Cunningham et al., 2003; Roopun et al., 2006; Johnson, 2016). Like the ING model, application of phasic $GABA_A$ receptor antagonists abolished gamma oscillations whilst pharmacologically enhancing the decay phase of the IPSCs reduced the frequency of the rhythm (Segal and Barker, 1984; Fisahn et al., 1998). Although it should be noted that manipulating the IPSC kinetics had more of an impact on ING than PING type oscillations suggesting that the addition of pyramidal cells to the network increases the stability of the rhythm (Whittington et al., 2000). In contrast to the ING model, application of AMPA receptor antagonists abolished PING type gamma oscillations, as phasic excitation is required to drive gamma (Fisahn et al., 1998; Cunningham et al., 2003). Carbachol induced oscillations in CA3 have been extensively investigated using pharmacology, dual extracellular and intracellular recordings and KO mouse studies; as such their mechanism is well understood. The preferential expression of mAChRs on pyramidal cells likely underlies the reliance on phasic excitation for pacing (Fisahn et al., 2002). The M1 receptor subtype is thought to generate gamma via tonic activation of pyramidal cells leading to increased action potential firing (Levey et al., 1995; Fisahn et al., 2002). Mathematical models have implicated axo-axonal gap junctions in the spread of excitation between pyramidal cells. Gap junctions between INs are thought to play a role in recruiting more INs to the network but are not fundamental for oscillation generation (Hormuzdi et al., 2001; Pais et al., 2003; Traub et al., 2003; Kopell and Ermentrout, 2004).

During carbachol induced gamma oscillations in CA3, the pyramidal cells and INs follow a highly coordinated sequence of events. In brief, the axons of pyramidal cells are excited via mAChR activation generating a very fast oscillation in the axon (VFO, ~70Hz). Rhythmic IPSPs generated by INs, and directed at the pyramidal cell soma interrupt the VFO and prevent the antidromic spread of excitation from the pyramidal cell axon to the soma. This VFO excitatory activity is therefore restricted to a window defined by the IPSPs. The excitation is spread to neighbouring pyramidal cells via axo-axonal gap junctions and generates axonal driven action potentials. These action potentials generate rhythmic (gamma frequency) EPSPs in synaptically connected INs which in turn initiates IN firing. The cycle repeats as this IN firing rhythmically interrupts VFO activity in pyramidal cell axons. The

observation that pyramidal cell firing leads IN firing by a few ms further confirmed this theory (Mann et al., 2005). During gamma oscillations, both pyramidal cells and INs are slightly depolarised but only by 5 mV and 0-1 mV respectively (Fisahn et al., 1998; Traub et al., 2000; Schmitz et al., 2001). Genetically reducing EPSCs specifically in the IN population, using $GluR_4$ KO mouse, reduced the power of gamma oscillations in CA3, implying phasic excitation to INs not pyramidal cells is required for gamma generation (Fuchs et al., 2007). Local application of an AMPA receptor antagonist to specific layers in CA3 during PING type gamma implicated perisomatic targeting INs in generation of the gamma (Mann et al., 2005). In CA3, these cells are most likely basket cells owing to their abundance, perisomatic targeting outputs, low spike threshold, interconnections with other interneurons and pyramidal cells and gamma frequency action potentials phase locked to local field gamma oscillations (Buhl et al., 1994; Cobb et al., 1995; Sik et al., 1995; Freund and Buzsaki, 1996; Penttonen et al., 1998; Gulyas et al., 1999; Hajos et al., 2004; Gloveli et al., 2005; Mann et al., 2005).

1.4 Human Epilepsy

The World Health Organisation (WHO) defines epilepsy as a "*chronic disorder characterised by recurrent (two or more, unprovoked) seizures as a result of excess electrical discharge in a group of brain cells*" (WHO, 2012). Approximately 70 % of diagnosed cases in the developed world are effectively controlled with AEDs (WHO, 2012). The risk of developing epilepsy is highest in childhood, the elderly and those living in developing countries (owing to increased incidence of infection and injury) (Bell and Sander, 2001; WHO, 2012). Mortality rates in epileptic patients are two-three times higher compared to the healthy population; death may be as a direct result of epilepsy, due to the underlying pathology or from unrelated conditions. Sudden unexpected death in epilepsy (SUDEP), the most common cause of mortality, is thought to affect 500 people in the UK per year (Hanna et al., 2002; Hitiris et al., 2007). Other epilepsy related mortality includes status epilepticus, suicide, accidents and death during surgery (Hitiris et al., 2007; Hamed et al., 2012).

1.4.1 Seizures

Seizures are a symptom of epilepsy defined by the International League Against Epilepsy (ILAE) as "*a transient occurrence of signs and/or symptoms due to abnormal excess or excess synchronous neuronal activity in the brain*" (Fisher et al., 2005). Seizure activity can be segregated into inter-ictal, pre-ictal, ictal and post-ictal states although the boundaries between these phases often overlap (Fisher et al., 2014).

1.4.1.1 Inter-ictal state

Patients spend the majority of their time in an inter-ictal state, a period between seizures in which abnormal behaviour is not usually present although occasional abnormal electrical activity (inter-ictal spikes) in the brain can be recorded in some patients. Inter-ictal spikes are

routinely used by clinicians in a pre-surgical assessment to identify the epileptic zone for resection (Barry et al., 1992; Wennberg et al., 1998; Hufnagel et al., 2000; Ishibashi et al., 2002). These spikes are generated when groups of neurons briefly depolarise (paroxysmal depolarising shift, PDS) to above threshold and generate a short (70 - 250 ms) burst of action potentials which are recorded with an EEG as fast discharges (Matsumoto and Marsan, 1964; Dichter and Spencer, 1969; Prince and Connors, 1985). These brief events are and are thought to be initiated by a reduction in inhibition and terminated with a inhibition driven fast hyperpolarisation (Prince and Futamachi, 1968; Dichter and Spencer, 1969; McCormick and Contreras, 2001). This reduction in inhibition can occur following interneuronal loss after extensive seizures or brain injury, such as in TLE (Toth et al., 1998; Kobayashi and Buckmaster, 2003). Areas with extensive connectivity of excitatory neurons, such as the hippocampus, are more vulnerable to this excess excitation (Wieser, 2004). It has been suggested that inter-ictal events in TLE drive abnormal axonal growth of excitatory neurons onto their original network which can lead to pathological feedback excitation (Kelley and Steward, 1997; Sutula, 2002; Staley et al., 2005). In addition, the glutamate released during PDS and corresponding depolarisation of postsynaptic membranes activates NMDA receptors which can lead to Ca^{2+} entry and induce long term potentiation of the synaptic connection (Meyer et al., 1984; Bains et al., 1999; Stoop et al., 2003; Behrens et al., 2005; Debanne et al., 2006). The combination of strengthening of excitatory synaptic connections and generation of new abnormal connections has been suggested to drive or sustain a network capable of producing ictal events (Staley et al., 2005; Staley and Dudek, 2006).

1.4.1.2 Pre-ictal

Prodromal symptoms in the 24 hours leading up to a seizure are reported in ~40 % of patients; behavioural changes (e.g irritability, anger), cognitive disturbances (e.g bradypsychia) and anxiety and mood changes are the most commonly reported symptoms (Petitmengin et al., 2006; Scaramelli et al., 2009). Some patients are able to predict, based on prodromal symptoms that they are at an increased likelihood of having a seizure, with those who had more regular seizures being better at predicting approaching seizures (Haut et al., 2007). Closer to seizure initiation, patients have reported shaking, tingling, twitching and double vision as predictors for an impending seizure. Up to 68 % of patients that had warning symptoms have reported an ability to prevent seizures by relaxation or distraction (Cull et al., 1996; Spector et al., 2000). Long-term EEG-video recording identified increased synchronous (4 - 15 Hz) activity in the brain in the hours preceding a seizure in ~70 % patients tested (Le Van Quyen et al., 2005). Pre-ictal discharges appear at the beginning of the ictal state.

Pre-ictal discharges differed from inter-ictal discharges as they are higher in amplitude, therefore they are likely corresponding to a larger number of neurons. Inter-ictal events have

been found to depend on both excitatory and inhibitory activity, whereas pre-ictal discharges were dependent on glutamatergic activity alone (Huberfeld et al., 2011; Stafstrom, 2011).

1.4.1.3 Ictal

Mass synchronisation of neuronal activity that interrupts the normal activity of the brain is known as an ictal event. The seizure trigger and resulting symptoms are dependent on the brain region affected and the type of epilepsy the patient has. Seizure classification has varied considerably over the years, in 2016 it was again reorganised, this time into three levels with revised terminology (figure 1.5) (Hirsch et al., 2016). First, seizures are classified as either generalised or focal (or unknown) onset depending on if one or both hemispheres participate, although focal can evolve into generalised (evolving to bilateral tonic-clonic). Next, seizures are classified based on symptoms, which are usually dependent on the brain area involved and cover both motor (e.g tonic-clonic, myoclonic) and non-motor symptoms (e.g absence seizures, sensory, cognitive or emotional impairments). Finally, awareness is considered and is split into three categories; aware, impaired awareness and unknown awareness. Awareness rather than responsiveness is used as patients may be unresponsive during seizures but may still be aware and able to recall it after the event. Awareness is not usually considered during generalised seizures as any form of awareness is uncommon (Hirsch et al., 2016).

Seizures are often diagnosed based on symptoms alone, as patients can have completely normal brain activity between seizures and seizures themselves may be rare making them difficult to capture using EEG recordings. If a clear lesion is not located via neuronal imaging in a pre-surgical assessment, long term EEG monitoring or intracranial electrodes may be necessary to identify the zone generating the seizures (dysplastic zone). EEG recordings of ictal events vary considerably between patients and types of epilepsy. Tonic-clonic seizures are the most well-known seizure type. Patients experience an initial tonic phase, with a fast muscle contraction that can be serious enough to impair breathing, followed by a clonic phase, characterised by rhythmic muscle contractions (Yo Ko, 2015). PDSs also occur during ictal events, however, this differs from those during inter-ictal events as the depolarisation is sustained rather than transient. The tonic phase consists of a long PDS accompanied by sustained action potential firing followed by the clonic phase, during which there are repeated PDSs accompanied by bursts of action potentials. Ictal events cause an increase in neuronal firing, decreased spike threshold, decreased afterhyperpolarisation, depolarisation of the membrane, decreased IPSPs and increased NMDA receptor activation leading to the PDS. As a result, the extracellular concentration of K^+ increases, which can itself depolarise cellular membranes and decrease spike threshold, generating a positive feedback loop (Matsumoto and Marsan, 1964; Traynelis and Dingledine, 1988; Jensen and Yaari, 1997; McCormick and Contreras, 2001).

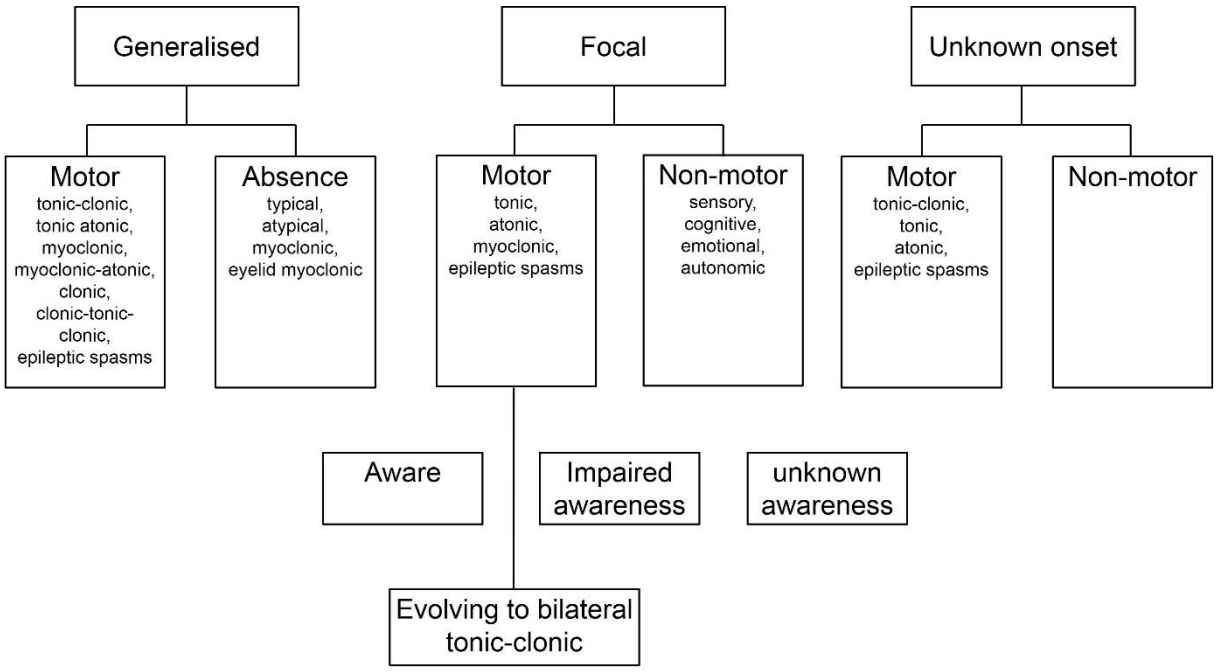

Figure 1.5 Seizure classification. Seizures are classified on three levels – 1. Focal/generalised/unknown. 2. Seizure symptoms. 3. Awareness. Additionally, seizures can begin as focal and evolve to generalised. Adapted from (Yo Ko, 2015).

1.4.1.4 Seizure termination and the post-ictal phase

Except in the case of *status epilepticus* (SE), seizures usually terminate without intervention after a few minutes and patients enter the post-ictal phase, which can last hours to days. Patients commonly report confusion, nausea, drowsiness, headaches, depression, psychosis and problems with memory (Fisher and Schachter, 2000). In the post-ictal EEG, the delta rhythm, a rhythm most prevalent during deep sleep, is the most common finding (Kaibara and Blume, 1988; Jan et al., 2001). Alterations in cerebral blood flow, receptor availability and increased inhibition in the post-ictal state have also been found (Fisher and Schachter, 2000; Koepp et al., 2010).

Human studies have found cortical perfusion increases significantly in the affected hemisphere during ictal events, and then reduces to below baseline levels following seizure termination (Weinand et al., 1994; Weinand et al., 1997). Decreased perfusion of the PC, hippocampus and amygdala has also been found 1-3 days following SE in animal models of epilepsy (Righini et al., 1994; Nakasu et al., 1995b; Nakasu et al., 1995a; Wang et al., 1996b). Whether or not this reduction in cerebral blood flow is a deliberate response by the brain to inhibit seizure activity, or a consequence of seizure induced intracellular Na^+

accumulation and cellular swelling is not known (Fisher and Schachter, 2000; Koepp et al., 2010).

Increased activation of fast, phasic $GABA_A$ receptors during ictal events is also likely to be important for seizure termination. Feed-forward inhibition is thought to prevent the spread of seizures outside the focal zone and $GABA_A$ receptor desensitisation has been reported to lead to SE (Chen et al., 2007a; Cruikshank et al., 2007; Goodkin et al., 2007; Trevelyan et al., 2007; Lado and Moshé, 2008). However, although GABA receptors are likely to participate in the termination of seizures, their short duration of action (ms – s) means they are unlikely to contribute much to the long term post-ictal state.

Following high frequency neuronal firing, opioids are released which may act as endogenous anticonvulsants (Frenk et al., 1979; Koepp et al., 2010). Opioid receptors have been found to be upregulated in the ictal zone during the post-ictal state in humans and administration of naloxone, an opioid receptor antagonist, between seizures has been found to significantly increase EEG recorded inter-ictal activity (Molaie and Kadzielawa, 1989; Hammers et al., 2007). Administering opioid receptor antagonists to rats following SE was able to reverse post-ictal depression. However, it also prevented the post-ictal inhibition of further seizures indicating opioids likely play a role in seizure termination (Frenk et al., 1979; Kelsey and Belluzzi, 1982; Martin et al., 1997).

Ictal events are highly energy-dependent. Much of this energy will come from ATP which when metabolised is converted to adenosine (McGaraughty et al., 2005). This resulting 6-31 fold increase (in humans) of adenosine in the brain, which persists during the post-ictal period, is at concentrations known to suppress ictal activity in human brain tissue *in vitro* (Kostopoulos et al., 1989; During and Spencer, 1992). Adenosine is thought to terminate seizures via presynaptic inhibition of neurotransmitter release, most likely via binding to A1 receptors (Dragunow et al., 1985; Young and Dragunow, 1994; Boison, 2005; Kochanek et al., 2006). Interestingly, these receptors are found to be significantly reduced in human epilepsy patients compared to healthy controls (Glass et al., 1996). However, adenosine's significant side effects and short half-life have so far precluded it from any clinical application (Lado and Moshé, 2008).

1.4.2 Temporal lobe epilepsy

TLE is thought to affect ~24 % of the epileptic population and is the most common form of focal onset seizures in the adult population (Semah et al., 1998). Seizures in TLE are usually focal, originating in the temporal regions of the brain but can evolve to generalised (Jasper, 2012). Seizure symptoms are dependent on the brain area involved but can range from brief aura-like symptoms to impaired consciousness and tonic-clonic seizures. TLE is sometimes preceded by an initial precipitating injury followed by a silent or latent period after which patients develop spontaneous recurrent seizures (SRS). The period of time spent in the

latent period varies depending on a number of factors including severity of insult and age before patients go on to develop SRS. In a process termed epileptogenesis, progressive changes in brain physiology including mossy fibre sprouting, hippocampal sclerosis and granular cell disorganisation precede SRS. This initial insult could be a febrile convulsion, hypoxia, trauma or infection with progressive changes in EEG and behaviour over the latent period (which may last years), which continue after seizures have become apparent (Mathern et al., 2002; Wieser, 2004).

Neuronal loss or hippocampal sclerosis has been found in TLE patients in post mortem tissue as well as in tissue removed during surgery, however there is some debate as to whether this causes or is as a result of seizures (Cavanagh and Meyer, 1956; Babb et al., 1984; Blümcke et al., 2000; Thom et al., 2005; Thom, 2009). Specific loss of dendritic targeting inhibition leading to disinhibition of pyramidal cells has been found in both TLE patients (De Lanerolle et al., 1989; Mathern et al., 1995; Wittner et al., 2001) and animal models (Ribak et al., 1982; Obenaus et al., 1993; Cossart et al., 2001; Dinocourt et al., 2003; Kobayashi and Buckmaster, 2003). The “dormant basket cell” hypothesis suggests that loss of excitatory input to dendritic targeting interneurons is responsible for this disinhibition (Sloviter, 1987; Babb et al., 1989; Sloviter, 1991; Sloviter et al., 2003). However, limited supporting evidence has led to this theory being strongly criticised (Bernard et al., 1998; Ben-Ari and Dudek, 2010).

In a heathy brain, the dentate gyrus granule cell layer is a single, closely packed band of neuronal cell bodies with a clear border to the molecular layer. Up to 90 % of TLE patients experience some form of granule cell disorganisation of which 40 % will be classified as severe dispersion with granular cell bodies dispersed into the molecular layer and no clear molecular-granular cell layer border (Houser, 1990; Thom et al., 2002). Synaptogenesis of the mossy fibres (axons) of the dentate granule cells is the third key difference in TLE patients compared to healthy controls. Mossy fibre sprouting is a form of synaptogenesis in which the axons of dentate granule cells form new, abnormal, excitatory synapses with the dendrites of granule cells is also found in TLE (Babb et al., 1991; Lim et al., 1997; Buckmaster et al., 2002; Nadler, 2003; Dudek and Shao, 2004; Freiman et al., 2011). The combination of increased excitatory feedback pathways from abnormal connections and decreased interneuron populations creates an imbalance between excitatory and inhibitory circuits and generates seizures.

1.4.3 Focal cortical dysplasia

Focal cortical dysplasia (FCD) is the most common form of intractable epilepsy found in paediatric patients undergoing surgery (Harvey et al., 2008). Symptoms are variable depending on the region affected with focal seizures which may or may not evolve to generalised being most common. Intellectual disability can also occur. Malformations in

cortical development lead to seizures that are often resistant to AEDs. Although originally thought of as rare (Taylor et al., 1971), better imaging equipment has increased diagnostic success and led to a rise in the number of confirmed cases (Bluemcke et al., 2011). Today FCD is defined as a congenital abnormality characterised by areas of the brain with disorganisation of normal cortical structure with or without abnormal cells with specific subtypes (I-III) depending on presentation (Bluemcke et al., 2011). Type I is the mildest form and patients do not usually develop seizures until early adulthood, type II is more severe and usually present during childhood. Type III can have any of the histopathological findings in types I and II but also co-presents with another epileptic lesion (such as a tumour), see table 1.4 (Palmini et al., 2004; Fauser et al., 2006; Bluemcke et al., 2011; Kabat and Król, 2012). Between 43% and 75% of patients who undergo surgery to treat FCD can expect to be seizure free a year after surgery with subtype of dysplasia being the most important factor in determining surgical success (Tassi et al., 2002; Colombo et al., 2003).

Type	Cortical layers	Cellular abnormalities	Co-presentation
Ia	Abnormal radial cortical lamination (>8 neurons aligned in vertical direction into micro columns).	Immature small diameter or hypertrophic pyramidal neurons outside layer V.	none
Ib	Abnormal tangential cortical layer (loss recognisable cortical layering).	Immature small diameter or hypertrophic pyramidal neurons outside layer V & normal neurons with disorientated dendrites.	none
Ic	Abnormal radial cortical lamination and tangential cortical layering.	Immature small diameter or hypertrophic pyramidal neurons outside layer V & normal neurons with disorientated dendrites.	none
IIa	Significant disorganisation – layers unidentifiable.	Dysmorphic neurons (enlarged cell soma and nucleus).	none
IIb	As above.	Dysmorphic neurons & balloon cells – very abnormal with large cell body and multiple nuclei connected via nuclear bridge.	none
IIIa	Cortical layering abnormalities.	Sometimes.	+ hippocampal sclerosis
IIIb	Cortical layering abnormalities.	Sometimes.	+ tumour
IIIc	Cortical layering abnormalities.	Sometimes.	+ vascular malformation
IIId	Cortical layering abnormalities.	Sometimes.	+ brain injury

Table 1.4 Focal cortical dysplasia subtypes (Bluemcke et al., 2011; Kabat and Król, 2012)

1.4.4 Antiepileptic drugs and drug resistance

AED therapy selected by the clinician is dependent on the type of seizures, epilepsy syndrome and age of patient. Initially monotherapy is used but if this is not successful more drugs are administered in place of the original or as adjunct therapies. Polytherapy has the added risk of drug interactions but is often more successful in preventing seizures. A variety of drugs are available with a variety of different drug targets; many drugs are promiscuous and affect multiple targets and can cause significant side effects (Rogawski and Löscher,

2004; Margineanu, 2012). AEDs are usually classified into three groups; those that modulate voltage-gated ion channels (e.g Na^+ and Ca^{2+} channel inhibitors), those that enhance synaptic inhibition and those that inhibit synaptic excitation. The ultimate aim of these drugs is to reduce or eliminate seizures by targeting the PDS, epileptic bursting and seizure synchronisation and spread (see section 1.4.1, seizures).

Patients do not respond adequately to AEDs in ~30 % of cases (Rogawski and Löscher, 2004). The point at which a patient's epilepsy is defined as intractable and surgery is recommended depends on the type of epilepsy. The ILAE defines drug resistance as *"failure of two adequate trials of two tolerated and appropriately chosen and used AED schedules (whether as monotherapies or in combination) to achieve sustained seizure freedom"* (Bourgeois, 2008). Failure to respond is the point at which unacceptable side effects occur without adequate seizure control (Hermanns et al., 1996).

There are a number of mechanisms thought to underlie drug resistance including failure of the drug to reach its target or altered drug targets (Kwan et al., 2011). Overexpression of the P-glycoprotein has been noted in resected tissue from drug resistant patients. P-glycoproteins are ATP-dependent efflux transporters which protect the blood brain barrier (BBB) by pumping drugs back into the capillaries thereby lowering the cerebral drug concentration (Tishler et al., 1995; Sisodiya et al., 2002; Aronica et al., 2003). However, more recent research has demonstrated that a number of commonly used AEDs including carbamazepine are not transported by the P-glycoprotein (Baltes et al., 2007). Reduced sensitivity to drugs might occur following prolonged use. Carbamazepine applied to resected tissue from carbamazepine resistant patients has been found to have a reduced effect on Na^+ channels when compared to tissue from carbamazepine sensitive patients (Remy et al., 2003). Proof of a reduced sensitivity to other drugs has been difficult to assess, particularly as most AEDs have multiple mechanisms of action, many of which are unknown (Kwan et al., 2011). It is also worth noting that issues in the management of the treatment may be the problem as "appropriately chosen" AEDs are crucial. Patients with poor compliance, the wrong diagnosis or treatment or an inappropriate dose are far more likely to experience drug resistance (Kwan et al., 2011).

There are a huge number of different AEDs available and to try them all is impractical, particularly as delaying surgical intervention is a risk factor for a poorer outcome both in seizure control and postoperative neurophysiological health (Janszky et al., 2005). After the patient is classed as drug refractory alternative treatments such as surgery may be considered (Kwan and Sperling, 2009).

1.4.5 Surgery

Patients with either FCD or TLE are the most likely to have drug refractory epilepsy (Semah et al., 1998). Medical intractability alone is not enough for the patient to undergo surgery, the

type of epilepsy, region of the brain generating the seizures and the type and severity of seizures are also considered in a pre-surgical assessment. Ideally a full resection of the affected brain region would be performed; if this is not possible, surgeons may consider partial resection, hemispherotomy, functional hemispherectomy, subpial transections, corpus callosotomy, vagal nerve stimulation, gamma knife surgery and deep brain stimulation (Noachtar and Borggraefe, 2009).

Before a resection is performed, non-invasive (MRI, EEG) and invasive tests (ECoG) are required to identify the region generating the seizures. Resections can be grouped into temporal and extra-temporal resection. In a randomised controlled trial, temporal resection was found to be effective in eliminating seizures in 64 % of patients compared to 8 % that continued with AED therapy (Wiebe et al., 2001). Similar results have also been demonstrated in uncontrolled studies and case reports (Engel et al., 2003). Extra-temporal resections which are performed on patients with a variety of different epilepsy syndromes, including FCD, involve removal of small areas of the brain not inside the temporal region. Postoperative seizure freedom varies widely depending on the region of the brain, if full or partial resection was achieved and how well the epileptic zone was identified (Noachtar and Borggraefe, 2009). Although surgery will not be carried out unless the clinician is confident that the patient's quality of life will be improved, surgery still carries risks and is not suitable for all patients indicating a need for further development of AEDs.

1.5 Animal models of temporal lobe epilepsy (TLE)

Animal models of human disease are a major area of medical research. Models allow researchers to investigate and manipulate the mechanisms of a disease. The better this is understood, the better they are equipped to target pharmaceutical interventions to diseases. The three most commonly used models of acquired TLE are the kindling model (Goddard, 1967), kainic acid model (Nadler et al., 1978) and the pilocarpine model (Turski et al., 1983b; Turski et al., 1983a). Each model shares some similarity with human disease, however, no model is a perfect (homologous) representation. By using models of acquired epilepsy, as opposed to genetic models, researchers can investigate the way in which the brain changes during epileptogenesis. This relies on an initial insult or injury to the brain, which in the case of the pilocarpine and kainic acid model is a period of SE, followed by a latent period in which epileptogenesis is thought to occur and ends when the chronic stage begins, with the first spontaneous recurrent seizure (SRS). The kindling model depends on repetitive insults and therefore does not strictly fit with this definition (Goddard, 1967; Turski et al., 1983b; Turski et al., 1983a; Ben-Ari, 1985).

Motor seizure activity is classified into five stages according to the Racine scale, from mild abnormal behaviour (stage one) to the more severe stage five tonic-clonic seizures, (table 1.5) (Racine, 1972).

Although first classified using the amygdala kindling model, the Racine Scale is the most commonly used assessment of seizure severity in all models without the need for concurrent EEG recording.

Stage	Activity (rats)
1	Facial/mouth movements including chewing
2	Head nodding
3	Forelimb contractions
4	Rearing (sitting up on hind limbs, forelimbs shaking)
5	Rearing and falling (like 4 followed by loss of postural control)

Table 1.5 Racine scale. The Racine scale is used to classify stages of seizure severity, stage 1 being the mildest and stage 5 being the most severe (Racine, 1972).

1.5.1 The kindling model

The kindling model is defined by a series of repetitive electrical stimulations to the brain resulting in an afterdischarge (AD). Over a number of repetitions the AD extends in duration, increases in amplitude and spike frequency and abnormal behaviour starts to appear (Goddard, 1967; Goddard et al., 1969). Abnormal behaviour typically follows the five stages of the Racine Scale (table 1.5), however, this is not always the case and is dependent on the area of the brain stimulated and susceptibility of the rat to kindling (Mcintyre, 2006). Initially the AD is only focal; however, over repetitive stimulations more areas of the brain are recruited and participate in the seizure activity (McIntyre, 1970). Over time the threshold for AD induction is reduced and weaker stimulation can be used (Racine et al., 1972; Löscher et al., 1993). The kindling model is classified as a model of partial seizures with secondary generalisation. This process of epileptogenesis differs from SE models (see below) as the brains response to stimulation gets progressively stronger without sustaining significant morphological damage (Morimoto et al., 2004). With no universally defined protocol, each research group has developed its own, with variations found in area of the brain kindled, stimulus strength or duration, interstimulus interval and AD threshold determination, all of which influence speed of kindling and response (Mcintyre, 2006). Different areas of the brain appear to have different AD/seizure thresholds, with the amygdala, piriform and perirhinal cortex being the most easily kindled (Kairiss et al., 1984; Racine et al., 1988a; Sato et al., 1998). Most experimenters class an animal as kindled when the stimulus applied reliably induces stage five seizures, however, others have continued to create an over kindled model in which spontaneous seizures occur independent of stimulation (Pinel et al., 1975; Pinel and Rovner, 1978; Michael et al., 1998). In that respect the kindling model is an excellent model for studying seizure progression, propagation and response to AEDs. However, as TLE

patients exhibit spontaneous seizures, most researchers wishing to study spontaneous seizures will select an SE model instead.

Chemical kindling is also possible via repeated application of sub-threshold doses of a variety of pro-convulsant drugs with the most commonly used being pentylenetetrazol (PTZ) (Cain, 1981, 1982; Gilbert and Goodman, 2006). Both direct intracerebral injections and systemic administration can be used, with differences in behaviour and electrophysiology dependent on route of administration, drug of choice and time between applications. Like the electrical kindling model, the chemical kindling model is considered to be a model of partial seizures with secondary generalisation. Rodents develop progressively worse seizures following each pro-convulsant administration, in line with the Racine scale. As many of these drugs can be delivered systemically, chemical kindling can be cheaper and easier to perform than electrical kindling and results in low levels of mortality. However, the disadvantages include less experimental control, lack of electrophysiological recording, the need to consider time between drug administration and entry into the brain, effects of drug absorption and distribution variation between animals and possible interaction between pro-convulsant and AED being tested (Gilbert and Goodman, 2006). As such, electrical kindling or SE models of epilepsy are generally more popular.

1.5.2 The kainic acid model

The kainic acid model is one of the most commonly used SE models of TLE. The model was developed when intracerebral injections of kainic acid were proposed as a model of hippocampal damage, but seizures were observed following injections prior to hippocampal CA3 damage (Nadler et al., 1978; Ben-Ari et al., 1979). Kainic acid is thought to induce seizures via a number of mechanisms including specific activation of $GluK_2$ receptors on mossy fibres postsynaptic to CA3 pyramidal synapses (Ben-Ari and Cossart, 2000). As a chronic model of epilepsy, an initial insult generates up to several hours of SE, followed by the latent period, a seizure free period that may last days or months before SRS develops (Dudek et al., 2006; Lévesque and Avoli, 2013). Kainic acid can either be injected systemically (ie. intraperitoneal or intravenous routes) or injected focally into the hippocampus or amygdala via the intracerebral route (Nadler et al., 1978; Ben-Ari et al., 1979; Ben-Ari et al., 1980). Both routes produce similarly high levels of successful seizure induction, with similar behavioural symptoms and length of latent period. Focal injections are however thought to more closely resemble human TLE pathology and behaviour than systemic induction (Mathern et al., 1995; Sloviter, 2005). Systemic injections generate a more widespread damage across the brain, whereas damage is more limited to the targeted regions with focal injections (Ben-Ari et al., 1980; Lancaster and Wheal, 1982; Drexel et al., 2012). However, a relatively low ratio of rats induced via the intracerebral route develop SRS, and of those, many spontaneously recover (Cavalheiro et al., 1982). This is likely due to the protective effects of anaesthesia, as a high percentage of animals that underwent focal

induction whilst awake entered SRS and did not spontaneously recover (Behrens et al., 2005). In 1987 ingestion of mussels contaminated with the kainic acid ligand domoic acid caused memory deficit, seizures, coma and death in a human population in eastern Canada. Similar to the kainic acid model in rodents, necrosis and neuronal loss were found *post-mortem* in numerous brain regions (Teitelbaum et al., 1990a; Cendes et al., 1995).

1.5.3 The pilocarpine model

The pilocarpine model is the third most commonly used model of epilepsy and is thought to more closely represent the natural history of acquired TLE than kindling (Turski et al., 1983b; Turski et al., 1983a; Cavalheuro et al., 2006). High doses (300 - 400 mg/kg) of pilocarpine, induce SE, after which if mortality has not occurred animals undergo a latent period in which they are seizure free followed by the development of SRS (Turski et al., 1983b; Turski et al., 1983a). The length of time spent in the latent period and mortality is dependent on a number of factors including dose, time spent in SE, age, weight and susceptibility to pilocarpine (Glien et al., 2001; Curia et al., 2008). Pre-treatment with lithium significantly reduces the threshold for seizure induction allowing for much lower doses of pilocarpine to be given (20 - 50 mg/kg) (Honchar et al., 1983). Pre-treatment increases the number of animals successfully entering SE, however, mortality still remains extremely high (Jope et al., 1986; Clifford et al., 1987; Sloviter, 2005; Curia et al., 2008). Despite the high mortality, the pilocarpine model is still popular due to its ease of induction, lower cost and is thought to be more representative of acquired TLE compared to the kindling model (Leite et al., 1990).

Pilocarpine is a non-specific mAChR agonist that initiates SE via M1 receptor activation (Clifford et al., 1987; Hamilton et al., 1997; Bymaster et al., 2003). M1 receptor activation is thought to upregulate phospholipase C, inositol trisphosphate and intracellular Ca^{2+} (Felder, 1995). Lithium potentiates this cholinergic effect by inhibiting inositol phosphate breakdown (Ormandy et al., 1991; Belmaker and Bersudsky, 2007; Hillert et al., 2014). Maintenance of SE following induction does not depend on AChRs but rather NMDA receptor activation and an imbalance between excitatory and inhibitory transmission (Jope et al., 1986; Clifford et al., 1987; Nagao et al., 1996; Priel and Albuquerque, 2002). SE severity is then increased by seizure induced BBB breakdown, with the PC demonstrating the greatest BBB breakdown (Rigau et al., 2007; Van Vliet et al., 2007).

The severity of mortality and morbidity resulting from traditional models has led to significant refinement of the lithium pilocarpine model in recent years (Glien et al., 2001; Sloviter, 2005; Modebadze et al., 2016). Administration of repeated lower doses of pilocarpine has been previously found to reduce mortality to ~10 % (Glien et al., 2001). The reduced intensity status epilepticus (RISE) model further refined the repeated doses model reducing the mortality rate to ~1 % (Modebadze et al., 2016). Seizure severity in the RISE model is reduced via administration of α_2 adrenergic receptor agonist xylazine during SE (Yang et al.,

2006), and limiting SE to one hour with a cocktail of anticonvulsant drugs (Tang et al., 2007; Modebadze et al., 2016). Xylazine is a potent muscle relaxant and a sedative, administered to circumvent hyperlocomotor activity and reduce the risk of seizure spread to the brainstem. Seizures were terminated via administration of MPEP, MK-801 and diazepam, an $mGluR_5$ antagonist, NMDA receptor antagonist and a $GABA_A$ receptor positive allosteric modulator respectively (Tang et al., 2007; Modebadze et al., 2016). Despite reducing the severity, the RISE model maintains its epileptogenicity and rats still develop SRS (Modebadze et al., 2016).

1.5.4 Brain slice acute models of epileptiform activity

There are a number of acute slice models of epileptiform activity that are utilised by researchers to investigate the mechanisms of seizure spread or efficacy of new AEDs. The most commonly used seizure models involve manipulation of the ionic concentration of the extracellular fluid. Seizure-like events (SLEs) can be induced by lowering the Ca^{2+} or Mg^{2+} or raising the K^+ concentration (Yaari et al., 1983). Simultaneous reduction of extracellular Ca^{2+} and raised K^+ generates repetitive non-synaptic mediated ictal events in areas of densely packed neurons e.g CA1 (Jefferys and Haas, 1982; Yaari et al., 1983; Heinemann et al., 2006). The reduction in Ca^{2+}-dependent currents, weakening of charge screening and increase in the persistent Na^+ current leads to a large (30 mV) membrane depolarisation and increase in action potential firing (Catterall, 1980; French et al., 1990; Azouz et al., 1996; Jensen et al., 1996; Shuai et al., 2003). Lowering extracellular Mg^{2+} can induce SLEs in a wider variety of brain areas. Removal of the Mg^{2+} block on NMDA receptors leads to cell membrane depolarisation and an increase in action potentials (Mayer and Westbrook, 1985; Anderson et al., 1986; Walther et al., 1986). A reduction in membrane surface charge screening and an elevation of intracellular Ca^{2+} through voltage sensitive Ca^{2+} channels is thought to contribute to epileptiform activity (Mody et al., 1987; Mangan and Kapur, 2004; Isaev et al., 2012). Raising extracellular K^+ also depolarises the cell membrane leading to enhanced neuronal firing and SLEs (Jensen and Yaari, 1988; Traynelis and Dingledine, 1988; Leschinger et al., 1993).

Alternatively, pharmacological application of epileptogenic drugs such as 4-aminopyridine (4-AP), kainic acid or pilocarpine can be used. The K^+ channel blocker 4-AP enhances the presynaptic release of excitatory and inhibitory neurotransmitters (Buckle and Haas, 1982; Perreault and Avoli, 1991). Giant EPSPs generate bursting activity even in the presence of enhanced inhibition (Perreault and Avoli, 1991). Kainic acid and pilocarpine are more commonly used in epileptic models *in vivo*, however, they have both also been utilised in *in vitro* slice preparations to induce epileptiform activity (Westbrook and Lothman, 1983; Nagao et al., 1996).

1.6 The piriform cortex and epilepsy

The human PC is smaller than the rodent cortex; however, it still shares a number of features, particularly its phylogenetically old trilaminate structure. The human PC is located close to the entorhinal cortex in the junction between the temporal and frontal lobes (Amunts et al., 2013; Mai et al., 2015). It is divided into the frontal and temporal regions which are thought to correspond to the rodent anterior and posterior regions respectively (Carmichael and Price, 1994).

Long before the PC was noted as a region of interest in rodents, the olfactory system was identified as participating in TLE in human patients (Jackson and Beevor, 1889; Jackson and Stewart, 1899). Epileptic auras are the perception of sensory information that can occur just before a seizure and can act as an early warning system. Olfactory hallucinations have been found to precipitate seizures in a small proportion of TLE patients (<10 %) (King and Marsan, 1977; Howe and Gibson, 1982; Gupta et al., 1983; Chen et al., 2003). The perceived odour is often unpleasant, with “rotten”, and “burning” smells commonly described (Acharya et al., 1998; Chen et al., 2003). More than half of TLE patients are reported to involuntarily wipe their nose in the post-ictal phase of a seizure; a process likely to involve the olfactory centres in the brain (Hirsch et al., 1998; Leutmezer et al., 1998; Geyer et al., 1999; Vaughan and Jackson, 2014). Specific recording from the PC has not been performed in patients with abnormal olfactory function. However, concurrent video and EEG recordings performed with an electrode in the PC of an epileptic patient identified epileptiform activity in the PC despite not reporting olfactory dysfunction. A temporal lobectomy and removal of the frontal PC significantly reduced this patient’s seizure incidence and severity (Vaughan and Jackson, 2014). Outside of the ictal/post-ictal state, reduced olfactory function has been reported, including reduced ability to identify or differentiate between odours and loss of odour memory (Martinez et al., 1993; Hummel et al., 1995; West and Doty, 1995; Lehrner et al., 1997; Savic et al., 1997; Hummel et al., 2013). Neuroimaging has also identified reduced activity and conduction delays in the PC following odour presentation between seizures compared to healthy controls (Hummel et al., 1995; Ciumas et al., 2008). Strong odour inhalation has been demonstrated to both induce seizures in some patients (Hughes and Andy, 1979) and arrest seizure development in others (Efron, 1956, 1957; Jaseja, 2008).

Domoic acid poisoning has been found to lead to extensive neuronal damage post-mortem across the brain including the hippocampus and PC (Teitelbaum et al., 1990b; Cendes et al., 1995). Neuronal loss has also been found in three patients who died days after experiencing prolonged SE. When compared to age-matched controls, damage was found in the hippocampus, amygdala, PC and in one patient the entorhinal cortex (Fujikawa et al., 2000). Since then, MR (magnetic resonance) volumetric imaging has demonstrated reduced volume within the PC, OB and cortical amygdala in deceased TLE patients compared to age-matched controls (Goncalves Pereira et al., 2005; Hummel et al., 2013). Increase in grey

matter volume in the PC, amygdala and parahippocampal gyrus has also been detected in the frontal lobe of epilepsy patients compared to age-matched controls (Centeno et al., 2014). EEG-fMRI (functional magnetic resonance imaging) found a correlation between inter-ictal epileptiform discharges and BOLD (measure of blood oxygen levels) increases in the PC (Laufs et al., 2011; Flanagan et al., 2014). 11C-labelled flumazenil positron emission tomography (PET) scans which demonstrate $GABA_A$ receptor binding, found reduced receptor binding in the PC particularly in those with more frequent seizures (Laufs et al., 2011). There is significant evidence to suggest the PC is involved in human epilepsy, however, it is not known if it is participating in seizure generation, propagation or if repeated seizures are leading to PC damage. To answer these questions researchers have turned to animal models.

Focal application of proconvulsant agents such as bicuculline, carbachol and kainic acid to the PC in rodents was found to induce seizures at a much lower concentration than that required in other brain areas (Piredda and Gale, 1985a). Kindling experiments have also implicated the PC as the dominant generator in epileptiform activity as it is the first brain area to develop inter-ictal spike activity, with transient spike activity seen before kindling had begun. This inter-ictal activity originates in the PC even when the kindling electrode is inserted into other brain regions (Kairiss et al., 1984; Racine et al., 1988a). Kindling of the PC specifically has been found to induce stage five seizures faster than the amygdala, entorhinal cortex and hippocampus (McIntyre and Gilby, 2008). Reduced neuronal density, neuronal and astrocytic death and increased oedema have been demonstrated in the PC at various stages post SE in the pilocarpine model of TLE (Nairismagi et al., 2004; Kim et al., 2010; Scholl et al., 2013; Woeffler-Maucler et al., 2014). Both whole brain and slice models of seizures have also implicated the PC in the manifestation and propagation of epileptiform activity to other limbic structures *in vitro* (De Curtis et al., 1994; Demir et al., 1998, 1999, 2001; Carriero et al., 2010; Panuccio et al., 2012).

Despite the evidence that the PC is more seizure sensitive than other areas of the brain more commonly associated with epilepsy, considerably less research exists in this area. On PubMed, there are 15-30 fold more papers citing the hippocampus and epilepsy compared to the PC (figure 1.6). This clearly indicates that the PC is an under-explored area of the brain implicated in epilepsy and further investigation might help in our understanding of epilepsy disorders.

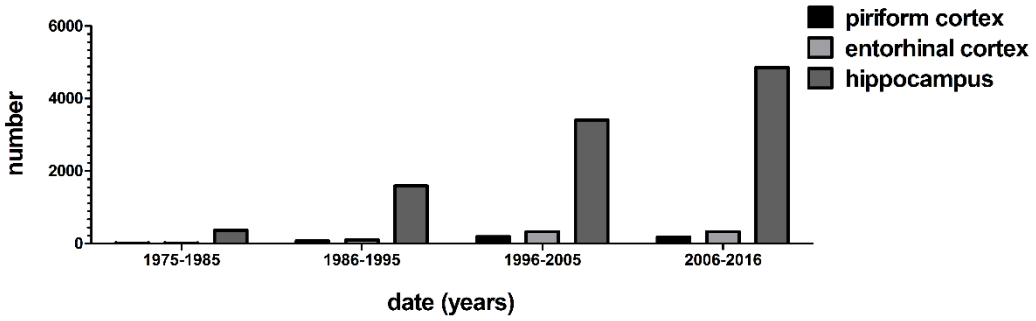

Figure 1.6 PubMed search conducted on 31/07/2016
A PubMed search was conducted on 31/07/2016 with the search terms “piriform” AND “epilepsy”, “pyriform” AND “epilepsy”, “olfactory cortex” AND “epilepsy”, “entorhinal” AND “epilepsy” and “hippocampus” AND “epilepsy”.

1.7 Aims and objectives

Given the relative lack of understanding of rhythmicity and neuronal network activity in the PC and its relation to epilepsy and epileptogenesis, we aimed to develop and explore neuronal oscillations and epileptiform activity in the PC *in vitro*, in both normal and epileptic brains. This aim comprised the following specific objectives:

- To develop a model of neuronal network oscillations in the aPC *in vitro*.
- To investigate the mechanisms that underlie neuronal network oscillations in the aPC in brain slices obtained from control adult rats.
- To investigate the mechanisms that underlie beta oscillations in human brain slices obtained from children undergoing surgery to treat drug refractory epilepsy.
- To investigate the sensitivity of four brain areas (hippocampal CA3, lateral entorhinal cortex, aPC and pPC) to zero Mg^{2+} ($0[Mg]^{2+}$) aCSF induced SLEs in slices from control animals *in vitro*.
- To characterise the sensitivity and properties of the aPC to $0[Mg]^{2+}$ aCSF *in vitro* at four stages of epileptogenesis in the new RISE model of epilepsy and compare to age-matched controls.
- To characterise the sensitivity of $0[Mg]^{2+}$ induced SLEs in the aPC *in vitro* to six combinations of commonly used anti-epileptic drugs at four stages of epileptogenesis compared to age-matched controls.

Chapter 2 Methods

2.1 Animal welfare

Experiments were performed in accordance with the Animals (Scientific Procedures) Act 1986, European Communities Directive 1986 (86/609/EEC) and Aston University ethical review documents. Male Wistar rats were housed in groups of 1-10 depending on size, in temperature and humidity controlled cages with a 12/12 light/dark cycle. Access to food and drink was provided *ad libitum*.

2.2 The reduced intensity status epilepticus (RISE) model of temporal lobe epilepsy

The RISE model of TLE is a modified lithium/pilocarpine model that was developed previously in our research group to reduce the mortality and extensive brain damage commonly found in standard pilocarpine/lithium model. Rats undergoing the protocol have a low mortality rate (1-3 %) and minimal brain damage (Modebadze et al., 2016).

Twenty four hours before epilepsy induction lithium chloride (127 mg/kg) was administered (subcutaneous – s/c) to male Wistar rats 1-3 days post weaning (postnatal day 21 - 24). The following day 1 mg/kg of (−)-scopolamine methyl bromide, a mAChR antagonist was administered (s/c) to reduce the peripheral effects of pilocarpine (diarrhoea and foaming at the mouth). 30 minutes later the general mAChR agonist pilocarpine (25 mg/kg) was administered (s/c). The rats were observed continually and were considered to be in status epilepticus (SE) when two stage 4+ Racine scale seizures (rearing, sitting up on hind limbs, forelimbs shaking, see table 1.5 for more details), were witnessed within 15 minutes of each other. The α_2 adrenergic receptor agonist xylazine 2.5 mg/kg (intramuscular - i/m) was then administered and rats were allowed to remain in modified SE for 1 hour. Any that failed to enter SE after 45 minutes were given up to two further doses of pilocarpine at least 30 minutes apart. SE was terminated using a “stop” solution consisting of the $GABA_A$ receptor positive allosteric modulator, NMDA receptor antagonist and $mGluR_5$ receptor antagonist (in mg/kg) 2.5 diazepam, 0.1 MK-801 and 20 MPEP respectively, see figure 2.1 for timeline of protocol. The rats were allowed to recover on a heat pad (33 ^{o}C) and (s/c) saline/glucose (0.9 % / 5 % NaCl/glucose) was given every 2 hours for 10 hours for rehydration. Following this, the rats were checked regularly for the next 72 hours to assess their health and wellbeing. Any failing to gain weight were closely monitored and given an oral gavage and/or encouraged to eat and drink. Breakthrough seizures were commonly observed over 12 - 48 hour period following induction which was found to be necessary for SRS development. None of the rats exceeded the maximum weight loss (25 % reduction of pre-induction weight), but rats occasionally exceeded (1 - 5 %) the moderate severity limit and were culled.

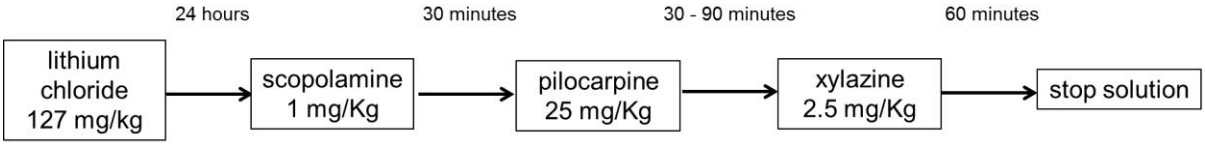

Figure 2.1. The RISE model of TLE.
The order and time between each drug used in the RISE model TLE.

2.2.1 Timeline of epileptogenesis

Following the RISE protocol, rats were tested for epilepsy development using the post-status behavioural battery (PSBB) to determine when SRS had developed. Rats were allowed one week post induction to recover before PSBB was performed twice a week. Rats were first prodded firmly in the rump with a blunt instrument (large pen) and the reaction was scored (1 - 7, see table 2.1), they were then picked up with a gloved hand and the reaction was scored (1 - 6, see table 2.1). These numbers were multiplied together and a rat was considered to be in SRS when they scored 10 or above for 4 consecutive sessions. These results were compared to twelve age-matched control rats. The rats were sacrificed at the following time points, 24 hours, 1 week, 4 - 6 weeks and 3 months+ post epilepsy induction and compared to age-matched controls. 24 hours, 1 week and 4-6 weeks post induction were time points considered to be in the latent period, see figure 2.2. Rats over 3 months, with confirmed epilepsy through PSBB were considered to have SRS. Rats took on average 20.33 ± 0.86 weeks to develop SRS (figure 2.3).

Score	Touch	Pick up
1	no reaction	Very easy pick up
2	rat turns towards the instrument	Easy pick up
3	rat moves away from the instrument	Some difficulty in pick up (rat rears and faces the hand)
4	rat freezes	Rat freezes
5	Rat turns towards the touch	Difficult pick up (rat moves away)
6	Rat turns away from the touch	Very difficult pick up (rats behaves defensively or attacks the hand)
7	Rat jumps (with or without vocalisation)	

Table 2.1 Post status behavioural battery (PSBB).
Two weeks following induction rats are monitored for the development of SRS using the PSBB task. Reaction to prodding in the rump and being picked up was scored and recorded.

Figure 2.2 Timeline of epileptogenesis.
Animals were sacrificed for experiments at 24 hours, 1 week, 4 - 6 weeks and 3 months+ post induction. Age and weight matched rats who did not undergo the protocol were used as controls.

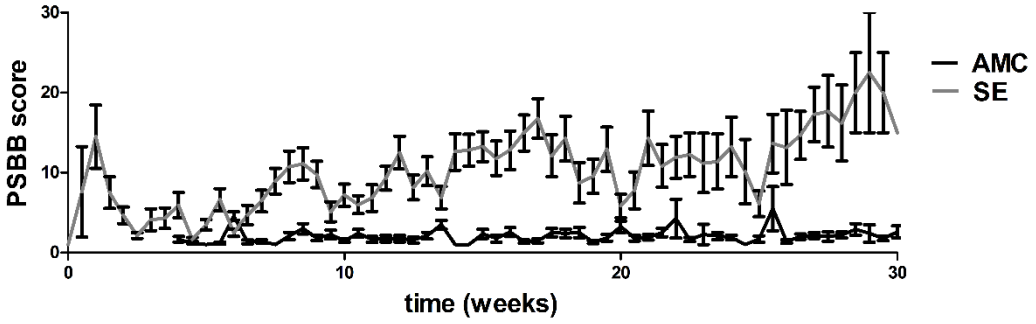

Figure 2.3 Average post status behavioural battery score
SE (n = 36) and age-matched control (AMC) (n = 12) rats were subjected to the touch and pick-up post status behavioural battery (PSBB) test twice a week. The scores for each test (table 2.1) were multiplied and rats were considered epileptic after four consecutive scores of ≥10.

2.2.2 Rodent "big brother" system

Eight rats were filmed following PSBB. This provided an independent comparison of seizure activity and validated PSBB. Rats were housed individually and recorded continuously 24 hours a day using an infrared light and a high resolution infrared video camera in the Rodent big brother system (AstraZeneca, UK). The rodent big brother system is currently in development by AstraZeneca to automatically detect when seizures occur. The rats were recorded and watched offline by members of our laboratory group and AstraZeneca. Videos were viewed offline using VLC media player (VideoLAN client).

2.3 Slice preparation

2.3.1 Control slice preparation

Brain slices were prepared from 70 - 100 g male Wistar rats (chapter 3). In brief, rats were anaesthetised with isoflurane then given injections consisting of pentobarbital (600 mg/kg, s/c), xylazine (100 mg/kg i/m) and ketamine (10 mg/kg i/m). The anaesthetic was considered sufficiently deep when the pedal and corneal reflexes disappeared. Sucrose based artificial cerebral spinal fluid (saCSF) was transcardially perfused and the brain quickly removed and placed in ice cold saCSF. 450 µm coronal (chapters 3, 6) or horizontal (chapter 5) slices

containing the piriform cortex (PC) were prepared using a vibrating microtome (Campden Instruments Ltd) and stored for at least 1 hour in an interface recording chamber at 30 - 33 ^{o}C containing aCSF bubbled with carbogen (95 % O_2 / 5 % CO_2) before commencing experiments. saCSF contained (in mM) 180 Sucrose, 2.5 KCl, 10 $MgCl_2$, 25 $NaCO_3$, 1.25 Na_2HCO_3, 0.5 $CaCl_2$, 10 D-glucose, 1 ascorbic acid with an osmolarity of 300 - 310 and pH 7.3, bubbled with carbogen. saCSF also contained a combination of neuroprotectants to enhance slice viability (mM) 2 N-acetyl cysteine, 1 taurine, 0.045 indomethacin, 0.3 uric acid, 20 ethylpyruvate, 0.2 ketamine and 0.2 aminoguanidine (Lacey et al., 2014; Prokic et al., 2015). aCSF was made up of (mM) 126 NaCl , 3 KCl, 1.6 $MgSO_4$, 2 $CaCl_2$, 26 $NaHCO_3$, 1.25 NaH_2PO_4, 10 D-glucose. The holding chamber aCSF also contained (mM) 0.045 indomethacin and 0.3 uric acid.

2.3.2 Choline cutting solution

Over the course of the project two different solutions were used to prepare brain tissue. Initially sucrose based cutting solution (section 2.3.1) was used in young rats (chapter 3, 70 - 100 g). However, when we used this solution with brain slices prepared from older animals, induced oscillatory activity was rare and cells appeared dead when investigated using an infrared microscope. Thus, a choline based cutting solution was found to more reliably produce healthy slices. Therefore all oscillation experiments (chapter 3) were performed using sucrose based cutting solution and the remaining experiments (chapters 4 - 6) were performed using slices that were prepared with choline based cutting solution. Experimental procedures were identical to those in 2.3.1 except the sucrose based cutting solution was replaced with a choline based solution containing (mM) 110 choline chloride, 26 $NaHCO_3$, 10 D-glucose, 11.6 ascorbic acid, 7 $MgCl_2$, 3.1 Na-pyruvate, 2.5 KCl, 1.25 $NaHPO_4$, 0.5 $CaCl_2$, 0.045 indomethacin, 0.3 uric acid and 0.19 ketamine.

2.3.3 Human brain slice preparation

Human brain tissue was obtained from children undergoing surgery to treat drug refractory epilepsy at Birmingham Children's Hospital. Children undergoing surgery were patients in which drug treatment had been unsuccessful at managing seizures to a reasonable level. In most cases patients had either FCD or TLE. Tissue was used in accordance with ethical permission granted by the Black Country LREC (protocol 'cellular studies in epilepsy' 10/H1202/23), Birmingham Children's Hospital NHS Trust (RECREF 10/H1202/23) and Aston University ethical review document (project 328). In brief, dysplastic tissue was removed by Mr Richard Walsh (consultant neurosurgeon, Birmingham Children's Hospital) from regions generating seizures identified by intraoperative and implanted ECoG. The tissue was placed in a sealed holding chamber containing ice-cold choline based cutting solution and transported within 10 minutes to the laboratory and sliced in the same way as animal tissue (section 2.3.1).

2.4 Extracellular recordings

450 µm brain slices were placed in an interface chamber (see figure 2.4) and superfused with aCSF at a flow rate of ~2 ml/min and maintained at 30-32 ^{o}C. Microelectrodes were pulled with a resistance of 1 - 5 MΩ using a Flaming Brown micropipette puller (Sutter Instruments, CA) and filled with aCSF. Four microelectrodes were inserted into layer II of the PC (Chapter 3, 6) or human tissue (chapter 4) of four separate slices or layer II of the aPC, pPC and lateral entorhinal cortex and stratum pyramidale of CA3 (Chapter 5) located using an Olympus SZ57 microscope. The signal was amplified 100x by an EXT-02F amplifier (NPI, Germany) and the 50 Hz electrical noise was removed by HumBugs (Quest Scientific, Canada). The signal was further amplified 10x by a LHBF-48X amplifier (NPI, Germany) and low pass filtered at 700 Hz and high pass filtered at 0.3 Hz with a sampling rate of 8.3 KHz. The signal was then digitised using a Digidata 1440A (Axon CNS, Molecular Devices, US) and recorded to disk (see figure 2.5). Recordings were viewed live using Clampex 10.3 and analysed offline using Spike2 7.1. Spontaneous activity was recorded in normal aCSF, oscillations were recorded in the presence of 400 - 600 nM kainate and 40 - 50 µM carbachol (chapters 3 - 4). 0[Mg^{2+}] recordings were performed in normal aCSF with the Mg^{2+} omitted (chapters 5 - 6). A modified aCSF solution (0.25 mM Mg^{2+}, 8 mM K^{+}) was used to induce epileptiform activity in human tissue (chapter 4). Drugs were applied for 40 minutes unless otherwise stated.

2.5 Multielectrode array recording

The multielectrode array recording was carried out using a 10 x 10 (4 mm x 4 mm) Utah array (Blackrock Microsystems, Salt Lake City, USA). 96 equally spaced platinum electrodes with an impedance of 170 – 461 KΩs were recorded from simultaneously. The signal was amplified by a RHD2132 amplifier board (Intan Technologies, Los Angeles, USA) and digitised by an Intan Technologies RHD2000 USB interface board. Signals were viewed online with Intan Technologies RHD2000 interface, recorded to disk and analysed offline using Spike2 7.1.

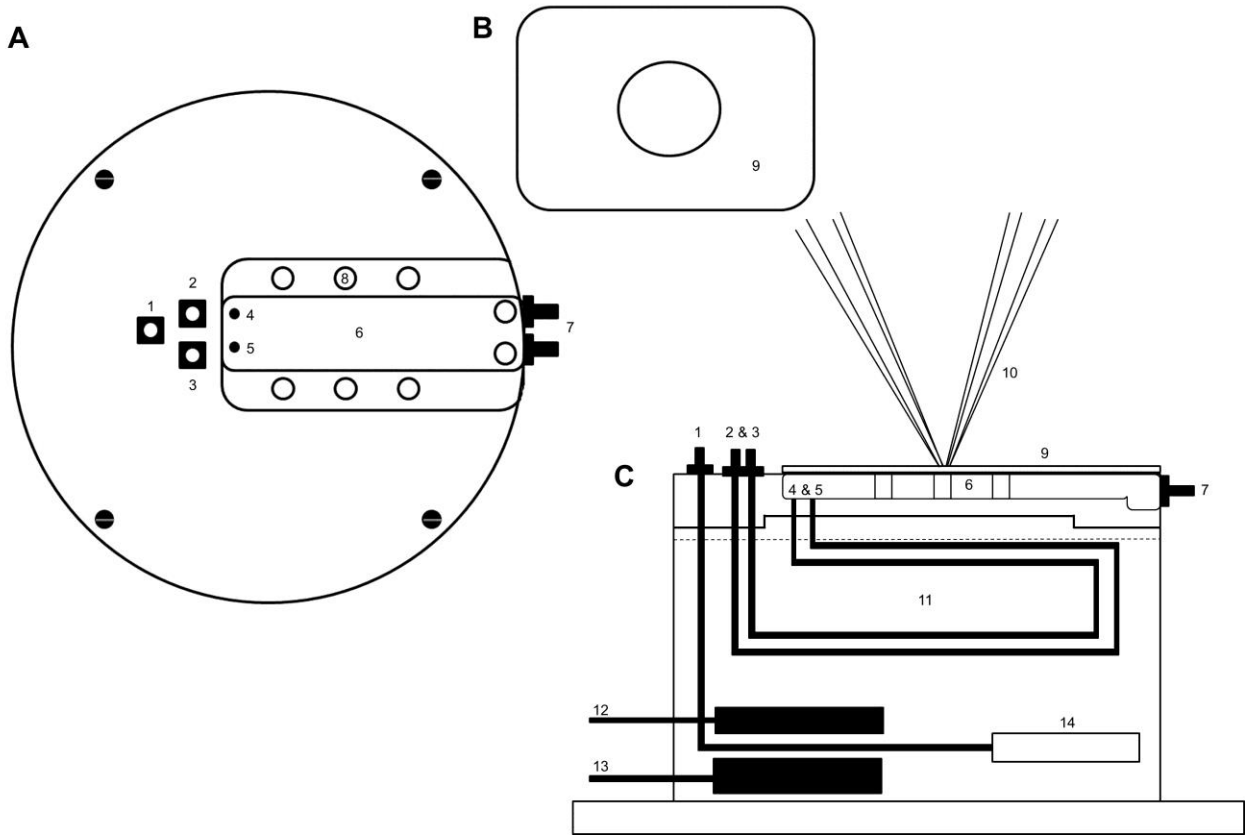

Figure 2.4 The recording interface chamber.
The interface chamber consisted of a top (A) in which the slices sat on a net in a tray (6) bathed in a continuous perfusion of aCSF. The top was screwed onto the bottom (C) which consisted of a chamber of warm water bubbled with carbogen to create the correct humidity and temperature for the slice. (1) Carbogen input into the water chamber was under the interface chamber (11). The aCSF was input into the chamber at (2) and (3) and then run into the bottom part of the chamber in tubing surrounded by warm water (11) and into the top of the tray (4 and 5), where it flowed over the netting under the slice (6) and out of the output drippers (7). To maintain the humidity the water in the bottom part of the chamber was bubbled with carbogen (14), the temperature was kept at 31 - 37 ^{o}C by a heater (12) and feedback sensor (13) allowing water to evaporate and flow over the slices (8). The acrylic lid (B, 9) prevented water droplets from hitting the slices. Up to four electrodes (10) were inserted into four slices via the hole in the acrylic lid (9) and the electrophysiological activity was recorded.

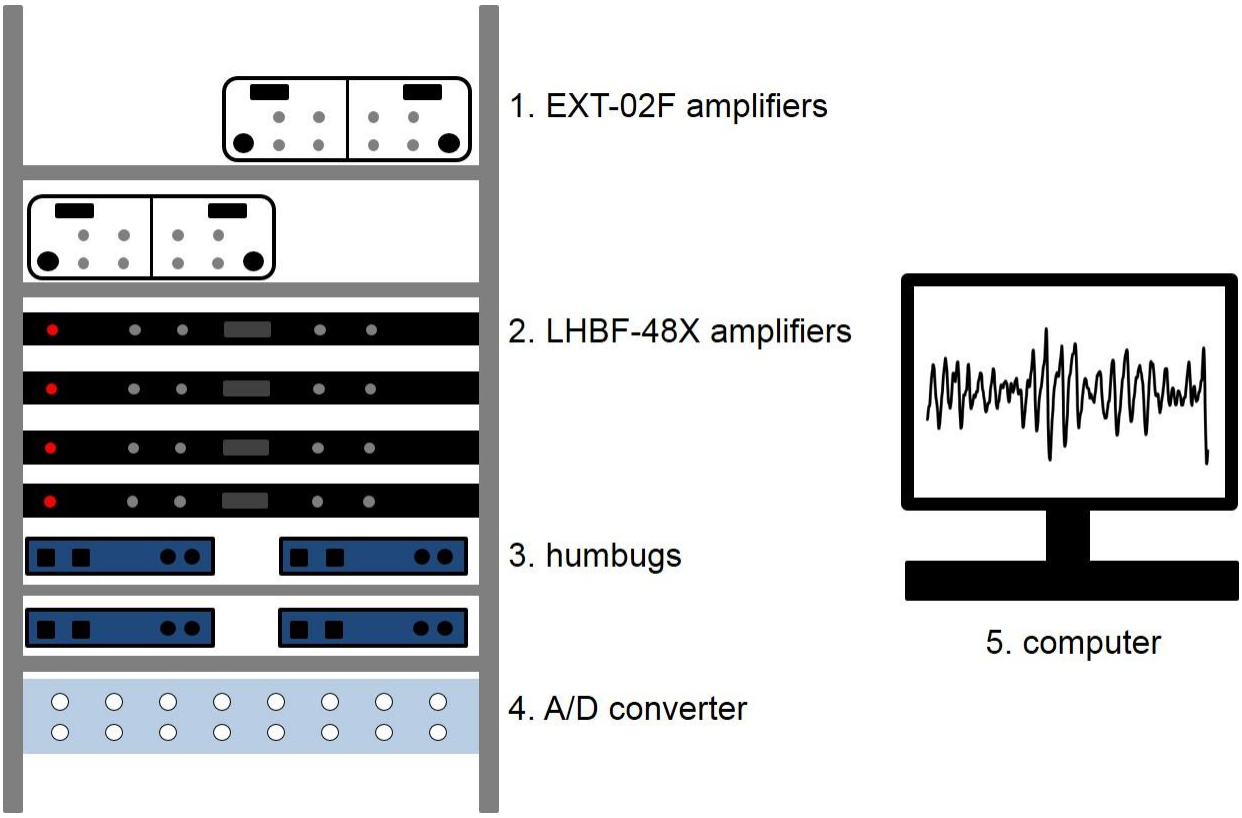

Figure 2.5 The recording electrical equipment.
Four microelectrodes were inserted into four separate slices. For each microelectrode the signal was then amplified 100x by a EXT-02F amplifier (1) and the 50Hz electrical noise was removed by the HumBugs (2). The signal then further amplified 10x and high and low pass filtered by a LHBF-48X amplifier (3). The signal was then digitised using a Digidata 1440A (4) and recorded and saved to a standard desktop computer (5).

2.5 Analysis

2.5.1 Local field potentials

Analysis of LFP recordings was performed offline using Spike2 7.1 software (Cambridge Electronic Design) and GraphPad Prism 5. Raw oscillations data was filtered using a band pass second order IIR digital filter between 10 and 45 Hz (gamma) or 2 and 40 Hz (beta). Power spectrums were not digitally filtered but determined from 60 second epochs of data using a fast Fourier transform (FFT) algorithm. Spectrograms were created in MATLAB (MathsWorks) using a Morlet-Wavelet approach and 1 - 2 seconds of raw data.

Single drug application to oscillations was presented as normalised mean ± SEM. The D'Agostino-Pearson normality test was used to test the normality of the oscillations. As the oscillation data presented in chapter 3 and 4 was found to not be normally distributed the non-parametric Wilcoxon signed rank test was performed in GraphPad Prism 5 (*P < 0.05, **P < 0.01, ***P < 0.001) and was used to detect significant differences unless otherwise stated.

The non-parametric Friedman test was performed in SPSS (IBM analytics) (*P < 0.05, **P < 0.01, ***P < 0.001) and was used to detect significant differences when more than one drug/drug dose was used and a Bonferroni adjusted Wilcoxon post hoc test (*P < 0.05, **P < 0.01, ***P < 0.001) was used to detect differences between conditions.

When multiple comparisons were made in chapter's 5 and 6, a between subjects ANOVA (univariate analysis of variance) was performed using SPSS (IBM analytics) on normalised, ranked data. The normality of the data was tested using a Kolmogorov-Smirnov and Shapiro-Wilk test of normality; all data were found to not be normally distributed. As the between subjects ANOVA requires the data to be normal and no outliers present the outliers were removed (1.5 x interquartile range) and the data were ranked before the between subjects ANOVA was performed. The Bonferroni post hoc test was used to detect differences between groups.

2.6 Drugs

Salts were obtained from Thermo Fisher Scientific and Sigma-Aldrich. Drugs were obtained from R&D systems, Sigma-Aldrich, Abcam, Eisai co and GW pharma. Drugs were diluted from powder into stock solutions of 1 - 200 mM in water, DMSO or ethanol depending on solubility and stored at -20 ^{o}C until use, see table 2.2 for more detail. Drugs were added to circulating aCSF at the required concentration for 40 minutes after the recording had stabilised unless otherwise stated.

Drug	Purchased from	Stock concentration and solution	Concentration used
(-)-scopolamine methyl bromide	Sigma	1 mg/ml water	1 mg/kg
atropine	Sigma	5 mM, water	5 µM
cannabidiol	GW pharma	60 mM, DMSO	30 µM
carbachol	Abcam	50 mM, water	variable
carbamazepine	Abcam	100 mM, DMSO	50 µM
carbenoxolone	Sigma	100 mM water	200 µM
CGP 55845	Abcam	100 mM, DMSO	5 µM
CNQX	Abcam	100 mM, DMSO	20 µM
CPCCOEt	Abcam	20 mM, DMSO	20 µM
diazepam	Hameln	2.5 mg/ml, ethanol	2.5 mg/kg
DL-AP5	Abcam	25 mM, water	50 µM
gabapentin	Abcam	100 mM, water	20 µM
gabazine	R&D systems	2.5 mM, DMSO	250 nM & 2.5 µM
kainate	Abcam	1mM water	variable
lamotrigine	Abcam	20 mM DMSO	20 µM
LY 341495	R&D systems	10 mM, DMSO	100 nM & 5 µM
MK-801	Abcam	20 mM, water*, in vitro*, 0.1 mg/ml in RISE model	20 µM *in vitro*, 0.1mg/kg in RISE model
MPEP	Abcam	100mM, DMSO, *in vitro*, 20 mg/ml, ethanol, RISE model	20 µM *in vitro*, 20mg/kg in RISE model
NBQX	Abcam	100 mM, DMSO	2.5 & 25 µM
pentobarbital	R&D systems / JML	10 mM *in vitro*, 200 mg/ml in terminal procedure	10 µM *in vitro*, 600 mg/kg in terminal procedure
perampanel	Eisai co.	100 mM DMSO	0.1 – 10 µM
picrotoxin	Sigma	100 mM DMSO	50 µM
pilocarpine	Sigma	20-25 mg/ml water	20-75 mg/kg (repeated doses)
pirenzepine	Abcam	10 mM,water	10 µM
SYM 2206	R&D systems	100 mM, DMSO	20 µM
tiagabine	Abcam	25 mM, water	50 µM
UBP 310	Abcam	30 mM, DMSO	3 µM
UPB 304	Abcam	100 mM water & NaOH	1 µM & 10 µM
valproate	Abcam	100 mM water	500 µM
xylazine	Bayer	20 mg/ml terminal procedure, 2.5 mg/ml, water, RISE	100 mg/kg terminal procedure, 2.5 mg/kg RISE
Zolpidem	R&D systems	1 mM, DMSO	10 – 500 nM
zonisamide	Abcam	100 mM, DMSO	100 µM

Table 2.2 Table of drugs used for experimental work conducted in this thesis.
Listed are the individual drugs, where they were obtained from, stock concentrations and circulating concentration.

Chapter 3 Pharmacologically induced persistent gamma (30 – 80 Hz) oscillations in layer II of the rat piriform cortex *in vitro*

3.1 Introduction

3.1.1 Neuronal network oscillations *in vitro*

Neuronal network oscillations *in vivo* have been observed for almost a century (Berger 1929). However, it was not until 1995 that researchers observed transient oscillations in an *in vitro* brain slice preparation (Whittington et al., 1995). These oscillations were induced by tetanic stimulation and lasted for only a few seconds. This was then followed by the development of a model of persistent oscillations which continued as long as the slice remained healthy (Fisahn et al., 1998). Pharmacologically induced persistent oscillations have since been reported in a number of brain regions including hippocampal CA3 (Fisahn et al., 1998) and CA1 regions (Gillies et al., 2002), entorhinal cortex (Cunningham et al., 2003), amygdala (Sinfield and Collins, 2006), cerebellar cortex (Middleton et al., 2008), somatosensory cortex (Buhl et al., 1998) and primary motor cortex (Yamawaki et al., 2008) using both cholinergic and/or kainate receptor agonists. The ability to induce these oscillations has been aided by advances in the preparation of *in vitro* neuronal tissue, notably the development of aCSF solutions specifically designed for neuroprotection during slicing, transcardial perfusion and the use of an interface chamber. Using these techniques improves slice viability and maintains the inhibitory network which is crucial for rhythmogenesis (Aghajanian and Rasmussen, 1989; Michaloudi et al., 2005). *In vitro* gamma oscillations have been separated into two mathematical models, ING (interneuron network gamma) and PING (pyramidal-interneuron network gamma) differentiated by the involvement of pyramidal cell input (discussed in more detail in section 1.3) (Whittington et al., 2000). Which model the oscillations more closely resembles is dependent on the method of induction and brain area.

3.1.2 The piriform cortex and neuronal network oscillations

The piriform cortex (PC) is the largest olfactory area in the brain and is thought to have roles in odour processing and memory consolidation. In 1985 it was first described as “area tempestas” owing to its heightened sensitivity to seizure induction (Piredda and Gale, 1985a). Since then, numerous studies have implicated it in the development of epilepsy (epileptogenesis) (Kairiss et al., 1984; Piredda and Gale, 1985a; Racine et al., 1988a). Persistent gamma oscillations have been extensively studied in other areas of the brain implicated in epileptogenesis including the hippocampus and entorhinal cortex (Whittington et al., 1995; Fisahn et al., 1998). To our knowledge, gamma oscillations have not been induced in the PC *in vitro* and this represents a key area yet to be explored.

The PC shares a number of structural and cellular properties with the cornu ammonis regions of the hippocampus indicating it might also show neuronal network oscillations with a high power. Within the PC, close alignment of pyramidal cells particularly in the densely populated layer II and dendrites that run parallel across the layers should make it easier to record network activity (Neville and Haberly, 2004). It is not unsurprising then, that rhythmic activity was reported in the PC and olfactory bulb (OB) in anesthetised hedgehogs *in vivo* in the

1940s (Adrian, 1942, 1950). Three neuronal network rhythms have since been identified in the animal olfactory system *in vivo*, low frequency (1 - 12 Hz), beta (15 - 30 Hz) and gamma (30 - 70 Hz) (Freeman, 1959). These rhythms are present spontaneously or in response to strong odour and have been found in number of different animals and man in a variety of behavioural states (Adrian, 1942, 1950; Dodge et al., 1956; Freeman, 1959, 1978; Bressler and Freeman, 1980; Boeijinga and Dasilva, 1988; Mori et al., 1992; Kashiwadani et al., 1999; Neville and Haberly, 2003). The intrinsic low frequency rhythm follows the respiratory cycle with the specific frequency modified by behaviour. The rhythm is generally referred to as theta owing to its similarity in frequency with hippocampal theta, however the frequency band is often lower than the classic definition of theta (4 - 12 Hz) (Kay and Stopfer, 2006; Rojas-Libano et al., 2014).

Less is known about olfactory beta oscillations which have been found to replace gamma in the OB and PC during odour sampling following learned association between odour and reward (Ravel et al., 2003; Martin et al., 2004a; Martin et al., 2004b; Martin et al., 2006). Others found either beta or gamma could be elicited depending on odorant concentration, with higher concentrations more likely to generate a higher frequency response (Neville and Haberly, 2003).

OB and PC odour induced bursts of gamma band activity were first identified in 1942 and were found to occur between inspiration and expiration (Adrian, 1942, 1950; Bressler and Freeman, 1980). A high level of coherence has been observed between PC and OB oscillations and removal or separation of the OB from the PC abolished PC gamma altogether (Freeman, 1968a, b). However, PC oscillations continued if the OB input was artificially replaced with electrical stimulation, implying PC gamma is locally generated but is reliant on OB input to excite the network into a state in which gamma generation is more favoured (Freeman, 1968a, b; Kay, 2014). Temporary block of the olfactory peduncle (PC to OB afferent connection) led to a significant increase in OB gamma amplitude indicating that feedback from the PC plays a role in modulating OB gamma (Kay and Freeman, 1998; Martin et al., 2004a; Martin et al., 2004b; Martin et al., 2006). The aPC produces a much greater oscillatory power compared to the pPC. This is most likely due to the aPC receiving a stronger input from the OB compare to the pPC (Freeman, 1959; Boeijinga and Dasilva, 1988).

In vitro investigations of oscillations in the PC have been previously limited to transient oscillations induced by stimulation of the lateral olfactory tract (LOT). Odour inhalation has been found to induce burst firing in mitral and tufted cells in the OB. This burst firing travels along fibres in the LOT to the afferent fibres in layer Ia of the PC (Cang and Isaacson, 2003). This activity can be replicated in PC brain slices via stimulation of the LOT (Cang and Isaacson, 2003; Suzuki and Bekkers, 2006). The response of individual cells to 40 Hz

stimulation was dependent on the strength of the afferent/associational connection and if the connection was facilitating or non-facilitating. The afferent input to superficial pyramidal cells (SP) was found to be facilitating, as each stimulation initiated burst firing in SP cells at a frequency ≥40 Hz. The afferent input to semilunar (SL) cells was found to be non-facilitating and large afterhyperpolarisations following each action potential led to less frequent firing (<40 Hz) (Suzuki and Bekkers, 2007, 2011). Facilitation of the afferent fibre input is also important for interneurons. Within each layer two distinct subtypes of interneurons exist with a 50 - 100 ms phase lag between them (Suzuki and Bekkers, 2010a). Mutually connected interneuron networks and phase lag between neurons in response to incoming stimulus is thought to play a role in both beta and gamma oscillations (Buzsáki and Draguhn, 2004).

PC gamma oscillations are thought to be locally generated within the PC following OB input to excite the network into a state in which oscillation generation is more likely (Freeman, 1968a, b; Kay, 2014). Stimulation experiments have gone some way to explore oscillations directly produced by LOT input (Suzuki and Bekkers, 2006, 2010a). To understand the mechanisms of locally generated PC oscillations we induced and characterised persistent gamma oscillations in the PC *in vitro* for the first time.

3.1.3 Gamma oscillations in the piriform cortex *in vitro*

In this study we have demonstrated, co-application of kainic acid and carbachol reliably induced persistent gamma oscillations in an *in vitro* brain slice preparation of the aPC. This activity was strongest in layer II and was found to be dependent on AMPA and $GABA_A$ receptors as well as gap junctions.

3.2 Results

3.2.1 Induction of gamma oscillations in layer II of the piriform cortex *in vitro*

The PC is a three layered structure which shares many characteristics with the hippocampal CA3 area (Neville and Haberly, 2003). Since hippocampal CA3 can generate spontaneous gamma oscillations *in vitro* (Lu et al., 2011; Modebadze, 2014), initial experiments were conducted to investigate if rhythmic activity was present in the aPC in the absence of bath applied drugs. Spontaneous rhythmic activity was not found (figure 3.2), therefore, pharmacological manipulation of network excitability was investigated. Nanomolar concentrations of kainic acid have previously been used to induce high power gamma oscillations in a number of brain regions (Hormuzdi et al., 2001; Roopun et al., 2006). Application of kainic acid alone was not sufficient to induce oscillations in the PC (figure 3.1). Kainic acid alone was also not sufficient to induce oscillatory activity in the motor cortex, or in the original somatosensory cortex study; co-application with the mAChR agonist, carbachol was also required (Buhl et al., 1998; Yamawaki et al., 2008). The addition of carbachol at concentrations similar to those used to induce oscillations in the motor cortex, reliably induced oscillations in the aPC (figure 3.1-2) (Yamawaki et al., 2008). Hence, co-application of kainic acid (600 nM) and carbachol (CCh) (50 μM) induced gamma oscillations with mean (± SEM) frequency of 35.93 ± 0.42 Hz and power of 44.87 ± 4.05 μV^2 (n = 120 slices) (figures 3.1-2). The oscillations appeared approximately 10 minutes after application of kainic acid and carbachol and stabilised after 1-3 hours (data not shown).

Dose response curves were performed to assess the dose of kainic acid and carbachol required to reliably induce oscillations. Increasing the concentration of kainic acid in the presence of 50 μM carbachol increased the gamma power in doses lower than 800 nM, application of higher doses of kainic acid reduced the gamma power (figure 3.1). Increasing the concentration of carbachol increased the gamma power up to 50 μM, after which application of further doses of carbachol reduced the gamma power (figure 3.1). Initial experiments were performed in the presence of 600 nM of kainic acid and 30 μM carbachol however this was found to not reliably induce gamma oscillations, therefore a dose of 600 nM of kainic acid and 50 μM carbachol was used throughout the study (figure 3.2).

Oscillations could be induced in both coronal and transverse slice preparations. More slices could be obtained from a coronal preparation than a transverse preparation and four slices could be simultaneously recorded from in the interface chamber with a coronal preparation, therefore this preparation was used to reduce animal usage. When three electrodes were simultaneously recorded in the PC in presumed layers I, II and III, the gamma oscillations were found to be highest in amplitude in layer II (figure 3.1 Ci-ii). There was also a low frequency component in layer I. Since layer II produced the most reliable and high-power oscillations, future experiments were performed therein.

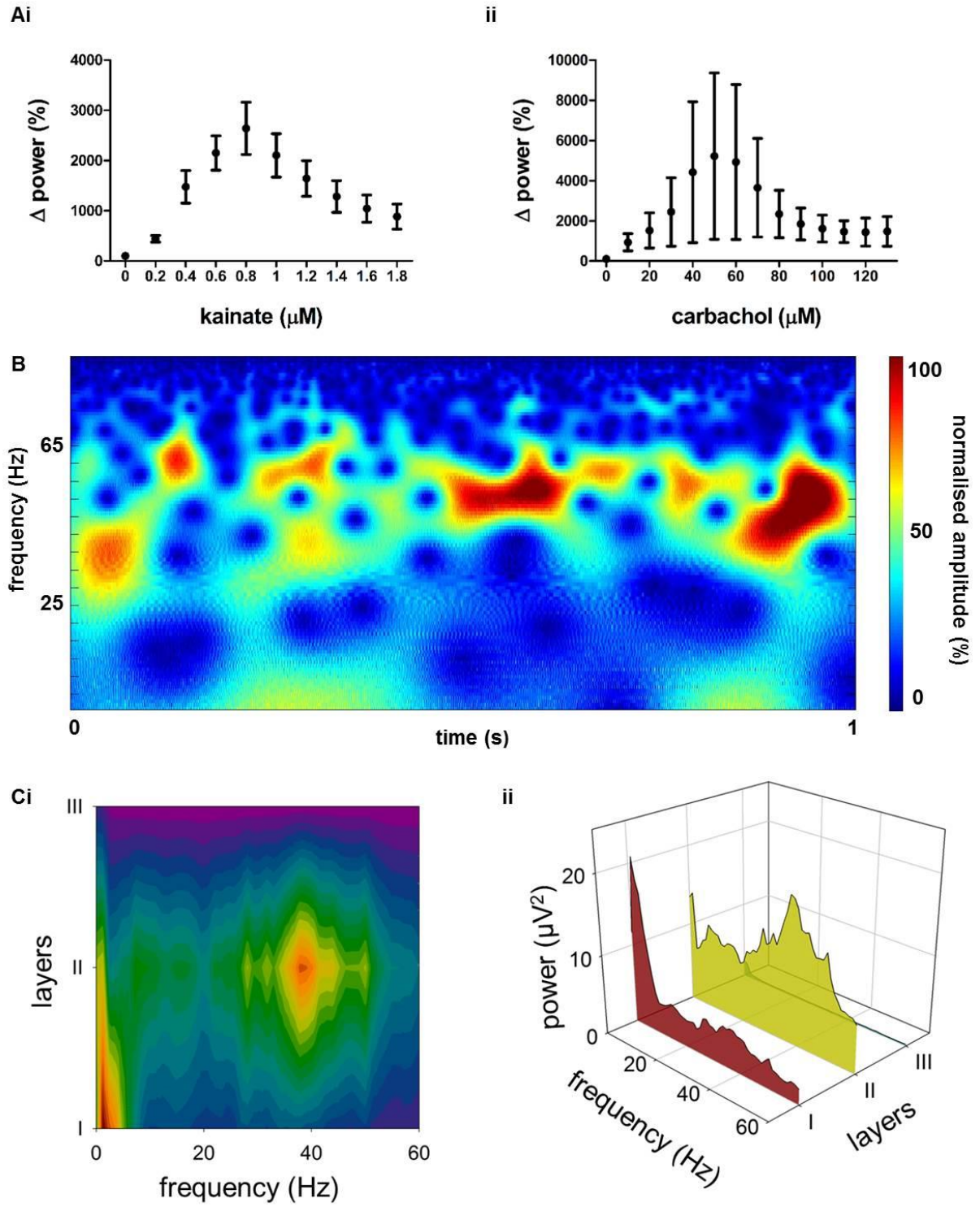

Figure 3.1 Application of kainic acid and carbachol induced gamma oscillations
Ai) Normalised mean increase in gamma peak power after doses of kainic acid were applied in the presence of 50 μM carbachol (n=8). Aii) Normalised mean increase in gamma peak power after doses of carbachol were applied in the presence of 600 nM kainic acid (n=6). B) Typical spectrogram (Morlet-Wavelet) demonstrating normalised amplitude and frequency of oscillations over a one second period. Ci/ii) Simultaneous recordings in layers I, II and III; gamma oscillations were found to be of greatest power in layer II.

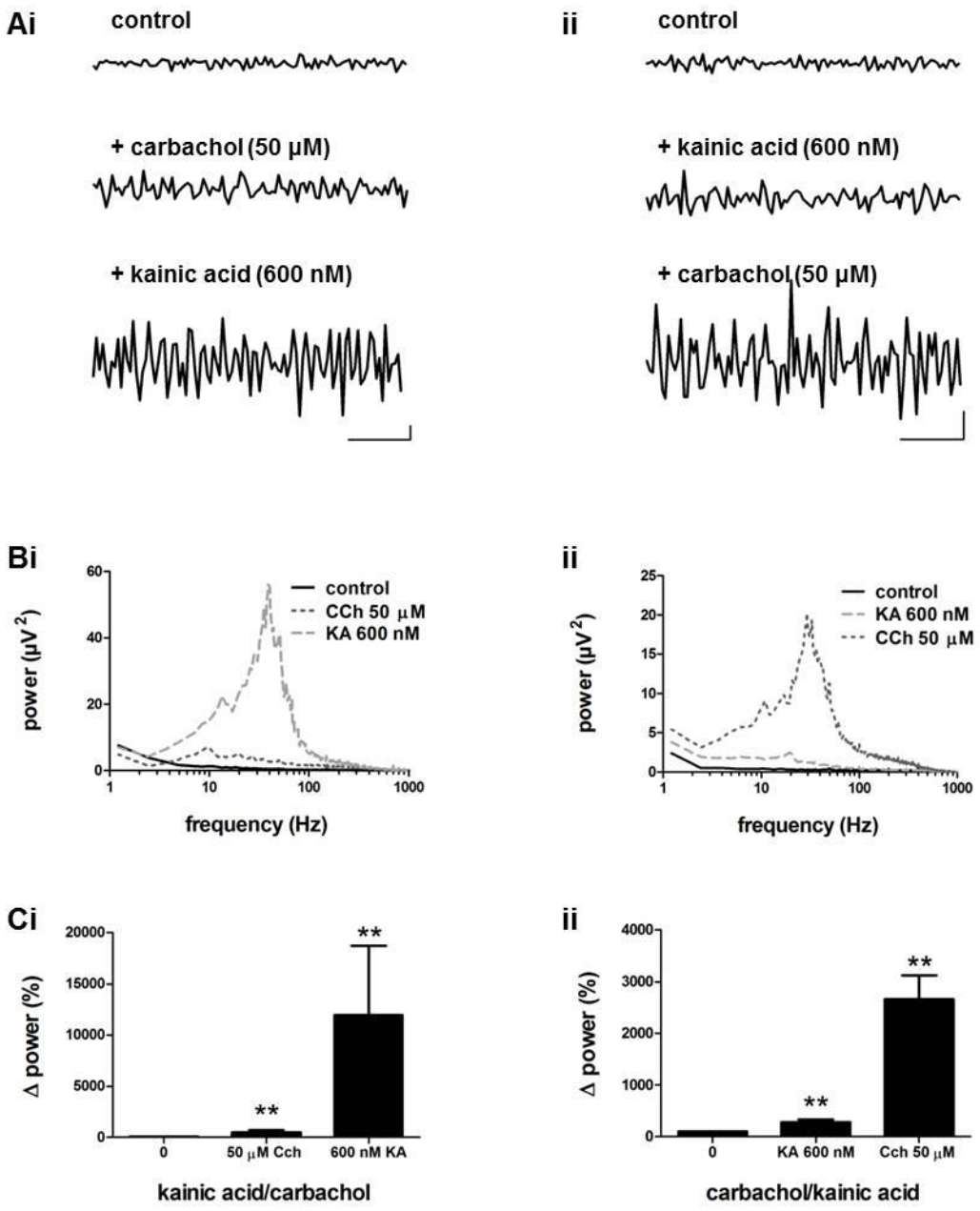

Figure 3.2 Pharmacological induction of gamma in layer II of the PC *in vitro*.

Application of both kainic acid and carbachol was required to induce gamma oscillations Ai) Recordings in normal aCSF were compared to recordings in which carbachol (50 µM) then kainic acid (600 nM) was applied. ii) Recordings in normal aCSF were compared to recordings in which kainic acid (600 nM) then carbachol (50 µM) was applied. A i/ii) One second of representative raw extracellular recordings taken from layer II of the PC (Scale – 20mV Vs 200ms). Bi/ii) Power spectrum corresponding to Ai/ii generated from 60 seconds of raw data Ci/ii) Normalised, pooled change in gamma peak power in layer II of the PC (n=8). Application of kainic acid or carbachol alone did not induce gamma oscillations; both kainic acid and carbachol were required.

3.2.2 Muscarinic acetylcholine receptor modulation of gamma oscillations

In the following experiments the control refers to slices in which gamma oscillations were induced by application of 600 nM kainic acid and 50 μM of carbachol and allowed to stabilise (approximately 1.5 - 3 hours) to the point that the oscillation peak power and frequency did not change in the 20 minutes prior to drug application. Further drugs were applied for 40 minutes unless otherwise stated and the gamma oscillations at the end of this period were compared to the control.

To demonstrate that carbachol is necessary for maintenance of the oscillations and confirm carbachol induced oscillations via the muscarinic acetylcholine receptors, 5 μM of atropine was applied. Atropine (5 μM) desynchronised the gamma network activity and significantly ($P < 0.01$, n=8) reduced gamma peak power by 93.2 ± 1.1 % (figure 3.3). In CA3 and CA1 gamma oscillations have been shown to be reliant specifically on the M1 mAChR (Fisahn et al., 1998). To test this, the M1 selective antagonist pirenzepine (10 μM) was applied. Pirenzepine significantly ($P < 0.01$, n=8) reduced the gamma peak power by 81.6 ± 7.4 % (figure 3.3).

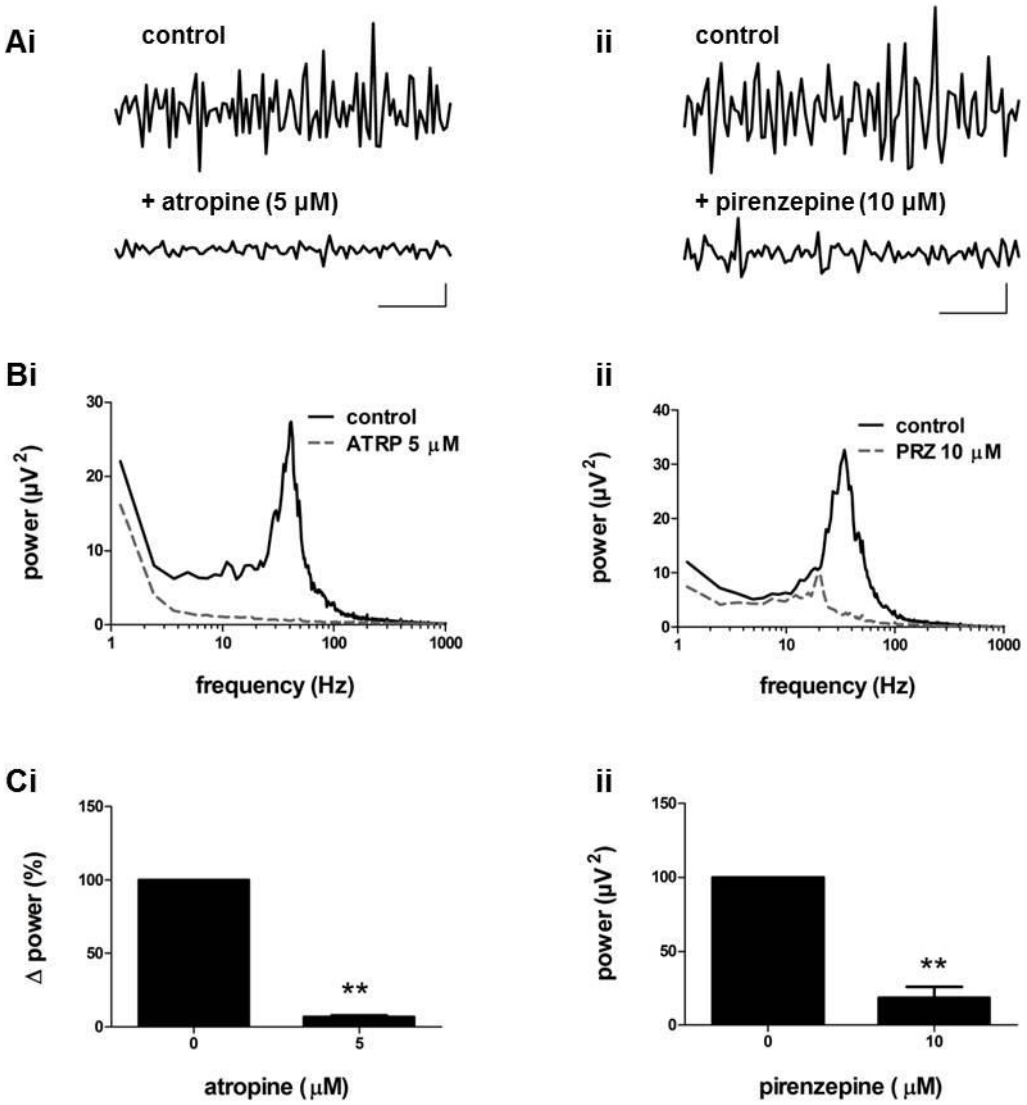

Figure 3.3 PC layer II gamma oscillations require muscarinic acetylcholine receptor activation.
Ai) Raw trace of a representative extracellular recording taken in layer II of the PC before (top) and after (bottom) atropine (5 µM) application (Scale – 20 µV Vs 200ms). Bi) Power spectrum (corresponding to Ai) of 60 seconds of raw data before and after atropine (5 µM) application. Ci) Normalised pooled data, atropine significantly ($P < 0.01$, n=8) reduced gamma peak power. Aii) Raw trace of a representative extracellular recording taken in layer II of the PC before (top) and after (bottom) pirenzepine (10 µM) application (Scale – 20 µV Vs 200ms). Bi) Power spectrum (corresponding to Aii) of 60 seconds of raw data before and after pirenzepine (10 µM) application. Cii) Normalised, pooled data, pirenzepine significantly ($P < 0.01$, n=8) reduced gamma peak power.

3.2.3 Gap Junction modulation of gamma oscillations

Gap junctions have been identified as essential for stable, high amplitude persistent gamma oscillations *in vitro* (Fisahn et al., 1998; Cunningham et al., 2003). To test whether gap junctions were necessary for persistent gamma in the PC the effect of the gap junction blocker carbenoxolone was investigated. Application of carbenoxolone (200 µM) for 2 hours desynchronised neuronal network activity and significantly ($P < 0.01$, n=8) reduced peak gamma power by 90.8 ± 2.7 % (figure 3.4).

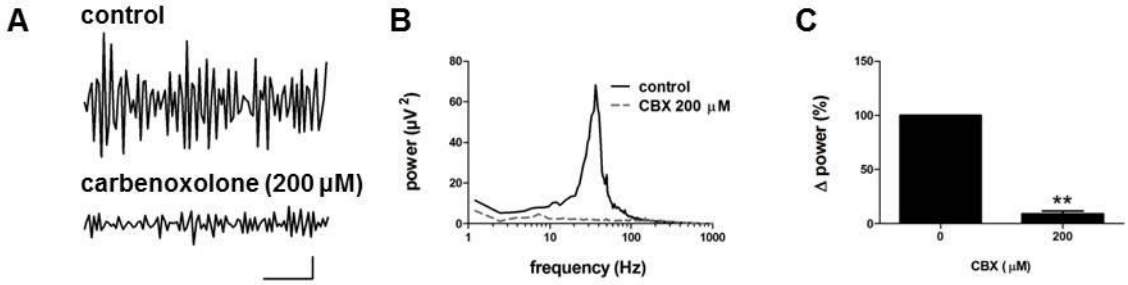

Figure 3.4 PC layer II gamma oscillations require gap junction function.
A) Raw trace of a representative extracellular recording taken in layer II of the PC before (top) and after (bottom) carbenoxolone (200 µM) application (Scale – 20 µV Vs 200ms). B) Power spectrum (corresponding to A) of 60 seconds of raw data before and after carbenoxolone (200 µM) application. C) Normalised pooled data, carbenoxolone significantly ($P < 0.01$, n=8) reduced gamma peak power.

3.2.4 $GABA_A$ receptor modulation of gamma oscillations

An intact inhibitory network is crucial for gamma induction and maintenance in other brain areas therefore the role of GABA receptors in PC oscillations was explored (Whittington et al., 1995; Fisahn et al., 1998). Picrotoxin (50 μM) is a 1:1 mix of picrotoxinin and picrotin which non-competitively blocks the $GABA_A$ receptor Cl^- channel preventing GABA triggered Cl^- entry into neuron. Picrotoxin significantly ($P < 0.01$, n=8) reduced the gamma peak power by 79 ± 3.9 % (figure 3.5). Gabazine competitively displaces GABA binding to the $GABA_A$ receptor, at low concentration it blocks synaptic (phasic) currents, whilst at higher concentration it also blocks extrasynaptic (tonic) currents (Stell and Mody, 2002). The effect of two doses of gabazine on gamma activity in the PC was explored. At 250 nM, gabazine significantly ($P < 0.05$, n=8) reduced peak gamma power by -67.1 ± 4.0 %, suggesting that the activity was exquisitely sensitive to $GABA_A$ receptor activity. At the higher concentration of 2 μM, gabazine significantly ($P < 0.05$, n=8) reduced gamma peak power by -86.5 ± 2.8 % (figure 3.5) which was significantly ($P < 0.05$, n=8) different to the 250 nM application.

Pentobarbital is a short acting barbiturate that acts as an allosteric modulator of the $GABA_A$ receptor. Pentobarbital binds to the β subunit of the $GABA_A$ receptor and enhances the effect of GABA binding by increasing the duration of Cl^- channel opening (Segal and Barker, 1984; Whittington et al., 2000). Pentobarbital (10 μM) had no significant effect on gamma peak power, but it significantly ($P < 0.01$) reduced the frequency by 5.96 ± 1.2 Hz (figure 3.6).

The main $GABA_A$ receptor subtypes in the CNS often contain a combination of subunits that confer sensitivity to benzodiazepines. Zolpidem is a positive allosteric modulator at the benzodiazepine site which lies at the junction between the α_1 and γ subunits of the $GABA_A$ receptor (figure 1.2). Zolpidem had different effects on the gamma oscillations depending on concentration used. Application of low dose (10 nM) zolpidem and subsequent 30 - 500 nM application had no effect on gamma oscillations (figure 3.7). Using a high starting dose of zolpidem (100 nM), followed by 500 nM application significantly ($P < 0.01$, n=8) increased gamma peak power by 73.2 ± 12.5 % and 125.6 ± 28.9 % respectively (figure 3.7).

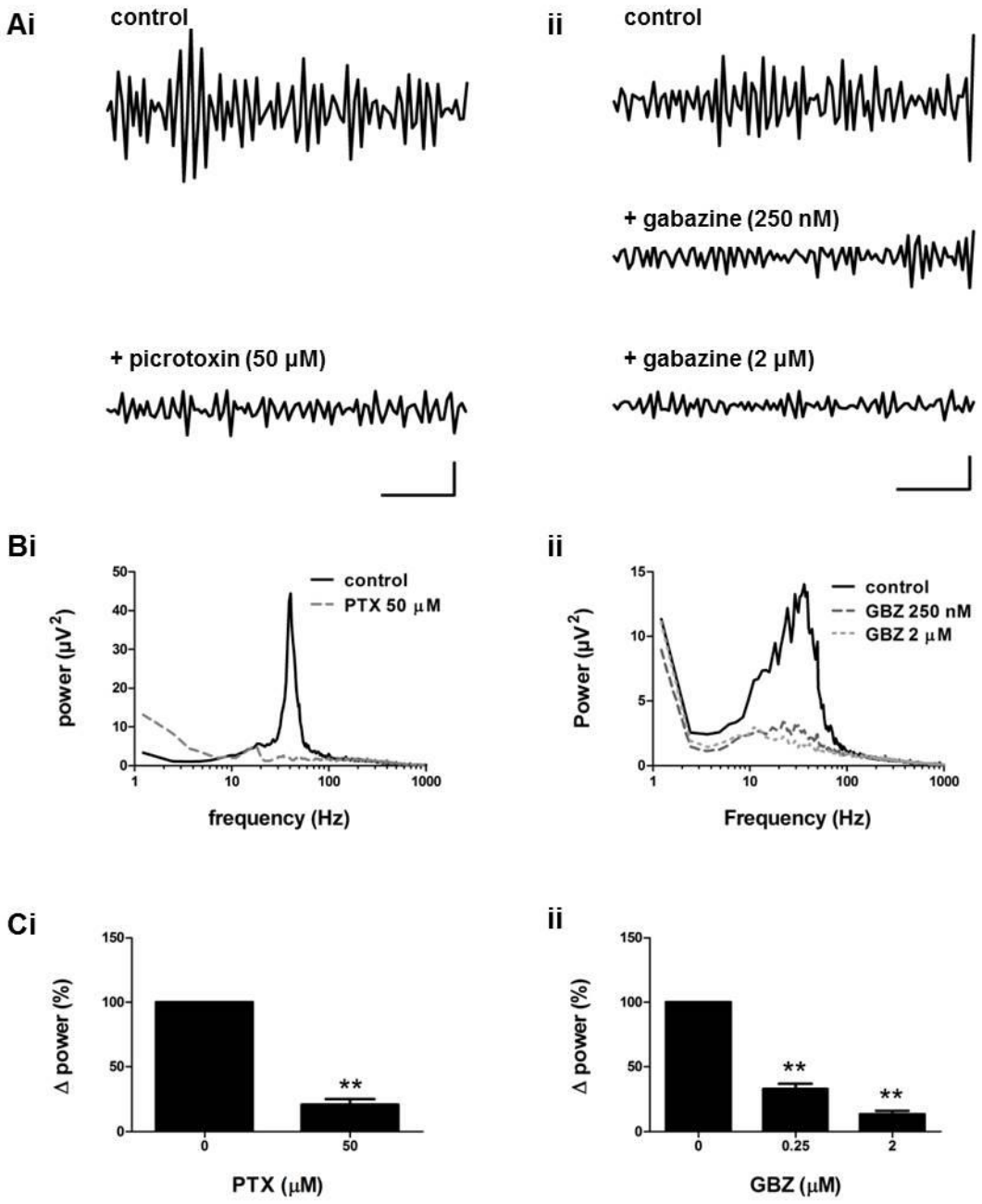

Figure 3.5 PC layer II gamma oscillations require synaptic and extrasynaptic $GABA_A$ receptor function. Ai) Raw trace of a representative extracellular recording taken in layer II of the PC before (top) and after (bottom) picrotoxin (50 µM) application (Scale – 20 µV Vs 200ms) Bi) Power spectrum (corresponding to Ai) of 60 seconds of raw data before and after picrotoxin (50 µM) application. Ci) Normalised, pooled data, picrotoxin (50 µM) significantly ($P < 0.01$, n=8) reduced gamma peak power. Aii) Raw trace of a representative extracellular recording taken in layer II of the PC before (top) gabazine at 250 nM (middle) and 2 µM (bottom). Bii) Power spectrum (corresponding to Aii) of 60 seconds of raw data before and after 250 nM and 2 µM application of gabazine. Cii) Normalised, pooled data, gabazine (0.25 and 2 nM) significantly ($P < 0.05$, n=8) reduced gamma peak power when compared to control, the two doses were also significantly different ($P < 0.05$, n=8) from each other.

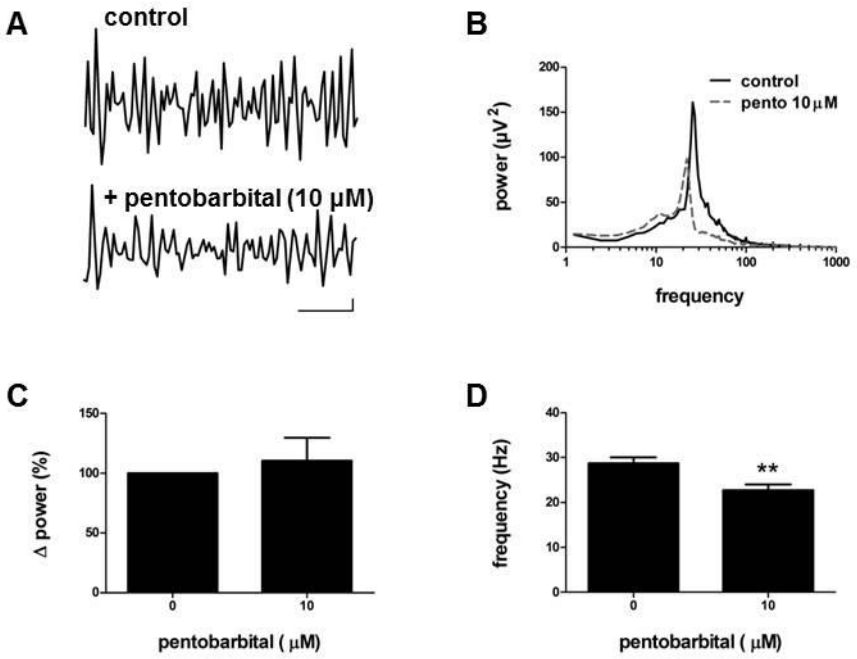

Figure 3.6 Modulation of PC layer II gamma oscillations by pentobarbital

A) Raw trace of a representative extracellular recording taken in layer II of the PC before (top) and after (bottom) pentobarbital (10 µM) application (Scale – 20 µV Vs 200ms). B) Power spectrum (corresponding to A) of 60 seconds of raw data before and after pentobarbital (10 µM) application. C) Normalised, pooled data, pentobarbital had no effect on the power of gamma peak ($P > 0.05$, n=8). D) Normalised, pooled data, pentobarbital significantly ($P < 0.01$, n=8) reduced gamma frequency.

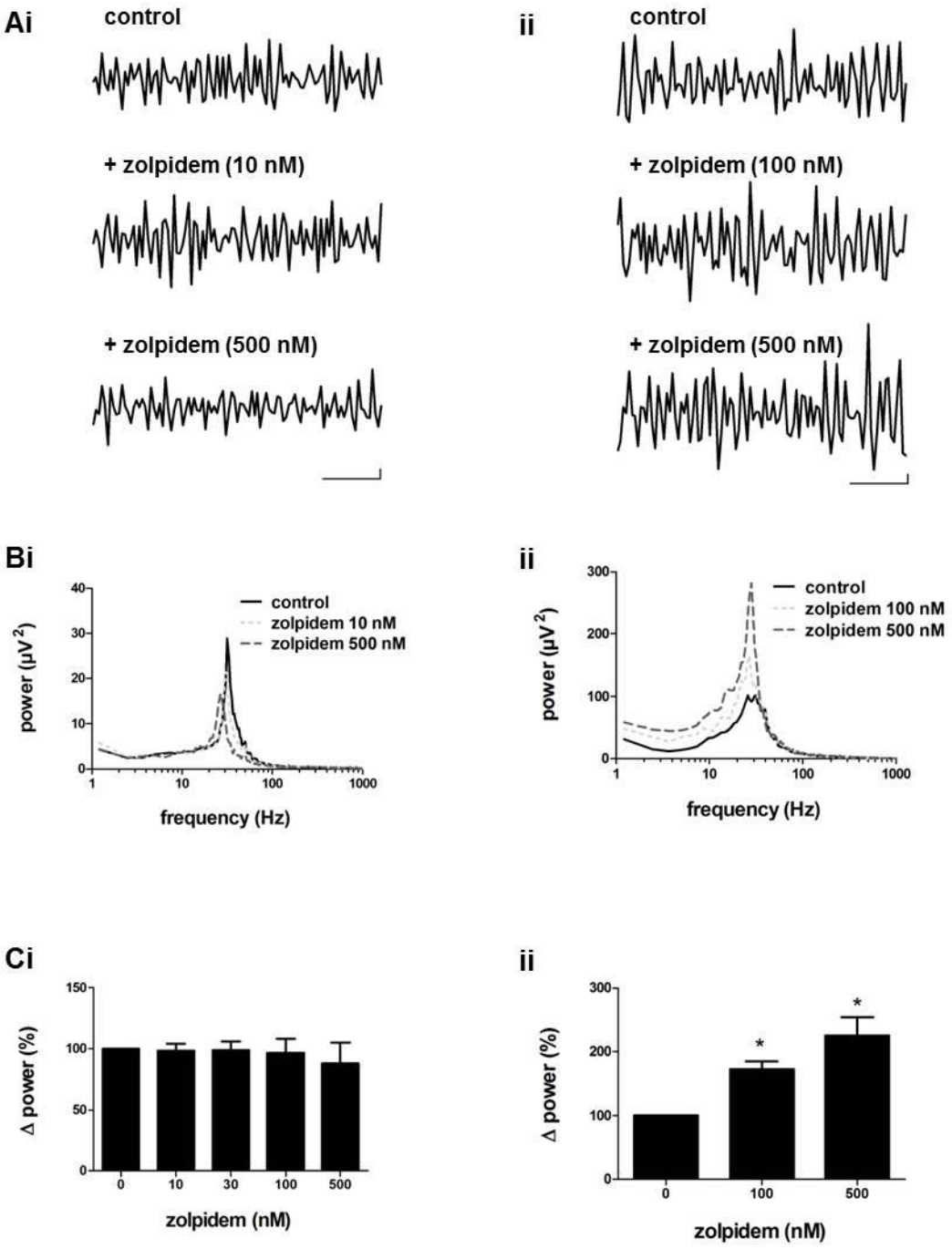

Figure 3.7 Concentration dependent modulation of PC layer II gamma oscillations by zolpidem.
Ai) Raw trace of a representative extracellular recording taken in layer II of the PC before (top) and after 10 nM (middle) and 500 nM (bottom) application of zolpidem (Scale – 20 μV Vs 200ms). Bi) Power spectrum (corresponding to Ai) of 60 seconds of raw data before and after 10 nM and 500 nM application of zolpidem. Ci) Normalised, pooled data, when a low dose was first applied zolpidem had no significant effect on gamma peak up to 500 nM ($P > 0.05$, n=13). Aii) Raw trace of representative extracellular recording taken in layer II of the PC before (top) and after 100 nM (middle) then 500 nM (bottom). Bii) Power spectrum (corresponding to Ai) of 60 seconds of raw data showing before and after 100 nM and 500 nM application of zolpidem. Cii) Normalised, pooled data, starting at a high dose zolpidem (100 nM and 500 nM) significantly enhanced ($P < 0.05$, n=8) gamma peak.

3.2.5 $GABA_B$ receptor modulation of gamma oscillations

$GABA_B$ receptors are G protein coupled receptors (GPCR) in which GABA binding initiates a secondary messenger cascade that opens K^+ channels and inhibits adenylate cyclase and presynaptic calcium release. $GABA_B$ receptors are thought to be involved in oscillatory activity in other brain regions, such as beta oscillations in the primary motor cortex (Yamawaki et al., 2008). However, application of the competitive $GABA_B$ receptor antagonist, CGP 55845 (5 µM) had no effect on PC layer II gamma oscillations (figure 3.8).

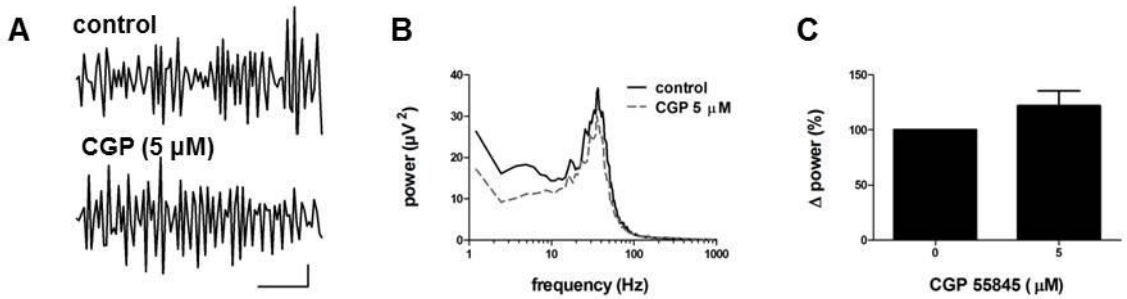

Figure 3.8 $GABA_B$ receptors do not contribute to PC layer II gamma oscillations
A) Raw trace of a representative extracellular recording taken in layer II of the PC before (top) and after (bottom) CGP 55845 (5 µM) application (Scale – 20 µV Vs 200ms). B) Power spectrum (corresponding to A) of 60 seconds of raw data before and after CGP 55845 (5 µM) application. C) Normalised, pooled data, CGP 55845 had no effect on the power of gamma peak power (n=9).

3.2.6 Ionotropic glutamate receptor modulation of gamma oscillations

Glutamate transmission is not always directly involved in gamma oscillation generation; it varies between brain regions and method of gamma induction (Bartos et al., 2007; Buzsaki and Wang, 2012). The sensitivity of PC gamma oscillations to glutamate receptor blockade was tested. The AMPA and kainate receptor antagonists NBQX and CNQX both reduced the gamma power (figure 3.9). CNQX, a competitive AMPA and kainate receptor antagonist significantly ($P < 0.01$, n=8) reduced gamma peak power by 89.8 ± 2.3 % (figure 3.9). NBQX, a competitive inhibitor of AMPA receptors at low dose (2.5 μM) and AMPA/kainate receptors at high dose (25 μM) significantly ($P < 0.05$, n=8) reduced gamma peak power by 54.9 ± 6.7 % and 90.5 ± 2.7 % respectively (figure 3.9). The changes affected by these doses were also significantly different to each other ($P < 0.05$, n=8).

To confirm the role of AMPA receptors, SYM 2206, a selective and potent non-competitive AMPA receptor antagonist was applied to gamma oscillations. SYM 2206 (20 μM) significantly ($P < 0.01$, n=8) reduced gamma peak power by 86.3 ± 3.9 % (figure 3.10).

Kainate receptor subtypes were investigated using kainate receptor antagonists UBP 304 and UBP 310. UBP 304 (1 μM), a $GluK_1$ receptor antagonist had no effect on gamma peak power ($P > 0.05$, n=8), at 10 μM it significantly ($P < 0.05$) reduced gamma peak power by 31.2 ± 4.4 % (figure 3.11) compared to control. UBP 310 (3 μM), a $GluK_{1/3}$ antagonist significantly ($P < 0.01$) reduced gamma peak power by 26.0 ± 5.4 % (figure 3.11).

NMDA receptors do not contribute to layer II PC gamma oscillations. The competitive NMDA receptor antagonist DL-AP5 (50 μM) and non-competitive antagonist MK-801 (20 μM) had no significant effect on gamma oscillations ($P > 0.05$) (figure 3.12).

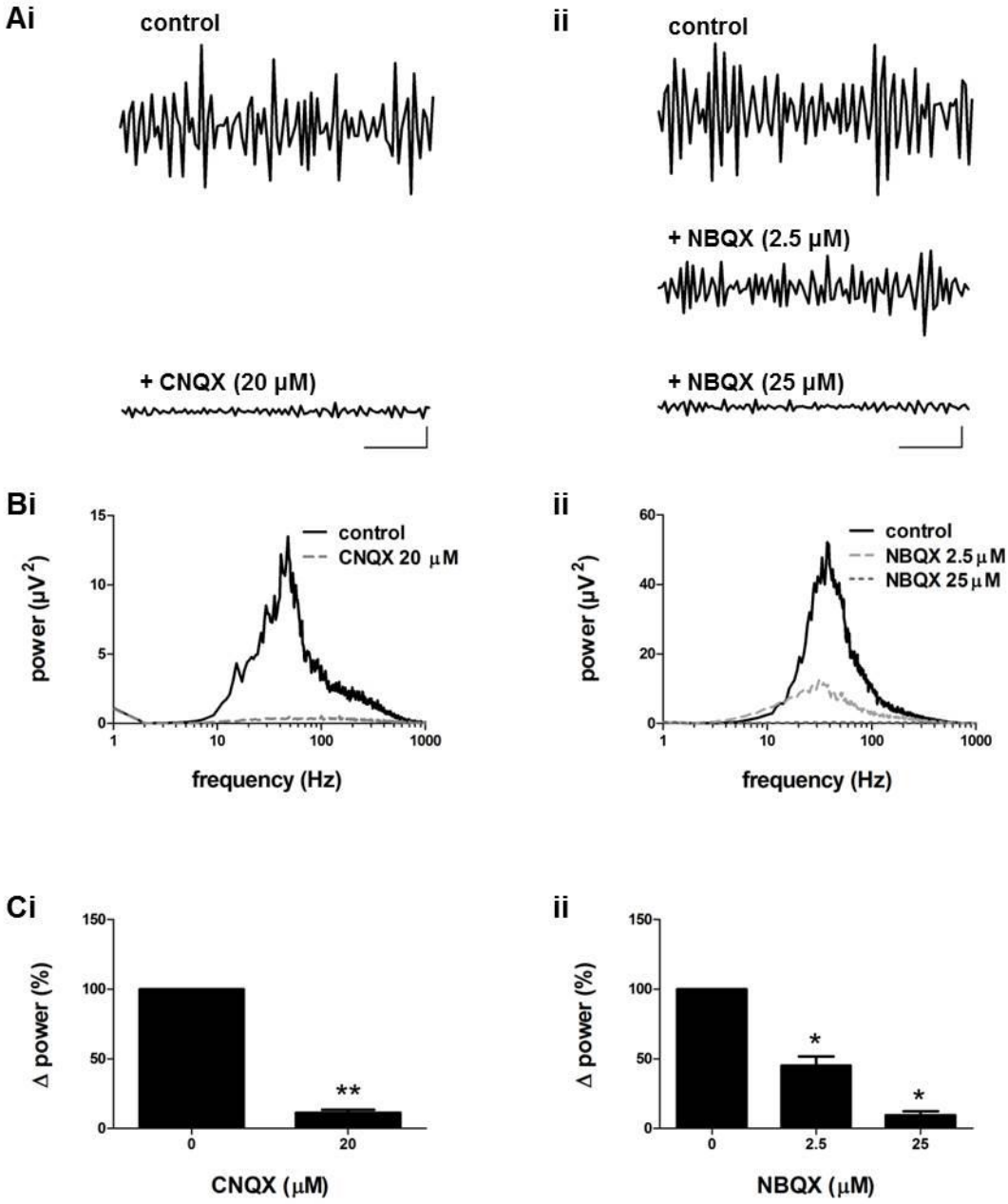

Figure 3.9 PC layer II gamma oscillations require glutamate transmission.
Ai) Raw trace of a representative extracellular recording taken in layer II of the PC before (top) and after (bottom) CNQX (20 µM) application (Scale – 20 µV Vs 200ms). Bi) Power spectrum (corresponding to Ai) of 60 seconds of raw data before and after CNQX (20 µM) application. Ci) Normalised, pooled data, CNQX (20 µM) significantly ($P < 0.01$ n=8) reduced gamma peak power. Aii) Raw trace of a representative extracellular recording taken in layer II of the PC before (top) and after 2.5 µM NBQX (middle) and 25 µM NBQX application (Scale – 20 µV Vs 200ms). Bii) Power spectrum (corresponding to Bi) of 60 seconds of raw data before and after NBQX (2.5 and 20 µM) application. Cii) Normalised, pooled data, NBQX (2.5 and 25 µM) significantly ($P < 0.05$, n=8) reduced gamma peak power when compared to control, the two doses were also significantly different ($P < 0.05$, n=8) from each other.

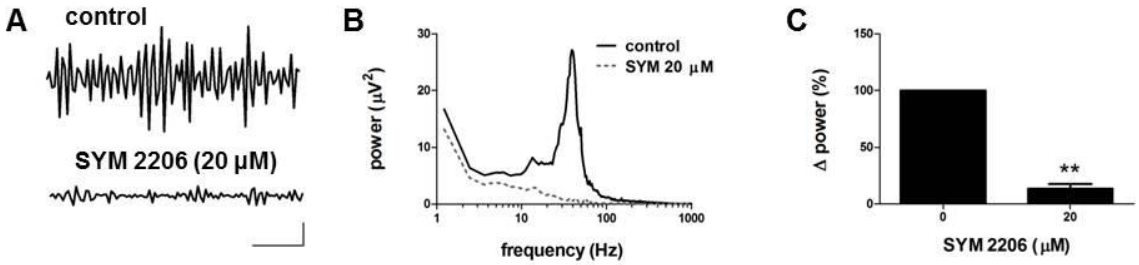

Figure 3.10 PC layer II gamma oscillations require AMPA receptors
A) Raw trace of a representative extracellular recording taken in layer II of the PC before (top) and after (bottom) SYM 2206 (20 µM) application (Scale – 20 µV Vs 200ms). B) Power spectrum (corresponding to A) of 60 seconds of raw data before and after SYM 2206 (20 µM) application. C) Normalised, pooled data SYM 2206 (20 µM) significantly ($P < 0.01$, n=8) reduced gamma peak power by -86.3 ± 3.9 % (n=8).

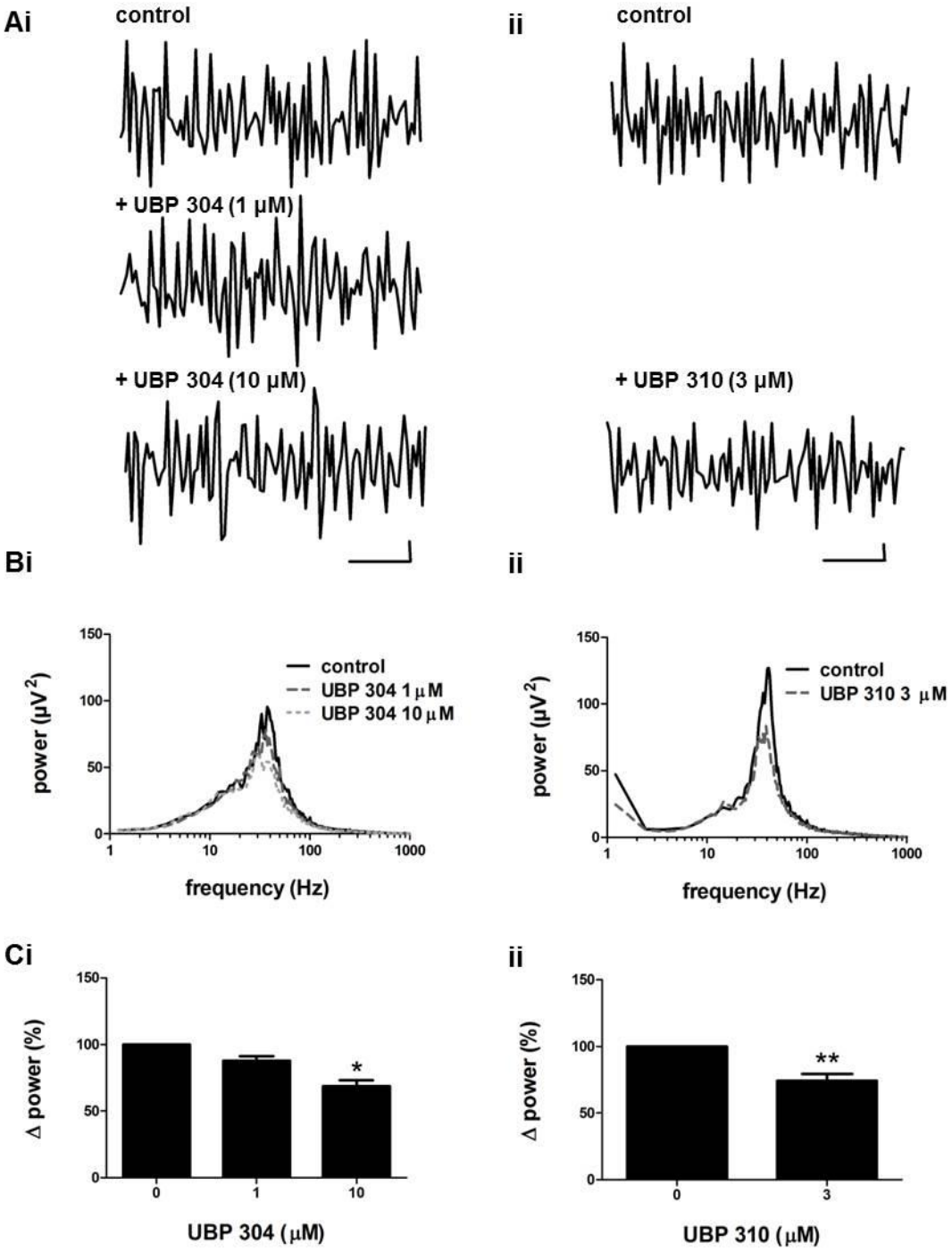

Figure 3.11 Kainate receptor modulation of PC layer II gamma oscillations.
Ai) Raw trace of a representative extracellular recording taken in layer II of the PC before (top) and after (bottom) UBP304 (1 µM and 10 µM) application (Scale – 20 µV Vs 200ms). Bi) Power spectrum (corresponding to Ai) of 60 seconds of raw data before and after UBP304 (1 µM and 10 µM) application. Ci) Normalised, pooled data, UBP304 (1 µM) did not significantly reduced gamma peak, UBP304 (10 µM) did significantly reduce gamma peak ($P < 0.05$, n=8) when compared to the control. Aii) Raw trace of a representative extracellular recording taken in layer II of the PC before (top) and after (bottom) UBP304 (3 µM) application (Scale – 20 µV Vs 200ms). Bii) Power spectrum (corresponding to Aii) of 60 seconds of raw data before and after UBP304 (3 µM) application. Ci) Normalised, pooled data, UBP304 (3 µM) significantly ($P < 0.01$, n=9) reduced gamma peak power.

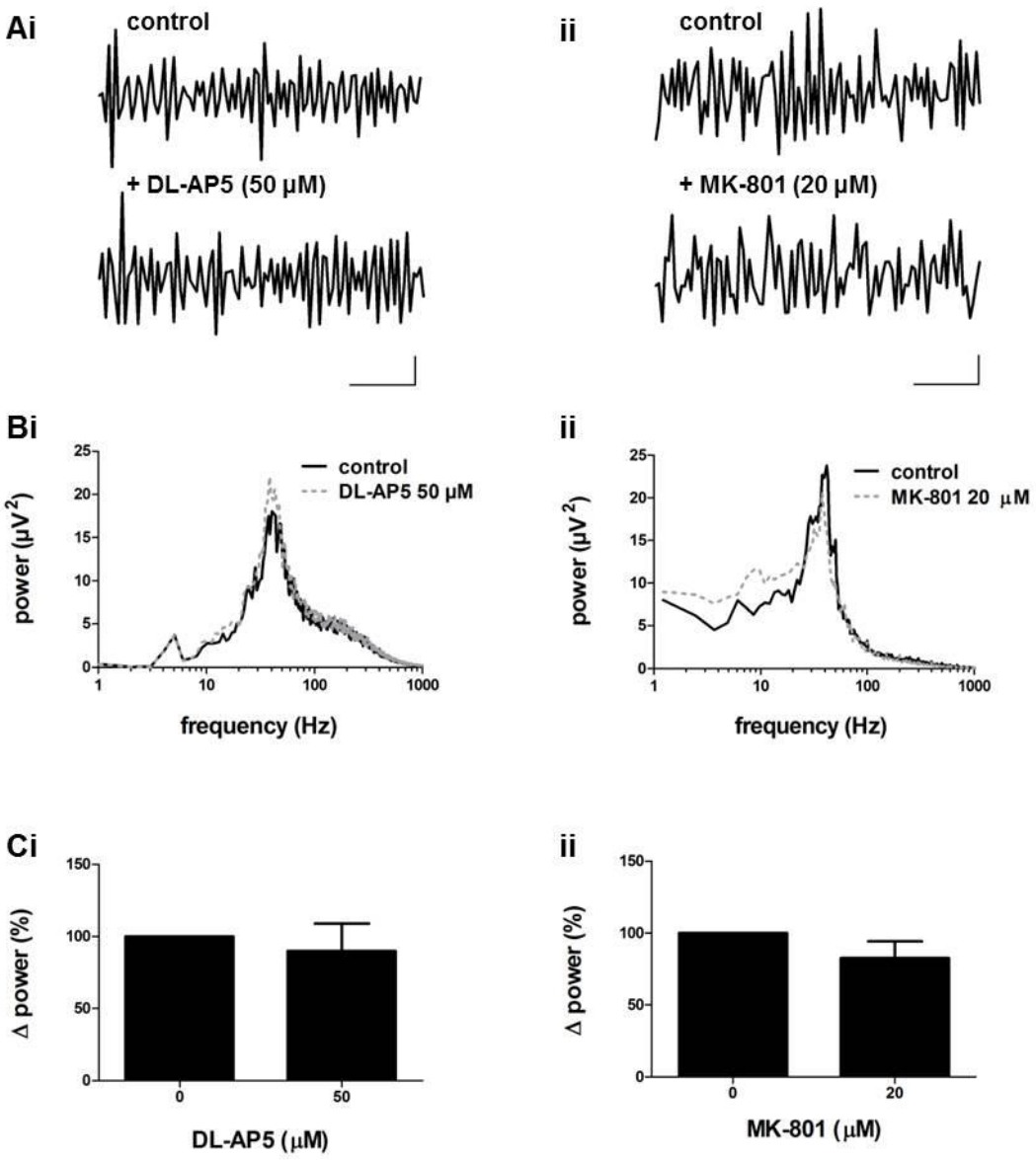

Figure 3.12 NMDA receptors do not contribute to PC layer II gamma oscillations.
Ai) Raw trace of a representative extracellular recording taken in layer II of the PC before (top) and after (bottom) DL-AP5 (50 µM) application (Scale – 20 µV Vs 200ms). Bi) Power spectrum (corresponding to Ai) of 60 seconds of raw data before and after DL-AP5 (50 µM) application. Ci) Normalised, pooled data, DL-AP5 had no effect on the gamma peak power ($P > 0.05$, n=8). Aii) Raw trace of a representative extracellular recording taken in layer II of the PC before (top) and after (bottom) MK-801 (20 µM) application (Scale – 20 µV Vs 200ms). Bii) Power spectrum (corresponding to Aii) of 60 seconds of raw data before and after MK-801 (20 µM) application. Cii) MK-801 (20 µM) (corresponding to Bii) had no effect on the gamma peak power ($P > 0.05$, n=8).

3.2.7 Metabotropic glutamate receptor modulation of gamma oscillations

The contribution of mGluRs to gamma oscillations was investigated using mGluR group I antagonists CPCCOEt, ($mGluR_1$) and MPEP ($mGluR_5$) and mGluR group II ($mGluR_{2/3}$) antagonist LY 341495. Application of MPEP (20 μM) had no effect ($P > 0.05$, n=8) on gamma oscillations (figure 3.13). CPCCOEt (20 μM) significantly ($P < 0.05$, n=8) increased gamma peak power by 13.3 ± 5.9 % indicating $mGluR_1$ would normally negatively modulate network synchronisation (figure 3.13). LY 341495 had no significant effect on gamma oscillations at low (100 nM) or high dose (5 μM) ($P > 0.05$, n=8) (figure 3.14).

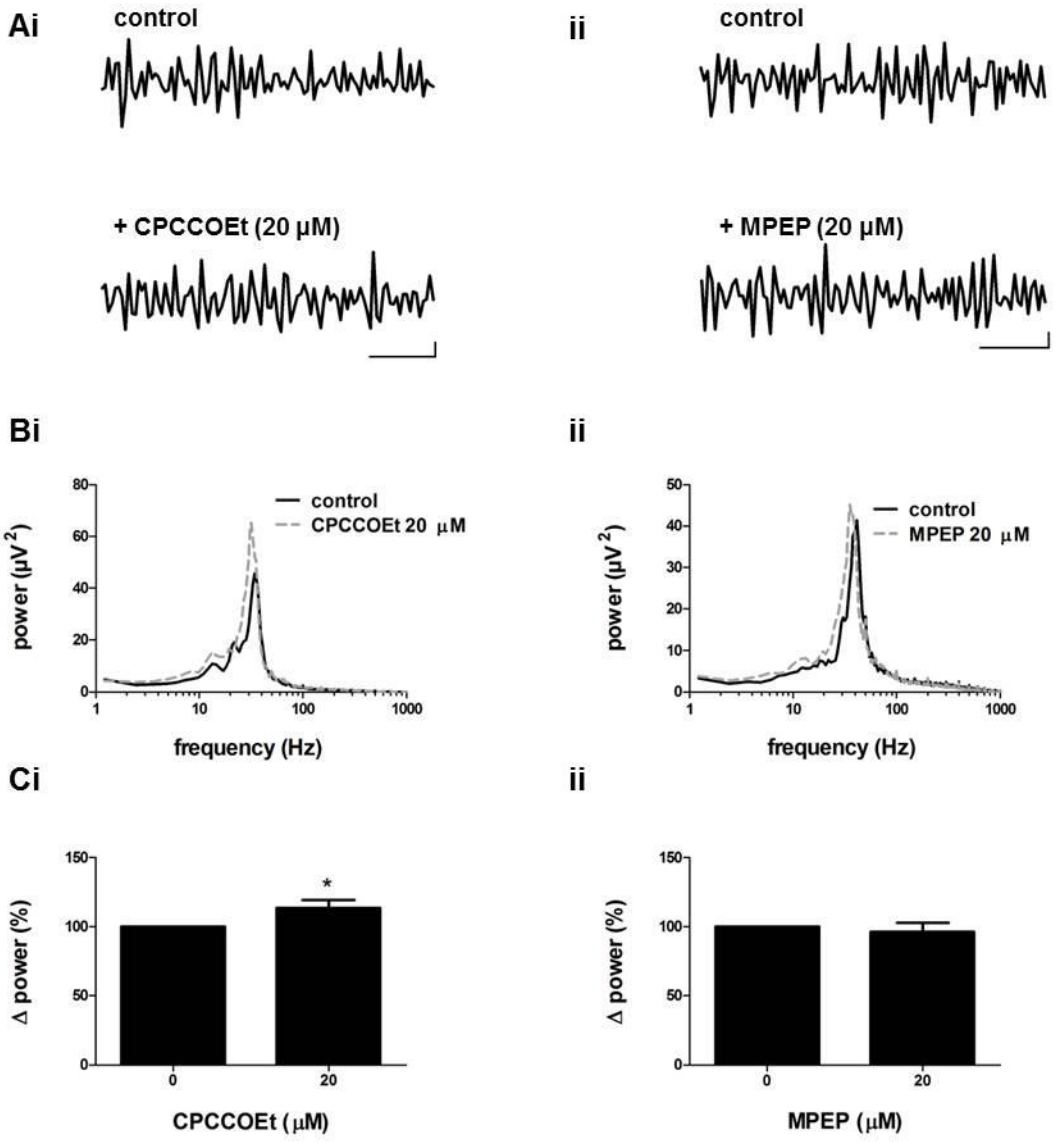

Figure 3.13 Modulation of PC layer II gamma oscillations by group I metabotropic glutamate receptor antagonists.

Ai) Raw trace of a representative extracellular recording taken in layer II of the PC before (top) and after (bottom) CPCCOEt (20 µM) application (Scale – 20 µV Vs 200ms). Bi) Power spectrum (corresponding to Ai) of 60 seconds of raw data before and after CPCCOEt (20 µM) application. Ci) Normalised, pooled data, CPCCOEt (20 µM) significantly ($P < 0.05$, n=8) increased gamma peak power by 13.3 ± 5.9 %. Aii) Raw trace of a representative extracellular recording taken in layer II of the PC before (top) and after (bottom) MPEP (20 µM) application (Scale – 20 µV Vs 200ms). Bi) Power spectrum (corresponding to Aii) of 60 seconds of raw data before and after MPEP (20 µM) application. Cii) Normalised, pooled data, MPEP (20 µM) had no significant effect on gamma peak power ($P > 0.05$, n=9).

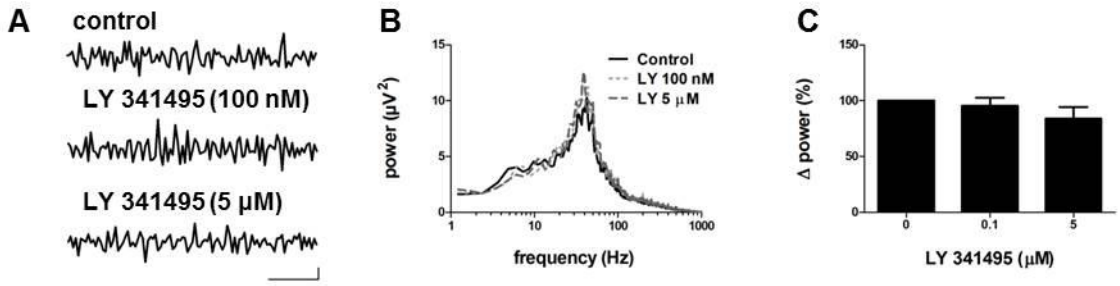

Figure 3.14 Group II metabotropic glutamate receptors do not contribute to PC layer II gamma oscillations.

A) Raw trace of a representative extracellular recording taken in layer II of the PC before (top) and after LY341495 application at 1 nM (middle) and 5 µM (bottom). (Scale – 20 µV Vs 200ms). B) Power spectrum (corresponding to A) of 60 seconds of raw data before and after LY341495 (100 nM and 10 µM) application. C) Normalised, pooled data, LY341495 had no effect on the gamma peak power ($p > 0.05$, n=8).

3.2.8 Summary of results

Table 3.1 summarises the effect of all pharmacological agents on the peak power of the PC gamma oscillations.

drug	n	Δ power (%)	frequency (Hz)
atropine (5 μM)	8	-93.2 ± 1.1 **	-5.79 ± 3.0 ns
pirenzepine (10μM)	8	-81.6 ± 7.44 **	-12.05 ± 3.4 *
carbenoxolone (200 μM)	8	-90.8 ± 2.7 **	-1.42 ± 2.8 ns
picrotoxin (50 μM)	8	-79 ± 2.7 *	-11.36 ± 5.2 ns
gabazine (250 nM / 2 μM)	8	-67.1 ± 4.0 * / -86.5 ± 7.8 *	-6.26 ± 2.3 ns / -9.16 ± 2.8 ns
zolpidem (100 nM / 500 nM)	8	+73.2 ± 12.5 * / +125 ± 28.9 *	-2.90 ± 0.9 ns / - 3.21 ± 1.0 ns
pentobarbital (10 μM)	8	+10.4 ±19.4 ns	-5.96 ± 1.2 **
CGP 55845 (5 μM)	9	+22 ± 13.2 ns	-1.77 ± 2.6 ns
CNQX (20 μM)	8	-89.8 ± 2.3 **	-2.08 ± 2.7 ns
NBQX (2.5 / 25 μM)	8	-54± 6.7 * / -90 ± 2.7 *	-6.86 ± 1.3 ns / -8.11 ± 1.7 *
SYM 2206 (20 μM)	8	-86.3 ± 3.9 **	-9.92 ± 0.7 **
UBP 310 (3 μM)	9	-26.0 ± 5.4 **	-1.22 ± 2.5 ns
UBP 304 (1 / 10 μM)	8	-12.5 ± 3.3 * / -31.2 ± 4.4 **	-0.0 ± 1.3 ns
DL-AP5 (50 μM)	8	-10.2 ± 19.2 ns	-1.02 ± 1.4 ns
MK-801 (20 μM)	8	-17.2 ± 11.7 ns	-2.74 ± 1.9 ns
LY 341495 (100 nM / 5 μM)	8	-6.6 ± 7.2 ns / -16 ± 10.2 ns	-1.53 ± 1.8 ns / -0.61 ± 1.7 ns
CPCCOEt (20 μM)	8	+13.3 ± 5.9 *	0.00 ± 1.6 ns
MPEP (20 μM)	9	-3.75 ± 6.7 ns	-5.61 ± 2.2 *

Table 3.1 Pharmacology of layer II gamma oscillations in the PC *in vitro*.
Change in gamma power and frequency after drug application is presented as normalised mean ± SEM, the change is indicated by – sign indicating a reduction in peak power or a + sign indicating an increase in peak power. The number of slices used is quoted as n values with a minimum of 3 animals used per drug. *P≤0.05, **P≤0.01.

3.3 Discussion

Neuronal network oscillations at gamma frequency have previously been demonstrated in the PC *in vivo*, but to our knowledge this is the first time persistent gamma has been described *in vitro* (Adrian, 1942, 1950). Application of both kainic acid and carbachol were required to initiate oscillatory activity, which was greatest in power in layer II. Sensitivity to $GABA_A$, AMPA, kainate and mACh (M1) receptor antagonists and gap junction blockade implies these oscillations require an intact inhibitory and excitatory network with both synaptic and non-synaptic connections.

3.3.1 Kainic acid and carbachol were required to induce gamma oscillations in layer II of the PC

Initial experiments were conducted to assess if any spontaneous rhythmic activity was present in the PC. The PC is structurally similar to the CA3 region of the hippocampus which has been previously found to generate robust, persistent gamma oscillations without pharmacological intervention (Lu et al., 2011; Modebadze, 2014). Despite the similarity in structure, spontaneous rhythmic activity was not found in the PC.

Application of kainic acid alone has been reported to reliably induce persistent gamma oscillations in limbic regions including CA3 and the entorhinal cortex (Fisahn et al., 1998; Cunningham et al., 2003). Nanomolar concentrations of the kainate receptor agonist kainic acid induced oscillations in the PC, however this was only possible in the presence of the mAChR agonist carbachol (figure 3.2). To demonstrate that kainate receptor activation is necessary for oscillation generation, as kainic acid is also known to activate AMPA receptors, application of a kainate receptor specific antagonist would be required (Huettner, 2003). However, at present, there are no kainate receptor antagonists that target all subunits, although a subunit selective pharmacological agent is available for $GluK_1$ (UBP 304). Other antagonists target mixed receptor subunits including $GluK_1$ and $GluK_3$ (UBP 310), $GluK_1$ and $GluK_{1/5}$ (ACET) and $GluK_1$, $GluK_{1/2}$ and $GluK_{1/5}$ (UBP 296 and LY382884).

All five kainate receptor subunits are expressed in the PC, although $GluK_3$ and $GluK_4$ are expressed at very low levels (Wisden and Seeburg, 1993). $GluK_{1/3}$ blockade with UBP 310 and $GluK_1$ blockade with UBP 304 reduced gamma peak power but did not abolish it, implying that $GluK_2$ or $GluK_5$ subunits may be more critical for gamma maintenance (figure 3.11). In CA3, kainic acid application has been found to induce oscillations by increasing interneuron axon excitability and reducing the threshold for antidromic spread of excitability to the soma (Semyanov and Kullmann, 2001; Fisahn et al., 2004). This depolarisation of the interneuron axon membrane potential has been found to increase action potential firing and sIPSC amplitude and frequency (Semyanov and Kullmann, 2001; Fisahn et al., 2004). Genetic KO of the $GluK_2$ receptor has been found to prevent kainate receptor induced gamma oscillations implying kainic acid exerts its effects specifically via the $GluK_2$ subunit (Fisahn et al., 2004). As $GluK_2$ subunit specific pharmacological agents are not currently

available, based on the current data we can only predict that kainic acid is inducing oscillations via a similar mechanism to the one described above.

In the PC, co-application of kainic acid and carbachol were necessary to provide sufficient excitation for gamma initiation (figure 3.2). Carbachol was found to be necessary for both induction and maintenance of these oscillations as application of atropine abolished gamma oscillations. Both carbachol and atropine are non-selective and act on all five subtypes of the mAChRs (M1-5). In CA3 and CA1, pirenzepine, an M1 mAChR specific antagonist has been found to abolish carbachol and muscimol induced gamma oscillations (Fisahn et al., 1998; Fisahn et al., 2002). This was also found in the PC as application of the M1 selective antagonist pirenzepine, also abolished the PC oscillations indicating these oscillations may have a similar mechanism of action (figure 3.3). Activation of M1 receptors in CA3 have been found to tonically activate pyramidal cells by enhancing the I_h and I_{cat} currents and increase action potential firing. M1 receptors in CA3 are preferentially expressed on pyramidal cells, thus interneurons are only activated indirectly via pyramidal cell driven EPSCs which also accounts for the sensitivity of carbachol induced oscillations to AMPA receptor blockade (Levey et al., 1995; Fisahn et al., 2002). In the PC, application of cholinergic agonists have been found to depolarise the membrane potential and increase action potential firing in layer II and III pyramidal cells (Tseng and Haberly, 1989a; Constanti et al., 1993; Barkai and Hasselmo, 1994; Libri et al., 1994). M1 receptors are found in the PC, however data describing which cells express which specific receptors has not been explored (Buckley et al., 1988).

Experiments were also conducted to assess which layer was most appropriate for oscillation recording. The long term objective of this project was to investigate the PC and its relationship with epilepsy, therefore the seizure prone layer III (‘area tempestas’) would have been the ideal area to explore (discussed further section 3.3.6). However, electrodes inserted into this layer failed to record oscillatory activity. Instead, layer II, the area dominated by pyramidal cell bodies was found to generate oscillations of the highest power and therefore experiments were conducted in this layer. It is also worth noting however, that the location of the recording electrodes was not confirmed histologically and therefore we can only approximate their location.

The oscillations in the PC were observed to take a similar period of time to stabilise as the hippocampus, but longer compared to the entorhinal or motor cortex (Modebadze, 2014; Johnson, 2016; Shah, 2017). Long lasting enhancement of synaptic potentials, termed LTP in the PC is thought to play a role in learning and memory of odour information and discrimination (Staubli et al., 1989). This NMDA-receptor dependent process has been found to be facilitated in the presence of carbachol (Barkai and Hasselmo, 1994). This may explain

why PC gamma oscillations, much like gamma in the hippocampus, an area also thought to be susceptible to LTP induction, took longer to stabilise (Bliss and Collingridge, 1993).

3.3.2 Dependence on gap junctions

Electrical synapses between cells (or gap junctions) are thought to play an important role in gamma oscillation generation (Hormuzdi et al., 2001; Bennett and Zukin, 2004; Kopell and Ermentrout, 2004). Transmission of both action potentials and subthreshold events via gap junctions are important for enhancing neuronal network synchronisation (power) and recruiting cells to the network. Pharmacological blockade of gap junctions with octanol or carbenoxolone in other brain regions has been shown to reduce or abolish gamma oscillations (Traub and Bibbig, 2000; Cunningham et al., 2003; Modebadze, 2014). In the PC, application of the gap junction blocker carbenoxolone abolished rhythmic activity when applied for two hours as is standard for this drug (figure 3.4) (Konopacki et al., 2004). Carbenoxolone was chosen due to its potency and water solubility at the high concentrations required to block gap junctions. Carbenoxolone or octanol have been previously used in numerous investigations into gap junction involvement in neuronal network oscillations (Traub et al., 2001a; Cunningham et al., 2003; Pais et al., 2003; Traub et al., 2003; Yamawaki et al., 2008). However, caution is required when interpreting our results as carbenoxolone acts on a number of other targets including $GABA_A$ receptor currents, input resistance and Ca^{2+} channels, for review see (Connors, 2012).

Pharmacological differentiation between gap junction proteins to differentiate between interneuron, pyramidal cell or glial gap junctions is not currently possible, therefore researchers have used mathematical models and KO mouse experiments to investigate which gap junctions are involved in gamma oscillation generation. Mathematical modelling identified axo-axonal coupling (pyramidal-pyramidal) not dendritic coupling (interneuron-interneuron) to be critical for gamma oscillation generation (Traub and Bibbig, 2000; Traub et al., 2003). This was further confirmed experimentally using a connexion-36 KO (Cx36) mouse. Cx36 KO mice were found to have almost no coupling between interneurons and yet carbenoxolone sensitive oscillations could still be induced in CA3 via carbachol application, although at a much lower power than wild type control (Deans et al., 2001; Hormuzdi et al., 2001; Buhl et al., 2003; Pais et al., 2003; Traub et al., 2003). It was also observed that low Ca^{2+} induced high frequency oscillations were also still present, and as these had been previously demonstrated to depend on gap junctions between pyramidal neurons it implied pyramidal cell gap junctions were still present (Deans et al., 2001; Hormuzdi et al., 2001; Buhl et al., 2003; Pais et al., 2003; Traub et al., 2003). Taken together, the above evidence indicated that interneuron dendritic gap junctions modulate the strength of the oscillation whilst pyramidal cell axo-axonal gap junctions were critical for oscillation generation in CA3 (see section 3.3.5 for further detail) (Traub et al., 2000; Traub et al., 2003; Kopell and Ermentrout, 2004). Further experimental work, utilising the Cx36 KO mouse, would be

required to investigate which of the gap junctions are responsible for oscillation generation in the PC.

3.3.3 Reliance on an intact GABA network

Mutually connected inhibitory interneuron networks can be driven to generate rhythmic activity if an appropriate excitatory drive is provided. Interneurons fire in phase with gamma oscillations with the frequency of both dependent on the IPSC kinetics (Bartos et al., 2007). $GABA_A$ receptors are GABA sensitive channels which, once activated, hyperpolarise neurons via Cl^- entry through the receptor ionophore. $GABA_A$ receptor channel blockade supressed PC gamma oscillations confirming the importance of inhibition in PC oscillation generation (figure 3.5) (Krishek et al., 1996). Low dose gabazine reduced gamma peak power by 67.1%, high dose gabazine reduced this by a further 19.4% implying both synaptic and extrasynaptic $GABA_A$ receptors contribute. Phasic (synaptic) and tonic (extrasynaptic) receptors have a similar affinity for gabazine, however, tonic receptors have a much higher affinity for GABA. Therefore higher concentrations of the competitive antagonist gabazine is required to out-compete GABA at tonic receptors (Stell and Mody, 2002). If phasic inhibition was pacing the network, pharmacological manipulation of $GABA_A$ receptor kinetics would be expected to alter the frequency whereas if tonic inhibition was contributing to the oscillations, altering the IPSC kinetics would be expected to change the gamma power (Segal and Barker, 1984; Whittington et al., 2000; Traub and Whittington, 2010). Pentobarbital was used to assess if phasic inhibition was pacing the network as it alters the $GABA_A$ receptor kinetics by increasing the amount of time the $GABA_A$ receptor is open (Segal and Barker, 1984). Pentobarbital significantly reduced the frequency of the PC gamma oscillations and had no significant impact on the power (figure 3.6) indicating that IPSC kinetics are responsible for the setting the frequency of the network.

Zolpidem, a benzodiazepine-like positive modulator of $GABA_A$ receptors, differentially affected gamma oscillations in the PC depending on dose (figure 3.7). A low starting dose of zolpidem (10 nM) had no effect on gamma oscillation peak power and nor did further application of higher doses subsequent to low dose zolpidem (30 - 500 nM). In contrast, a higher starting dose of 100 nM significantly enhanced gamma peak power at both 100 nM and 500 nM. This effect has been previously demonstrated in our research group in primary motor cortex beta oscillations (Prokic et al., 2015). Application of low-dose zolpidem (10 nM) reduced the power of the beta oscillations and prevented augmentation of power at subsequently applied higher doses, whereas initial application of higher doses enhanced the oscillatory power. Patch clamp recordings of interneurons found tonic inhibition was enhanced in the presence of 10 nM zolpidem, whereas high doses reduced this current. Mathematical modelling found 10 nM increased the proportion of $GABA_A$ receptors entering a slowly desensitising state whereas rapid desensitisation was more favourable when higher doses of zolpidem were applied. Rapid desensitisation of $GABA_A$ receptors allowed more

rapid cycling between states and therefore increased $GABA_A$ receptor binding and enhanced the oscillatory activity (Prokic et al., 2015). This may also explain why the power of gamma oscillations in the PC was enhanced in the presence of high concentrations of zolpidem but unaltered in the presence of low concentrations.

$GABA_B$ receptors are metabotropic, inhibitory GPCRs. $GABA_B$ receptors open K^+ channels, hyperpolarise the cells and inhibit adenylate cyclase and presynaptic calcium release (Dunlap and Fischbach, 1981; Hill, 1985; Newberry and Nicoll, 1985). In contrast to motor cortex gamma and beta and hippocampal gamma, $GABA_B$ receptor antagonist CGP 55845 had no effect on gamma peak power implying $GABA_B$ receptors do not contribute to gamma oscillations (figure 3.8) (Yamawaki et al., 2008; Dugladze et al., 2013).

3.3.4 Glutamate transmission modulation

A comparison of PC layer II oscillations to the widely used PING and ING models of neuronal network oscillations indicates PING better represents the gamma oscillations observed. The key difference between the two models is the reliance on phasic excitatory transmission for pacing (Cobb et al., 1995; Traub et al., 1996b; Whittington et al., 2000). Oscillation sensitivity to mixed AMPA and kainate receptor blockade was initially examined using the AMPA and kainate receptor blocker CNQX. Gamma oscillations were abolished in the presence of CNQX implying that either kainate, AMPA or both receptors were required for gamma oscillation pacing (figure 3.9). The AMPA/kainate receptor antagonist NBQX blocks AMPA receptors at low dose and blocks both AMPA and kainate receptors at a high dose. Low dose application reduced gamma peak power by 54.9%, which was further reduced by an additional 35.6% after application of a high dose implying both AMPA and kainate receptors are required for oscillation pacing (figure 3.9). SYM 2206, a potent antagonist of AMPA receptors has no effect on kainate receptors and was found to abolish gamma oscillations (figure 3.10). AMPA specific receptor blockade would be expected to have no effect on ING-like oscillations but abolish PING-like oscillations, as EPSPs are required for gamma oscillation generation (Hajos et al., 2004; Mann et al., 2005). Carbachol induced oscillations in CA3 have previously been found to be sensitive to AMPA receptor blockade, which likely reflects preferential expression of mAChRs on pyramidal cells in CA3 (Fisahn et al., 1998; Fisahn et al., 2002). Application of mAChR agonists was found to generate gamma oscillation by selectively exciting pyramidal cell axons via the M1 mAChRs in CA3 (see section 3.3.5 for more detail) (Levey et al., 1995; Traub et al., 2000; Fisahn et al., 2002). The subcellular location of mAChRs in the PC is not currently known. Given that AMPA receptor blockade abolished gamma oscillations in the PC, these oscillations more closely resemble the PING model than ING.

NMDA receptor blockade had no significant effect on gamma oscillations in the PC (figure 3.12). NMDA receptors positively modulate beta frequency oscillations in the motor cortex

and spontaneous and kainic acid (but not carbachol) induced oscillations in CA3 (Yamawaki et al., 2008; Modebadze, 2014). $mGluR_{2-3}$ and $mGluR_5$ receptors did not appear to contribute to oscillatory activity, however, $mGluR_1$ negatively modulated the oscillations, as application of CPCCOEt increased the oscillatory power. This was unsurprising given that $mGluR_1$ agonists have been previously found to depress IPSCs (Yu et al., 2013). As the gamma oscillations in the PC are likely to be dependent on rhythmic IPSCs for oscillation generation, a reduction in IPSC amplitude would be expected to reduce the amplitude of the oscillations.

3.3.5 Mechanism of gamma oscillations

The above pharmacological data indicate that in the PC, gamma oscillations induced by carbachol and kainic acid application most closely resemble previously found PING-type oscillations in CA3 (figure 1.4). The oscillations in the PC were initiated by kainic acid and carbachol. In CA3, kainic acid has been found to activate $GluK_2$ receptors on interneurons and enhance axonal excitability leading to increased action potential firing and enhanced IPSC amplitude and frequency (Semyanov and Kullmann, 2001; Fisahn et al., 2004). M1 mACh receptors in CA3 have been found to tonically activate pyramidal cell axons and generate VFO in the axons by potentiating the I_h and I_{cat} currents (Levey et al., 1995; Fisahn et al., 1998; Fisahn et al., 2002). The PC gamma oscillations, like those characterised in CA3, were found to depend on AMPA and $GABA_A$ receptors and gap junctions. In CA3, the VFO has been found to be interrupted by rhythmic IPSPs, accounting for the sensitivity to $GABA_A$ receptor blockade, and spread to neighbouring pyramidal cells via axo-axonal gap junctions, explaining the sensitivity to gap junction blockade. This excitation has been found to build up in the axon within the temporal window dictated by the IPSP frequency and produce axon driven action potential firing. This generates EPSCs in interneurons leading to interneuron firing, therefore accounting for the sensitivity of these oscillations to AMPA receptor blockade. The frequency of this rhythm in CA3 was found to be dictated by the kinetics of the IPSCs (Fisahn et al., 1998; Traub and Bibbig, 2000; Schmitz et al., 2001). Given that our oscillations are pharmacologically similar to those previously explored in CA3, we predict that a similar mechanism of action occurs during persistent PC gamma oscillations. In order to confirm this, further experiments would need to be performed including dual intra- and extracellular recordings and KO mouse studies.

3.3.6 Experimental limitations and future work

The question as to why both kainic acid and carbachol are essential for oscillation generation in the PC is likely related to the brain area in question and not the experimental setup or technique. Oscillations in CA3 and the entorhinal cortex were readily induced when kainic acid was applied alone using the same experimental technique. Similarly high levels of kainic acid and carbachol were required to induce beta frequency oscillations in primary motor cortex slices and gamma in somatosensory cortex slices (Buhl et al., 1998; Yamawaki et al., 2008). The sucrose based cutting solution used by (Yamawaki et al., 2008) has since been

refined to contain a number of neuroprotectants and was used in the experimental work presented in this chapter. Neuroprotective agents such as taurine, aminoguanidine and N-acetyl cysteine were previously found to enhance slice viability allowing much lower concentrations of kainic acid and carbachol to be used to induce oscillations in the primary motor cortex (Prokic, 2011; Johnson, 2016). Oscillations could still be elicited in the PC when sucrose based solution not containing neuroprotectants or choline based solution was used, however the concentration of kainic acid and carbachol required to induce oscillations remained the same as when it was prepared in sucrose based cutting solution.

The PC has been implicated in the development of TLE (Piredda and Gale, 1985a; Piredda and Gale, 1985b; McIntyre and Gilby, 2008). Extensive research has been undertaken on network changes during epileptogenesis in the hippocampus and entorhinal cortex using extracellular *in vitro* recordings. A reduction in the power of spontaneous gamma oscillations has been previously observed in CA3 of slices prepared during the mid-latent period (5-6 weeks) from the RISE model of epilepsy compared to age-matched controls (AMCs) (Modebadze et al., 2016). The gamma peak power was found to be identical in CA3 in slices prepared from animals which were displaying spontaneous recurrent seizures (SRS, chronic period) to those prepared from AMCs. These data indicate there are alterations in the pathophysiology of CA3 during the mid-latent period that resolves before the start of the chronic period. These spontaneous oscillations have been previously found to be similar to PING-type oscillations which depend on a mutually connected network of interneurons and pyramidal cells for oscillations generation. The preferential degradation of interneurons during epileptogenesis could therefore account for this reduction in oscillatory power found during the latent period (Ribak et al., 1982; De Lanerolle et al., 1989; Obenaus et al., 1993; Mathern et al., 1995; Cossart et al., 2001; Wittner et al., 2001; Dinocourt et al., 2003; Kobayashi and Buckmaster, 2003). The study of neuronal network activity in the PC *in vitro* may also be a useful technique for investigating network changes that underlie epilepsy.

In order to evaluate alterations in network activity during epileptogenesis, we needed to be able to reliably induce neuronal network oscillations in the PC in older (4 – 7 months) animals *in vitro*. When we induced oscillations in the PC prepared from older animals using the sucrose based cutting solution used in this chapter, <1 slice per animal displayed reliable oscillatory activity. Choline based cutting solutions are thought to improve interneuron viability to a similar degree as sucrose solutions in young animals. In older animals, choline has been found to be more effective at preserving slice viability than sucrose based solutions (Hoffman and Johnston, 1998; van Praag et al., 2002; Momiyama, 2003; Tanaka et al., 2008). When we induced oscillations in PC slices prepared in a choline based cutting solution (see methods) oscillatory activity in slices prepared from older animals was still rare (~1 slice per animal). This prevented us from investigating alterations in neuronal network activity in older and epileptic animals (although see appendix one).

3.3.7 Final Conclusions

The study of neuronal network oscillations *in vitro* represents a useful technique for investigating network changes in during pathological conditions such as epilepsy. For the first time persistent gamma oscillations have been induced and characterised in the PC *in vitro*. These oscillations have a similar mechanism to gamma oscillations in other limbic regions of the brain (Fisahn et al., 2002; Cunningham et al., 2003). Oscillations were initiated by kainic acid and carbachol and were dependent on an intact excitatory and inhibitory network connected by both chemical and electrical synapses.

Chapter 4 Pharmacologically induced persistent beta (12 – 30 Hz) oscillations in human neocortical slices *in vitro*

4.1 Introduction

Approximately 50 million people worldwide live with epilepsy, of which 30 % fail to adequately respond to antiepileptic drugs (AEDs) (Cockerell et al., 1995; Kwan and Brodie, 2000; WHO, 2012). In the most severe cases, the only course of action is a surgical resection of the epileptic focus. Certain types of epilepsy are more likely to be resistant to AED treatment than others; temporal lobe epilepsy (TLE) is the most common in the adult population and focal cortical dysplasia (FCD) in the paediatric population (Semah et al., 1998; Kwan and Brodie, 2000; Harvey et al., 2008). Post-operative seizure freedom is variable depending on diagnosed epilepsy type, duration of disease, age at treatment, lesion location and if a full or partial resection was undertaken (Wass et al., 1996; Wiebe et al., 2001; Stavem and Guldvog, 2005; Noachtar and Borggraefe, 2009). Surgery carries significant risk and has to be balanced with the risks associated with living without adequate seizure control (Behrens et al., 1997; Sperling et al., 1999; Sperling et al., 2005). Many drug resistant patients are also not good candidates for surgery.

4.1.1 Human brain tissue *in vitro*

Laws governing clinical research practice prevent invasive analysis of human cellular behaviour in all but the most exceptional cases. Instead, researchers have turned to both *in vivo* and *in vitro* electrophysiology of animal models to analyse cellular and network behaviour, explore the mechanisms of epilepsy and screen for new AEDs. However, no model perfectly represents human disease and a significant proportion of epilepsy patients remain resistant to currently available AEDs, indicating a need for new models to investigate epilepsy and screen new AEDs.

Surgically removed brain tissue offers a unique opportunity for researchers to investigate epilepsy in a more clinically relevant model. Tissue is only removed in patients with high seizure severity who are not adequately controlled by AED therapy, allowing researchers to try and better understand the mechanisms underlying drug resistant epilepsy. Despite the significant barriers associated with obtaining human tissue there has been a notable increase in the number of publications using human tissue in the last 40 years (Koehling and Avoli, 2006; Jones et al., 2015). Considerable organisation and coordination is required between researchers and clinical members of staff to obtain ethical approval and informed consent before considering the issues associated with collecting tissue from the surgical theatre. Close proximity of the laboratory to the operating theatre is essential and tissue availability is sporadic and often cancelled at very short notice. Similarly, whilst animal models tend to be genetically inbred and have undergone the same procedure to induce epilepsy, making the tissue collected easily comparable, human patients are unique and the tissue comes from a variety of different ages, history of AED use, seizure disorder and a mixture of brain regions (Koehling and Avoli, 2006; Jones et al., 2015). However, notwithstanding these disadvantages, human tissue is still the best ‘model’ of epilepsy possible *in vitro* and

represents an exciting opportunity to test theories developed in rodent brain slices in tissue that is more clinically relevant to human disease.

4.1.2 Human tissue and neuronal network oscillations

Much of the electrophysiological recordings conducted in human slices have focused on individual cellular behaviour or induced epileptiform activity. Despite significant research into neuronal network oscillations in rodent brain slices, research into neuronal network behaviour in human cortical tissue is severely lacking. To date, only one study investigating oscillations in human brain slices *in vitro* exists (Florez et al., 2015). Both theta and gamma oscillations were found to be induced following bath application of kainic acid and carbachol, however, the transient (2 - 3 minutes) nature of these oscillations prevented pharmacological evaluation of synaptic mechanisms (Florez et al., 2015). Much of our understanding of rodent cortical oscillations comes from pharmacological intervention and analysis of cellular and synaptic behaviour of persistent oscillations induced *in vitro*. The profile of human cortical oscillations *in vivo* are similar to those found in rodents *in vivo*, therefore it is assumed the mechanisms generating rodent oscillations may be similar to those in humans. However, this has not been rigorously explored, indicating a need for further research into the mechanisms of human neuronal oscillations.

4.1.3 Beta oscillations in rodent cortical tissue

Beta frequency oscillations (12 – 30 Hz) have garnered much less attention than gamma oscillations, particularly *in vitro*. Beta oscillations in the motor, premotor, parietal and sensory cortex and cerebellum *in vivo* are thought to be involved in movement preparation and initiation (Sanes and Donoghue, 1993; Murthy and Fetz, 1996; Lee, 2003; Courtemanche and Lamarre, 2005; Tkach et al., 2007). In the olfactory bulb and related regions, beta is thought underlie odour learning and memory (Martin et al., 2004a; Martin et al., 2004b; Martin et al., 2006). Beta oscillations have also been found in the hippocampus and temporal lobe regions although their function in this area is not clear (Leung, 1992). Alterations in beta oscillations have been found in a number of neurological disorders, including increased amplitude and highly synchronous oscillations observed in Parkinson's disease patients (Brown, 2003) and patients during status epilepticus (Bonati et al., 2006), and reduced amplitude in patients with schizophrenia (Uhlhaas et al., 2006; Roopun et al., 2008).

Application of kainic acid or carbachol have been found to induce persistent gamma oscillations in a number of brain areas including CA3, CA1, the entorhinal cortex and somatosensory cortex (discussed in detail in section 1.3) (Fisahn et al., 1998; Cunningham et al., 2003; Roopun et al., 2006). However, application of similar concentrations of these pharmacological agents has also been used to induce beta oscillations in the secondary somatosensory and primary motor cortex (Roopun et al., 2006; Yamawaki et al., 2008). Some temporal lobe areas have also been found to display beta oscillations following activation of muscarinic acetylcholine (mACh) (Shimono et al., 2000; Arai and Natsume,

2006), serotonin (5-HT) (Bibbig et al., 2007) or metabotropic glutamate (mGlu) (Boddeke et al., 1997) receptors or following tetanic stimulation (Traub et al., 1999). The best characterised of these are beta oscillations found in the secondary somatosensory cortex and primary motor cortex (Roopun et al., 2006; Yamawaki et al., 2008).

One of the defining features of beta oscillations in the secondary somatosensory cortex and primary motor cortex is that they occur in the absence of AMPA receptor input much like the ING model of gamma oscillations (figure 1.4). Independent gamma and beta oscillations were found to coexist within layer IV of the secondary somatosensory cortex (Roopun et al., 2006). Beta was found to be generated in the deeper layers and gamma in the more superficial areas allowing for the unique opportunity to investigate the mechanisms of both of these oscillations within a single slice preparation. AMPA blockade abolished gamma but not beta and NMDA receptor blockade increased beta power and abolished gamma (Roopun et al., 2006). Blockade of phasic $GABA_A$ receptors abolished gamma but enhanced beta, whereas blockade of both phasic and tonic $GABA_A$ receptors abolished beta (and gamma), implying the rhythm was driven independently of synaptic excitation and inhibition. This non-synaptic rhythm was found to be driven by beta frequency spikelets, spread via axo-axonal gap junctions in intrinsically bursting (IB) pyramidal cells in layer V. The frequency of these spikelets and therefore the frequency of the rhythm was modulated by the M type K^+ current I_M (Roopun et al., 2006).

In the primary motor cortex, the cellular mechanisms that underlie beta frequency oscillations more closely resemble ING type oscillations (see section 1.3) than beta in the secondary somatosensory cortex (Roopun et al., 2006; Yamawaki et al., 2008). Layer V cells fired low frequency (~7 Hz) spikes that were phase locked to the beta rhythm. Rhythmic IPSPs recorded in layer V cells had a beta frequency component suggesting the inhibitory network was pacing the beta oscillation (Yamawaki et al., 2008; Lacey et al., 2014).

4.1.4 Human beta oscillations *in vitro*

In this study, for the first time we demonstrate application of kainic acid and carbachol induced persistent beta frequency oscillations in brain slices prepared from tissue removed from paediatric patients undergoing surgery to treat drug resistant epilepsy. This activity was dependent on mACh, AMPA and $GABA_A$ receptors as well as gap junctions.

4.2 Results

4.2.1 Human cortical tissue *in vitro*

Human brain slices were obtained from patients aged <16 years of age undergoing surgery to alleviate the symptoms of drug refractory epilepsy between December 2013 and August 2016. Information about the patients was often limited due to confidentiality; table 4.1 contains known information on all patients included in this study. The tissue was collected from 19 patients with FCD (15/19) or TLE (4/19). The patients with FCD were not classified into subtype, however as type II and III are the most likely to present in childhood and type I is more commonly diagnosed in adulthood therefore the tissue is likely to be from patients with type II and III FCD (Bluemcke et al., 2011; Kabat and Król, 2012). All tissue used was from the dysplastic region.

Some of the data points presented here was collected by other members of the research group (Tamara Modebadze, Darshna Shah, Swetha Kalyanapu, and Nicholas Johnson). Tissue was collected and sliced as a collective effort within the group. Some of the results presented in this chapter have previously been presented in Tamara Modebadze's thesis (Modebadze, 2014).

Age	Gender	Diagnosis	Type of tissue obtained
6	F	FCD II	Dysplastic
		FCD	Dysplastic
		FCD	Dysplastic (central gyrus)
11	F	FCD	Dysplastic (temporal gyrus)
	M	FCD	Dysplastic (left frontal lobe)
	F	FCD	Dysplastic (temporal cortex)
	F	TLE	Dysplastic (parahippocampal region)
	M	TLE	Dysplastic (amygdala)
	F	FCD	Dysplastic (frontal lobe)
	M	FCD	Dysplastic (sensory motor cortex)
4	F	TLE	Dysplastic (amygdala)
15	M	FCD	Dysplastic (inferior frontal gyrus)
5	F	FCD	Dysplastic (frontal area between sensory and motor)
		FCD	Dysplastic (frontotemporal cortex)
		TLE	Dysplastic (amygdala and medial temporal gyrus)
6	M	FCD IIIb	Dysplastic (left parietal lobe)
1	F	FCD	Dysplastic (primary motor cortex)
6	M	FCD	Dysplastic (medial temporal gyrus)
7	M	FCD	Dysplastic (medial temporal gyrus)
11	F	FCD	Dysplastic (lateral temporal lobe)

Table 4.1 Origin of human cortical tissue
Chronologically ordered information on patient's age, gender, diagnosis and type/area of brain removed. Some of this information was not available.

4.2.2 Induction of beta oscillations

Initial experiments were conducted to identify any spontaneous activity present in the human neocortical brain slices *in vitro*. Electrodes were inserted into the brain slices, in the superficial layers with care taken to avoid areas with a high density of blood vessels and white matter (fibre tracts). Spontaneous epileptiform was rarely found (although see section 4.2.5) and spontaneous rhythmic activity was never found in any of the slices tested.

Neuronal network oscillations have previously been induced in rodent brain slices via application of the pharmacological agents kainic acid and carbachol either alone or in combination (Buhl et al., 1998; Fisahn et al., 1998; Gillies et al., 2002; Cunningham et al., 2003; Sinfield and Collins, 2006; Middleton et al., 2008; Yamawaki et al., 2008). Previously in our research group, application of (0.15 – 1.2 μM) of kainic acid alone has been found to induced rhythmic activity in human slices with a power of up to 7 μV^2 (1.2 μM kainic acid) and a variable frequency depending on the concentration (Modebadze, 2014). However, as these oscillations were small and unreliable, further experiments were conducted using a combination of kainic acid and carbachol. This combination has been used previously to induce gamma in the rodent piriform cortex (PC) (chapter 3), primary motor cortex and somatosensory cortex and beta oscillations in the primary motor cortex in rodent slices *in vitro* (Buhl et al., 1998; Yamawaki et al., 2008; Johnson, 2016). Similar concentrations to those used previously in rodent PC (chapter 3) were used to induce oscillations in human brain slices *in vitro*.

Application of 400 - 600 nM kainic acid and 30 – 50 μM carbachol induced oscillations with a mean peak power of 12.1 ± 2.0 μV^2 and frequency of 20.3 ± 1.2 Hz (n = 33) (figure 4.1), which we have termed beta oscillations. A Morlet-Wavelet analysis (figure 4.1 C) demonstrated that these oscillations were formed of bursts of beta oscillations with varying power. These beta frequency oscillations persisted for an extended period of time (up to 3 hours). The optimal dose of kainic acid and carbachol was variable between patients.

Both gamma and beta frequency oscillations have been extensively characterised in a number of brain regions in *in vitro* brain slices (Traub and Whittington, 2010). We therefore investigated the pharmacological mechanisms of these induced beta oscillations in human brain slices to evaluate if they were mechanistically similar to oscillations found in slices prepared from animal tissue *in vitro*. Low n numbers are presented owing to the limited availability of tissue.

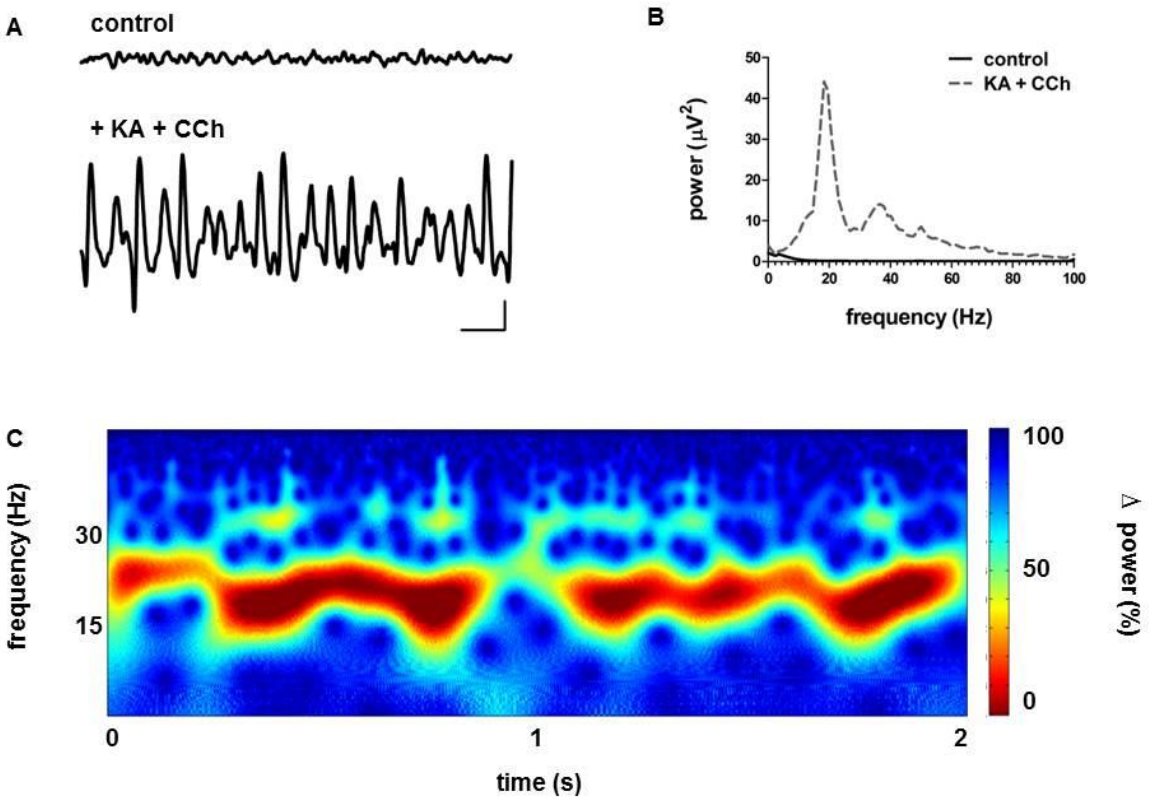

Figure 4.1 Application of kainic acid and carbachol induced beta oscillations in human slices
Application of both kainic acid and carbachol was required to induce beta oscillations A) One second of raw extracellular recordings taken from human cortical tissue before (control) and after kainic acid (400 nM) and carbachol (40 μM) application (Scale – 20 μV^2 Vs 100 ms). B) Power spectrum generated from 60 seconds of raw data before and after kainic acid (400 nM) and carbachol (40 μM) application. C) Typical spectrogram (Morlet-Wavelet) of 2 seconds of data demonstrating frequency and power of induced beta oscillations in human cortical tissue.

4.2.3 Muscarinic acetylcholine receptor modulation of beta oscillations

In the following experiments the control refers to slices in which beta oscillations were induced by application of 400 - 600 nM kainic acid and 30 - 50 µM of carbachol. The oscillations were allowed to stabilise (approximately 0.5 - 1.5 hours) to the point that the oscillations peak power and frequency did not change in the 20 minutes prior to drug application. Drugs were applied for 40 minutes unless otherwise stated and the beta oscillations at the end of this period were compared to the control.

To demonstrate that carbachol is necessary for the maintenance of the beta oscillations and confirm carbachol induced oscillations via the mAChRs, the competitive mAChR antagonist atropine was applied to human brain slices. Atropine (5 µM) application abolished the beta oscillation peak power (n = 2) (figure 4.2 A-B). Gamma oscillations in other brain regions such as CA3, CA1 and the PC (chapter 3) have been shown to rely specifically on the M1 receptor subtype of the mAChRs (Fisahn et al., 1998; Fisahn et al., 2002). To our knowledge, this has not been tested in beta oscillations. To test if carbachol induced beta oscillation via activation of the M1 subtype, the M1 selective antagonist pirenzepine (10 µM) was applied. Pirenzepine (10 µM) also abolished the beta oscillatory peak power (n = 2) (figure 4.2 C).

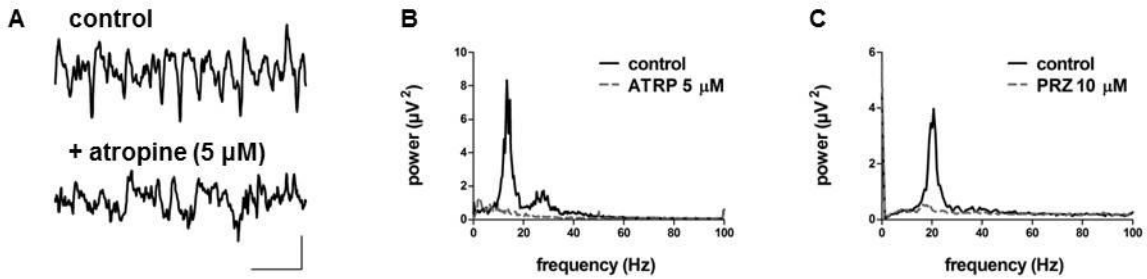

Figure 4.2 Human beta oscillations require muscarinic acetylcholine receptor activation.
A) Raw trace of an extracellular recording taken in human cortical tissue before (top) and after (bottom) atropine (5 µM) application (Scale – 20 µV Vs 200 ms). B) Power spectrum of 60 seconds of raw data (corresponding to A) before and after atropine (ATRP) (5 µM) application. C) Power spectrum of 60 seconds of raw data before and after pirenzepine (PRZ) (10 µM) application.

4.2.4 Gap junction modulation of beta oscillations

Gap junctions have been identified as critical for beta oscillations generation *in vitro* (Roopun et al., 2006; Yamawaki et al., 2008). To test if gap junctions were necessary for beta oscillation in human neocortical brain slices the gap junction blocker carbenoxolone was applied. Application of carbenoxolone (200 μM) for 2 hours significantly ($P < 0.05$, $n = 6$) reduced peak beta power by 79.5 ± 8.17 % (figure 4.3).

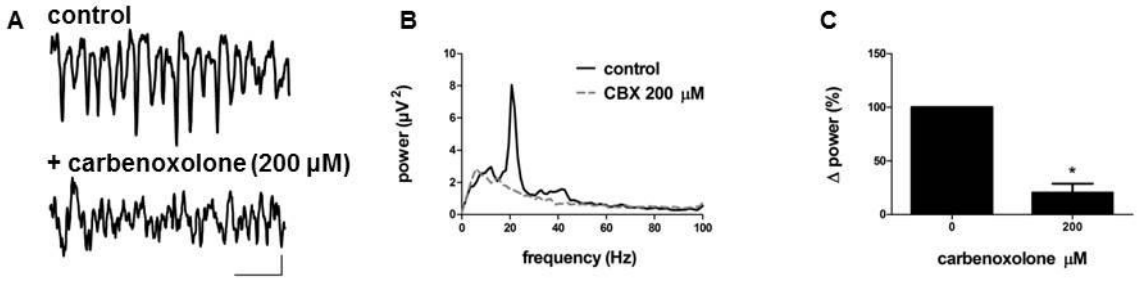

Figure 4.3 Human beta oscillations require gap junctions

A) Raw trace of an extracellular recording taken in human cortical tissue before (top) and after (bottom) carbenoxolone (200 μM) application (Scale – 10 μV Vs 200 ms). B) Power spectrum of 60 seconds of raw data (corresponding to A) before and after carbenoxolone (CBX) (200 μM) application. C) Normalised, pooled data, carbenoxolone significantly ($P < 0.05$, $n=6$) reduced beta peak power.

4.2.5 $GABA_A$ receptor modulation of beta oscillations

$GABA_A$ receptors have been previously found to be required for beta oscillation generation in the motor and somatosensory cortex (Roopun et al., 2006; Yamawaki et al., 2008). This was tested in human beta oscillations via application of the $GABA_A$ receptor non-competitive channel blocker picrotoxin (50 μM). Picrotoxin significantly ($P < 0.05$, $n = 6$) reduced the gamma peak power by 75.63 ± 3.81 % (figure 4.4). The short acting barbiturate pentobarbital was used to investigate if phasic $GABA_A$ receptors were pacing the oscillation. Pentobarbital binds to the β subunit of the $GABA_A$ receptor and enhances the effect of GABA binding by increasing the duration of Cl^- channel opening when GABA binds to the $GABA_A$ receptor (Segal and Barker, 1984; Whittington et al., 2000). Pentobarbital increased the beta peak power, and reduced the frequency of the oscillations ($n = 1$) (figure 4.5).

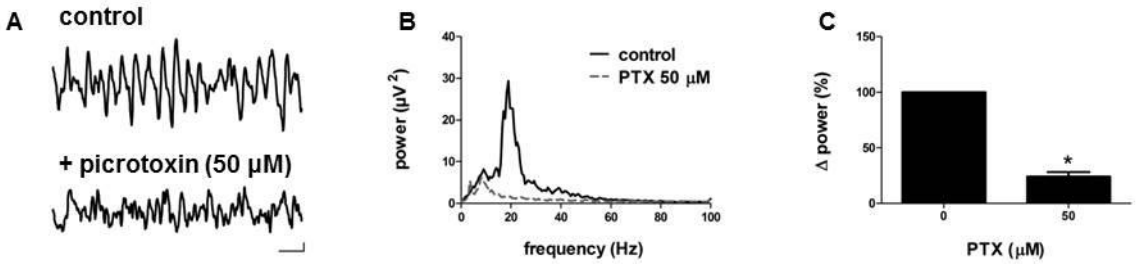

Figure 4.4 Human beta oscillations require $GABA_A$ receptors.
A) Raw trace of a representative extracellular recording taken in human cortical tissue before (top) and after (bottom) picrotoxin (50 µM) application (Scale – 10 µV Vs 100 ms). B) Power spectrum of 60 seconds of raw data (corresponding to A) before and after picrotoxin (50 µM) application. C) Normalised, pooled data, picrotoxin (50 µM) significantly ($P < 0.05$, n=6) reduced beta peak power.

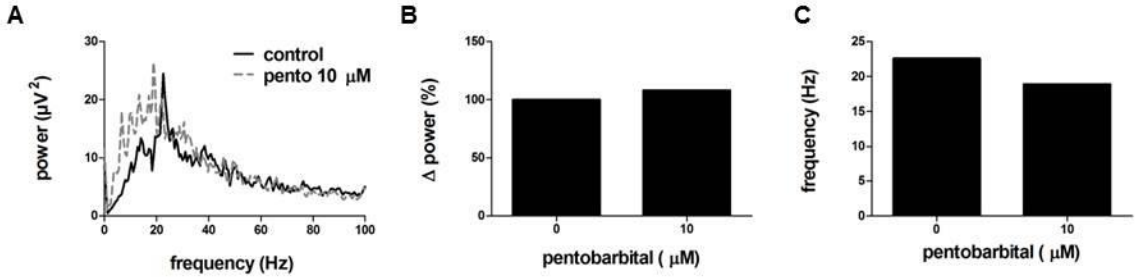

Figure 4.5 Human beta oscillations are paced by phasic $GABA_A$ receptors
A) Power spectrum of 60 seconds of raw data (corresponding to A) before and after pentobarbital (pento) (10 µM) application. B) Normalised change in beta oscillation power following pentobarbital (10 µM) application (n = 1). C) Alteration in frequency of human oscillations following pentobarbital (10 µM) application (n = 1).

4.2.6 Glutamate receptor modulation of beta oscillations

AMPA receptors are required for the generation of PING type oscillations *in vitro* (Traub and Whittington, 2010). In contrast, beta oscillations and ING-type oscillations in CA3 have been found to occur independently of AMPA receptors in both in the secondary somatosensory cortex and primary motor cortex (Fisahn et al., 2004; Roopun et al., 2006; Yamawaki et al., 2008). Therefore the sensitivity of human beta oscillations *in vitro* to glutamate receptor blockade was tested. Application of NBQX, a competitive AMPA and kainate receptor antagonist reduced the beta frequency peak (n = 4) (figure 4.6). This suggested both AMPA and kainate receptor function was required for oscillation maintenance. The role of AMPA receptors was investigated separately via application of non-competitive AMPA receptor antagonist SYM 2206. SYM 2206 (20 µM) significantly ($P < 0.05$) reduced the beta peak power by 74.77 ± 7.9 % (figure 4.7).

Beta oscillations have been found to be abolished in the presence of NMDAR antagonists in the primary motor cortex, however in the secondary somatosensory cortex, NMDAR blockade increased beta oscillation power (Roopun et al., 2006; Yamawaki et al., 2008). To evaluate if NMDAR were contributing to beta oscillation generation in human brain slices *in vitro*, the non-competitive NMDA receptor antagonist MK-801 was applied. MK-801 (20 µM) did not significantly alter the power of beta oscillations in human brain slices (n = 4) (figure 4.8).

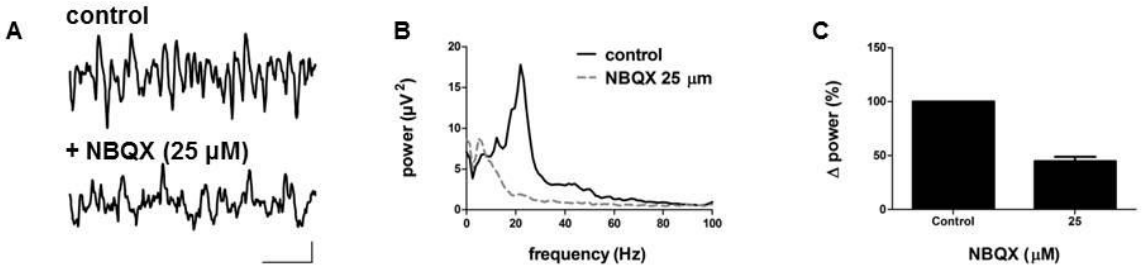

Figure 4.6 Human beta oscillations require kainate/AMPA receptors.
A) Raw trace of a representative extracellular recording taken in human cortical tissue before (top) and after (bottom) NBQX (20 µM) application (Scale – 20 µV Vs 200 ms). B) Power spectrum (corresponding to A) of 60 seconds of raw data before and after NBQX (25 µM) application. C) Normalised, pooled data, NBQX (25 µM) reduced the gamma peak (n = 4).

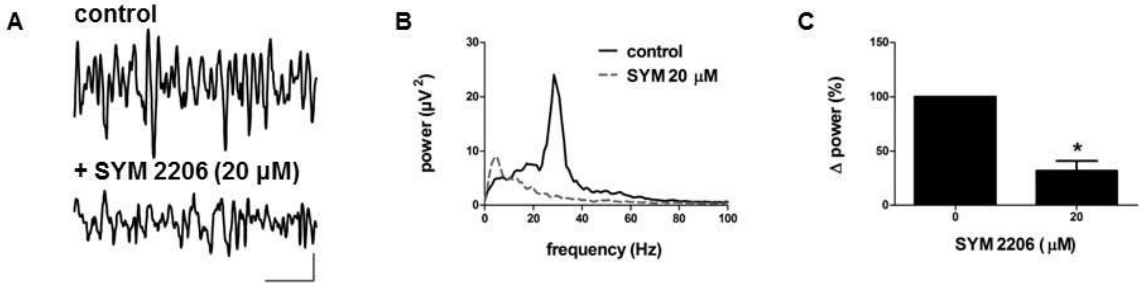

Figure 4.7 Human beta oscillations require AMPA receptors.
A) Raw trace of a representative extracellular recording taken in human cortical tissue before (top) and after (bottom) SYM 2206 (20 µM) application (Scale – 10 µV Vs 100 ms). B) Power spectrum of 60 seconds of raw data (corresponding to A) before and after SYM 2206 (20 µM) application. C) Normalised, pooled data, SYM 2206 (20 µM) significantly ($P < 0.05$, n=6) reduced beta peak power.

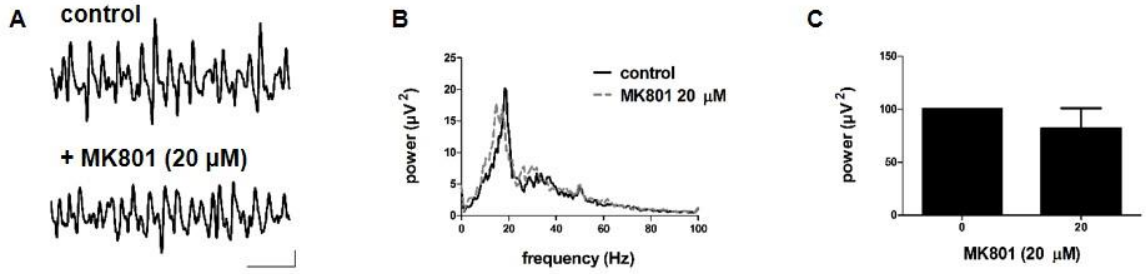

Figure 4.8 Human beta oscillations do not require NMDA receptors.
A) Raw trace of a representative extracellular recording taken in in human cortical tissue before (top) and after (bottom) MK-801 (20 µM) application (Scale – 10 µV Vs 100 ms). B) Power spectrum (corresponding to A) of 60 seconds of raw data before and after MK-801 (20 µM) application. C) Normalised, pooled data, MK-801 (20 µM) did not significantly ($P > 0.05$, n=4) alter beta peak power.

4.2.7 Spontaneous and induced epileptiform activity

Spontaneous epileptiform activity was occasionally observed in human brain slices (figure 4.9 A-B). The most commonly occurring epileptiform event was inter-ictal activity (figure 4.9 A) and bursts (lasting <1s) of high frequency oscillations (HFO) (figure 4.9 B). This spontaneous activity did not persist; however, lasting epileptiform activity could be induced by altering the ionic concentration of the circulating artificial cerebral spinal fluid (aCSF). Application of aCSF containing zero Mg^{2+} ions has been previously found to induce epileptiform activity in human slices with a low level of reliability (Shah, 2017). Application of high K^{+} (8 mM) and low Mg^{2+} (0.5 mM) induced epileptiform activity in 4/4 slices tested (Huberfeld et al., 2011). Epileptiform activity comprised of either regular (5.57 ± 0.78 /hr, n = 3) slow DC shifts in baseline (figure 4.9 C) termed seizure-like events (SLEs) or higher frequency (4 Hz, n = 1) repetitive, brief depolarisations (figure 4.9 D) referred to as inter-ictal bursting (IIB).

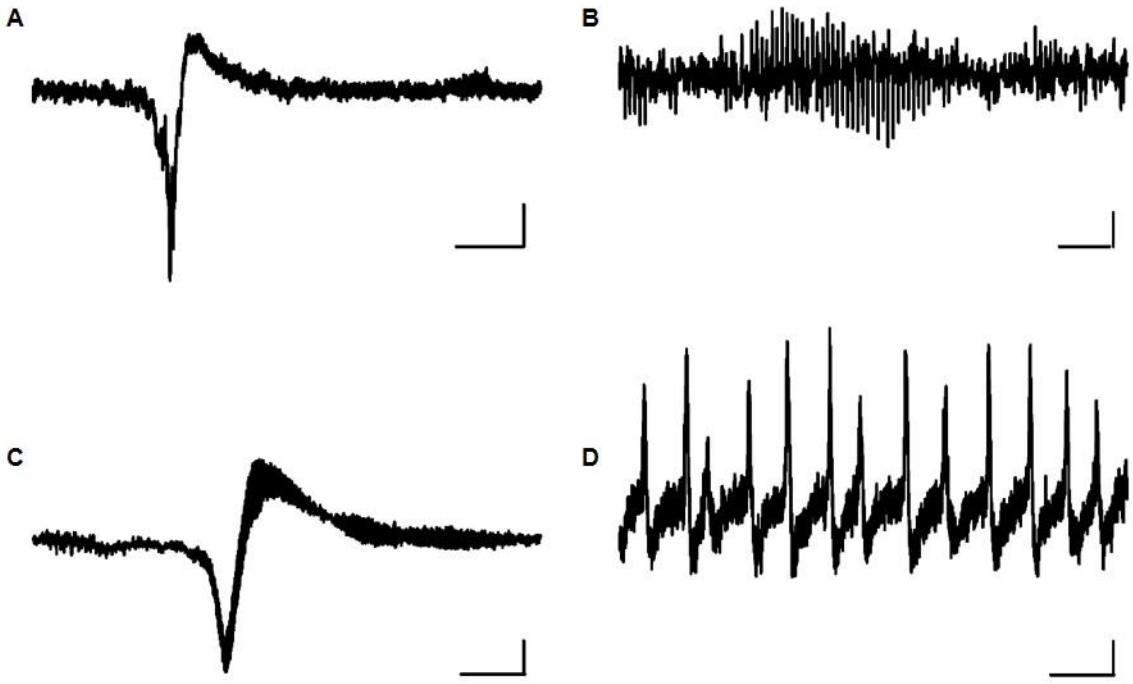

Figure 4.9 Spontaneous and induced epileptiform activity in human slices *in vitro*
A) Raw trace of spontaneous inter-ictal activity in human neocortical slices (scale - 2s Vs 50 μV^2). B) Spontaneous high frequency oscillatory activity in human neocortical slice (scale – 100 ms V 10 μV^2). C) Seizure-like event induced (application of high K^+/low Mg^{2+} aCSF) in human neocortical brain slice *in vitro* (scale – 2s Vs 500 μV^2). D) Induced (application of high K^+/low Mg^{2+} aCSF) repetitive epileptiform activity in human neocortical slices *in vitro* (scale 500 ms Vs 20 μV^2).

4.2.8 Sensitivity of epileptiform activity to perampanel

The sensitivity of this induced epileptiform activity to the recently licenced AED perampanel (0.1 – 10 μM), was tested in collaboration with M Cunningham's laboratory (Newcastle, UK). Perampanel is a non-competitive AMPAR antagonist used as an adjunct therapy in patients with refractory epilepsy (Rogawski and Hanada, 2013). Perampanel application (30 minutes per dose) reduced the frequency of SLEs (n = 3) and the amplitude of IIBs (n = 1) at low concentrations (0.1 – 1 μM) (figure 4.10). Application of higher concentrations (3 – 10 μM) abolished all epileptiform activity in human brain slices (figure 4.10).

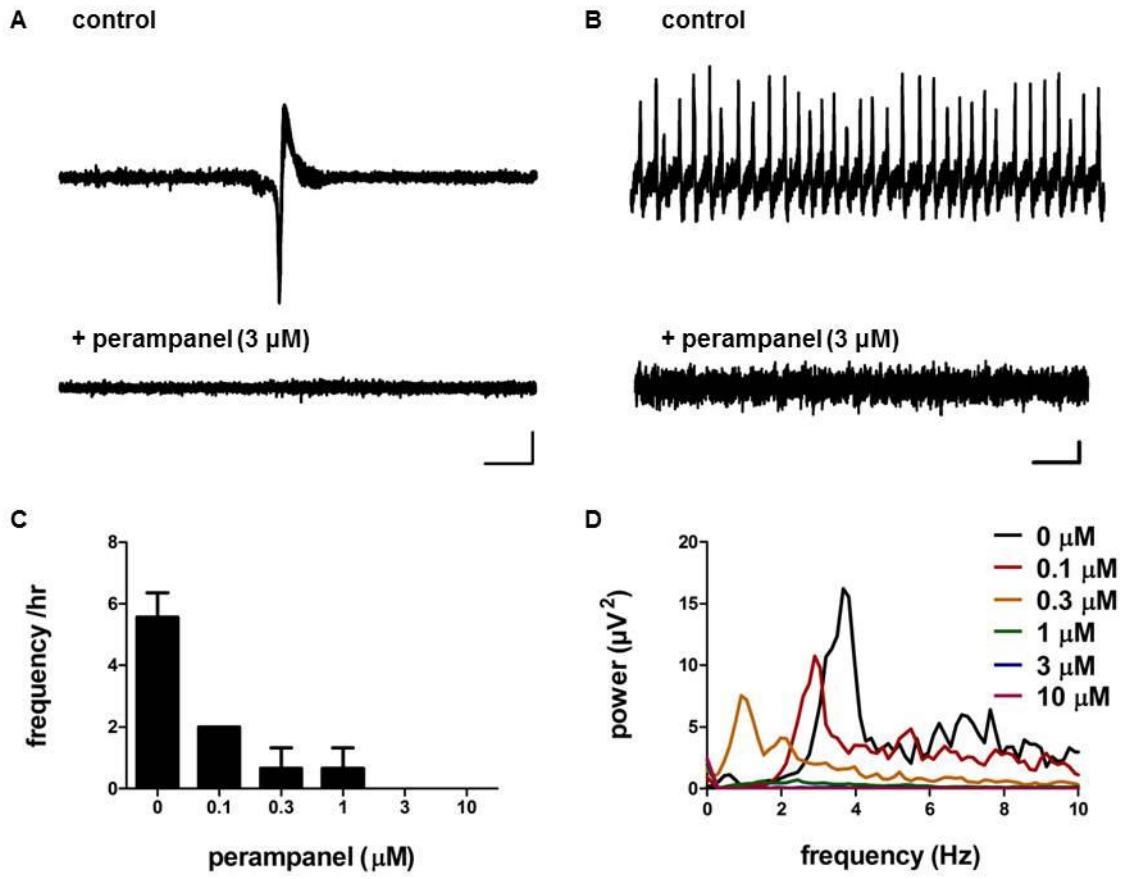

Figure 4.10 Perampanel and induced epileptiform activity *in vitro*

A) Raw trace of induced SLE in human neocortical slices before (top) and after (bottom) 3 μM perampanel application (scale - 500 μV^2 Vs 10s). B) Raw trace of induced IIB in human neocortical slice before (top) and after (bottom) 3 μM perampanel application (scale – 1 s V 20 μV^2). C) Pooled (n = 3) effect of variable doses of perampanel on induced SLEs in human brain slices *in vitro*. D) Power spectrum of 60 s of raw data demonstrating the effect of variable doses of perampanel on the power and frequency of IIB activity (n = 1) in human cortical slices *in vitro*.

4.3 Discussion

Persistent beta and gamma frequency oscillations have previously been found in numerous brain regions in rodent brain slices *in vitro* (Traub and Whittington, 2010). To our knowledge, this is the first time persistent beta frequency oscillations have been induced and characterised in slices prepared from human brain tissue. These were found to be dependent on AMPA and $GABA_A$ receptors as well as gap junctions for oscillation generation. The pharmacological profile of these oscillations was unexpectedly more closely related to rodent PING-type oscillations (Cobb et al., 1995; Traub et al., 1996a) than previously found rodent beta oscillations (Roopun et al., 2006; Yamawaki et al., 2008). In addition, we induced epileptiform activity in the human cortical slices and found this activity to be acutely sensitive to the new AED perampanel.

4.3.1 Beta frequency oscillations in epileptic human tissue *in vitro*

Epilepsy is a disorder of neuronal network synchrony, with alterations in excitation and inhibition thought to underlie changes in network activity leading to seizures (Fisher et al., 2005; WHO, 2012). Much of our understanding of network activity and in particular neuronal network oscillations comes from experiments performed on rodent brains both *in vivo* and *in vitro*. *In vitro* recordings of oscillatory activity in rodent brain slices has been comprehensively utilised as a tool to investigate the mechanisms of oscillation generation in a way not possible in either human or animal brains *in vivo* (Traub and Whittington, 2010). Despite the extensive use of human brain slices utilised from patients undergoing surgery to treat drug resistant epilepsy (Jones et al., 2015), neuronal network oscillations have not been mechanistically explored in human brain slices (Florez et al., 2015). Instead, researchers have been limited to the assumption that rhythms recorded in animals might be mechanistically similar to those found in humans. Human brain slices therefore offer the rare opportunity to explore the mechanisms of neuronal network oscillations *in vitro* in tissue that is more directly comparable to human patients.

Initial experiments were carried out to find spontaneous activity in the brain slices. In rodent brain slices, spontaneous rhythmic activity has been found in the hippocampus (Lu et al., 2011; Modebadze, 2014), and spontaneous inter-ictal events (IIE) and seizure-like events in the piriform cortex (see chapter 5). The tissue used in this study was always from the dysplastic zone, the area identified by intra or extracranial EEG as generating seizure activity. It might therefore be expected to be spontaneously active, however apart from IIEs consisting of brief depolarisations or transient bursts of HFOs (considered further below); spontaneous activity was rarely recorded in this study. In order to study rhythmic activity pharmacological manipulation was required.

Application of kainic acid or carbachol or a combination of both has been previously used to induce beta (Roopun et al., 2006; Yamawaki et al., 2008) and gamma oscillations (Fisahn et al., 1998; Hormuzdi et al., 2001; Cunningham et al., 2003) in rodent brain slices *in vitro*.

Application of kainic acid and carbachol consistently induced beta frequency oscillations in human brain slices. However, the concentration of each pharmacological agent required varied considerably between patients. This likely reflects differences in brain area used, extent of cortical disorder (such as in FCD), and method of removal. The method of removal is likely to influence slice viability, which is an important factor in oscillation generation (Aghajanian and Rasmussen, 1989; Michaloudi et al., 2005; Prokic, 2011). Brain tissue that was removed quickly, with minimal cauterisation required lower doses of kainic acid or carbachol to induce beta oscillations.

Application of kainic acid alone could also induce oscillations, however, higher concentrations (>1 μM) were required and the power of the oscillations generated was low (<10 μV^2). Furthermore, this method was less reliable than when kainic acid and carbachol were applied in combination. Kainic acid has been previously found to induce oscillations by depolarising interneurons and increasing sIPSC frequency and amplitude in the hippocampus (Semyanov and Kullmann, 2001; Fisahn et al., 2004). As neither mIPSC frequency nor the paired pulse ratio were found to be enhanced, kainate receptors are thought to enhance interneuron excitability specifically in the axons (Semyanov and Kullmann, 2001; Fisahn et al., 2004). This tonic depolarisation of interneurons is thought to be mediated via the $mGluR_2$ receptor subtype (Fisahn et al., 2004). The role of kainate receptor subtypes was not tested in this study owing to the limited availability of pharmacological agents. Oscillations were never found in the presence of carbachol alone; therefore kainate receptor activation might be expected to be critical for oscillation generation. However, kainic acid is also known to activate AMPA receptors and as AMPA receptors have been found to be required for beta oscillation generation (discussed further below), the role of kainate receptors is more debatable and would require further investigation (Hampson et al., 1992).

The role of mAChR activation for oscillation generation was confirmed when application of atropine, a mAChR antagonist abolished oscillations in the presence of 400 – 600 nM kainic acid and 30 - 40 μM carbachol. This also confirmed the need for either high concentrations (>1 μM) of kainic acid alone or lower concentration (400 – 600 nM) when used in combination with carbachol. Carbachol is a non-selective mAChR agonist, however, gamma oscillations induced by mAChR activation in CA3 and CA1 in rodent tissue have been found to depend specifically on activation of the M1 receptor subtype (Fisahn et al., 1998; Fisahn et al., 2002). This was also the case for our oscillations in human brains slices as pirenzepine, an M1 receptor specific antagonist also abolished neuronal oscillations. In CA3, during muscimol induced gamma oscillations, activation of the M1 receptor has been found to potentiate the I_h and I_{cat} currents without modulating I_M in pyramidal cells leading to pyramidal cell depolarisation (Fisahn et al., 2002). To our knowledge, the subtype of mAChR generating beta oscillations in rodent brain slices has not been tested. However, given that I_M

current blockade has been found to modulate beta in the somatosensory cortex but not gamma in CA3, either different subtypes of mAChRs induced beta oscillations, or the effect of M1 mAChRs is different depending on the brain area. Indeed, M1 receptors have been found to modulate I_M in sympathetic ganglion neurons (Hamilton et al., 1997) but not in the hippocampus (Rouse et al., 2000; Fisahn et al., 2004). Further experimental work would be required to investigate which currents M1 receptors modulate to generate beta oscillations in human cortical tissue.

Application of kainic acid and carbachol has previously been found to induce theta and gamma oscillations in human brain slices (Florez et al., 2015). However, the transient nature of these oscillations prevented a full pharmacological characterisation, although application of atropine before kainic acid and carbachol application did prevent these oscillations from developing (Florez et al., 2015). Differences in experimental set-up including the use of a submerged slice chamber likely account for the disparities between our experimental findings and these previous results.

4.3.1.1 Beta frequency oscillation pharmacology

The persistent nature of the beta oscillations induced in human cortical slices meant unlike the transient oscillations found previously found (Florez et al., 2015) it was possible to perform a pharmacological analysis.

Gap junctions have been previously found to play an important role in gamma and beta oscillations (Fisahn et al., 1998; Hormuzdi et al., 2001; Roopun et al., 2006; Yamawaki et al., 2008). Application of carbenoxolone abolished our beta oscillations and confirmed the role of gap junctions in slices prepared from human brain tissue. As discussed in detail earlier (see section 1.3) axo-axonal gap junctions between pyramidal cells have been found to be critical for the generation of carbachol induced gamma oscillations in CA3 and carbachol/kainic acid induced beta in the secondary somatosensory cortex (Fisahn et al., 1998; Traub et al., 2000; Schmitz et al., 2001; Roopun et al., 2006). Based on our results, we are unable to explain exactly how gap junctions contribute to oscillation generation, however the mechanisms are likely to be similar to those found previously for either gamma or beta oscillations.

$GABA_A$ receptor channel blockade abolished beta oscillations in human brain slices in this study. $GABA_A$ receptors have been previously found to pace gamma oscillations in temporal lobe regions (Segal and Barker, 1984; Fisahn et al., 1998; Whittington et al., 2000). The $GABA_A$ receptor agonist pentobarbital increased the power and decreased the frequency of the oscillations implying that rhythmic IPSCs might be pacing the network and tonic $GABA_A$ receptors may also contribute to the rhythm. Caution is required when interpreting this result however, as this is based on n=1. Further experiments are required to understand the role phasic $GABA_A$ receptors play in human beta oscillation generation. Pentobarbital has been previously used in rodent brain slices to assess if phasic $GABA_A$ receptors were pacing the

network (Fisahn et al., 1998). If phasic receptors were pacing the oscillations altering IPSC kinetics, pentobarbital would be expected to alter the frequency of the oscillation (Segal and Barker, 1984; Fisahn et al., 1998; Whittington et al., 2000). Pentobarbital alters the kinetics of IPSCs by enhancing the decay phase thereby increasing the duration of the IPSC (Segal and Barker, 1984). When applied to gamma oscillations the frequency of the oscillations was reduced implying the frequency was being set by the $GABA_A$ receptor kinetics (Fisahn et al., 1998; Whittington et al., 2000). The involvement of $GABA_A$ receptors in beta oscillations are more debatable (Roopun et al., 2006; Yamawaki et al., 2008). Pentobarbital was also found to reduce the frequency of the primary motor cortex beta oscillations, implying phasic IPSPs were pacing the network (Yamawaki et al., 2008). Pentobarbital has not been used in secondary somatosensory cortex beta oscillations, however application of gabazine at low concentrations (250 nM) which is known to block phasic, not tonic $GABA_A$ receptors, increased the oscillation peak indicating the beta oscillations found in this brain area were not dependent on phasic synaptic inhibition (Stell and Mody, 2002; Roopun et al., 2006). We have demonstrated that $GABA_A$ receptors are also important for beta oscillation generation and that phasic $GABA_A$ receptors likely contribute to the rhythm, although more n numbers are required to confirm this.

Glutamate receptor pharmacology indicates beta oscillations in human brain slices are mechanistically more comparable to previously found rodent gamma oscillations than beta oscillations (Cobb et al., 1995; Traub et al., 1996a). Suppression of both AMPA and kainate receptors was found to abolish the oscillations in this study, an effect also found in most gamma oscillations (Fisahn et al., 1998; Cunningham et al., 2003; Roopun et al., 2006). The role of AMPA receptors alone was then assessed separately. SYM 2206, an AMPA receptor specific antagonist abolished beta oscillations in human brain slices. This is at odds with previously found beta oscillations in the secondary somatosensory cortex and primary motor cortex as these oscillations continued in the presence of AMPA receptor blockade (Roopun et al., 2006; Yamawaki et al., 2008). Gamma oscillations are often segregated into two mathematically distinct models; ING- and PING-type (discussed in section 1.3), with ING oscillations insensitive to AMPA receptor blockade and the more common PING-type model being dependent on AMPA EPSCs for oscillation generation. The disappearance of our beta oscillations in the presence of AMPA receptor blockade indicates our oscillations more closely resemble PING pharmacologically than ING or even previously found beta oscillations in rodent tissue.

NMDA receptor blockade was found to have no effect on our beta oscillations. NMDA receptor involvement in gamma oscillations has been found to be variable depending on brain region, or method of induction (Fisahn et al., 2004; Lu et al., 2011; Modebadze, 2014). The amplitude of beta oscillations in the secondary somatosensory cortex has been found to be increased in the presence of NMDA receptor blockade, whereas beta oscillations in the

primary motor cortex were unaffected (although the frequency was slightly reduced) (Roopun et al., 2006; Yamawaki et al., 2008).

4.3.1.2 Limitations of experimental results and future work

Care should be taken when interpreting these results. Despite our best efforts to maintain experimental similarity between patients, there were a number of factors that may influence these results that were outside our control. The age and gender of patients, history of AED use, epileptic condition, severity of seizures, the brain area in which tissue was removed from, the care taken when removed (scalpel or cauteriser), the speed of removal and the time between oxygenation of cutting solution and collection of specimen were all different between patients. Given these differences, ideally all experiments performed here would be performed on at least one slice from every patient in order to identify if there were any differences in pharmacological mechanisms between patients. The limited availability of tissue prevented this, and also accounts for the low n numbers within some experiments. However, all results reported in this chapter came from a minimum of two patients (except in the case of n=1 experiments). One final consideration should be given to the origin of the above tissue. All tissue removed came from the dysplastic zone, an area identified by clinicians as the area generating seizures. All of the above pharmacological mechanisms have been compared to brain slices prepared from healthy rodents. Therefore the mechanism of these beta oscillations could be due to the cellular and synaptic reorganisation that occurs in FCD or TLE patients.

Further experiments are required to increase the n numbers for some pharmacological agents. These experiments should also be repeated in “control” human tissue. Superficial tissue originating outside the dysplastic area is occasionally removed to gain access to the dysplastic zone. This tissue could be used in the future as a form of “control” for the above experiments.

Despite these limitations, the use of human brain tissue presents a unique and exciting opportunity to explore the neuronal networks involved in drug resistant epilepsy in a clinically relevant model. After a full characterisation of these oscillations is performed, human beta oscillations could be used to explore alterations in network and synchronous activity that lead to epilepsy and could be utilised in the future for the development of new pharmaceutical agents targeted at patients with drug resistant epilepsy.

4.3.2 Epileptiform activity and perampanel

4.3.2.1 Epileptiform activity

Epileptiform activity has been extensively investigated previously in human brain slices (Jones et al., 2015). Initially, epileptiform activity was only reported when pro-convulsants were applied or when the ionic composition of aCSF was altered (Koehling and Avoli, 2006; Jones et al., 2015). More recently, groups have reported spontaneous activity *in vitro*;

however, this is usually limited to inter-ictal activity and bursts of HFOs (Wittner et al., 2009; Roopun et al., 2010; Huberfeld et al., 2011; Cunningham et al., 2012; Simon et al., 2014). Induction of SLEs has been noted to be extremely difficult in *in vitro* human slices, leading to the use of greater pro-convulsant conditions for SLE induction in human compared to rodent brain slices (Heinemann and Staley, 2014). In our laboratory, application of zero Mg^{2+} aCSF (0$[Mg]^{2+}$) has been found to rarely induce persistent epileptiform activity (Shah, 2017), therefore we applied aCSF with low Mg^{2+} (0.5 mM) and high K^{+} (8 mM) which reliably induced epileptiform activity in all slices tested. This epileptiform activity consisted of either SLEs or IIBs. Previously, application of 0 mM Mg^{2+} and 8 mM K^{+} has been found to induce IIBs, SLEs and pre-ictal discharges, which were similar in properties to seizures recorded in patients prior to surgery (Huberfeld et al., 2011). Pre-ictal discharges were not noted in the brains slices we tested, however this may be due to differences in brain region tested. The SLEs in this study were similar in shape and properties as those found in the rodent piriform cortex, CA3 of the hippocampus and the lateral entorhinal cortex (chapter 5).

4.3.2.2 Perampanel

Perampanel is a recently developed AED and a highly selective antagonist of AMPA receptors. It is currently licenced as an adjunct therapy for both children and adults with partial onset seizures with or without secondary generalisation (Rogawski and Hanada, 2013). Perampanel has been demonstrated to be effective in multiple animal models of epilepsy *in vivo* including pentylenetetrazol, maximal electrical shock, 6 Hz seizure test and kindling (Hanada et al., 2011; Zwart et al., 2014). Application of 10 µM perampanol to human brain slices from patients with TLE in modified aCSF (high K^{+}, low Mg^{2+} and 10 µM picrotoxin) has been previously found to reduce the amplitude and frequency of epileptiform events (Zwart et al., 2014). In this study we assessed the effect of perampanel on induced epileptiform activity (high K^{+}, low Mg^{2+}) in tissue originating from patients with FCD type II in collaboration with M Cunningham's laboratory (Newcastle). Perampanel reduced the frequency of SLEs and power of IIBs after 0.1 µM application and completely abolished both types of epileptiform activity after 3 µM application. This was a lower concentration than that found in TLE patient tissue, however, as lower concentrations were not tested previously it is not known if lower concentrations would reduce epileptiform events in brain slices from TLE patients (Zwart et al., 2014).

4.3.3 Final conclusions and future work

For the first time we have induced and partially characterised the pharmacological mechanisms of persistent beta oscillations in the human neocortical slices *in vitro*. These oscillations were found to be generated by application of kainic acid and carbachol and depended on $GABA_A$ and AMPA receptors as well as gap junctions for oscillation generation. Although the frequency of these oscillations was in the beta band, they were found to be mechanistically more closely related to PING-type oscillations than ING or beta oscillations

previously found in rodent cortical tissue. These induced oscillations could be used in the future as a tool to investigate alterations in network activity in patients with drug resistant epilepsy. In addition to this, epileptiform was found to be reliably induced in tissue removed from patients with FCD. This epileptiform activity was acutely sensitive to perampanel application even at low doses.

Chapter 5 The piriform cortex and epilepsy

5.1 Introduction

5.1.1 The piriform cortex and epilepsy

The piriform cortex (PC) first caught the attention of epilepsy researchers when it was noted to have a significantly lower threshold for seizure induction using chemoconvulsants (Piredda and Gale, 1985a; Piredda and Gale, 1985b; Piredda and Gale, 1986) compared to other areas of the brain more commonly associated with epilepsy such as the hippocampus or amygdala (Baxter, 1967; Vosu and Wise, 1975; Schwarcz et al., 1978; Ben-Ari et al., 1980; Wasterlain and Jonec, 1983). Gale named the area "area tempestas" (from the Latin for storm or sudden storm), a term which originally only referred to the deep anterior PC (aPC) layer III/endopiriform nucleus. However, this has since been expanded to include the aPC layer II (Maggio and Gale, 1989; Wardas et al., 1990). The location of area tempestas was further confirmed in slice experiments using the $GABA_A$ receptor antagonist, bicuculline, as epileptiform activity was found to originate in layer III/endopiriform nucleus and propagated to layers I/II (Demir et al., 1998, 2001).

The PC is also more sensitive to kindling induced seizures than the entorhinal cortex (EC), hippocampus and amygdala (McIntyre and Gilby, 2008). However, the most sensitive region, as determined by kindling-induced afterdischarge (AD) threshold, was identified in the mid/posterior deep layers of the PC, not area tempestas (Morimoto et al., 1986; Cain et al., 1988; Ludvig and Moshe, 1988; Honack et al., 1991; Löscher et al., 1995). Despite this, *in vitro* brain slices prepared from kindled animals and a slice model of kindling identified area tempestas as the origin of epileptiform activity (Hoffman and Haberly, 1991a; Hoffman and Haberly, 1991b). For full kindling to occur, the AD needs to extend in amplitude and duration and propagate to other brain regions (Goddard, 1967; Goddard et al., 1969). Even when the PC was not the site of electrical stimulation it has been implicated in amplification and propagation of the AD to other brain regions. During kindling, inter-ictal spikes (IISs) were found to originate in the PC, despite the stimulating electrode being located in other brain areas and in fact the PC often displayed IIS activity before induction began (Kairiss et al., 1984; Racine et al., 1988a). AD's have been recorded in the ipsilateral PC as early as the first stimulation when the stimulating electrode was located in the amygdala (Loscher and Ebert, 1996). Increased glucose metabolism and neuronal activation has also been found in the PC during stage 1-2 seizures even before it was detected in the amygdala (Engel et al., 1978; Clark et al., 1991).

Disruption of PC activity has been demonstrated in a number of studies to influence kindling. For example, local microinjections of NMDA (and to a lesser extend AMPA/kainate) receptor antagonists into the PC prevented the development of discharges and motor seizures during kindling, but continued stimulation beyond drug treatment induced epilepsy as normal (Croucher et al., 1988). Similarly, infusion of a GABA transaminase inhibitor into the PC elevated the threshold for seizure induction (Stevens et al., 1988). However, when physical

(Racine et al., 1988b) or chemical lesions (Wahnschaffe et al., 1993) were made in the PC or pPC, epileptogenesis was not blocked. Indeed, there was only a small increase in the number of stimulations required in amygdala kindling to produce a fully kindled animal (Racine et al., 1988b; Wahnschaffe et al., 1993). Perineuronal nets provide structure and support for synapses onto interneurons and control the synaptic plasticity underlying so-called 'critical periods' in cortical structures, as well as being responsible for maintaining the balance between excitation and inhibition in local circuits (Hensch, 2005). Perineuronal nets have been found to be significantly degraded in PV positive (fast spiking multipolar) interneurons in the PC following kindling (Pollock et al., 2014). Preventing the breakdown of perineuronal nets with doxycycline was found to suppress seizure activity in a rat model of epilepsy (Pollock et al., 2014). The firing patterns of a subset of interneurons in the PC was also found to be changed from non-adapting (fast spiking and regular spiking multipolar) to an adapting response to depolarising current injection. This alteration was thought to be due to an upregulation of the $K_v1.6$ voltage-dependent K^+ current, not loss of a subset of interneurons, thereby reducing interneuron excitability and reducing inhibitory neurotransmitter release (Gavrilovici et al., 2012). An increase in mIPSC amplitude and duration recorded in interneurons and not pyramidal cells and an enhanced phosphorylation of $GABA_A$ receptors has also been found following kindling (Gavrilovici et al., 2006; Kia et al., 2011). Combined, this interneuron reorganisation and reduction in interneuron excitability might lead to disinhibition of pyramidal cells and thus increase network excitability facilitating seizure initiation and propagation.

Status epilepticus (SE) based models of epilepsy, such as the soman, pilocarpine and kainic acid models, have also identified the PC as being critical in epileptogenesis. The acetylcholinesterase inhibitor, soman, induces seizures via excess stimulation of AChRs. Lesioning of the PC, but not the EC, hippocampus or amygdala increased the latency to first seizure following soman administration in rats (Myhrer et al., 2008). Neuronal hyperactivity assessed via c-fos immunodetection identified the PC as activated earlier (30 minutes) following pilocarpine administration than the hippocampus and amygdala (60 - 90 minutes) (Sinel'nikova et al., 2013). Neuronal loss and oedema has been found earlier in the PC and EC (6 hours) than in the hippocampus (36 - 48 hours) following pilocarpine induced epilepsy (Wall et al., 2000; André et al., 2007). This difference in responsiveness to pilocarpine induced epilepsy might be due to the tendency of PC cells to burst fire following mAChR activation (Postlethwaite et al., 1998; Whalley et al., 2005). This burst firing activity is more evident in young animals and it may also account for the observed drop in sensitivity to pilocarpine induced epilepsy in rats after postnatal day 22 (Cavalheiro et al., 1987; Postlethwaite et al., 1998; Whalley et al., 2005). Furthermore, the enzyme responsible for converting glutamate to GABA (glutamate decarboxylase (GAD) 65 and 67) is upregulated 8

hours following kainate or pilocarpine induced SE in the PC, perhaps acting as a compensation mechanism in response to enhanced excitability (Freichel et al., 2006).

Cellular loss, particularly of PV positive (fast spiking multipolar) inhibitory neurons has been reported across the PC and endopiriform nucleus in the chronic stage of induced epilepsy (Druga et al., 2003; Chen et al., 2007b). Astrocytic loss, neurodegeneration, reduced neuronal density and oedema has also been found (Kim et al., 2010; Scholl et al., 2013; Woeffler-Maucler et al., 2014). Cell death was reduced in a number of areas including the PC when SE was stopped by an NMDA receptor antagonist injection, whilst development of SRS was unaffected (Brandt et al., 2003). It was suggested the damage is not important for SRS induction but it could be that this damage is responsible for altered behaviour seen in rat models and TLE patients with lesions (Pinel et al., 1977; Trimble, 1991; Brandt et al., 2003). Neuronal death and injury has also been found in the PC (and other regions) following kainic acid induced TLE (Covolan and Mello, 2000; Candelario-Jalil et al., 2001; Chen et al., 2005).

The reasons underlying the PC's sensitivity to epilepsy induction is likely to be due to a combination of its unusual structure and extensive connectivity. Like the hippocampus, another area of the brain with enhanced seizure susceptibility, the PC comprises of a three layer allocortex with extensively connected excitatory network. The extensive connectivity of the PC with other brain regions, in particular the hippocampus, amygdala and entorhinal cortex allows it to spread epileptiform activity between brain regions generating secondary generalised seizures.

5.1.2 The reduced intensity status epilepticus (RISE) model of temporal lobe epilepsy (TLE)

The reduced intensity status epilepticus (RISE) model of TLE was developed following a critical assessment of the currently available status models of epilepsy. Sloviter (2005) criticised the disparity in pathophysiology and cognitive/behavioural abnormalities of rats subjected to a SE type induction compared to TLE patients. Traditional SE models are associated with severe, widespread brain damage, increased aggression and hypersensitivity. Additionally, traditional models have significantly high levels of mortality (up to 100 %) with variables such as period spent in SE, pilocarpine concentration, single or divided doses and age all thought to influence mortality (Curia et al., 2008). The RISE model was developed in line with the NC3Rs (the National Centre for Refinement, Replacement and Reduction in animal research) and is a modified lithium-pilocarpine model in which SE severity is reduced with a potent muscle relaxant (xylazine) and then stopped after 1 hour (MPEP, MK-801 and diazepam) resulting in a mortality rate of ~1 % (Modebadze et al., 2016).

Like other SE models of epilepsy, the rats undergo a latent period in which progressive changes in the brain lead up to the first spontaneous seizure, after which, spontaneous

recurrent seizures (SRS) regularly occur (Curia et al., 2008). The length of the latent period varies between laboratories, with the Whalley laboratory at Reading University reporting up to 12 weeks whereas those induced at Aston University were on average 20 weeks (see PSBB, methods) after which, SRS develops. This difference is likely to be due to differing ages of induction and differences in rat source. During the latent period progressive changes in behaviour and *in vitro* network activity were observed. In the hippocampus, normal gamma band activity was replaced by theta, gamma and high frequency oscillations (HFO) at 24 hours post induction. This was followed by a depression of gamma power during the latent period and a return to high power gamma in SRS. Histological analysis of brain regions following the development of SRS in older pilocarpine models has been associated with extensive morphological and cellular damage particularly in the hippocampus and PC (Sloviter, 2005). This was not found in the RISE model, with little difference in histology found in the hippocampus and PC between chronic and age-matched control animals (Modebadze et al., 2016).

5.1.3 The zero magnesium model of epileptiform activity *in vitro*

The *in vitro* zero Mg^{2+} ($0[Mg]^{2+}$) model of epileptiform activity in hippocampal brain slices was developed over thirty years ago (Mayer et al., 1984; Anderson et al., 1986; Walther et al., 1986) and has since been used in cell culture studies (Coulter and Lee, 1993; Sombati and Delorenzo, 1995). Mg^{2+} had been associated with seizures some years before the development of the $0[Mg]^{2+}$ model in *in vitro* brain slices. Hypomagnesaemia in humans has been found to induce seizures that can be rescued by magnesium sulphate ($MgSO_4$) replacement therapy (Arnold et al., 1983; Nuytten et al., 1991). Treatment with $MgSO_4$ has also been found to be more effective than diazepam at reducing the risk of seizures and maternal death in pregnant women with eclampsia (Duley et al., 2010). A low Mg^{2+} diet in rats has been found to increase susceptibility to seizure induction (Greenberg and Tufts, 1935) and intravenous Mg^{2+} suppresses seizure activity in rats, cats, dogs and primates (Borges and Giicer, 1978; Buck et al., 1979). Under normal conditions NMDA receptors are blocked by a Mg^{2+} ion preventing their activation unless there is a sufficient depolarisation of the cell membrane. If the Mg^{2+} is not present, NMDA receptors are activated at resting membrane potential when glutamate (and D-serine/glycine) binds. This leads to membrane depolarisation, an increase in action potentials (APs), abnormal neuronal synchrony and raised intracellular Ca^{2+} which can lead to excitotoxicity, cell death and seizures (Mayer et al., 1984; Traub et al., 1994; Heinemann et al., 2006; Ghasemi and Schachter, 2011). Two types of epileptiform events have been identified following $0[Mg]^{2+}$ application; seizure-like events (SLEs) which transition into late recurrent discharges (LRD) in temporal regions of the brain. Whilst initial SLEs are sensitive to common AEDs, the LRD are not, although both maintain their sensitivity to NMDA receptor antagonists (Walther et al., 1986; Stanton et al., 1987; Dreier and Heinemann, 1990; Zhang et al., 1995; Dreier et al., 1998). The transition is

thought to be due to a reduction in synaptically available GABA (Heinemann et al., 1994; Mody et al., 1994; Pfeiffer et al., 1996).

In addition to its effects on NMDA receptors, the absence of Mg^{2+} may also increase presynaptic intracellular Ca^{2+} by reducing surface charge screening (Isaev et al., 2012). Under normal ionic conditions, there is a voltage-dependent block of Ca^{2+} channels by Mg^{2+} ions. At rest, the neuronal membrane has a negative surface charge attracting divalent cations (Mg^{2+}/Ca^{2+}) which compete to form a layer of positive charge. This reduces the Ca^{2+} available for influx when Ca^{2+} channels open (Muller and Finkelstein, 1974). The absence of Mg^{2+} enhances the Ca^{2+} available in the extracellular space close to the presynaptic Ca^{2+} receptors leading to enhanced intracellular Ca^{2+} and neurotransmitter release (Mody et al., 1987; Mangan and Kapur, 2004; Isaev et al., 2012). Increased extracellular K^{+} is also present during epileptiform activity including 0$[Mg]^{2+}$ induced SLEs (Lux et al., 1985; Dreier and Heinemann, 1991). This rise has been found to occur before SLEs are initiated and has been suggested to spread seizure activity to neighbouring brain regions (Yaari et al., 1983; Konnerth et al., 1986; Dreier and Heinemann, 1991).

5.1.4 The piriform cortex and epileptiform activity *in vitro*

The entire PC has been found to be sensitive to induction of epileptiform activity via application of 0$[Mg]^{2+}$ or low Cl^{-} aCSF, 4-AP or bicuculline *in vitro* (Hoffman and Haberly, 1989, 1991b; Demir et al., 1999; Whalley et al., 2009). 0$[Mg]^{2+}$ application in the PC has been found to induce paradoxical depolarising shifts (PDS) in neurons and rhythmic burst firing of APs which are sensitive to NMDA receptor blockade (McIntyre and Plant, 1993; Libri et al., 1996; Whalley et al., 2009). This bursting activity originates from pyramidal cells located in the endopiriform cortex and layer III of the PC and propagates up to the superficial layers (Hoffman and Haberly, 1991b). In the OB, 0$[Mg]^{2+}$ application induced delta frequency (2-4 Hz) activity and SLEs which consist of a slow-DC shift superimposed on repetitive spiking activity (Igelström et al., 2011). Blockade of K^{+} channels via 4-AP application has also been found to induce spontaneous burst firing of APs (Libri et al., 1996; Whalley et al., 2009). Beta – gamma frequency (20 – 60 Hz) oscillations have been found to be induced by 4-AP application in an isolated guinea pig whole brain preparation. These oscillations propagated from the PC to the lateral entorhinal cortex (LEC) and occasionally the medial entorhinal cortex (MEC). This activity in the PC was found to precede IIEs and SLEs in the hippocampus and EC, which did not propagate to the PC (Uva et al., 2005; Carriero et al., 2010). Since then, SLEs/IIEs have been recorded in PC brain slices following 4-AP application, with the highest amplitude activity recorded in layer II. SLEs (HFOs) were primarily generated in the aPC and propagated to the pPC whereas IIEs originated from either sub region (Panuccio et al., 2012). Bicuculline application in isolated whole brain induced SLEs in the hippocampus and EC which could propagate to the PC; unless IIEs were present, in which case invasion of SLEs into the PC was prevented (Librizzi and de

Curtis, 2003). High frequency IIEs induced by bicuculline in the pPC, in slices containing PC and neocortex, were found to drive activity in the neocortex. High frequency IIE persisted in the pPC following separation of the PC from the neocortex, whilst the frequency of IIE in the neocortex slowed (Rigas and Castro-Alamancos, 2004). Interestingly, similar experiments with aPC and neocortex showed that the IIE frequency remained unaltered following separation of the two regions (Rigas and Castro-Alamancos, 2004), suggesting that the pPC is more important in driving epileptiform activity than the aPC.

5.1.5 Enhanced sensitivity to epileptiform activity in the piriform cortex *in vitro*

In this study we demonstrate that epileptiform activity can be reliably induced in PC brain slices *in vitro* via removal of Mg^{2+} ions from the perfusate. These induced SLEs were similar in appearance to seizures recorded in epileptic patients *in vivo*. In brain slices containing aPC, pPC, CA3 and LEC, SLEs are first observed in the PC in the majority of slices tested. The properties of induced SLEs in the PC were found to change during epileptogenesis in comparison to age-matched controls.

5.2 Results

5.2.1 The PC is more sensitive to induction of SLEs than CA3 and the lateral entorhinal cortex

Initial experiments were conducted to assess if epileptiform activity was present spontaneously in the PC slice *in vitro*. Spontaneous SLEs were recorded in horizontal slices prepared from 100g rats (29 - 31 days) containing both the aPC (figure 5.1 Ai-Ei) and the pPC (figure 5.1 Aii-Eii). These SLEs consisted of HFO activity (figure 5.1 Ai/ii and Di-ii) followed by a slow DC shift (figure 5.1 Ai/ii and Ci/ii). However, spontaneous SLEs were unreliable and did not persist. Application of 0$[Mg]^{2+}$ aCSF increased the excitability of the slices and reliably induced SLEs with a higher amplitude DC shift and HFO activity (figure 5.1 B-Ci/ii and Ei/ii).

A multielectrode array (MEA) recording (figure 5.2) was performed in a horizontal slice to assess if the area of SLE origin could be detected. The 96 channel array was inserted into a slice across the aPC, pPC, endopiriform cortex and striatum (figure 5.2 A-B). Simultaneous recordings of 40 seconds of raw data is presented in 5.2 C. SLEs occurred across most of the electrodes but not at exactly the same time. In both the aPC and pPC the SLEs appear to be generated in the deeper layers (including the endopiriform cortex) before propagating to the superficial layers close to the lateral olfactory tract. There appeared to be multiple sites of onset of SLEs with SLEs observed in the striatum and regions outside the PC which seem to be unrelated to the SLEs observed in the PC. However, caution is required when interpreting these results as the location of the MEA was not confirmed histologically.

In order to assess the relative excitability of four brain regions commonly associated with epilepsy, horizontal slices were prepared from 100g rats and electrodes were inserted into layer II of the aPC and pPC, stratum pyramidale in CA3 and layer II of the LEC as shown in figure 5.3 A. 0$[Mg]^{2+}$ aCSF was applied to ten slices for up to 2 hours to induce epileptiform activity. Slices containing all four brain areas were used to assess excitability without introducing bias. SLEs were similar across the four regions with HFOs before a slow DC shift (figure 5.3 A-D).

SLEs were observed in the aPC in 9/10 slices, 10/10 in the pPC, 5/10 in the LEC and 9/10 in CA3. 8/10 of the slices showed SLEs in either the aPC or pPC first, the remaining slices showed SLEs in either CA3 (1/10) or the LEC (1/10) first (figure 5.3). SLEs were simultaneously observed in all four brain areas in 4/10 slices. SLEs occurred with an inter-event interval (IEI) of 12.83 ± 3.21 mins in the pPC (n = 9), 13.45 ± 3.1 mins in the aPC (n =9), 10.05 ± 1.3 mins in the LEC (n = 5) and 12.75 ± 3.4 in CA3 (n = 8) (figure 5.4 A). The SLEs occurred with a frequency of 6.20 ± 1.0 /hr in pPC, 5.89 ± 0.8 /hr in aPC, 6.42 ± 0.9 /hr in the LEC and 5.59 ± 0.7 /hr in CA3. The maximal power of the slow DC shift was calculated using a custom Spike2 script in which the maximal power in the 0 - 3 Hz frequency range

was calculated every 100 ms (FFT size 32768). The average power (calculated from the maximal power of the first three SLEs in each recording) of the SLEs was 188.1 ± 132.0 μV^2 in the pPC (n = 10) 324.4 ± 148.3 μV^2 in the aPC (n = 9), 196.0 ± 150.5 μV^2 in the LEC (n = 5) and 250.8 ± 82.2 μV^2 in CA3 (n = 9) (figure 5.4 C). The latency to first SLE following 0$[Mg]^{2+}$ was 19.41 ± 3.9 mins in pPC (n = 10), 18.22 ± 1.9 mins in aPC (n = 9), 18.98 ± 4.9 mins in the LEC (n = 5) and 19.57 ± 3.2 mins in CA3 (n = 9) (figure 5.4 D). A Kruskal-Wallis test was used to identify significant differences between the four areas. There was no identifiable significant difference in power, IEI, frequency of SLEs or latency to first SLE between brain areas (figure 5.4 A-D).

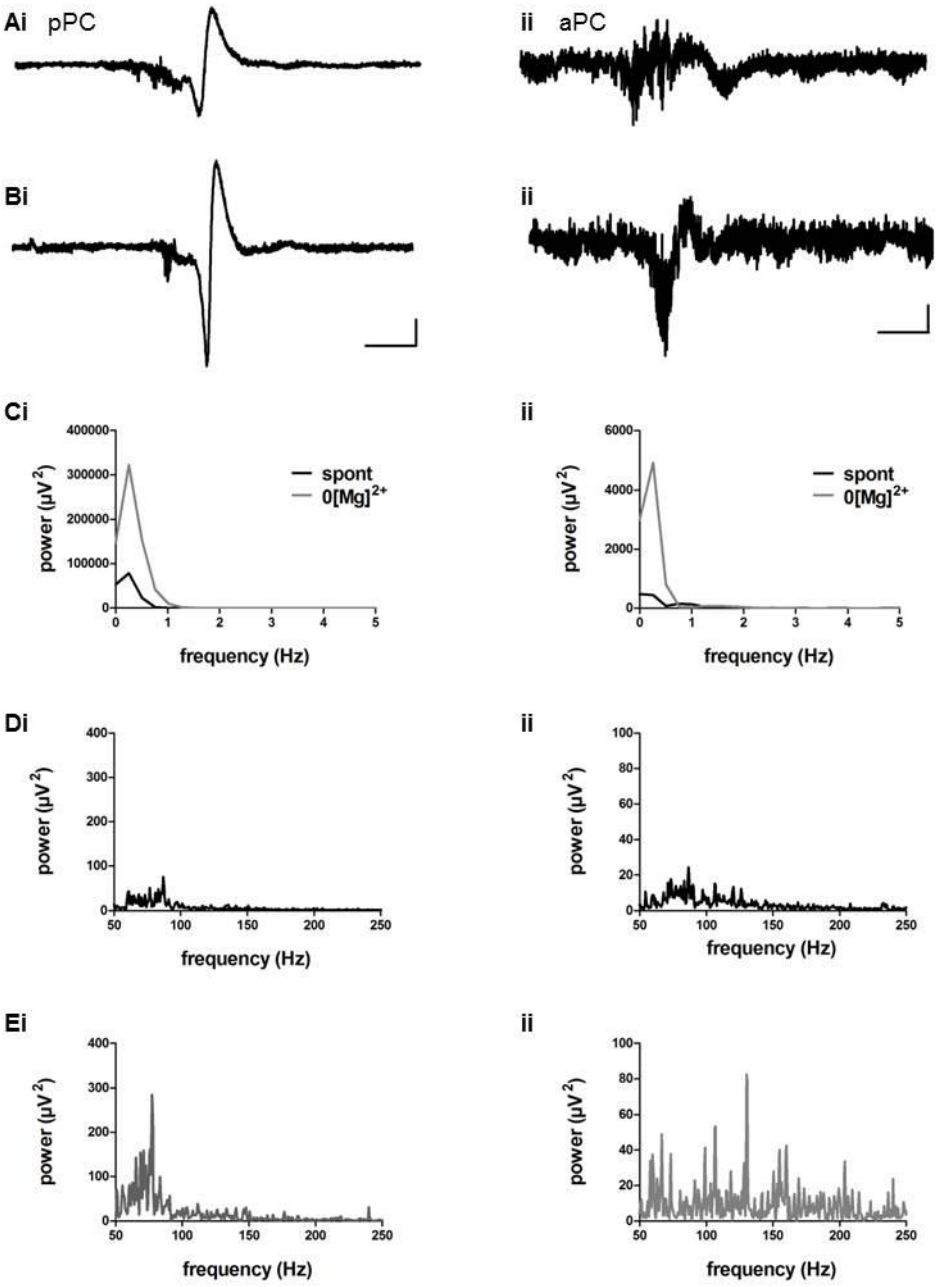

Figure 5.1 Comparison of spontaneous and 0[Mg]$^{2+}$ induced SLEs in the pPC (left) and aPC (right)
A) Example of spontaneous SLEs in the pPC (i) and aPC (ii) recorded in a horizontal slice preparation. Scale 5s Vs 500 μV^2 pPC, 5 s Vs 100 μV^2 aPC. B) Example of SLE in same brain slice following application of 0[Mg]$^{2+}$ aCSF for one hour in the pPC (i) and aPC (ii). C) Power spectrum generated from 10 seconds of raw data (FFT size 32768) showing the low frequency (DC shift) component of spontaneous (black) and 0[Mg]$^{2+}$ (grey) induced SLEs in the pPC (i) and aPC (ii). D) Power spectrum generated from 2 - 5 seconds of raw data (FFT size 32768) showing the HFO (50 – 250Hz) component of spontaneous (black) SLEs in the pPC (i) and aPC (ii). E) Power spectrum generated from 2 - 5 seconds of raw data (FFT size 32768) showing the HFO (50 – 250Hz) component of 0[Mg]$^{2+}$ (grey) induced SLEs in the pPC (i) and aPC (ii).

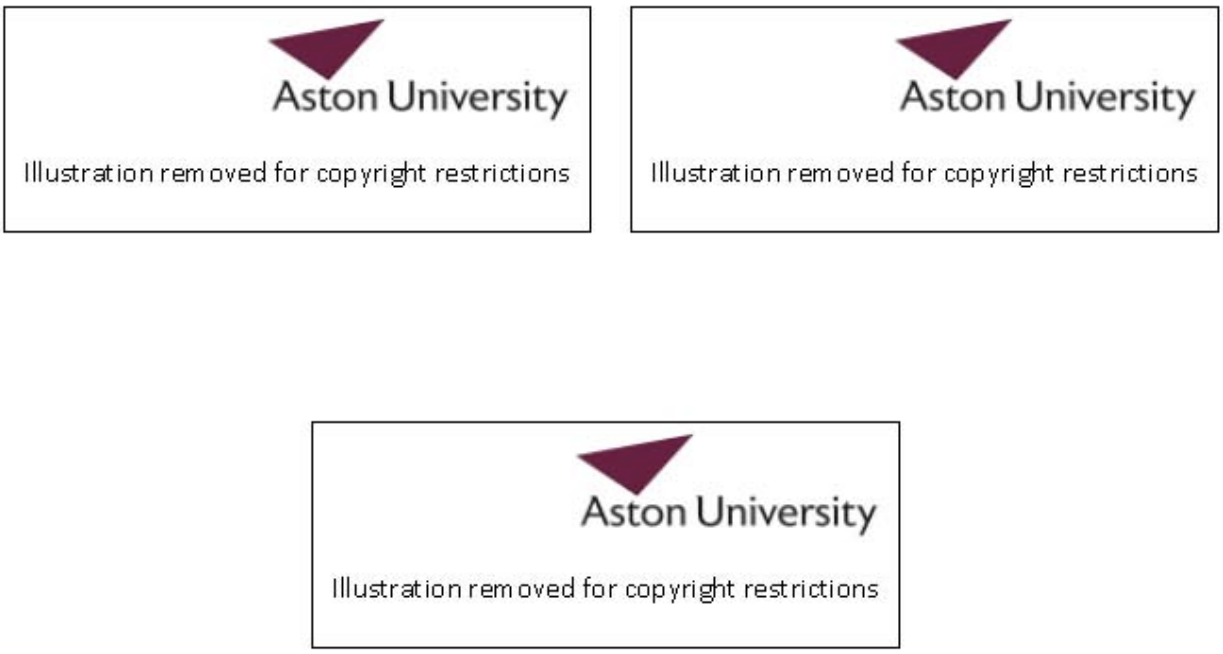

Figure 5.2 Multielectrode array recording of 0[Mg]$^{2+}$ induced epileptiform activity in the PC and surrounding areas *in vitro*

A) Image of a brain slice demonstrating the brain areas recorded with the multielectrode array. B) Multielectrode array placement. aPC – anterior piriform cortex, pPC – posterior piriform cortex, LOT – lateral olfactory tract, DEn – dorsal endopiriform cortex and CPu – striatum. C) 40s raw trace of multielectrode array recording. Each recording corresponds to electrode placement in B. Scale - 5 s Vs 200 µV. Slice image from (Williams and Rosen, 2003)

Figure 5.3 0[Mg]$^{2+}$ induced SLEs in the pPC, aPC, LEC and CA3 in connected slices *in vitro*
A) Image of a brain slice with electrode placement. Bi) Raw trace of representative SLE in the pPC, aPC, LEC and CA3 of a connected slice (scale 20 s Vs 500 μV^2). PC SLEs precede SLEs in the LEC and CA3. Bii) Expanded view of SLEs from Bi (see bars on Bi). Scale (2s Vs 500 μV^2). C) Graph demonstrating the maximal power in the 0 - 3 Hz frequency band (FFT size 32768) over time for the pPC (black), aPC (red), LEC (blue) and CA3 (green). D) Power spectrum generated from 2 - 5 seconds of raw data (FFT size 32768) showing the HFO (50 – 250Hz) component of pPC (black, i), aPC (red, ii), EC (blue, iii) and CA3 (green, iv). Slice image from (Williams and Rosen, 2003).

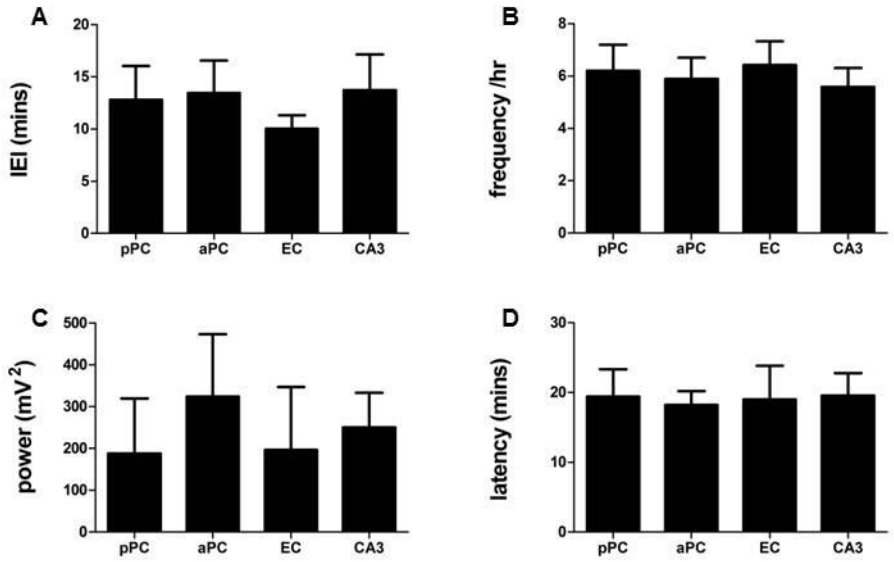

Figure 5.4 Properties of 0[Mg]$^{2+}$ SLEs in the pPC, aPC, LEC and CA3 in connected slices *in vitro*
A) Average IEI between the first three SLEs. B) Average frequency of SLEs per hour calculated from the first three SLEs. C) Maximal power in the 0 - 3 Hz frequency band (FFT size 32768) averaged from the first three SLEs. D) Average latency to first SLE. Data collected from pPC (n= 9), aPC (n = 9), EC (n = 5), CA3 (n = 9), data from brain areas which did not have SLEs were not included in this analysis

5.2.2 Connectivity between the temporal and olfactory regions does not alter the properties 0[Mg]$^{2+}$ induced SLEs

As there were no significant differences between frequency, power, IEI or latency to first SLE between the four brain regions, the experiments were repeated with slices that had been cut, separating the PC from the LEC and CA3 (figure 5.5 A). This was to assess if the excitability was influenced by reciprocal connections present between the brain areas.

Of the 10 slices tested, SLEs were recorded in 10/10 in aPC, 10/10 in pPC, 5/10 in LEC and 6/10 in CA3. SLEs appeared first in the PC in 7/10 of the slices tested (3/10 in pPC, 4/10 in aPC). SLEs were found simultaneously in all four brain regions in 4/10 slices tested. SLEs occurred with an average IEI of 14.17 ± 1.3 mins in pPC (n = 10), 14.69 ± 1.3 mins in aPC (n = 9), 11.21 ± 1.9 mins in LEC (n = 4) and 13.35 ± 1.8 mins in CA3 (n = 5) (figure 5.6 A). The frequency of SLEs was 4.5 ± 0.3 /hr in pPC, 4.35 ± 0.32 /hr in aPC, 5.88 ± 1.0 /hr in EC and 4.86 ± 0.7 /hr in CA3 (figure 5.5 B). The average maximum power of the SLEs DC shift was 55.07 ± 34.3 mV^2 in the pPC (n =10), 15.14 ± 4.4 mV^2 in the aPC (n = 9), 4.14 ± 2.5 mV^2 in the LEC (n = 5) and 189.80 ± 176.4 mV^2 in CA3 (n = 6) (figure 5.6 C). The latency to first SLE following 0[Mg]$^{2+}$ applications was 30.20 ± 5.9 mins in pPC, 29.71 ± 6.6 mins in aPC, 35.15 ± 6.4 mins in LEC and 22.65 ± 6.0 mins in CA3 (figure 5.6 D). A Kruskal-Wallis test

identified no significant differences in power, IEI, frequency of SLEs or latency to first SLE between brain areas (figure 5.6 A-D).

Figure 5.5 0[Mg]$^{2+}$ induced SLEs in the pPC, aPC, LEC and CA3 in cut slices *in vitro*
A) Image of a brain slice with electrode placement in a cut slice. B) Raw trace of representative SLEs in the pPC, aPC, LEC and CA3 of a cut slice (scale 2 s Vs 200 μV^2). SLEs did not occur at the same time. Slice image from (Williams and Rosen, 2003)

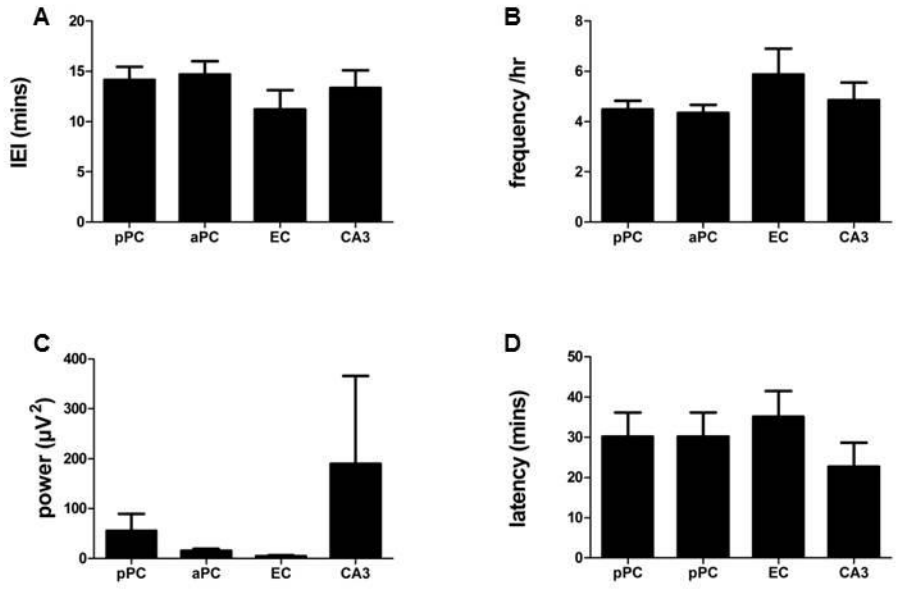

Figure 5.6 Properties of 0[Mg]$^{2+}$ SLEs in the pPC, aPC, LEC and CA3 in cut slices *in vitro*
A) Average IEI between the first three SLEs. B) Average frequency of SLEs per hour calculated from the first three SLEs. C) Maximal power in the 0 - 3 Hz frequency band (FFT size 32768) averaged from the first three SLEs. D) Average latency to first SLE. Data collected from pPC (n= 10), aPC (n = 9), EC (n = 4), CA3 (n = 5), data from brain areas which did not have SLEs were not included in this analysis

5.2.3 Comparison between cut and connected slices

Next, the difference in excitability of all four brain areas was assessed in connected (figure 5.3) and cut (figure 5.5) slices.

5.1.3.1 Posterior piriform cortex

There was no significant difference in IEI, frequency, power or latency to first SLE (figure 5.7) in 0$[Mg]^{2+}$ induced SLEs between connected (n = 9) and cut slices (n = 10) in the pPC.

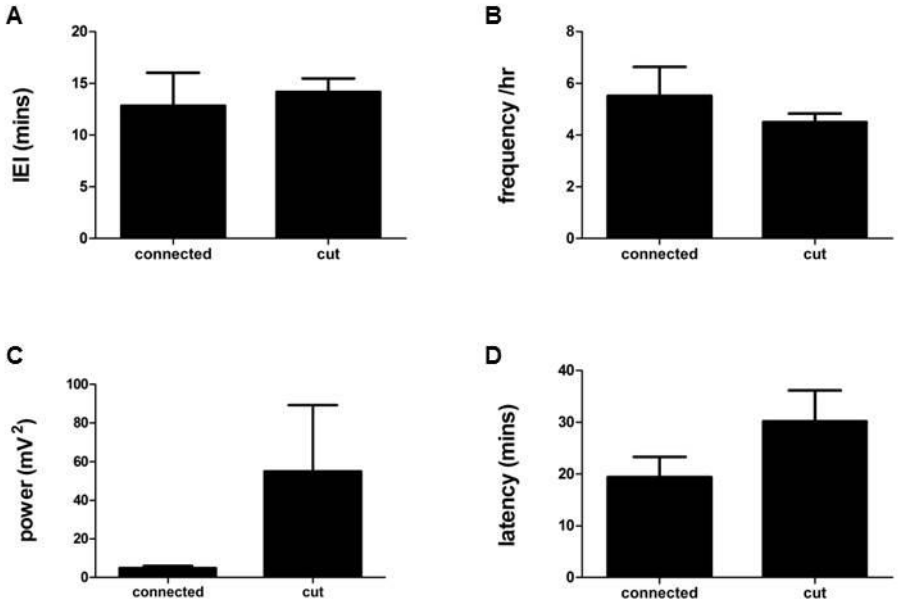

Figure 5.7 Comparison of 0$[Mg]^{2+}$ SLEs in pPC in cut and connected slices i*n vitro*

A) Average IEI between the first three SLEs. B) Average frequency of SLEs per hour calculated from the first three SLEs *in vitro*. C) Maximal power in the 0 - 3 Hz frequency band (FFT size 32768) averaged from the first three SLEs. D) Average latency to first SLE. Data collected from connected (n = 9) and cut (n = 10) slices. Data not included if no SLEs found in the brain region.

5.2.3.2 Anterior piriform cortex

There was no significant difference in IEI or frequency of 0[Mg]$^{2+}$ induced SLEs between connected (n = 9) and cut (n = 9) slices of aPC (figure 5.8). There was a general trend towards lower amplitude of the power in cut slices; however this was not significant (P > 0.05) (figure 5.8 C). Connected slices (18.22 ± 1.9 mins) had a significantly (P < 0.05) shorter latency to first SLE compared to cut slices (29.71 ± 6.6 mins).

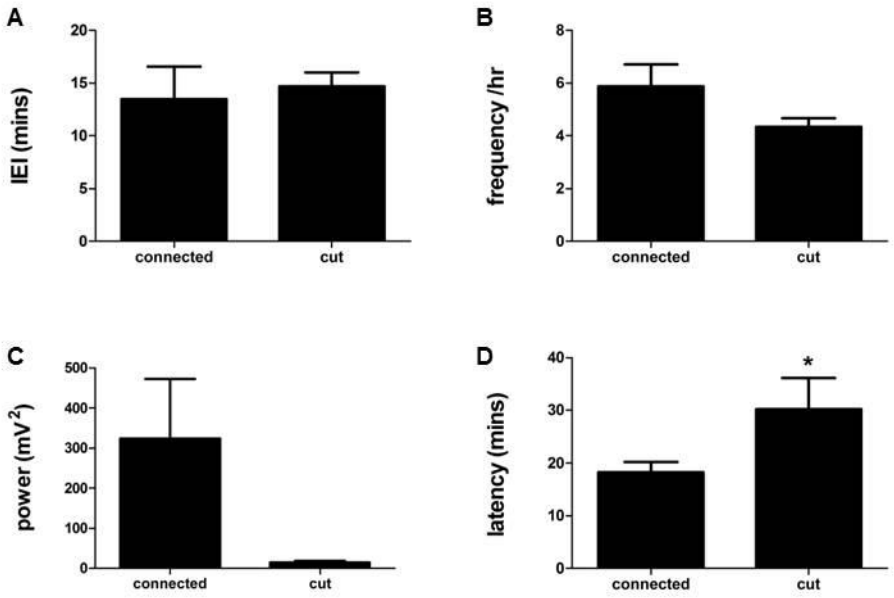

Figure 5.8 Comparison of 0[Mg]$^{2+}$ SLEs in aPC in cut and connected slices i*n vitro*

A) Average IEI between the first three SLEs. B) Average frequency of SLEs per hour calculated from the first three SLEs *in vitro*. C) Maximal power in the 0 - 3 Hz frequency band (FFT size 32768) averaged from the first three SLEs. D) Average latency to first SLE. Data collected from connected (n = 9) and cut (n = 9) slices. Data not included if no SLEs found in the brain region.

5.2.3.3 Lateral entorhinal cortex

There was no significant difference in IEI, frequency or latency to first SLE in 0[Mg]$^{2+}$ induced SLEs between cut (n = 4) and connected (n = 5) LEC slices (figure 5.9). Connected slices had a significantly higher amplitude low frequency (0 - 3 Hz) DC shift (196.0 ± 150.5 mV^2) than cut slices (4.14 ± 2.5 mV^2).

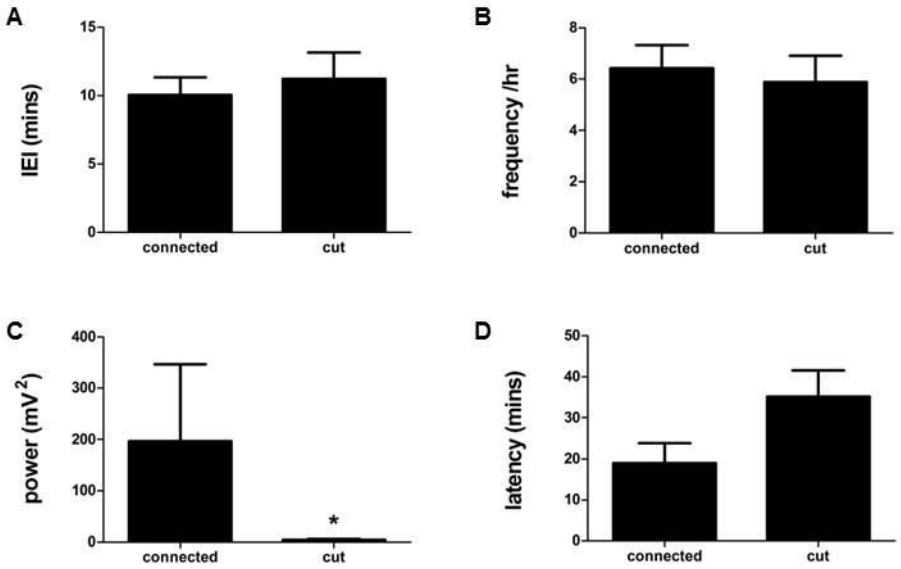

Figure 5.9 Comparison of 0[Mg]$^{2+}$ SLEs in LEC in cut and connected slices i*n vitro*

A) Average IEI between the first three SLEs. B) Average frequency of SLEs per hour calculated from the first three SLEs *in vitro*. C) Maximal power in the 0 - 3 Hz frequency band (FFT size 32768) averaged from the first three SLEs. D) Average latency to first SLE. Data collected from connected (n = 5) and cut (n = 4) slices. Data not included if no SLEs found in the brain region.

5.2.3.4 CA3

There was no significant difference in IEI, frequency, power or latency to first SLE (figure 5.10) in 0[Mg]$^{2+}$ induced SLEs between connected (n=9) and cut slices (n = 5) in the CA3 region of the hippocampus.

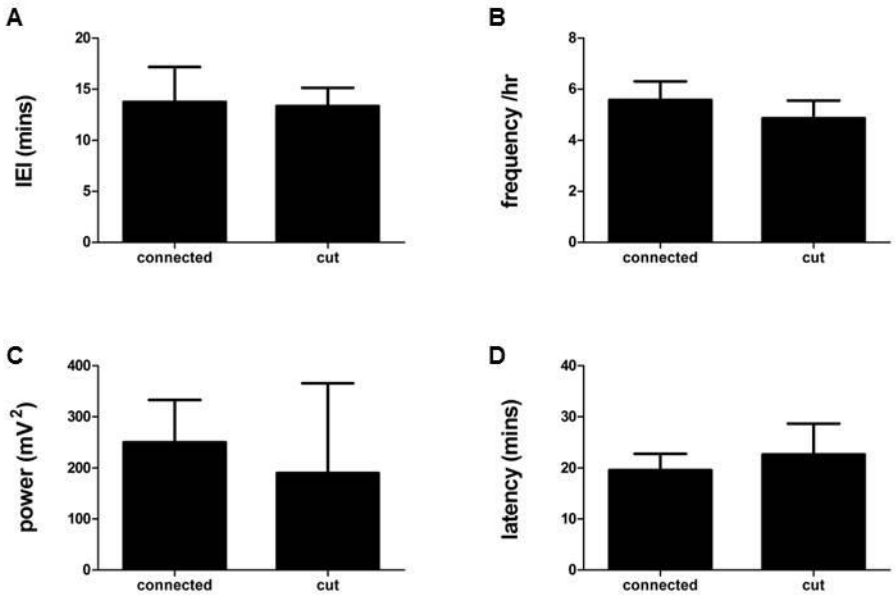

Figure 5.10 Comparison of 0[Mg]$^{2+}$ SLEs in CA3 in cut and connected slices i*n vitro*

A) Average IEI between the first three SLEs. B) Average frequency of SLEs per hour calculated from the first three SLEs *in vitro*. C) Maximal power in the 0 - 3 Hz frequency band (FFT size 32768) averaged from the first three SLEs. D) Average latency to first SLE. Data collected from connected (n = 9) and cut (n = 5) slices. Data not included if no SLEs found in the brain region.

5.2.4 Enhanced excitability of piriform cortex slices prepared during epileptogenesis

The frequency of 0[Mg]$^{2+}$ induced SLEs was no different between the cut and connected slices in any of the four brain regions tested suggesting that the reciprocal connections were not conducting the SLEs between brain regions in the slice preparation. As the PC was found to be more sensitive to SLE induction than CA3 and the LEC, the properties of SLEs in this brain region were assessed over the course of epileptogenesis. The sensitivity of the recently developed RISE (Modebadze et al., 2016) model of epilepsy to 0[Mg]$^{2+}$ induced SLEs was evaluated at four time points (24 hours, 1 week (early latent period), 4 weeks (mid latent period) and 3 months+ (chronic period)) post SE compared to age-matched controls (AMCs). To maximise data collection and minimise animal usage coronal aPC slices were used. The properties of these SLEs were evaluated from the first three SLEs; following this the slices were used to assess sensitivity to AEDs (chapter 6). This accounts for the high n numbers presented (n = 48 for each condition). The IEI between SLEs, the frequency of SLEs, latency to first SLE and the percentage of slices which showed SLEs were compared (figure 5.11). All data presented in graphs were ranked to make the data normally distributed and a

between subjects ANOVA was used to assess significant differences between groups (figure 5.11). The raw mean (and standard error of the mean) data for each condition is presented in table 5.1.

5.2.4.1 SLE inter-event interval

The IEI between 0$[Mg]^{2+}$ induced SLEs were compared at four stages of epileptogenesis to AMCs (figure 5.11 A). One outlier was identified (1.5 x interquartile range) and removed. There was a significant interaction effect between age and epileptic state F(degrees freedom, error) = (3, 335) = 8.550 P < 0.000. Specifically, the IEI between SLEs in slices prepared from SE animals was significantly longer at 24 hours post SE (P = 0.016) compared to AMCs. The IEI between SLEs in slices prepared from SE animals was significantly shorter at 4 weeks (P < 0.000) and 3 months+ (P = 0.018) post SE compared to AMC. There was an overall significant difference between SE and AMCs F(degrees freedom, error) = (3, 335) = 9.328 P = 0.002. There was also an overall significant difference between age groups F(degrees freedom, error) = 11.898 P < 0.000. Specifically, the IEI between SLEs was significantly shorter in slices prepared from SE and AMC animals at 24 hours post SE compared to 4 weeks (P = 0.012) and 3 months+ (P < 0.000) post SE. The IEI was also significantly shorter in slices prepared from SE and AMC animals at 1 week compared to 4 weeks (P = 0.037) and 3 months+ (P < 0.000) post SE.

5.2.4.2 Frequency of SLEs

The frequency of 0$[Mg]^{2+}$ induced SLEs at four stages of epileptogenesis were compared to AMCs (figure 5.11 B). One outlier was identified and removed. There was a significant interaction effect between epileptic state and age F(degrees freedom, error) = (3, 375) = 11.319 P < 0.000. Specifically, the frequency of SLEs was lower in slices prepared from AMC compared to SE animals at 24 hours post SE (P = 0.002). The frequency of SLEs was higher in slices prepared from SE compared to AMC animals at 4 weeks post SE (P < 0.000) and 3 months+ post SE (P = 0.001). There was an overall significant difference between SE and AMC F(degrees freedom, error) = (3,375) = 8.716 P = 0.003. There was also an overall significant difference between age groups F(degrees freedom, error) = (3, 375) = 8.716 P < 0.000. Specifically, there was a significantly lower frequency of SLEs in slices prepared from SE and AMC animals at 3 months+ compared to 24 hours (P = 0.003) and 1 week (P = 0.050) post SE.

5.2.4.3 Latency to first SLE

The latency to first 0$[Mg]^{2+}$ induced SLE in slices prepared at four stages of epileptogenesis was compared to AMCs (figure 5.11 C). No outliers were identified. There was a significant interaction effect between status and age F(degrees freedom, error) = (3, 328) = 3.548 P = 0.015. Specifically, the latency to first SLE was significantly shorter in slices prepared from SE compared to AMC at 4 weeks post SE (P < 0.000). There was an overall significant difference between SE and AMC F(degrees freedom, error) = (3, 328) = 4.199 P = 0.041.

There was also an overall significant difference between age groups F(degrees freedom, error) = (3, 328) = 15.293 P < 0.000. Specifically, the latency to first SLE for slices prepared from SE and AMC animals was significantly longer at 3 months+ post SE compared to 24 hours (P < 0.000), 1 week (P < 0.000) and 4 weeks (P = 0.01) post SE. The latency to first SLE was significantly longer for slices prepared from SE and AMC animals at 4 weeks post SE compared to 1 week post SE (P = 0.015).

5.2.4.4 Percentage of slices that had SLEs

The percentage of slices that showed SLEs when 0$[Mg]^{2+}$ aCSF was applied was compared to AMCs at 4 stages of epileptogenesis (figure 5.11 D). There was no significant interaction effect between epileptic state and age. There was also no significant difference between SE and AMC. There was no significant difference between age groups.

In summary, the main finding from these experiments was the notable increased frequency of SLEs in the PC from SE-experienced animals compared to controls, which was especially robust at later stages after SE (4 weeks and 3 months).

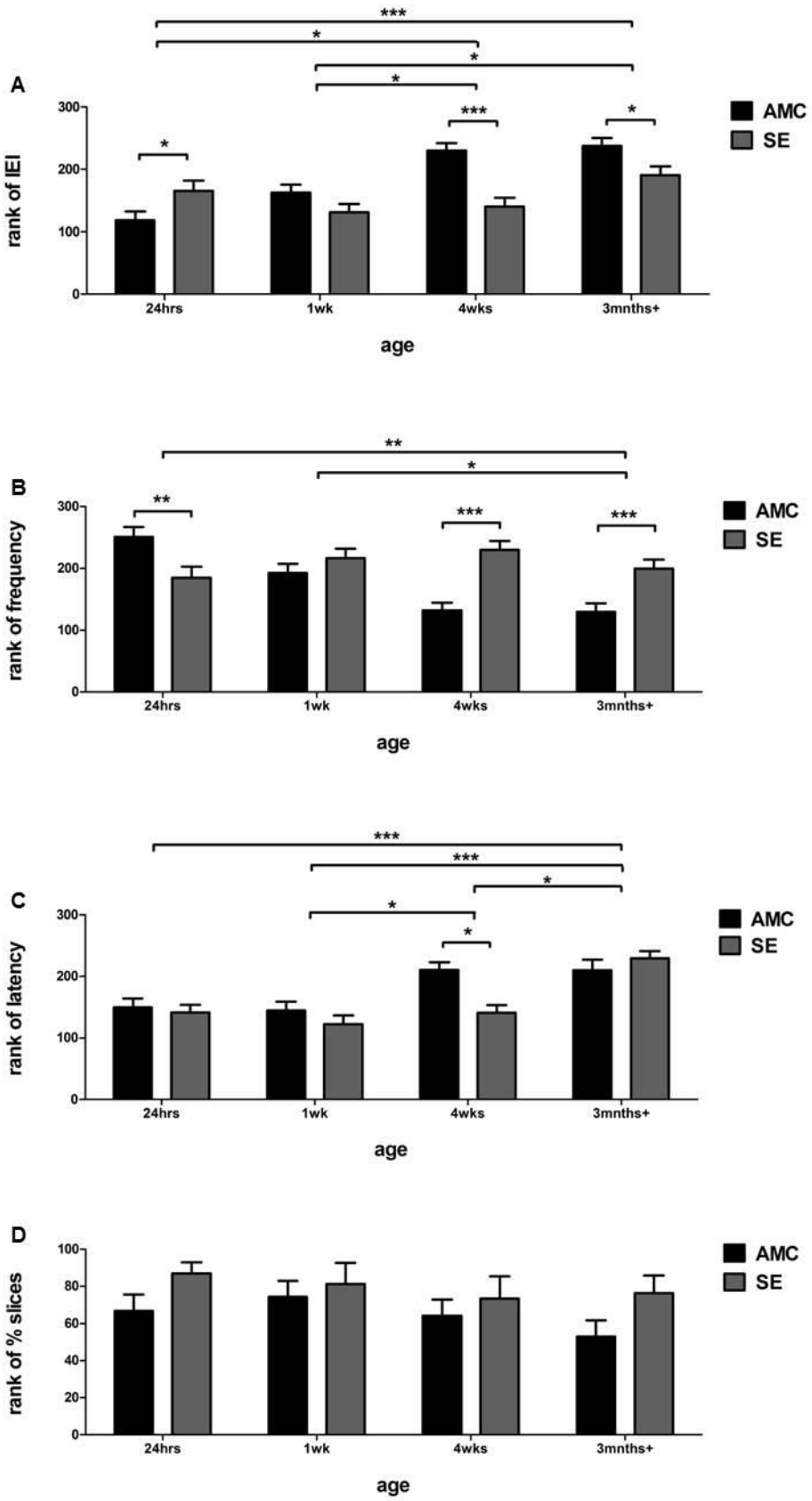

Figure 5.11 Comparison of the properties of 0[Mg]$^{2+}$ induced SLEs in the piriform cortex in slices prepared from rats at four time points after epilepsy induction compared to AMC

A) Ranked inter-event interval (IEI) between SLEs. B) Ranked frequency of SLEs per hour. C) Ranked latency to first SLE. D) Ranked percentage of slices that had SLEs.

age/status	n	IEI (mins)	frequency (/hr)	latency to first SLE (mins)	% slices with SLEs
24hrs AMC	48	12.86 ± 0.95	5.64 ± 0.30	31.34 ± 2.38	75.00 ± 5.41
24hrs SE	48	15.38 ± 1.02	4.54 ± 0.26	30.24 ± 2.21	87.72 ± 3.08
1 wk AMC	48	14.98 ± 0.85	4.50 ± 0.22	31.08 ± 2.80	80.10 ± 5.00
1 wk SE	48	13.02 ± 0.66	5.04 ± 0.30	27.70 ± 2.54	82.14 ± 7.35
4 wks AMC	48	19.96 ± 1.34	3.67 ± 0.15	42.30 ± 2.62	73.33 ± 5.56
4 wks SE	48	14.08 ± 1.02	5.10 ± 0.24	29.25 ± 1.91	78.47 ± 7.50
3 mnths+ AMC	48	23.96 ± 2.79	3.69 ± 0.18	48.33 ± 4.29	65.53 ± 5.78
3 mnths + SE	48	17.65 ± 1.33	4.57 ± 0.21	50.52 ± 4.21	81.25 ± 5.67

Table 5.1 Table summarising the properties of 0[Mg]$^{2+}$ induced SLEs in the PC in slices prepared from rats at four time points after epilepsy induction compared to AMCs.
Raw inter-event interval, frequency (per hour), latency to first SLE (minutes) and percentage of slices that showed SLEs in slices prepared from the PC at four stages of epileptogenesis (24 hours, 1 week, 4 weeks and 3 months) and age-matched controls. Mean ± standard error of the mean.

5.2.4.5 Persistence of SLEs in vitro

In order to assess the PC's sensitivity to AEDs (chapter 6), the SLEs needed to persist for the length of the experiment. 0[Mg]$^{2+}$ was applied to slices at four stages of epileptogenesis (and AMCs) and recorded for an extended period of time (5 hours). In order to perform the experiments SLEs would need to persist for at least 120 minutes. The SLEs persisted for more than this at all eight time points tested (table 5.2).

	AMC		**SE**	
time point	n number	time (mins)	n number	time (mins)
24 hrs	4	254.6 ± 15.2	3	238.6 ± 37.1
1 wk	4	285.7 ± 21.1	4	290.9 ±25.0
4 wks	4	283.8 ±13.2	4	216.4 ± 61.6
3 mnths +	6	216.1 ± 32.5	4	159.3 ±31.8

Table 5.2 The length of time SLEs persisted for during 0[Mg]$^{2+}$ application in the piriform cortex
The persistence of the SLEs was investigated at 4 stages of epileptogenesis and equivalent AMCs. Mean ± standard error of the mean.

5.3 Discussion

The hippocampus and EC have dominated the field of epilepsy research in the past, despite identification of the PC in 1985 as being more sensitive to seizure induction than these regions (Piredda and Gale, 1985a; Piredda and Gale, 1985b; McIntyre and Gilby, 2008). This has been further confirmed in this chapter as 0$[Mg]^{2+}$ aCSF induced SLEs were observed in the PC first in 9/10 brain slices containing aPC, pPC, LEC and CA3. The properties of these SLEs were very similar in all four brain regions investigated. To assess if the properties of these SLEs were intrinsic to the brain regions or influenced by connections between regions, the slices were cut between the temporal and olfactory areas. The majority of these properties remained the same with SLEs still beginning in the PC first in the majority (7/10) of slices tested. The excitability of slices prepared from animals that had undergone the RISE protocol for epilepsy induction were assessed via 0$[Mg]^{2+}$ induction of epileptiform activity and compared to AMCs. The IEI and latency to first SLE, was lower in SE compared to AMCs indicating PC slices prepared from the RISE model of epilepsy are more excitable than AMCs.

5.3.1 The piriform cortex is more susceptible to SLE induction than CA3 and the lateral entorhinal cortex *in vitro*

Application of 0$[Mg]^{2+}$ aCSF induced both inter-ictal events (IIEs) (data not shown) and SLEs in the anterior and posterior PC *in vitro*. These SLEs consisted of HFOs (50 – 250 Hz) at the beginning of a slow DC shift. The MEA data suggested that these SLEs originate in the deeper PC layers as previously found (Hollmann et al., 1991). The MEA also identified a very similar pattern of epileptiform activity in the anterior and posterior PC and the surrounding areas with HFO activity at the beginning of the slow shift in baseline followed by a period of decreased electrical activity.

The slow DC shift has been under reported both in human and animal studies possibly due to high pass filtering being set too high during EEG recordings (Rodin and Modur, 2008). This shift in baseline closely resembles tonic seizures recorded *in vivo* in patients (Ikeda et al., 1997), which consist of sustained muscle contraction resulting from prolonged neuronal depolarisation (Traynelis and Dingledine, 1988; McNamara, 1994). The DC shift is further associated with a rise in extracellular K^+ and has been found in a number of brain regions *in vitro* including the olfactory bulb and CA1 (Lux et al., 1985; Konnerth et al., 1986; Lewis et al., 1990; Jensen and Yaari, 1997; Igelström et al., 2011). Earlier intracellular recordings in the PC with 0$[Mg]^{2+}$ aCSF have demonstrated paradoxical depolarising shifts and rhythmic bursting of action potentials (Libri et al., 1996; Whalley et al., 2009). Previous extracellular recordings have reported much shorter duration, higher frequency epileptiform activity compared to those found in this study (Libri et al., 1996; Whalley et al., 2009). Those reported previously more closely resemble a period of SE whereas the SLEs found in this

study more closely resemble tonic seizures. This likely reflects differences in preparation of neuronal tissue.

HFOs were found during the few seconds preceding a SLE (pre-ictal stage) and the first few seconds of the SLE. This oscillatory activity was found to be of a lower amplitude than the DC shift and primarily in the high gamma (60 - 100 Hz) frequency range. HFO activity commonly occurs during the pre-ictal phase and seizure initiation in epileptic patients (Arroyo and Uematsu, 1992; Traub et al., 2001b; Jirsch et al., 2006; Jacobs et al., 2009; Khosravani et al., 2009). This activity is thought to be independent of synaptic activity, instead depending on gap junctions, although this was not assessed in this study (Traub et al., 2001b). Lower frequency oscillatory activity (30 - 60 Hz) has also been observed in the PC following 4-AP application in a whole guinea pig brain preparation. These oscillations were generated in the aPC and propagated to the pPC and LEC (Uva et al., 2005; Carriero et al., 2010). Interestingly, in the studies of Uva and Carreiro, SLEs were not found in the PC but were found in the EC and CA1. However, since then IIE and SLEs have been reported in the PC in both coronal and sagittal PC brain slices (Panuccio et al., 2012).

The PC has been previously identified as more sensitive to chemical kindling than other areas of the brain more commonly associated with epilepsy (hippocampus and amygdala) (Piredda and Gale, 1985a; Piredda and Gale, 1985b). Since then, the PC has been identified as one of the most sensitive areas of the brain to electrical kindling and one of the regions most damaged in SE models of epilepsy (Wall et al., 2000; André et al., 2007; McIntyre and Gilby, 2008). In a whole brain preparation *in vitro*, epileptiform activity has been found to begin in the PC before the EC and hippocampus (Uva et al., 2005; Carriero et al., 2010). To further confirm the PC's sensitivity to induction of epileptiform activity in comparison to the hippocampus and EC these four (separating the PC into aPC and pPC) areas were investigated in a brain slice preparation. A brain slice containing all four areas, removes much of the bias that can be introduced when using multiple slices, ie differences in slicing speed or section, differences in period of time spent in incubation chamber, recording chamber flow rate, humidity and temperature. The SLEs induced by $0[Mg]^{2+}$ aCSF application were very similar in all four areas, with a slow DC shift and HFO activity. In the majority of slices tested (9/10), SLEs induced by $0[Mg]^{2+}$ aCSF application were first recorded in either the aPC or pPC, although this did not translate to a significant difference in latency to first SLE. This is most likely because latency to first SLE varied considerably between slices whilst in general SLEs were found in the pPC or aPC earlier than in CA3. This further reinforced the need to compare these four areas in joined slices subjected to the same conditions.

Epileptiform activity induced by $GABA_A$ receptor blockade in slices has been found to be similar in frequency in the pPC and surrounding neocortex (Rigas and Castro-Alamancos,

2004). When the connections between the pPC and neocortex were severed, the epileptiform activity in the pPC continued at the same frequency, whilst the frequency in the surrounding neocortex slowed down implying the pPC had been driving this activity (Rigas and Castro-Alamancos, 2004). In this study no significant differences in SLE IEI, frequency or power between PC, CA3 and EC were found, therefore the possibility that one of these regions was driving the SLEs was investigated. To explore this, the experiments were repeated with a cut between the temporal and olfactory regions to assess if the properties of 0$[Mg]^{2+}$ induced SLEs were intrinsic to the brain areas tested, or influenced by possible connections between the regions. The SLEs were similar in appearance to those produced in connected slices with HFOs and a slow DC shift found in the majority of recordings. As before, SLEs were recorded in the PC regions before the EC/CA3 in the majority of slices tested and again this did not translate to a significant difference in latency to first SLE. SLEs were found in the aPC and pPC in the majority of slices tested, but, unlike in connected slices, SLEs were found in CA3 in only 6/10 (compared to 9/10) slices tested. This difference was not subjected to any statistical analysis, but nonetheless it could suggest that excitability of CA3 is influenced by the PC. However, as there were no significant differences in the properties of 0$[Mg]^{2+}$ induced SLEs between the brain areas, or between cut and connected slices in CA3, this is unlikely to be the case. The MEA recording in the PC and surrounding area also suggested excitatory activity does not originate in the PC and spread to other regions of the brain in horizontal brain slices, instead the SLEs have multiple sites of origin.

5.3.2 Alterations in the properties of induced epileptiform activity in the piriform cortex during epileptogenesis *in vitro*

The electrophysiological properties of SLEs induced via application of 0$[Mg]^{2+}$ aCSF were compared at four stages of epileptogenesis to AMCs. Although SLEs were found in a similar percentage of slices in AMC compared to SE at all time points, there were significant differences in the IEI, frequency and latency to first SLE.

The PC is a highly excitable area of the brain; even before kindling IIEs have been observed in the PC *in vivo* (Kairiss et al., 1984; Racine et al., 1988a). A high proportion of slices developed SLEs in slices prepared from PC (65 - 88 %), with a similar proportion of SLEs found in slices prepared from SE and AMC animals for all age groups. Spontaneous discharges (IIEs) and 0$[Mg]^{2+}$ induced SLEs have been previously found in a similar proportion of slices prepared from fully kindled animals compared to AMCs in the PC (McIntyre and Plant, 1993). In contrast, 0$[Mg]^{2+}$ induced SLEs occured in <50 % slices in the EC for SE animals and <20 % for AMCs (3 months+) (Shah, 2017). This further supports the hypothesis that the EC is less excitable and less seizure sensitive than the PC.

An age-dependent increase in latency to first SLE was observed in PC slices in this study. This was not unexpected as an age-dependent increase in latency has been previously demonstrated in 0$[Mg]^{2+}$ induced SLEs in the EC (Gloveli et al., 1995; Buchheim et al., 1999;

Holtkamp et al., 2011). Although one study has found no difference in latency to first SLE between 3 - 4 month and 24 month old rats (Holtkamp et al., 2003). However, as the risk of seizures is thought to be highest in the very young and the very old, seizure threshold is highest in middle age (Tallis et al., 1991; Bell and Sander, 2001; WHO, 2012). As the oldest rats in this study (4 – 8 months) were younger than those in the previous study (Holtkamp et al., 2003), the longer latency to first seizure likely reflects an increased seizure threshold in middle age.

The latency to first SLE was identical in SE and AMC in this study, except at 4 weeks post SE. A previous study found the latency to first SLE to be significantly shorter in SE (kindled) compared to AMC in the EC (Holtkamp et al., 2011) . However, in the PC, kindling has been found to be associated with an increase in latency to first IIE compared to AMCs (McIntyre and Plant, 1993). In this study, the latency to first SLE was significantly shorter in SE compared to AMC at 4 weeks alone. For all other age groups the latency to first SLE was mirrored in both SE and AMC. This may reflect transient changes in excitability of the PC over the course of epileptogenesis.

The frequency of SLEs in the PC was significantly lower in SE animals compared to AMC at 24 hours post SE. At one week there was no difference between SE and AMC and at 4 weeks and 3 months+ the frequency was significantly lower in AMC compared to SE. This difference in frequency of SLEs appears to be due to decreased frequency of SLEs with age in slices prepared from AMC animals. This effect is absent in slices prepared from SE animals as they maintain a high frequency of SLEs which is comparable to the frequency found in young animals. This indicates an enhanced level of excitability usually associated with slices prepared from young animals is maintained in slices prepared from animals during epileptogenesis. A similar trend has also been observed in the EC following kindling induced SE (Holtkamp et al., 2011). No difference in frequency of 0$[Mg]^{2+}$ induced SLEs was found at 1 week, however at 4 weeks (latent period) and 8 weeks (chronic) post SE the frequency was observed to be higher in SE compared to AMC indicating increased excitability of slice (Holtkamp et al., 2011). Increased SLE frequency has been previously proposed to result from a reduction in feed-forward inhibition (Trevelyan et al., 2007). Alterations in inhibition have been commonly reported in a number of brain regions including the PC in the latent period (Lehmann et al., 1998; Loscher et al., 1998; Holtkamp et al., 2005; Freichel et al., 2006). NMDA receptor expression and function are also altered over the course of epileptogenesis. In particular, NMDA autoreceptors were found to be decreased during development, an effect not seen in slices prepared from chronic (pilocarpine) epileptic rats (Yang et al., 2006). As 0$[Mg]^{2+}$ application induces SLEs primarily by unblocking NMDA receptors, the increased NMDA receptor expression might explain why the frequency of SLEs remains stable during epiletogensis whilst there is a decrease in excitability in slices prepapred from AMC animals.

No difference in SLE amplitude or duration has been recorded in EC slices prepared from AMC compared to kindled animals (Holtkamp et al., 2011). Amplitude and duration were not analysed in this chapter as it might have introduced bias into the data set. Duration in particular is subject to substantial analytical bias particularly as the SLEs were analysed manually and dependent on the experimenter identifying the start and end of an SLE. SLE amplitude was not recorded, as many SLEs saturated the amplifier thereby exceeding the recording window and making assessment of SLE amplitude difficult. Excluding those that saturated the window or recording the amplitude as the maximal power the amplifier allowed were considered, however this would likely introduce bias particularly if one group was more likely to saturate the amplifier than others.

For the first time SLEs have been induced by 0$[Mg]^{2+}$ aCSF in the PC over the course of epileptogenesis in comparison to AMCs. The persistence of these SLEs over time and the high proportion of slices which develop SLEs, in comparison to the EC, indicates this model of epileptiform activity is better suited for the screening of antiepileptic drugs (AEDs) than classically used EC slices (Walther et al., 1986; Stanton et al., 1987; Dreier and Heinemann, 1990; Zhang et al., 1995; Dreier et al., 1998).

5.3.3 Final Conclusions

0$[Mg]^{2+}$ application reliably induced both IIEs and SLEs in the aPC and pPC *in vitro*. These SLEs consisted of HFO activity and a slow DC shift in baseline and were similar to tonic epileptic seizures recorded in human patients *in vivo*. Furthermore, the PC was found to be more sensitive to SLE induction than other areas of the brain more commonly associated with epilepsy (LEC and CA3). SLEs in the PC were generated independently of the LEC and CA3 regions but shared similarities in frequency, IEI and power. The latency to first SLE, IEI and frequency of SLEs induced by 0$[Mg]^{2+}$ application in the PC were altered during ageing with an increased latency to first SLE and increased IEI observed. The alteration in frequency and IEI were absent in slices prepared from animals which had undergone the RISE protocol for epilepsy induction. The differences in the properties of 0$[Mg]^{2+}$ induced SLEs in the PC over epileptogenesis indicates the excitability of the slices changes during the establishment of epilepsy when compared to AMCs suggesting that epileptogenesis is a dynamic process. The sensitivity of these SLEs to AED treatment may also change over the time course of epileptogenesis.

Chapter 6 Characterisation of the sensitivity of piriform cortex slices prepared using the RISE model of epilepsy to antiepileptic drug treatment

6.1 Introduction

Epilepsy is one of the most common neurological disorders, affecting ~50 million people worldwide (WHO, 2012). Despite a range of available antiepileptic drugs (AEDs), drug resistance in found in ~30 % of patients (Cockerell et al., 1995; Kwan and Brodie, 2000; WHO, 2012). Some of these patients may be offered surgery to remove the epileptic focus, however, surgery carries significant risk and many patients are not good candidates (e.g area of the brain not possible to remove without neurological impact). This clearly indicates a need for further development of AEDs and effective screening models. A number of animal models of epilepsy are available and used for AED screening (Goddard, 1967; Nadler et al., 1978; Turski et al., 1983b), however, many are associated with very high mortality and morbidity and the pathophysiology does not always closely resemble that found in human disease. The RISE model of epilepsy, a modified lithium-pilocarpine model, was developed to reduce morbidity and mortality associated with older models whilst maintaining epileptogenicity (Modebadze et al., 2016).

The piriform cortex (PC) is a highly excitable, seizure sensitive region of the brain, which is thought to be involved in epileptogenesis (Piredda and Gale, 1985a; McIntyre and Gilby, 2008). This view was supported by data presented in chapter 5, as the PC was found to be more susceptible to induction of epileptiform activity *in vitro* compared to the lateral entorhinal cortex (LEC) and the CA3 region of the hippocampus. In traditional pilocarpine models, the PC is extensively damaged following status epilepticus (SE) making assessment of the electrophysiological properties of slices very difficult (Sloviter, 2005). In contrast, we have shown that there is minimal damage in PC slices prepared from the RISE model (Modebadze et al., 2016), indicating networks of excitatory and inhibitory neurons critical for PC function are still present and that gross neuronal network damage *per se* is not critical for the development of chronic epilepsy. Hence, the RISE model provides an opportunity to investigate PC function in the development of epilepsy.

The zero Mg^{2+} ($0[Mg]^{2+}$) model is one of the most widely used acute *in vitro* models of epileptiform activity. Bath application of aCSF with $0[Mg]^{2+}$ elicits seizure-like events (SLEs) and inter-ictal events (IIEs). AED efficacy and mechanism of action can be assessed in a basic preparation before other factors (e.g pharmacokinetics and drug interactions) are considered (Heinemann et al., 2006; Reddy and Kuruba, 2013). To date, entorhinal-hippocampal slices have primarily been used for this purpose. Initial epileptiform activity (SLEs) induced by $0[Mg]^{2+}$ has been found to be sensitive to blockade with common AEDs (carbamazepine, phenobarbital, midazolam, valproate and ethosuximide). However, this epileptiform activity has been reported to transition into late recurrent discharges (LDRs) which become AED insensitive 1-2 hours following $0[Mg]^{2+}$ application (Zhang et al., 1995; Dreier et al., 1998; Quilichini et al., 2003). Application of $GABA_A$ receptor agonists or GABA was found to abolish these LRDs whilst $GABA_A$ receptor positive modulators (such as

phenobarbital) had no effect, implying the transition from pharmacosensitivity to pharmacoresistance might be due to diminishing GABA (Heinemann et al., 1994; Pfeiffer et al., 1996). In the hippocampus and entorhinal cortex, the switch between SLEs and LRDs is accompanied by a change in epileptiform pattern that is not seen in the PC (chapter 5). 0$[Mg]^{2+}$ application in a PC slice preparation has been previously found to induce paroxysmal depolarising shifts and burst firing, originating in deep layer III and the endopiriform layer (Hoffman and Haberly, 1991a; Hoffman and Haberly, 1991b; McIntyre and Plant, 1993; Libri et al., 1996; Whalley et al., 2009). We found that spontaneous (i.e. without 0$[Mg]^{2+}$ application) SLEs were observable in slices prepared following RISE animals (from now on referred to as post SE) and sometimes in age-matched control (AMC) animals (chapter 5), however, these were not reliable and were of a low amplitude. Hence, 0$[Mg]^{2+}$ application was used to reliably induce regular, high amplitude SLEs in slices prepared from both SE and AMC animals in the PC (chapter 5), and this method was chosen to perform further studies.

6.1.1 Antiepileptic drugs and the piriform cortex

Despite identification of the PC as more epileptogenic than other brain areas more commonly associated with epilepsy (chapter 5) (Piredda and Gale, 1985a; McIntyre and Gilby, 2008), the sensitivity (or resistance) of this area to AEDs has never been explored (although see Whalley et al., 2009). In chapter 5, the PC was found to be acutely sensitive to SLE induction via 0$[Mg]^{2+}$ application in slices prepared from both SE and AMC animals. However, this sensitivity was altered with age, with a decrease in SLE frequency and an increase in latency to first SLE in aged animals. These effects were less prominent in slices prepared from animals that had undergone the RISE protocol for epilepsy induction, indicating a state of underlying hyperexcitability in the post SE condition. Given that this alteration likely indicates an adaptive or maladaptive change in excitability of the PC in RISE animals, the sensitivity or resistance to AED treatment might also vary. Using the 0$[Mg]^{2+}$ model of seizures *in vitro* with the RISE model of epilepsy allows for the assessment of an individual brain area's sensitivity to AEDs.

New AED treatments are usually tested as an adjunct therapy in patients in which AED treatment has failed. This population is highly pharmacoresistant and therefore complete seizure freedom is often an unrealistic expectation. Instead, a >50 % reduction in seizure frequency is the commonly reported primary outcome of a successful drug trial. Those patients in which seizures are not reduced by >50% are considered resistant to the AED tested (Beyenburg et al., 2010; Guekht, 2011). Patients are usually classified as pharmacoresistant following *"failure of two adequate trials of two tolerated and appropriately chosen and used AED schedules (whether as monotherapies or in combination) to achieve sustained seizure freedom*" (Bourgeois, 2008). Despite this, previous *in vitro* studies have largely classified tissue as resistant when it does not respond to a range of single AEDs

(Zhang et al., 1995; Dreier et al., 1998; Quilichini et al., 2003). Therefore, in order address both the monotherapy and drug combination aspects of drug resistance in this study we investigated the sensitivity and resistance to both single and double drug combinations in the PC over the course of epileptogenesis in comparison to AMCs.

The drugs were chosen to include a number of different drug targets, first and second line treatments and adjunct therapies and one new drug currently undergoing clinical assessment (cannabidiol) (table 6.1). Na^+ channels are one of the most important targets for AED treatment as sustained high frequency bursting during seizure activity is acutely reliant on Na^+ channels rapidly cycling between open, inactivated and closed states (Kwan et al., 2001; Rogawski and Löscher, 2004). For this reason, a pure Na^+ channel (carbamazepine or lamotrigine) modulator or a drug with mixed mechanisms including Na^+ channel modulation (valproate) were included in every AED combination. The Na^+ channel blocker CBZ is one of the most effective AEDs used in both mono- and polytherapy therefore it was included in five of the six AED combinations.

drug	primary target	use	interactions	therapeutic dose	dose used
CBZ	Voltage-dependent Na^+ channels	First line, mono and adjunct therapy. Partial, secondary generalised and generalised tonic-clonic seizures.	VPA + CBZ = ↑CBZ + ↓VPA. LTG/TGB/ZNS + CBZ = ↓LTG/TGB/ZNS. Neurotoxic with LTG.	Adult dose = 800 - 1200 mg/day. Plasma concentration = 17 - 51 μM/L.	50 μM
VPA	Multiple mechanisms	First line therapy. Mono and adjunct therapy for all types of epilepsy.	LTG/CBZ + VPA = ↑LTG/CBZ + ↓VPA. ZNS + VPA = ↓ZNS.	Adult dose = 500 - 2500 mg/day Plasma concentration = 350 - 700 μM/L.	500 μM
ZNS	Multiple mechanisms	Secondary line therapy. Adjunct therapy in partial and secondary generalised seizures.	VPA/CBZ + ZNS = ↓ZNS.	Adult dose = 100 - 600 mg/day. Plasma concentration = 47 - 188 μM/L	100 μM
GBP	Multiple mechanism	Limited use. Mono or adjunct therapy in partial with or without secondary generalisation.	None reported.	Adult dose = 900 - 3600 mg/day Plasma concentration = 12 - 117 μM/L	20 μM
LTG	Voltage-dependent Na^+ channels	Mono and adjunct therapy for partial, primary and secondary generalised.	CBZ + LTG = ↓LTG. VPA + LTG = ↓VPA.	Adult dose = 100 – 700 mg/day Plasma concentration = 12 - 58 μM/L	20 μM
CBD	Multiple mechanisms	New AED, still in pre-clinical assessment. Adjunct therapy.	Unknown.	Adults = 25 – 50 mg /kg Plasma concentration = unknown	30 μM
TGB	GABA reuptake	Adjunct therapy in partial seizures with or without secondary generalisation.	CBZ + TGB = ↓CBZ. VPA + TGB = ↓VPA + ↑TGB.	Adult dose =15 - 45 mg/day. Plasma concentration = 53 - 532 nM/L	20 μM

Table 6.1 Antiepileptic drug mechanisms of action, use, interaction and dosing
Drug interactions indicate changes in blood plasma levels of drugs when co-administered (Jones et al., 2010; Patsalos and Bourgeois, 2010; Jones et al., 2012; Devinsky et al., 2016).

6.1.1.1 Carbamazepine

One of the most effective and commonly used AEDs is the Na^+ channel blocker carbamazepine (CBZ). First developed in 1968, it was approved for use in the treatment of epilepsy in the USA in 1974 and today is listed on the WHOs list of essential medicines (WHO, 2015). CBZ is effective in partial and generalised seizures but contraindicated in absence and myoclonic seizures (Rogawski and Löscher, 2004). The primary mechanism of action of CBZ is thought to be blockade of voltage-dependent Na^+ channels (Ambrósio et al., 2002). During ictal activity, prolonged abnormal depolarisation of neurons leads to bursts of action potential (AP) firing. Whilst bursting, voltage-dependent Na^+ channels cycle between open (activated), inactivated and closed states. During the inactivated state, which may last 3 - 5 ms, Na^+ channel activation is not possible and the channel must enter the closed state before activation can occur. Rapid cycling between these states facilitates high frequency firing during epileptiform activity. CBZ is thought to work by prolonging the length of time the channel is in the inactivated state, therefore reducing neuronal capacity for high frequency repetitive firing. CBZ also shifts the voltage dependence of inactivation to more hyperpolarised levels and the activation threshold to a more depolarised level, thereby decreasing the window current (the overlap between inactivation and activation curves). The high ratio of Na^+ channels in an inactivated state during high frequency firing compared to single action potential firing allows CBZ to be selective for pathological activity only (Willow and Catterall, 1982; Courtney and Etter, 1983; Willow et al., 1984; Willow et al., 1985; Macdonald, 1989; Elliott, 1990; Kuo et al., 1997; Hebeisen et al., 2015; Shaheen et al., 2015). Enhancing the time spent in an inactivated state is thought to lead, via a reduction of spike firing, to a decrease in neurotransmitter release, with glutamatergic cells more strongly affected than GABAergic cells (Pothmann et al., 2014). Like many AEDs, CBZ is promiscuous and evidence for other channel involvement is debated, it has been found to inhibit Ca^{2+} channels (Schirrmacher et al., 1993, 1995; Yoshimura et al., 1995; Patsalos and Bourgeois, 2010), although see (Zona et al., 1990; Sayer et al., 1993). CBZ has also been found to potentiate K^+ channels (Zona et al., 1990), although other reports indicate no effect (Wooltorton and Mathie, 1993; Lee et al., 1997; Rundfeldt, 1997) and even K^+ channel block (Matsumoto et al., 1998; Dreixler et al., 2000). Effects on adenosine receptors have also been reported (Skerritt et al., 1983; Gasser et al., 1988; Daval et al., 1989; Weir et al., 1990; Vancalker et al., 1991; Okada et al., 1997; Biber et al., 1999).

6.1.1.2 Lamotrigine

Lamotrigine (LTG) was originally licenced for use (in Europe) in 1991 as an alternative to CBZ. With a similar mechanism of action, LTG is not as effective as CBZ, but is active across a broader spectrum of epilepsies and is better tolerated with fewer side effects (Patsalos and Bourgeois, 2010). Like CBZ, LTG is used in partial and generalised tonic-clonic seizures, but unlike CBZ it is also useful for absence seizures (Rogawski and Löscher, 2004). The use-dependent blockade of voltage-dependent Na^+ channels is achieved the same way as in

CBZ (see 6.1.1.1) (Lang et al., 1993; Xie et al., 1995). This blockade has also been found to reduce glutamate release (Leach et al., 1986; Sitges et al., 2007). A reduction in high voltage activated (HVA) Ca^{2+} channel currents (N- and P/Q-type) has also been reported. This can also reduce glutamate release, although to a lesser extent than via Na^{+} channel modulation (Stefani et al., 1996; Wang et al., 1996a). However, it has also been noted that this presynaptic inhibition of glutamate release persists in the presence of TTX implying neither Ca^{2+} or Na^{+} channels are responsible. Instead, it has been suggested that LTG reduces glutamate release via interaction with downstream release machinery (Cunningham and Jones, 2000). Additionally, both presynaptic enhancement (Cunningham and Jones, 2000) and reduction of GABA release has been reported (Leach et al., 1986; Teoh et al., 1995). When used as an adjunct therapy in both adult and paediatric patients, a number of studies have demonstrated a significant reduction (17 – 59%) in the frequency of seizures (Matsuo, 1999).

6.1.1.3 Valproate

Valproate (VPA) is a broad spectrum first line treatment for generalised seizures and has multiple mechanisms of action. VPA is effective in partial, generalised tonic-clonic, absence and myoclonic seizures (Rogawski and Löscher, 2004). VPA has been found to raise ambient GABA levels, block Na^{+} channels, inhibit T-type Ca^{2+} channels and decrease ambient aspartate levels in the brain (Patsalos and Bourgeois, 2010). Ambient GABA levels have been reported to increase in the rodent brain by 15 - 45 % following VPA administration (Godin et al., 1969; Kukino and Deguchi, 1978). Increased GABA levels have also been found in human plasma (30 % higher) following two day administration (Löscher and Schmidt, 1980). This increased GABA is thought to be due to enhanced GABA availability through inhibition of GABA degradation, increased GABA release and blockade of GABA uptake (Rowley et al., 1995; Sills et al., 1996; Löscher, 1999). A reduction in aspartate, an agonist of NMDA receptors, in the brain has also been noted (Schechter et al., 1978; Löscher et al., 1993). Blockade of Na^{+} channels has also been found to inhibit high frequency firing, but not via interaction with the inactivated state (like LTG and CBZ) (Van den Berg et al., 1993; Albus and Williamson, 1998). Instead, it is thought that VPA inhibits the persistent Na^{+} channel, which remains active during prolonged depolarisation and shifts the voltage dependence of the inactivation state to a more hyperpolarised level, thereby decreasing the window current (Taverna et al., 1998; Vreugdenhil et al., 1998b; Stafstrom, 2007). VPA is also thought to inhibit low voltage activated (LVA) T-type Ca^{2+} currents, however this effect is small, requiring very high concentrations of VPA and is therefore unlikely to contribute in a significant way to its antiepileptic effects (Kelly et al., 1990). VPA's broad spectrum of action has made it a very popular choice of AED particularly in patients presenting with generalised seizures (Patsalos and Bourgeois, 2010).

6.1.1.4 Zonisamide

Zonisamide (ZNS) is another broad spectrum AED with multiple targets and, as such, is used in a wide range of different epilepsy syndromes, including partial, generalised, absence, and myoclonic seizures, infantile spasm and Lennox-Gastaut syndrome (Patsalos and Bourgeois, 2010). ZNS is thought to block the spread of ictal events by reducing Na^+ channel-dependent high frequency AP firing and blocking LVA T-type Ca^{2+} channels (Kwan et al., 2001; Leppik, 2004). T-type Ca^{2+} channel activation can lead to neuronal bursting and activation of intracellular second messenger cascades and is thought to play a critical role in epileptiform activity (Suzuki and Rogawski, 1989; Huguenard, 1996; Perez-Reyes, 2003). ZNS has been found to block T-type Ca^{2+} channels and suppress this bursting activity (Suzuki et al., 1992). Like LTG and CBZ, ZNS also increases the time the Na^+ channels spend in an inactivated state thus increasing the time period in which the Na^+ channel is unable to open and reducing cell firing (Schauf, 1987; Rock et al., 1989). During rest, ZNS has also been found to enhance GABA release without affecting glutamate release (Okada et al., 2002; Yoshida et al., 2005; Yamamura et al., 2009). Despite a broad spectrum of action and studies supporting its potential as first-line therapy (Pack, 2013), ZNS is usually used as a second line or adjunct therapy (Patsalos and Bourgeois, 2010).

6.1.1.5 Gabapentin

As the name might suggest, gabapentin (GBP) was originally developed with a similar chemical structure to GABA, however analysis of its pharmacological properties revealed despite the similarity in structure, gabapentin does not bind to GABA receptors or transporters (Su et al., 1995; Taylor et al., 1998; Kwan et al., 2001). GBP has a number of mechanisms of action, however, its therapeutic use is restricted to partial and generalised tonic-clonic seizures with a low percentage of patients responding to it (Patsalos and Bourgeois, 2010). GBP has little effect on Ca^{2+} channel currents, however it has been found to bind to the $\alpha_2\delta$ auxiliary subunit on voltage-gated Ca^{2+} channels (Ca_v1 (L) and Ca_v2 (N, P/Q and R)) and thereby prevent ion channel trafficking, which subsequently reduces channel expression at the cell membrane (Hendrich et al., 2008). Increased GABA has also been observed in the cortex of epileptic patients following GBP dosing and human slices incubated in GBP had a significantly higher GABA concentration; an effect that is absent in rodent slices (Petroff et al., 1995; Errante et al., 2002; Kuzniecky et al., 2002; Cai et al., 2012). In animal models, GBP has been shown to activate GAD thereby increasing GABA synthesis. Increased non-vesicular GABA release, reduced GABA-transaminase and decreased glutamate concentration has also been found (Götz et al., 1993; Leach et al., 1997). No change in glutamate concentration has been observed in human patients (Cai et al., 2012).

6.1.1.6 Tiagabine

Tiagabine (TGB) is a narrow spectrum AED which is used as an adjunct therapy when other AEDs have failed (Patsalos and Bourgeois, 2010). TGB administration has been found to prolong the time GABA spends in the synaptic cleft both in human TLE patients and in rodent studies (During et al., 1992; Fink-Jensen et al., 1992; Sills et al., 1999). TGB enhances synaptically available GABA by selectively inhibiting its reuptake by the GABA uptake transporter GAT-1 (Borden et al., 1994). This corresponds to an increase in the duration (but not amplitude) of IPSCs, in rodent hippocampal slices (Roepstorff and Lambert, 1992). As TGB has a narrow spectrum of efficacy against focal seizures its use it rather limited (Patsalos and Bourgeois, 2010).

6.1.1.7 Cannabidiol

A small group of patients received cannabidiol (CBD) in the 1980s in a phase two clinical trial with a reported decrease in seizure frequency (Cunha et al., 1980). However, it was not until more recently that an in-depth analysis of the anticonvulsant properties of CBD was performed. An open-label clinical trial in the USA found a significant reduction (>30 %) in the frequency of seizures in a small number of patients with drug refractory epilepsy that took CBD in addition to their normal medication (Devinsky et al., 2016). An adequate safety profile was found, but a randomised controlled clinical trial is required to comprehensively test CBD's AED properties. CBD has been found to reduce seizure incidence and severity in *in vitro* and *in vivo* models of epilepsy (Jones et al., 2010; Jones et al., 2012). The mechanism of action of CBD are not well understood (Devinsky et al., 2014; Bih et al., 2015). Surprisingly, CBD does not interact with either of the known endocannabinoid receptors, CB1 or CB2. Instead, CBD is thought to modulate Ca^{2+} homeostasis, block voltage-gated Ca^{2+} channels, act as an agonist to the 5-HT_{1A} receptor and reduce adenosine uptake. During pathological conditions, such as enhanced extracellular K^{+}, or following application of 4-AP, CBD reduced intracellular Ca^{2+} by modulating the mitochondrial Na^{+}-Ca^{2+} exchanger. This effect was absent under normal conditions (Drysdale et al., 2006; Ryan et al., 2009). At physiologically relevant concentrations CBD inhibits low voltage activated T-type Ca^{2+} channels (Ross et al., 2008). CBD has also been found to activate the 5-HT_{1A} receptor (inhibitory GPCR - serotonin receptor) in cell culture and in animals models of epilepsy this has been found to be anticonvulsant (Russo et al., 2005). CBD also blocks the equilibrative nucleoside transporter, thereby reducing adenosine reuptake (Carrier et al., 2006; Pandolfo et al., 2011). Adenosine is thought to be involved in seizure termination, with raised levels found in the post-ictal phase leading to inhibition of neurotransmitter release (Dragunow et al., 1985; Young and Dragunow, 1994; Boison, 2006; Carrier et al., 2006).

6.1.3 The piriform cortex's sensitivity to antiepileptic drug treatment during epileptogenesis

In this study pharmacoresistance was investigated in the PC following epilepsy induction using the RISE protocol compared to AMCs. A high proportion of pharmacoresistance was found in the younger age groups in response to single and double AED application compared to older animals. During the mid-latent period, significant differences were observed in both single and double AED treatment between SE and AMC particularly with regard to the Na^+ channel modulators. During the chronic period the majority of slices tested were found to be pharmacosensitive in response to both single and double drug combinations in slices prepared from both SE and AMC animals.

6.2 Results

6.2.1 Alterations in resistance to anti-epileptic drugs over the course of epileptogenesis

This study was conducted in parallel with work carried out in the medial EC (MEC) by Darshna Shah. Data presented here were collected in collaboration with Katherine Murrall, an undergraduate placement student. In this chapter, the effects of six different combinations of AEDs have been mapped out in PC brain slices prepared from the new RISE model of TLE (Modebadze et al., 2016). The effect of these AEDs was investigated at 4 time points following epilepsy induction (SE); 24 hours (early latent period), 1 week (early latent period), 4 weeks (mid latent period) and 3 months+ (chronic period) and compared to age-matched controls (AMC). Seizure-like events (SLEs) were induced by replacing normal aCSF with $0[Mg]^{2+}$ aCSF perfusate one hour after slice preparation. A single drug was applied to slices that had a minimum of 3 SLEs <30 minutes apart. A second drug was then applied for a further hour. The frequency of SLEs was calculated (per hour) for the 15 - 60 minutes after drug application and compared to SLE frequency (per hour) before drug application. Each drug combination at every time point was performed on 8 slices prepared from a minimum of 3 animals (totalling 384 slices, table 6.2). In this study, alterations in the frequency of SLEs was assessed as this is the measure most commonly used in clinical practice to measure AED efficacy. Frequency is presented as mean ± standard error of the mean (SEM, graphs) and normalised change in mean frequency (tables). The proportion of slices that continued to display SLEs in the presence of drug and the proportion of slices that were resistant to drug application (defined as <50 % reduction in SLE frequency) are also presented (tables).

age/epi state	VPA + CBZ	CBZ + ZNS	CBZ + GBP	LTG + GBP	CBD + CBZ	TGB + CBZ
SE 24 hrs	8 / 3	8 / 3	8 / 3	8 / 4	8 / 4	8 / 3
AMC 24 hrs	8 / 3	8 / 3	8 / 3	8 / 4	8 / 3	8 / 3
SE 1 wk	8 / 3	8 / 4	8 / 3	8 / 3	8 / 3	8 / 3
AMC 1 wk	8 / 3	8 / 3	8 / 3	8 / 4	8 / 3	8 / 3
SE 4 wks	8 / 3	8 / 3	8 / 5	8 / 4	8 / 3	8 / 4
AMC 4 wks	8 / 4	8 / 4	8 / 5	8 / 5	8 / 3	8 / 4
SE 3 mnths+	8 / 3	8 / 5	8 / 5	8 / 6	8 / 3	8 / 4
AMC 3 mnths+	8 / 4	8 / 3	8 / 3	8 / 6	8 / 4	8 / 4

Table 6.2 Experimental matrix.
Number of slices / number of animals. Every drug combination was tested in 8 slices from a minimum of 3 animals from SE and AMC animals at four time points. Epi state – epileptic state AMC or SE.

6.2.2 Twenty four hours post status epilepticus

Twenty-four hours after animals had undergone the RISE protocol for epilepsy induction animals were still recovering from the protocol and were having sporadic spontaneous seizures (Modebadze et al., 2016). The effect of six combinations of AEDs on $0[Mg]^{2+}$

induced SLEs in PC slices prepared 24 hours post-epilepsy induction and AMCs was investigated (22 - 25 days old, 45 - 65 g). The Bonferroni adjusted Wilcoxon test was used to detect significant differences between the columns as the Friedman test indicated a significant difference in all graphs (figure 6.1).

Figure 6.1 summarises the effect of single and double drug application on slices prepared from AMC (figure 6.1 A-Fi) and SE (figure 6.2 A-Fii) animals. Table 6.3 shows the percentage of slices that continued to show SLEs, the percentage of slices resistant to drug application (defined as <50 % reduction in SLE frequency) and the alteration in normalised frequency of SLEs following single and double drug application for both AMC and SE animals. In summary, CBZ (CBZ + GBP only) alone significantly reduced the frequency of SLEs in slices prepared from AMC animals (figure 6.1 Ci). TGB alone reduced the frequency of SLEs in slices prepared from SE animals only (figure 6.1 Fii). All other single drug applications had no significant ($P > 0.05$) effect on slices prepared from either SE (figure 6.1 Aii-Fii) or AMC animals (figure 6.1 Ai-Fi). There were no significant differences between the application of the first drug and second drug in slices prepared from SE or AMC animals. All double drug combinations significantly reduced the frequency of SLEs in slices prepared from AMC animals (figure 6.1 Ai-Fi) except the two drug combinations CBZ + GBP and LTG + GBP. All double drug combinations except CBZ + ZNS and CBZ + GBP reduced the frequency of SLEs in slices prepared from SE animals (figure 6.1 Aii-Fii). None of the single or double drug combinations abolished all seizures in all slices tested.

	AMC			24 hours post SE		
drug(s)	slices with SLEs	resistant slices	frequency (%)	slices with SLEs	resistant slices	frequency (%)
VPA	8/8	7/8	ns	7/8	7/8	ns
VPA + CBZ	6/8	5/8	-57.4 ± 10.4*	6/8	5/8	-42.9 ± 15.1*
CBZ	6/8	3/8	ns	7/8	5/8	ns
CBZ + ZNS	3/8	1/8	-84.9 ± 8.2*	8/8	6/8	ns
CBZ	7/8	5/8	-43.8 ± 15.2*	8/8	5/8	ns
CBZ + GBP	7/8	4/8	ns	7/8	5/8	ns
LTG	6/8	5/8	ns	5/8	5/8	ns
LTG + GBP	5/8	3/8	ns	4/8	3/8	-66.4 ± 14.2*
CBD	8/8	5/8	ns	5/8	5/8	ns
CBD + CBZ	7/8	1/8	-69.4 ± 7.6*	3/8	1/8	-84.2 ± 8.2*
TGB	8/8	4/8	ns	7/8	6/8	-32.1 ± 14.6*
TGB + CBZ	6/8	0/8	-72.8 ± 6.4*	7/8	4/8	-55.1 ± 7.4*

Table 6.3 Table showing the effect of single and double AED combinations on SLEs in slices prepared from SE animals 24 hours post SE and AMCs

The number of slices (slices with SLEs) that continued to show SLEs after drug application is presented on the left, the number of slices which were resistant (<50 % reduction in frequency) is in the middle and the percentage change in frequency (if significant) is presented on the right. * $P < 0.05$ for both SE and AMC.

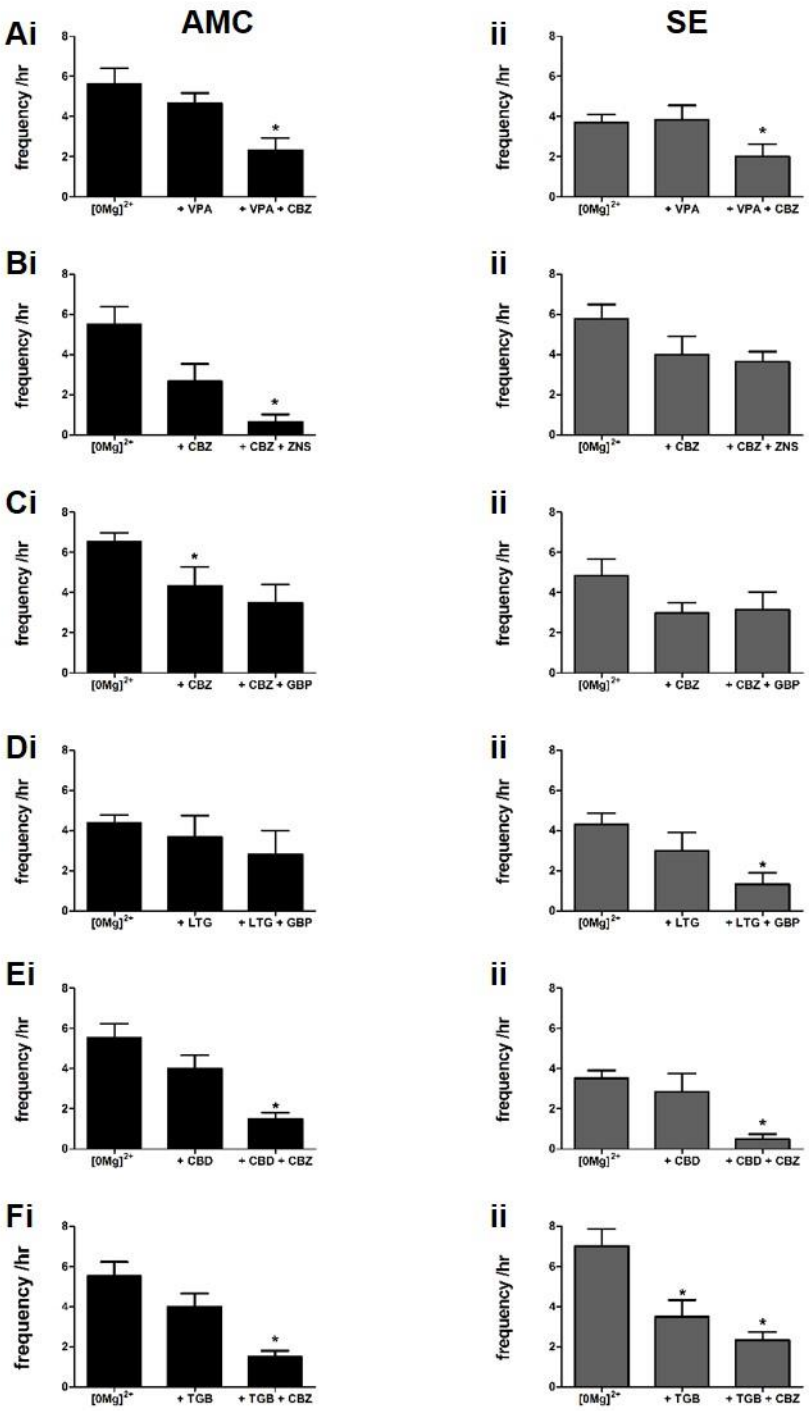

Figure 6.1 The effect of single and double AED combinations on SLEs in slices prepared from SE animals 24 hours post SE and AMCs

The raw frequency of SLEs per hour before and after single and double drug application in animals which had undergone the RISE protocol for epilepsy induction 24 hours previously (right, grey) and AMC (left, black). N = 8 for all conditions.* $P < 0.05$.

6.2.2.1 Comparison of antiepileptic drugs at twenty four hours post status epilepticus

To investigate if there were any significant differences between the frequency of SLEs following application of different single drugs and between slices prepared from AMC and SE animals (epileptic state) a between subjects ANOVA was used. The data were normalised to the 0$[Mg]^{2+}$ control period as there were significant differences in the frequency of SLEs between SE and AMC during 0$[Mg]^{2+}$ application (chapter 5). One outlier (1.5 x interquartile range) was identified and removed and the data were ranked to make them normally distributed. Figure 6.2 A shows the ranked data, to see the raw data see figure A2.1 A (appendix). There was no significant interaction between drug and epileptic state. There was no overall significant effect of epileptic state. There was no overall significant effect between single drugs for SLE frequency.

To investigate if there were any significant differences between the frequency of SLEs following different double drug combinations and between slices prepared from AMC and SE animals (epileptic state) a between subjects ANOVA was used. The data were normalised to the 0$[Mg]^{2+}$ control period. One outlier was identified and removed and the data were ranked to make them normally distributed. Figure 6.2 B shows the ranked data, to see the raw data see figure A2.1 B (appendix). There was no significant interaction between drug and epileptic state. There was no overall significant effect of epileptic state. There was no overall significant effect between double drugs for SLE frequency.

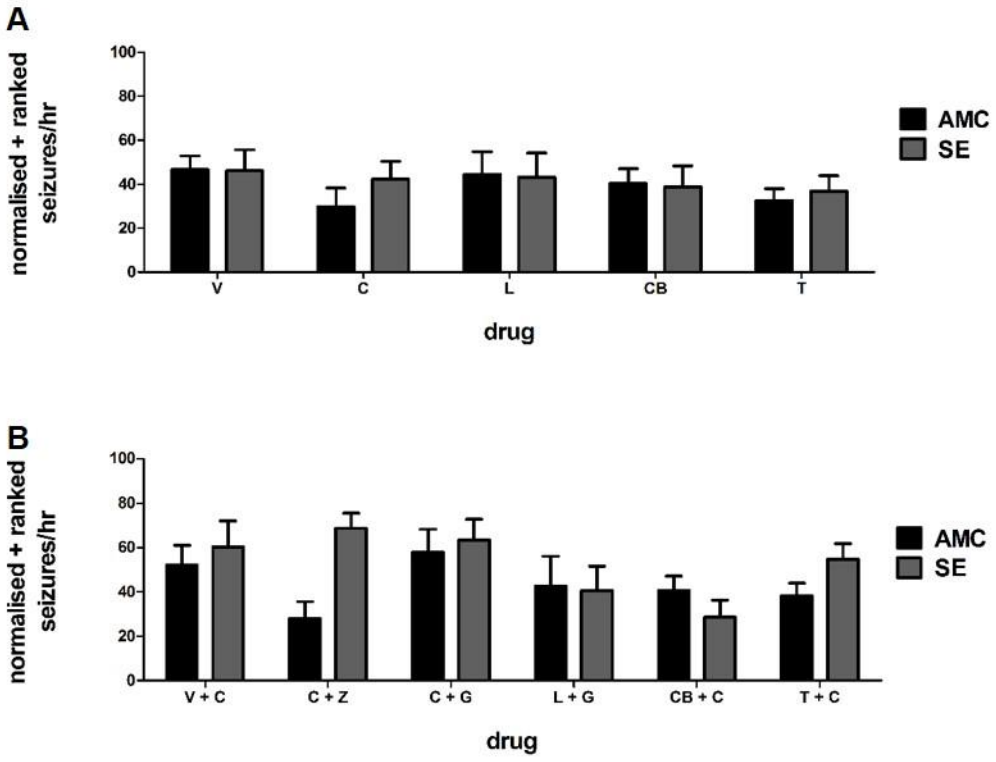

Figure 6.2 Comparison of different drugs on SLEs in slices prepared from animals 24 hours post SE and AMCs.
Ranked mean SLEs per hour (normalised to 0[Mg]$^{2+}$) after single (A) and double (B) drug application. N = 8 for all conditions. V – valproic acid, C – carbamazepine, L – lamotrigine, CB – cannabidiol, T – tiagabine.

6.2.3 One week post status epilepticus

One week following epilepsy induction using the RISE protocol, the animals had recovered and were no longer experiencing spontaneous seizures. This time point represents the early latent period. The effect of six combinations of AEDs on 0[Mg]$^{2+}$ induced SLEs in PC slices prepared 1 week post epilepsy induction and AMCs was investigated (29 - 31 days old, 75 - 100 g). The Bonferroni adjusted Wilcoxon test was used to detect significant differences between the columns as the Friedman test indicated a significant difference in all graphs (figure 6.3).

Figure 6.3 summarises the effect of single and double drug application on slices prepared from AMC (figure 6.3 Ai-Fi) and SE (figure 6.3 Aii-Fii) animals. Table 6.4 shows the percentage of slices that continued to show SLEs, the percentage of slices resistant to drug application (defined as <50 % reduction in SLE frequency) and the alteration in normalised frequency of SLEs following single and double drug application for both AMC and SE animals. In summary, only CBZ (CBZ + GBP only) significantly reduced the frequency of SLEs in slices prepared from AMC (figure 6.3 Ai-Fi) and SE animals (figure 6.3 Aii-Fii). All other single drugs had no significant effect on the frequency of SLEs in slices prepared from AMC and SE animals. All the double drug combinations tested significantly reduced the

frequency of SLEs in slices prepared from AMC animals (figure 6.3 Ai-Fi) except LTG + GBP (figure 6.3 Di) and CBD + CBZ (figure 6.3 Eii). CBZ + ZNM (figure 6.3 Bii), CBZ + GBP (figure 6.3 Cii), and LTG + GBP (figure 6.3 Dii), significantly reduced the frequency of SLEs in slices prepared from SE animals, no other double drug combination significantly reduced the frequency. There were no significant differences between the application of the first drug and second drug in slices prepared from SE or AMC animals.

	AMC			1 week post SE		
drug(s)	slices with SLEs	resistant slices	frequency (%)	slices with SLEs	resistant slices	frequency (%)
VPA	7/8	3/8	ns	7/8	7/8	ns
VPA + CBZ	5/8	2/8	-67.7 ± 11.9*	4/8	3/8	ns
CBZ	5/8	2/8	ns	2/8	4/8	ns
CBZ + ZNS	2/8	1/8	-91.2 ± 6.2*	2/8	1/8	-36.5 ± 22.0*
CBZ	5/8	1/8	-77.5 ± 9.1*	6/8	1/8	-68.6 ± 10.7*
CBZ + GBP	2/8	1/8	-85.2 ± 10.3*	3/8	2/8	-75.9 ± 12.3*
LTG	7/8	7/8	ns	7/8	3/8	ns
LTG + GBP	5/8	2/8	ns	6/8	3/8	-53.9 ± 14.6*
CBD	8/8	6/8	ns	8/8	7/8	ns
CBD + CBZ	6/8	4/8	ns	6/8	3/8	ns
TGB	7/8	5/8	ns	8/8	6/8	ns
TGB + CBZ	5/8	4/8	-57.6 ± 14.3*	6/8	2/8	ns

Table 6.4 Table showing the effect of single and double AED combinations on SLEs in slices prepared from SE animals 1 week post SE and AMCs

The number of slices (slices with SLEs) that continued to show SLEs after drug application is presented on the left, the number of slices which were resistant (<50 % reduction in frequency) is in the middle and the percentage change in frequency (if significant) is presented on the right. * $P < 0.05$.

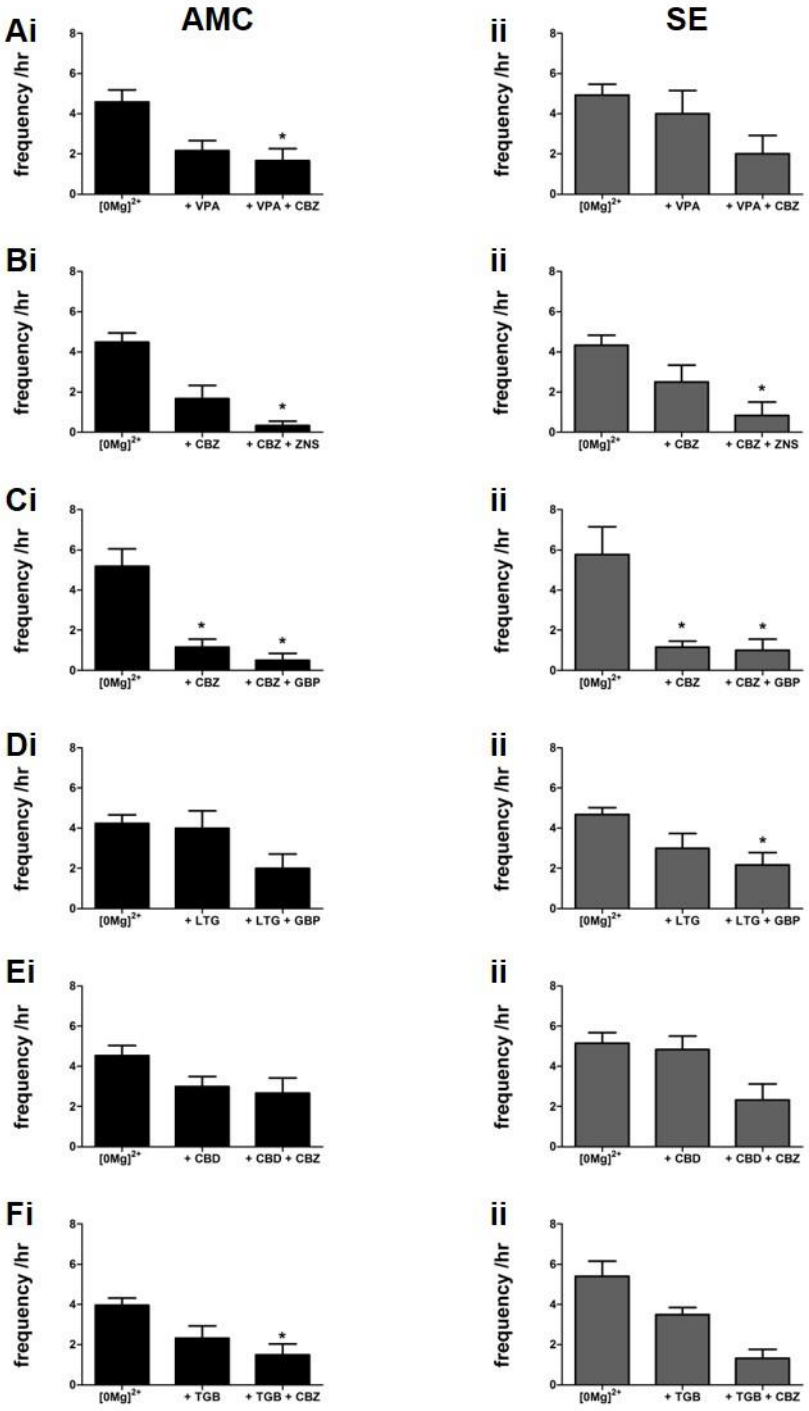

Figure 6.3 The effect of single and double AED combinations on SLEs in slices prepared from SE animals 1 week post SE and AMCs

The raw frequency of SLEs per hour before and after single and double drug application in animals which had undergone the RISE protocol for epilepsy induction 24 hours previously (right, grey) and AMC (left, black). N = 8 for all conditions.* $P < 0.05$.

6.2.3.1 Comparison of antiepileptic drugs at one week post status epilepticus

To investigate if there were any significant differences between frequency of SLEs following application of different single drugs and between slices prepared from AMC and SE animals (epileptic state) a between subjects ANOVA was used. The data were normalised to the 0$[Mg]^{2+}$ control period. One outlier was identified and removed and the data were ranked to make them normally distributed. Figure 6.4 A shows the ranked data, to see the raw data see figure A2.2 A (appendix). There was no significant interaction between drug and epileptic state. There was no overall significant effect of epileptic state. There was no overall significant effect of different drugs on frequency of SLEs.

To investigate if there were any significant differences between frequency of SLEs following application of different double drug combinations and between slices prepared from AMC and SE animals (epileptic state) a between subjects ANOVA was used. The data were normalised to the 0$[Mg]^{2+}$ control period. One outlier was identified and removed and the data were ranked to make them normally distributed. Figure 6.4 B shows the ranked data, to see the raw data see figure A2.2 B (appendix). There was no significant interaction between drug and epileptic state. There was no overall significant effect of epileptic state. There was no overall main effect difference between different drug combinations on frequency of SLEs.

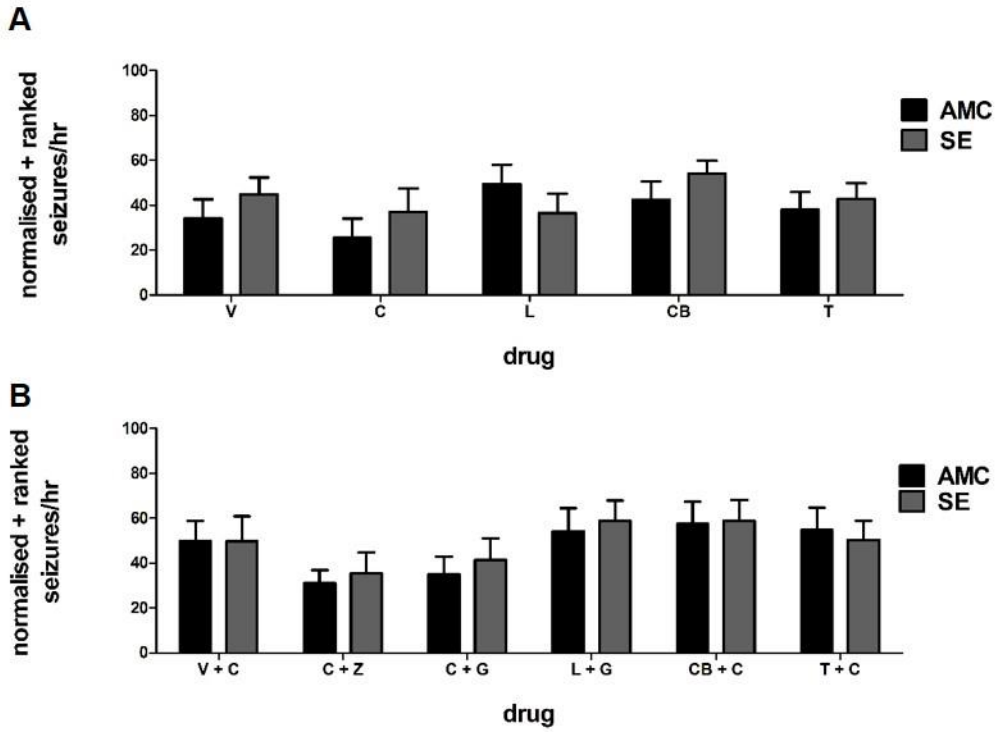

Figure 6.4 Comparison of different drugs on SLEs in slices prepared from animals 1 week post SE compared to AMCs.
Ranked mean SLEs per hour (normalised to 0[Mg]$^{2+}$) after single (A) and double (B) drug application. N = 8 for all conditions. V – valproic acid, C – carbamazepine, L – lamotrigine, CB – cannabidiol, T – tiagabine.

6.2.4 Four weeks post status epilepticus

Four weeks after animals have undergone the RISE protocol for epilepsy induction represents the middle latent period (Modebadze et al., 2016). The effect of six combinations of AEDs on 0[Mg]$^{2+}$ induced SLEs in PC slices prepared 4 weeks post epilepsy induction and AMCs was investigated (48 - 53 days old, 200 - 250 g). The Bonferroni adjusted Wilcoxon test was used to detect significant differences between the columns as the Friedman test indicated a significant difference in all graphs (figure 6.5).

Figure 6.5 summarises the effect of single and double drug application on slices prepared from AMC (figure 6.5 A-Fi) and SE (figure 6.5A-Fii) animals. Table 6.5 shows the percentage of slices that continued to show SLEs, the percentage of slices resistant to drug application (defined as <50 % reduction in SLE frequency) and the alteration in normalised frequency of SLEs following single and double drug application for both AMC and SE animals. In summary, all the single drugs tested significantly reduced the frequency of SLEs in slices prepared from SE animals (figure 6.5 Aii-Fii) except CBZ (CBZ + GPT only, figure 6.5 Cii) and CBD (figure 6.5 Eii). All the single drugs tested significantly reduced the frequency of SLEs in slices prepared from AMC animals (figure 6.5 Ai-Fi) except VPA, CBZ (CBZ + ZNS, figure 6.5 Ai) and CBD (figure 6.5 Ei). Application of LTG abolished all SLEs in all slices prepared from SE animals (figure 6.5 Dii). All the drug combinations tested significantly

reduced the frequency of SLEs in slices prepared from both SE (figure 6.5 Aii-Fii) and AMCs (figure 6.5 Ai-Fi). CBD + CBZ was significantly more effective at reducing SLE frequency than CBD alone in slices prepared from SE animals (figure 6.5 Eii). None of the double drug combinations tested abolished all SLEs in all slices prepared from AMC animals (figure 6.5 Ai-Fi). The drug combinations VPA + CBZ (figure 6.5 Aii), LTG + GBP (figure 6.5 Dii) and CBD + CBZ (figure 6.5 Eii) abolished all SLEs in all slices prepared from SE animals.

	AMC			**4 weeks post SE**		
drug(s)	slices with SLEs	resistant slices	frequency (%)	slices with SLEs	resistant slices	frequency (%)
VPA	8/8	8/8	ns	7/8	3/8	-57.8 ± 10.3*
VPA + CBZ	4/8	2/8	-74.8 ± 10.0*	0/8	0/8	-100 ± 0.0*
CBZ	5/8	2/8	ns	4/8	0/8	-58.7 ± 16.0*
CBZ + ZNS	5/8	1/8	-74.9 ± 9.0*	4/8	0/8	-78.9 ± 9.0*
CBZ	5/8	2/8	-66.1 ± 12.0*	3/8	2/8	ns
CBZ + GBP	2/8	1/8	-88.9 ± 7.6*	1/8	1/8	-95.5 ± 4.5*
LTG	6/8	3/8	-59.1 ± 11.9*	0/8	0/8	-100 ± 0.0*
LTG + GBP	4/8	1/8	-68.3 ± 14.1*	0/8	0/8	-100 ± 0.0*
CBD	7/8	6/8	ns	8/8	5/8	ns
CBD + CBZ	1/8	0/0	-95.5 ± 4.5*	0/8	0/0	-100 ± 0.0*
TGB	2/8	1/8	-84.9 ± 10.1*	8/8	0/8	-67.8 ± 2.5*
TGB + CBZ	2/8	0/8	-89.5 ± 6.9*	7/8	0/8	-74.4 ± 4.5*

Table 6.5 Table showing the effect of single and double AED combinations on SLEs in slices prepared from SE animals 4 weeks post SE and AMCs

The number of slices (slices with SLEs) that continued to show SLEs after drug application is presented on the left, the number of slices which were resistant (<50 % reduction in frequency) is in the middle and the percentage change in frequency (if significant) is presented on the right. * $P < 0.05$.

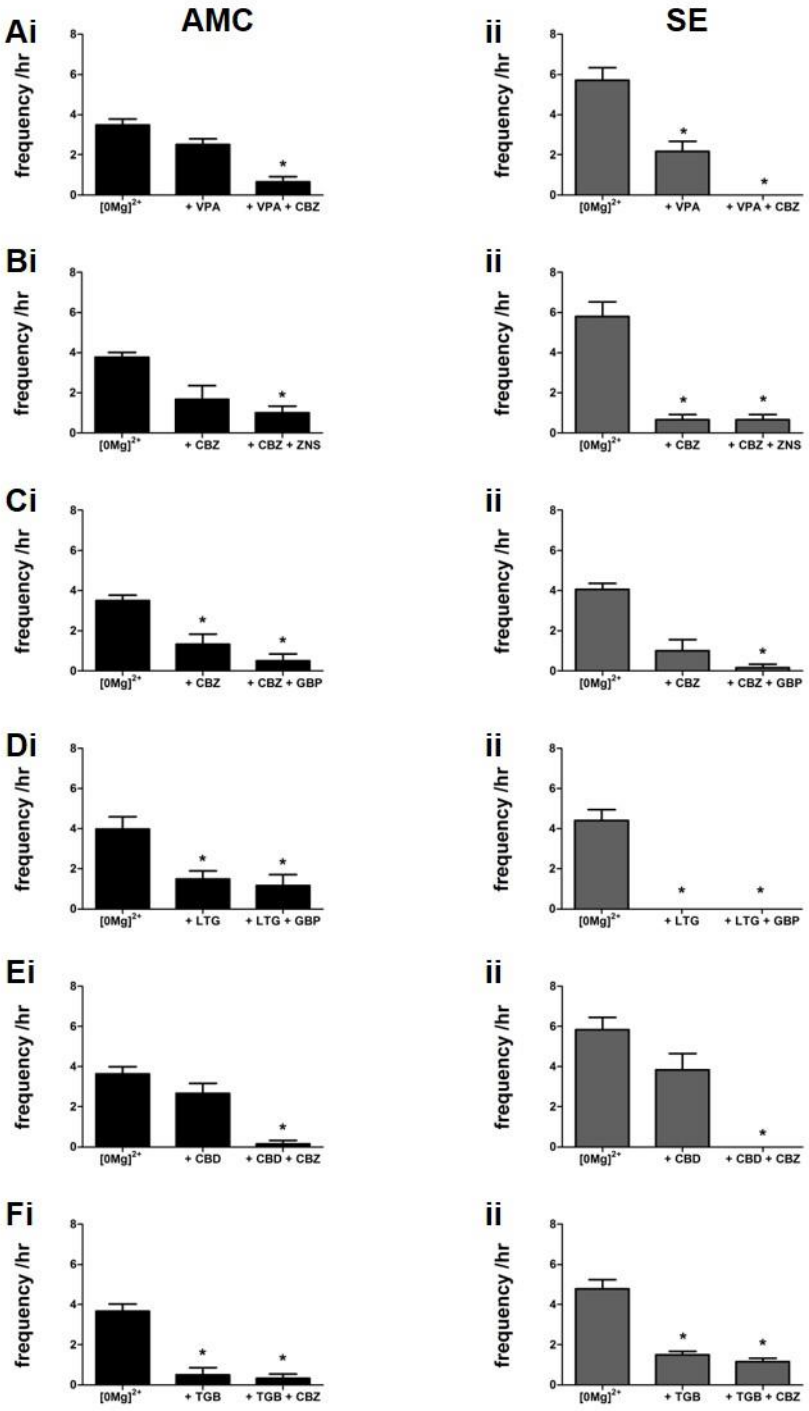

Figure 6.5 The effect of single and double AED combinations on SLEs in slices prepared from SE animals 4 weeks post SE and AMCs

The raw frequency of SLEs per hour before and after single and double drug application in animals which had undergone the RISE protocol for epilepsy induction 24 hours previously (right, grey) and AMC (left, black). N = 8 for all conditions.* $P < 0.05$.

6.2.4.1 Comparison of antiepileptic drugs at four weeks post status epilepticus

To investigate if there were any significant differences between frequency of SLEs following application of different single drugs and between slices prepared from AMC and SE animals (epileptic state) a between subjects ANOVA was used. The data were normalised to the 0$[Mg]^{2+}$ control period. One outlier was identified and removed and the data were ranked to make them normally distributed. Figure 6.6 A shows the ranked data, to see the raw data see figure A2.3 A (appendix). There was a significant interaction effect between epileptic state and drug F (degrees freedom, error) = (4,69) = 4.183, P = 0.04. Specifically, VPA (P = 0.018), CBZ (P = 0.042) and LTG (P = 0.001) were significantly more effective at reducing the SLE frequency in slices prepared from SE compared to AMC animals. An overall significant difference was seen between slices prepared from SE compared to AMC animals F (degrees of freedom, error) = (1, 69) = 7.784, P = 0.007. An overall significant difference was found between drugs F(degrees of freedom, error) = (4, 69) = 10.460, P < 0.001. Specifically, LTG (P = 0.002), TGB (P = 0.007) and CBZ (P = 0.003) were significantly more effective at reducing SLE frequency in slices prepared from SE and AMC animals than VPA. CBD (P = 0.001) was significantly less effective at reducing SLE frequency in slices prepared from SE and AMC animals than CBZ. LTG (P < 0.001) was significantly more effective at reducing SLE frequency in slices prepared from SE and AMC animals than CBD. TGB (P = 0.001) was significantly more effective at reducing the frequency of SLEs in slices prepared from SE and AMC animals than CBD.

To investigate if there were any significant differences between frequency of SLEs following application of different double drug combinations and between slices prepared from AMC and SE animals (epileptic state) a between subjects ANOVA was used. The data were normalised to the 0$[Mg]^{2+}$ control period. Two outliers were identified and removed and the data were ranked to make them normally distributed. Figure 6.6 B shows the ranked data, to see the raw data see figure A2.3 B (appendix). There was a significant interaction effect between epileptic state and drug F(degrees freedom, error) = (5,82) = 2.665, P = 0.008. Specifically, the drug combinations VPA + CBZ (P = 0.006) and LTG + GBP (P = 0.021) were significantly more effective at reducing the frequency of SLEs in slices prepared from SE animals than AMC animals. The drug combination TGB + CBZ was significantly (P = 0.019) more effective at reducing the frequency of SLEs in slices prepared from AMC animals compared to SE animals. There was no overall significant difference between SE and AMCs. There was an overall significant difference between different drugs F(degrees of freedom, error) = (5, 82) = 2.665, P = 0.028. Specifically, the drug combination of CBD + CBZ was more effective at reducing the frequency of SLEs in slices prepared from SE and AMC animals than TGB + CBZ (P = 0.033).

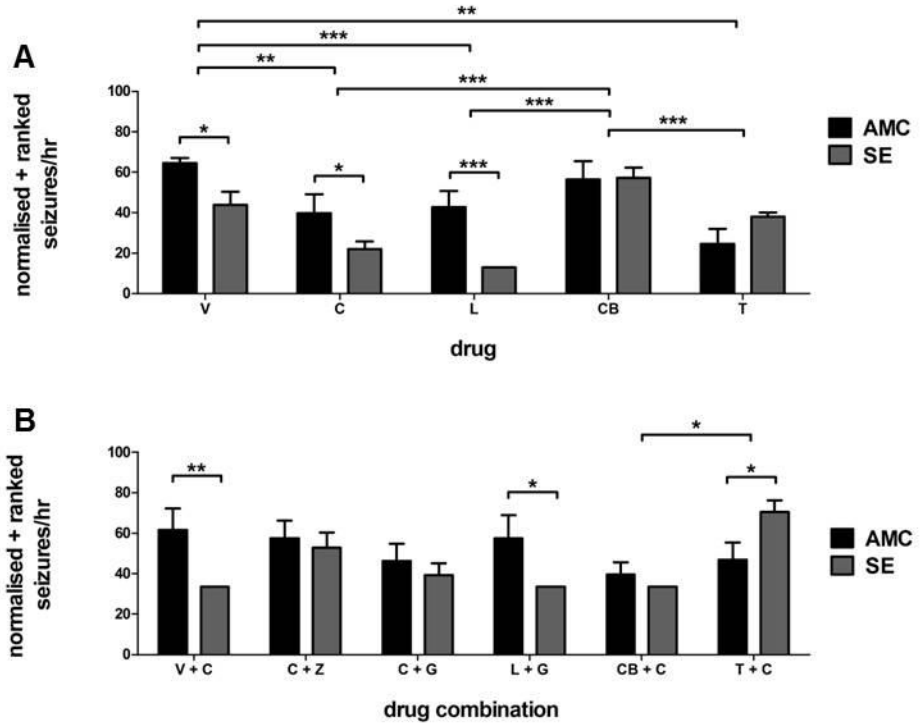

Figure 6.6 Comparison of different drugs on SLEs in slices prepared from animals 4 weeks post SE compared to AMCs.
Ranked mean SLEs per hour (normalised to 0[Mg]$^{2+}$) after single (A) and double (B) drug application.
N = 8 for all conditions. * P < 0.05, ** P < 0.01, *** P < 0.001. V – valproic acid, C – carbamazepine, L – lamotrigine, CB – cannabidiol, T – tiagabine.

6.2.5 Three months+ post status epilepticus

Three months+ post induction is the stage in which spontaneous recurrent seizures (SRS) are present. The length of time taken to enter SRS was dependent on the animal (see methods). Animals were used for experiments following a high (≥10) PSBB score on a minimum of 4 consecutive sessions (Modebadze et al., 2016). The effect of six combinations of AEDs on 0[Mg]$^{2+}$ induced SLEs in the PC in slices prepared ~3 months post induction were compared to AMCs. The AMC animals were carefully selected to mirror the ages of SE animals used as the period of time taken for SRS to develop was on average 20 weeks but ranged from 8 – 30 weeks (77 - 231 days old, 300 - 600 g). The Bonferroni adjusted Wilcoxon test was used to detect significant differences between the columns as the Friedman test indicated a significant difference in all graphs (figure 6.7).

Figure 6.7 summarises the effect of single and double drug application on slices prepared from AMC (figure 6.7 A-Fi) and SE (figure 6.7A-Fii) animals. Table 6.6 shows the percentage of slices that continued to show SLEs, the percentage of slices resistant to drug application (defined as <50 % reduction in SLE frequency) and the alteration in normalised frequency of SLEs following single and double drug application for both AMC and SE animals. In summary, all the single drugs tested significantly reduced the frequency of SLEs in slices

prepared from SE animals (figure 6.7 Aii-Fii) except VPA (figure 6.7 Aii) and LTG (figure 6.7 Dii). All the single drugs tested significantly reduced the frequency of SLEs in slices prepared from AMC animals (figure 6.7 Ai-Fi). None of the single drugs tested abolished all SLEs in all slices tested in slices prepared from SE (figure 6.7 Aii-Fii) or AMC animals (figure 6.7 Ai-Fi). All the double drug combinations tested significantly reduced the frequency of SLEs in slices prepared from both SE (figure 6.7 Aii-Fii) and AMC animals (figure 6.7 Ai-Fi). None of the double drugs tested abolished all SLEs in all slices tested in slices prepared from SE animals (figure 6.7 Aii-Fii). The drug combinations CBD + CBZ (figure 6.7 Ei) and TGB + CBZ (figure 6.7 Fi) abolished all SLEs in all slices tested in slices prepared from AMC animals (figure 6.7 Ai-Fi).

	AMC			3 months+ post SE		
drug(s)	slices with SLEs	resistant slices	frequency (%)	slices with SLEs	resistant slices	frequency (%)
VPA	7/8	2/8	-57.9 ± 7.5*	8/8	5/8	ns
VPA + CBZ	5/8	0/8	-81.8 ± 5.9*	4/8	0/8	-84.7 ± 6.0*
CBZ	4/8	3/8	-68.2 ± 12.9*	6/8	2/8	-65.8 ± 11.3*
CBZ + ZNS	2/8	0/8	-92.0 ± 5.2*	2/8	0/8	-90.1 ± 6.5*
CBZ	2/8	1/8	-87.0 ± 9.3*	7/8	1/8	-64.0 ± 7.3*
CBZ + GBP	1/8	0/8	-95.5 ± 4.5*	1/8	0/8	-97.1 ± 2.9*
LTG	3/8	2/8	-71.7 ± 15.6*	7/8	2/8	ns
LTG + GBP	1/8	0/8	-95.0 ± 5.0*	4/8	1/8	-76.7 ± 12.0*
CBD	2/8	1/8	-86.0 ± 9.5*	5/8	3/8	-55.2 ± 16.0*
CBD + CBZ	0/8	0/8	-100 ± 0.0*	2/8	0/8	-90.0 ± 7.7*
TGB	4/8	2/8	-73.7 ± 10.4*	2/8	0/8	-93.4 ± 4.4*
TGB + CBZ	0/0	0/8	-100 ± 0.0*	2/8	0/8	-92.3 ± 5.3*

Table 6.6 Table showing the effect of single and doubles AED combinations on SLEs in slices prepared from SE animals 3 months+ post SE and AMCs

The number of slices (slices with SLEs) that continued to show SLEs after drug application is presented on the left, the number of slices which were resistant (<50 % reduction in frequency) is in the middle and the percentage change in frequency (if significant) is presented on the right. * $P < 0.05$.

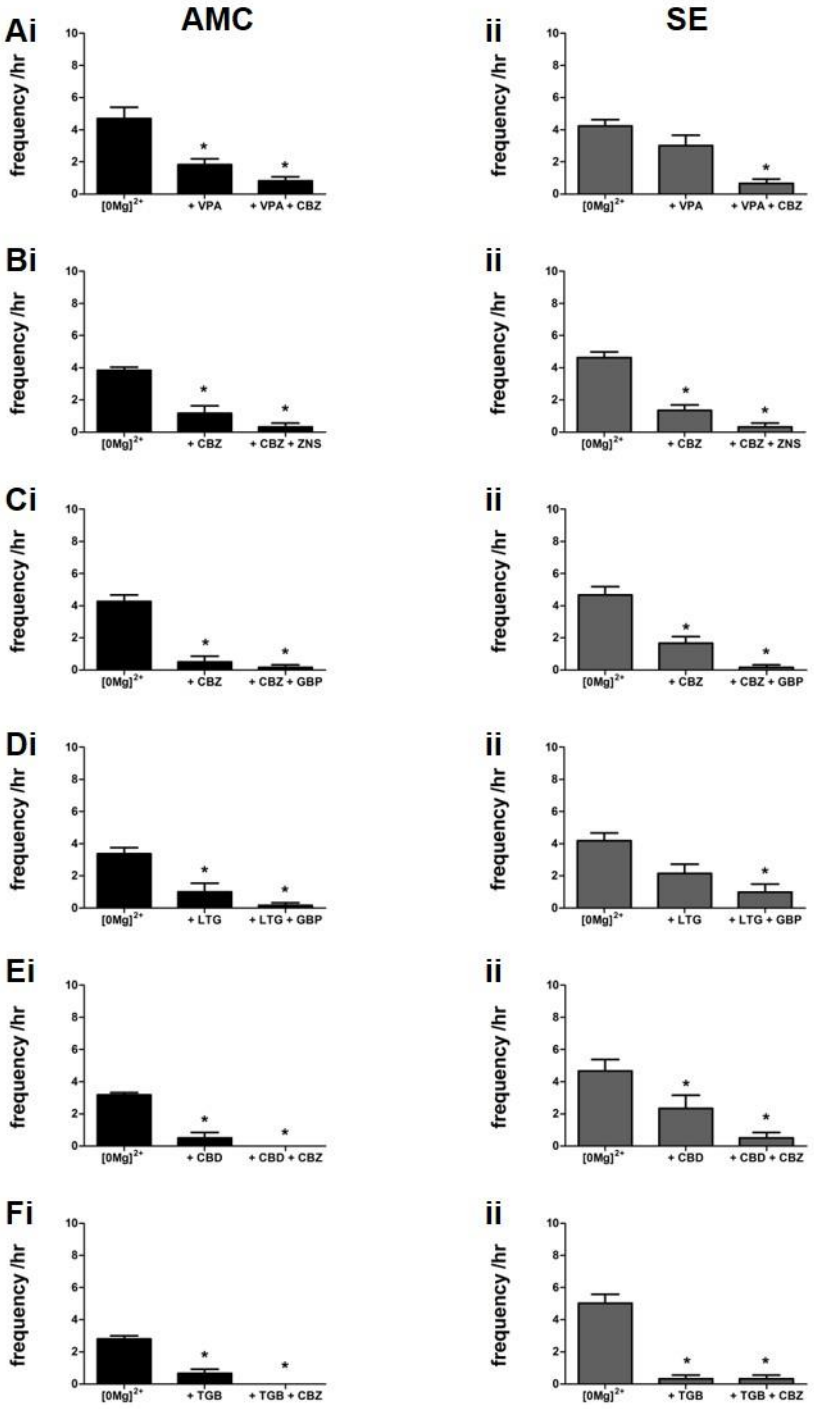

Figure 6.7 The effect of single and double AED combinations on SE animals 3 months+ post SE and AMCs

The raw frequency of SLE per hour before and after single and double drug application in animals which had undergone the RISE protocol for epilepsy induction 24 hours previously (right, grey) and AMC (left, black). N = 8 for all conditions.* $P < 0.05$.

6.2.5.1 Comparison of antiepileptic drugs at three months post status epilepticus

To investigate if there were any significant differences between different single drugs and between AMC and SE animals (epileptic state) a between subjects ANOVA was used. The data were normalised to the 0$[Mg]^{2+}$ control period. No outliers were identified and the data were ranked to make them more normally distributed. Figure 6.8 A shows the ranked data, to see the raw data see figure A2.4 A (appendix). There was no significant interaction effect between epileptic state and drug. No overall significant differences were seen between SE and AMC. An overall significant difference was seen between different drugs F(degrees of freedom, error) = (4, 70) = 3.523, P = 0.010. Specifically, TGB was significantly more effective at reducing the frequency of SLEs in slices prepared from SE and AMC animals than VPA (P = 0.006).

To investigate if there were any significant differences between different double drug combinations and between AMC and SE animals (epileptic state) a between subjects ANOVA was used. The data were normalised to the 0$[Mg]^{2+}$ control period. Two outliers were identified and removed and the data were ranked to make them more normally distributed. Figure 6.8 B shows the ranked data, to see the raw data see figure A2.4 B (appendix). There was no significant interaction effect between epileptic state and drug. There was no overall significant difference between SE and AMC. There was an overall significant difference different drugs F(degrees of freedom, error) = (5, 82) = 3.003, P = 0.015. Specifically, the drug combination CBD + CBZ was found to be more effective at reducing SLEs than VPA + CBZ.

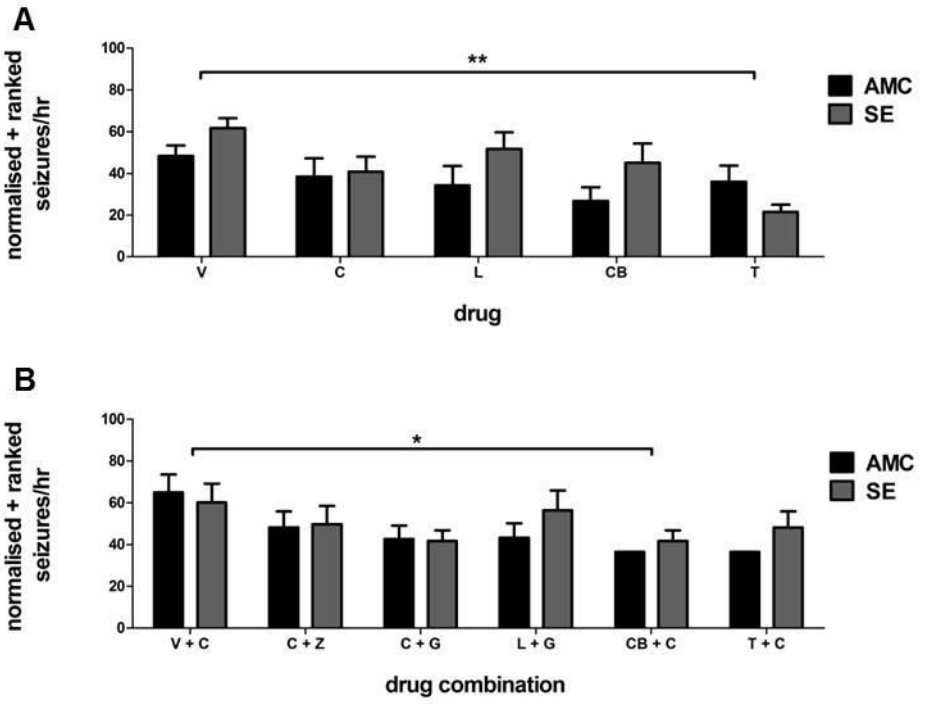

Figure 6.8 Comparison of different drugs on SLEs in slices prepared from 3 months+ post SE compared to AMCs.
Ranked mean SLE per hour (normalised to 0[Mg]$^{2+}$) after single (A) and double (B) drug application.
N = 8 for all conditions. * P < 0.05, ** P < 0.01. V – valproic acid, C – carbamazepine, L – lamotrigine, CB – cannabidiol, T – tiagabine.

6.2.6 Alterations in sensitivity to antiepileptic drugs with age

Previously, differences in efficacy between single and doubled drug combinations for each stage of epileptogenesis were investigated. Next, differences between age groups were explored for each individual drug and double drug combination (data previously presented). A between subjects ANOVA was used to investigate these differences. Frequency data was used to assess this and all data were normalised to the control period in which 0[Mg]$^{2+}$ was applied alone. The data were ranked to make it normally distributed, see figure A2.5 (single drugs) and A2.6 (double drugs), appendix for unranked data.

The effect of VPA alone was compared between age groups (figure 6.9 A). No outliers were identified. There was no significant interaction effect between age and epileptic state for application of VPA. There was no overall significant difference between SE and AMC. Overall significant differences were seen between different age groups F(degrees freedom, error) = (3,56) = 4.662, P = 0.006. Specifically, VPA was significantly less effective at reducing the frequency of SLEs in slices prepared from SE and AMCs at 24 hours compared to 4 weeks (P = 0.017) and 3 months+ (P = 0.009) post induction.

The effect of CBZ alone was compared between age groups (figure 6.9 B). No outliers were identified. There was no significant interaction effect between age and epileptic state. There

was no significant difference between SE and AMC. There was also no significant difference identified between age groups.

The effect of LTG alone was compared between age groups (figure 6.9 C). No outliers were identified. There was no significant interaction effect between age and epileptic state. There was no significant difference between SE and AMCs. There was an overall significant difference found between age groups F(degrees freedom, error) = (3,56) = 5.587, P = 0.002. Specifically, LTG was significantly less effective at reducing the frequency of SLEs in slices prepared from SE and AMC animals at 24 hours (P = 0.007) compared to 4 weeks. LTG was also significantly less effective at reducing the frequency of SLEs in slices prepared from SE and AMC animals at 1 week (P = 0.007) compared to 3 months+ post induction.

The effect of CBD alone was compared between age groups (figure 6.9 D). No outliers were identified. There was no significant interaction effect between age and epileptic state. There was no significant difference between SE and AMCs. There was an overall significant difference between age groups F(degrees freedom, error) = (3,56) = 5.077, P = 0.004. Specifically, CBD was more effective at reducing the frequency of SLEs in slices prepared from SE and AMC animals at 3 months+ post induction compared to 24 hours (P = 0.031) and 1 week (P = 0.003).

The effect of TGB alone was compared between age groups (figure 6.9 E). One outlier was identified and removed. There was no significant interaction effect between age and epileptic state. There was no significant difference between SE and AMCs. There was an overall significant difference between age groups F(degrees freedom, error) = (3,55) = 12.142, P < 0.000. Specifically, TGB was significantly more effective at reducing the frequency SLEs in slices prepared from AMC and SE animals at 4 weeks (P = 0.001) and 3 months+ (P < 0.00) post induction compared to 24 hours post induction. Additionally, TGB was significantly more effective at reducing SLEs in slices prepared from AMC and SE animals at 4 weeks (P = 0.003) and 3 months+ (P < 0.000) post induction compared to 1 week post induction.

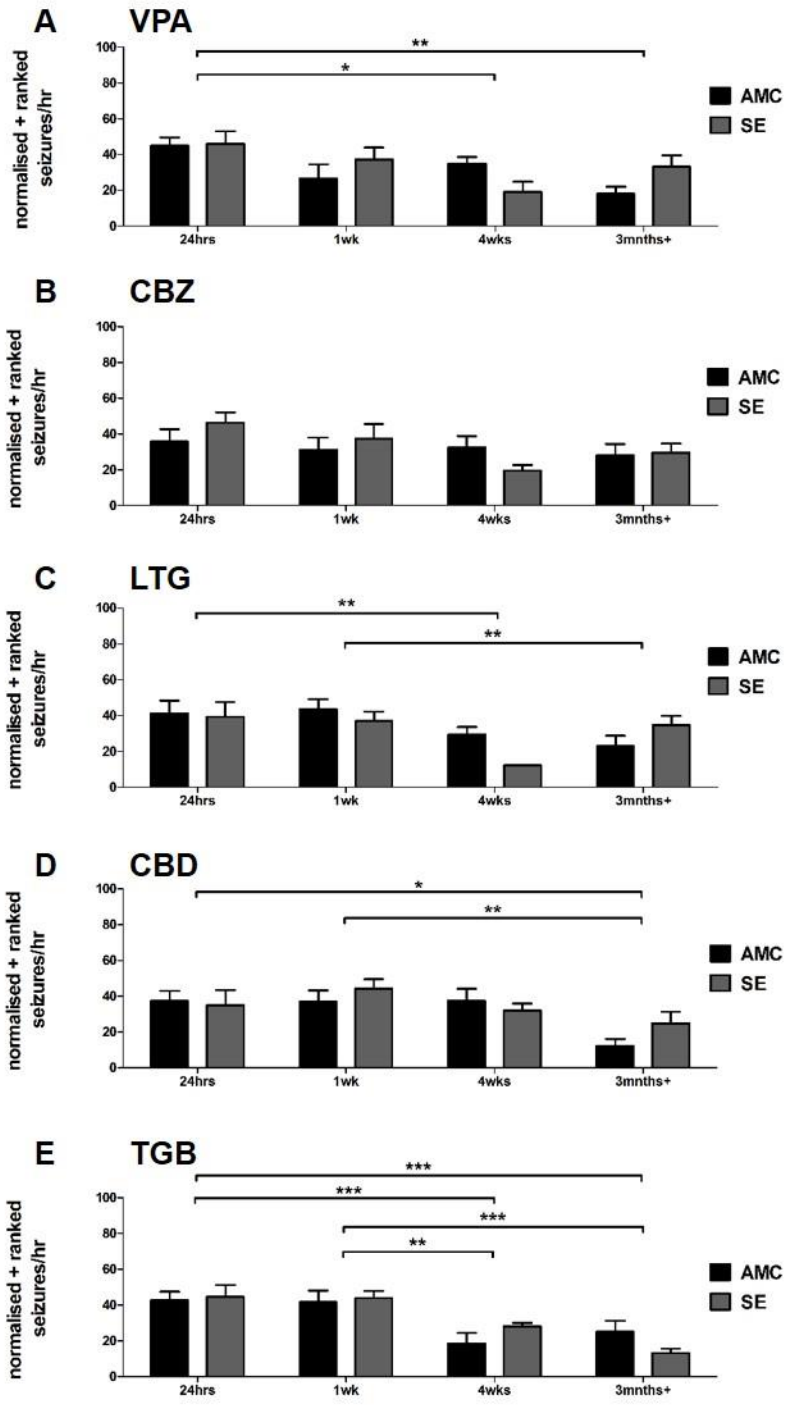

Figure 6.9 Comparison of the effect of 5 AEDs on SLEs at 4 stages post SE compared to AMC
Ranked mean SLE per hour (normalised to 0$[Mg]^{2+}$) after single drug application at 24 hours, 1 week, 4 weeks and 3 months+ post epilepsy induction (SE – grey) and age-matched controls (AMC - black)
N = 8 for all conditions. * $P < 0.05$, ** $P < 0.01$, *** $P < 0.001$.

The effect of VPA + CBZ was compared between age groups (figure 6.10 A). One outlier was identified and removed. There was no significant interaction effect between age and epileptic state. There was no overall significant difference between SE and AMCs. There was an overall significant difference between age groups F(degrees freedom, error) = (3,55) = 4.738, P = 0.005. Specifically, VPA + CBZ was significantly more effective at reducing the frequency of SLEs in slices prepared from AMC and SE animals at 4 weeks (P = 0.005) and 3 months+ (P = 0.038) compared to 24 hours post induction.

The effect of CBZ + ZNS was compared between age groups (figure 6.10 B). Two outliers were identified and removed. There was a significant interaction effect between age and epileptic state for application for application of CBZ + ZNS F(degrees freedom, error) = (3,54) = 1.365, P = 0.009. Specifically, CBZ + ZNS was significantly (P < 0.000) more effective at reducing SLEs in slices prepared from AMC compared to those prepared from SE animals at 24 hours post induction. There was no overall significant difference between SE and AMC. There was an overall significant difference between age groups F(degrees freedom, error) = (3,54) = 5.873, P = 0.009. Specifically, CBZ + ZNS was significantly less effective at reducing the frequency of SLEs at 24 hours post induction compared to 1 week (P = 0.003) and 3 months+ (P = 0.008) post induction.

The effect of CBZ + GBP was compared between age groups (figure 6.10 C). Two outliers were identified and removed. There was not a significant interaction effect between age and epileptic state. There was no overall significant difference between AMC and SE. There was an overall significant difference between age groups F(degrees freedom, error) = (3,54) = 10.666, P < 0.000. Specifically, CBZ + GBP was significantly less effective at reducing SLEs at 24 hours post induction compared to 1 week (P = 0.004), 4 weeks (P < 0.000) and 3 months+ (P < 0.000) post induction.

The effect of LTG + GBP was compared between age groups (figure 6.10 D). Two outliers were identified and removed. There was no significant interaction effect between age and epileptic state. There was no overall significant difference between AMC and SE. There was an overall significant difference between age groups F(degrees freedom, error) = (3,54) =3.098, P = 0.034. However post-hoc analysis did not identify any specific differences between groups.

The effect of CBD + CBZ was compared between age groups (figure 6.10 E). One outlier was identified and removed. There was no significant interaction effect between age and epileptic state. There was no overall significant difference between SE and AMCs. There was an overall significant difference between age groups F(degrees freedom, error) = (3,55) = 12.305, P < 0.000. Specifically, CBD + CBZ was found to more effectively reduce the frequency of SLEs in slices prepared from SE and AMC animals at 4 weeks (P = 0.005) and 3 months+ (P = 0.015) compared to 24 hours post induction. Additionally, CBD + CBZ was

found to more effectively reduce the frequency of SLEs in slices prepared from SE and AMC animals at 4 weeks ($P < 0.000$) and 3 months+ ($P < 0.000$) post induction compared to 1 week post induction.

The effect of TGB + CBZ was compared between age groups (figure 6.10 F). Two outliers were identified and removed. There was no significant interaction effect between age and epileptic state. There was no overall significant difference between SE and AMCs. There was an overall significant difference between age groups F (degrees freedom, error) = (3,54) = 8.269, $P < 0.000$. Specifically, TGB + CBZ was found to more effectively reduce the frequency of SLEs in slices prepared from SE and AMC animals at 3 months+ post induction compared 24 hours ($P < 0.000$) and 1 week ($P = 0.020$) post induction.

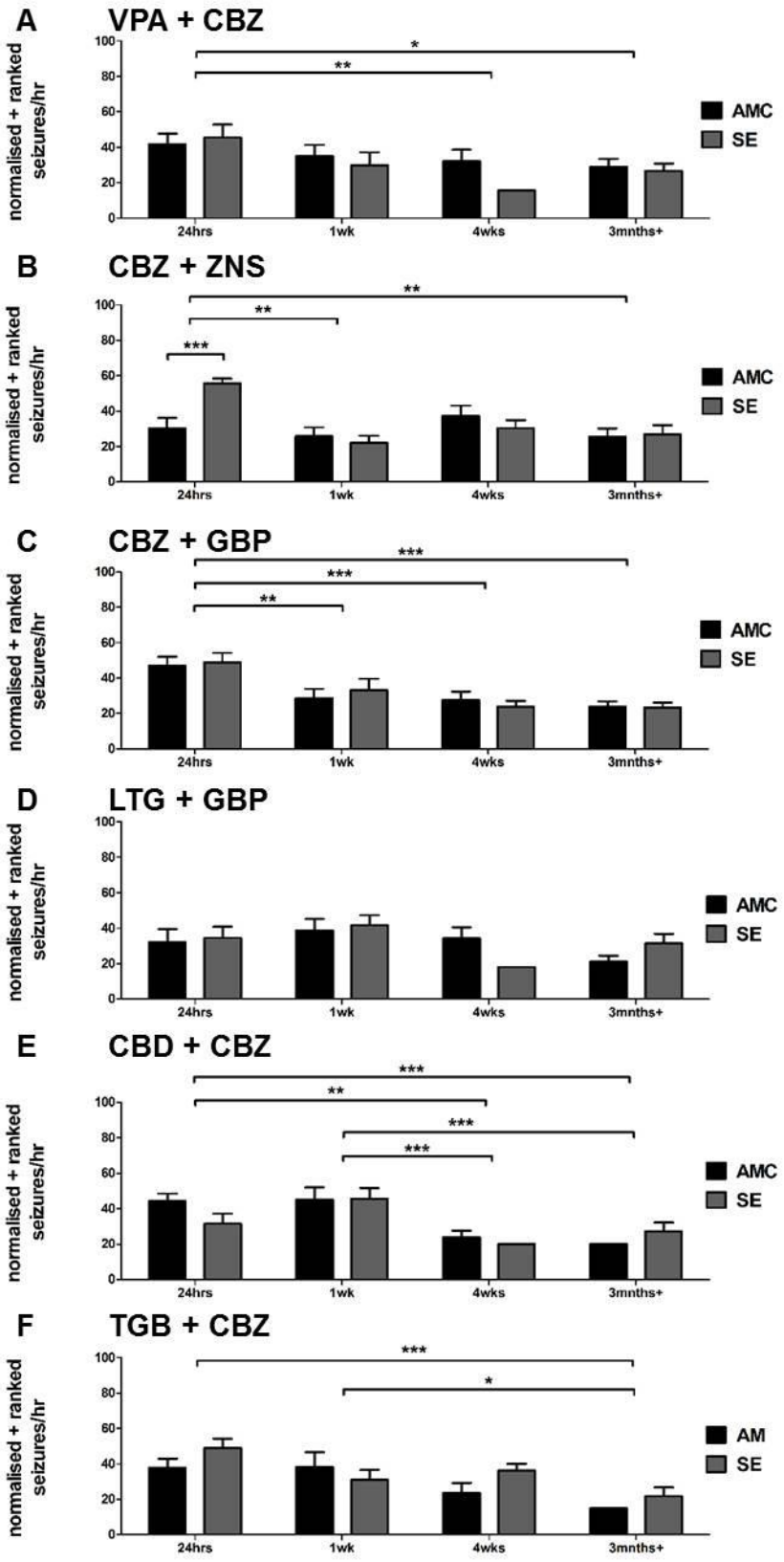

Figure 6.10 Comparison of the effect of 6 combinations of AEDs on SLEs at 4 stages post SE compared to AMC

Ranked mean SLE per hour (normalised to 0$[Mg]^{2+}$) after double drug application at 24 hours, 1 week, 4 weeks and 3 months+ post epilepsy induction (SE – grey) and age-matched controls (AMC - black)
N = 8 for all conditions. * P < 0.05, ** P < 0.01, *** P < 0.001.

6.2.7 Alterations in antiepileptic drug resistance with age

Previously we have established an age-dependent increase in sensitivity to AEDs (above). Next we assessed if a similar pattern was observed for resistance to AEDs. Slices were defined as resistant if SLE frequency, increased, stayed the same or decreased by <50 %. This was plotted against time for single (figure 6.11 Ai-Fi) and double (figure 6.11 Aii-Fii) drugs. As the data presented is a percentage, statistical analysis was not performed, however there was a trend in most single and double drug combinations towards decreased resistance with age. Next, all the single drugs (figure 6.12 A) and double drug combinations (figure 6.12 B) were pooled at each age group to assess the overall resistance to AEDs over time.

The percentage of slices that displayed resistance for each single drug was pooled at every time point and compared using a between subjects ANOVA to further assess if resistance to AEDs was age-dependent or epileptic state-dependent. The data were ranked (figure 6.12 A) to normalise them, the unranked mean ± SEM is presented in table 6.7. There was no significant interaction effect between age and epileptic state. There was no overall significant difference between SE and AMC. There was an overall significant difference between age groups $F(3,40) = 8.409$ $P < 0.000$. Specifically, slices prepared from SE and AMC animals at 3 months+ post induction were significantly less resistant than 24 hrs ($P < 0.000$) and 1 week ($P = 0.008$) post induction. Slices prepared from SE and AMC animals at 4 weeks post induction were also significantly less resistant than 24 hours post induction ($P = 0.017$).

The percentage of slices that displayed resistance for each double drug were pooled at each time point and compared using a between subjects ANOVA to further assess if resistance to AEDs was age-dependent or epileptic state-dependent. The data were ranked (figure 6.12 B) to normalise them and the unranked mean ± SEM is presented in table 6.7. There was no significant interaction effect between age and epileptic state. There was no overall significant difference between SE and AMC. There was an overall significant difference between age groups $F(3,40) = 23.276$ $P < 0.000$. Specifically, slices prepared from SE and AMC animals at 3 months+ post induction were significantly less resistant than those prepared at 24hrs ($P < 0.000$) and 1 week ($P < 0.000$) post induction. Slices prepared from SE and AMC animals at 4 weeks post induction were also significantly less resistant than those prepared at 24 hours ($P < 0.000$) and 1 week ($P = 0.001$) post induction.

In summary, the data indicates that like sensitivity, resistance is also age-dependent. When individual single and double drug combinations were considered most displayed a trend towards decreased resistance with time. When resistance for every drug was pooled together and compared at different time points more resistance was observed in younger (24 hours and 1 week) compared to older (4 weeks and 3 months+) animals.

Figure 6.11 (following page) Percentage of resistant slices for each single and double drug at every time point.

The percentage of slices displaying resistance (defined as a <50 % reduction in SLE frequency) is plotted for each single (Ai-Fi) and double (Aii-Fii) drug for both SE (grey) and AMC (black) slices. N = 8 for all conditions.

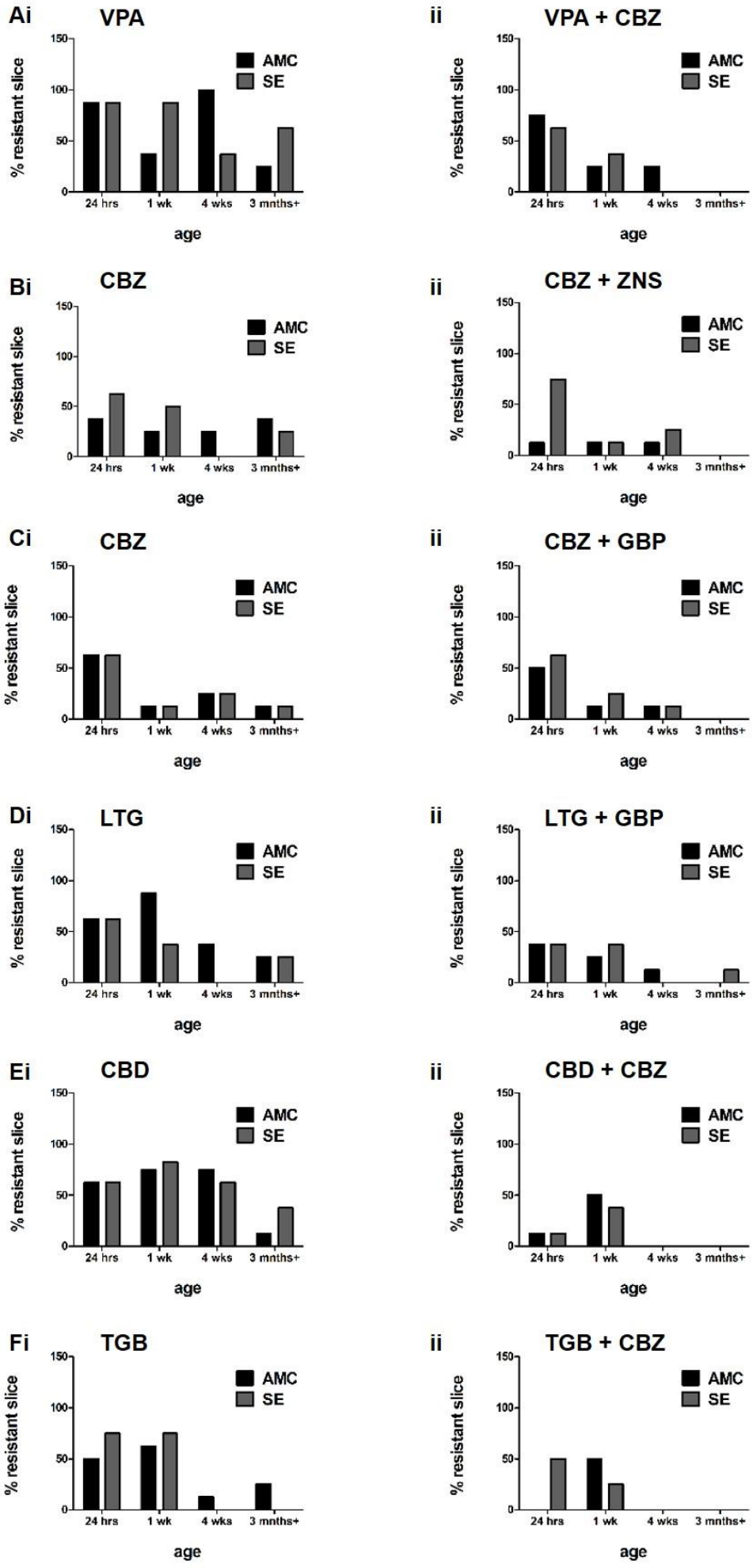
Ai
VPA
ii
VPA + CBZ
Bi
CBZ
ii
CBZ + ZNS
Ci
CBZ
ii
CBZ + GBP
Di
LTG
ii
LTG + GBP
Ei
CBD
ii
CBD + CBZ
Fi
TGB
ii
TGB + CBZ
% resistant slice
150
100
50
0
AMC
SE
24 hrs
1 wk
4 wks
3 mnths+
age

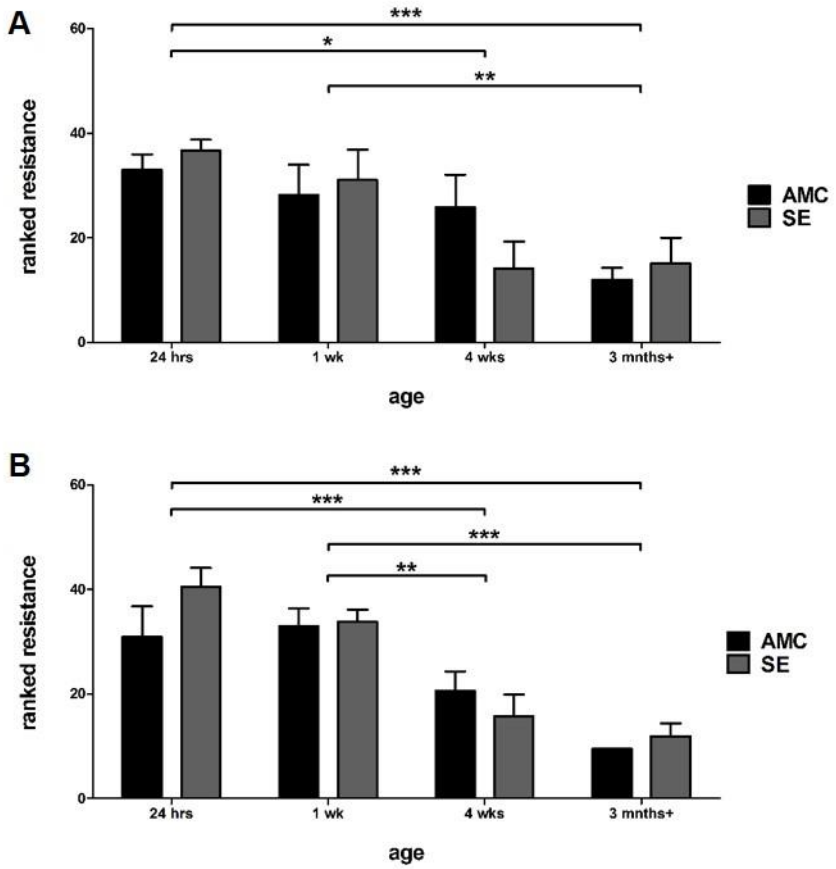

Figure 6.12 Ranked pooled resistance to AEDs at 4 time points of epileptogenesis compared to AMC
Ranked mean percentage of slices that displayed resistance pooled for all the single (A) and double (B) drugs tested for (SE – grey) and age-matched controls (AMC - black)
N = 48 for all conditions. * P < 0.05, ** P < 0.01, *** P < 0.001.

	AMC		SE	
time point	single drug (%)	double drug (%)	single drug (%)	double drug (%)
24 hrs	60.4 ± 6.8	31.5 ± 11.5	68.8 ± 4.3	50.0 ± 9.1
1 wk	50.0 ± 12.1	29.2 ± 7.0	55.4 ± 12.4	29.2 ± 4.2
4 wks	45.8 ± 13.9	10.4 ± 3.8	20.8 ± 10.5	6.3 ± 4.3
3 mnths+	16.7 ± 4.2	0.0 ± 0.0	22.9 ± 9.9	2.1 ± 2.1

Table 6.7 Mean pooled percentage of slices that displayed resistance to AEDs at 4 time points during epileptogenesis compared to AMC
Mean ± SEM of percentage of slices that displayed resistance pooled for all the single and double drugs. N = 48 for each condition.

6.3 Discussion

The RISE model was recently developed as an alternative to traditional epilepsy models which often display high levels of morbidity and mortality (Sloviter, 2005; Modebadze et al., 2016). While the model maintains its epileptogenicity, its sensitivity (or resistance) to AED treatment was unknown, and therefore this was assessed in the PC at four stages of epileptogenesis. 0$[Mg]^{2+}$ was applied to PC slices prepared from the RISE model of TLE and AMCs to reliably induce SLEs. Single and double drug combinations were tested as both mono- and polytherapy are used clinically. The majority of the single and double AED combinations assessed in this study significantly reduced the frequency of 0$[Mg]^{2+}$ induced SLEs in the PC at 4 weeks and 3 months+ post epilepsy induction regardless of epilepsy state. However, in the younger age groups (24 hours and 1 week) reduced sensitivity or resistance to a single AED treatment was found. This time-dependent decrease in resistance to AED treatment is age, not epileptic state-dependent. Significant differences in sensitivity to AEDs between SE and AMC were primarily found at 4 weeks post induction with AED treatment being more effective in slices prepared from SE compared to AMC animals.

6.3.1 Pharmacoresistance during the early latent period

Single doses of AEDs were rarely (2/12) able to significantly reduce SLEs in slices prepared from either SE or AMC animals during the early latent period (24 hours and 1 week post epilepsy induction). The percentage of slices resistant to single AED intervention was found to be between 50 and 60 %.

A number of single AEDs have been previously assessed on 0$[Mg]^{2+}$ induced SLEs in cortico-hippocampal formation slices prepared from young animals with only 5/10 AEDs assessed effectively eliminating or reducing the frequency of SLEs (Quilichini et al., 2003). They found VPA to be effective whereas TGB, GBP, CBZ and LTG were either completely ineffective (TGP or GBP) or worsened SLEs (CBZ, LTG) (Quilichini et al., 2003). In this thesis, LTG and TGB were rarely effective, with a small, but significant reduction in SLE frequency noted at 24 hours but not 1 week post induction in AMC (LTG) and SE (TGB) animals. In contrast with previous work, VPA was found to be completely ineffective in both age groups and CBZ significantly reduced SLE frequency at both 24 hours and 1 week and GBP was not tested alone. However, it is worth noting the Quilichini study was performed in very young (post-natal day 7-8) animals (Quilichini et al., 2003). In slices prepared from older (6 - 8 weeks, corresponding to our 2 - 4 weeks post induction) rats, initial SLEs were sensitive to CBZ and VPA application in temporal lobe slices, however they lost this sensitivity when they transitioned to late recurrent discharges (LRDs) and became pharmacoresistant (Dreier and Heinemann, 1990; Zhang et al., 1995). As these time points (postnatal 7 - 8 days and 6 - 8 weeks) were either side of the 24 hour (3 weeks postnatal) and 1 week (4 weeks postnatal) time points used in this study, it is difficult to make comparisons. *In vivo*, CBZ has been found to prevent and VPA prolong the time course to

pilocarpine induced SE, and both were ineffective when given after SE had begun (Morrisett et al., 1987). However, another study found that pre-treatment with CBZ had no effect but VPA prevented SE, although this may be accounted for by differing concentrations of AEDs used (Turski et al., 1987).

Application of two AEDs significantly reduced the frequency of SLEs in 4/6 drug combinations tested in slices prepared from SE and AMC animals at 24 hours and 1 week post induction (except at 1 week SE, only 3/6 were effective). The addition of a second drug reduced the percentage of slices displaying resistance from 50 – 60 % to 30 - 50 %. This is similar to the level of pharmacoresistance seen clinically after prescription of one and two AEDs, further reinforcing the need to consider both single and double AED treatments (Semah et al., 1998; Kwan and Brodie, 2000; Rogawski and Löscher, 2004). The level of resistance was indistinguishable between 24 hours and 1 week in both AMC and SE animals. Similar results were obtained in both SE and AMC (although see below), implying this resistance is an intrinsic property of 0$[Mg]^{2+}$ induced SLEs in the PC.

When applied in combination, at 24 hours post induction, CBZ + ZNS was significantly more effective in slices prepared from AMC than in SE animals (figure 6.10), with only 3/8 slices continuing to show SLEs following ZNS application in AMC compared to 8/8 in slices prepared from SE animals, a trend that is not repeated in any other age group. Resistance to this combination was found in 1/8 slices prepared from AMC, compared to 6/8 prepared from SE animals. ZNS is a broad spectrum AED which modulates Na^+ channels and T-type Ca^{2+} channels. In CA1 pyramidal neurons, a transient upregulation of the T-type Ca^{2+} channel $Ca_v3.2$ has been found in slices prepared a few days following pilocarpine SE in rats and mice and kindling in rats. This enhanced the magnitude of T-type Ca^{2+} currents in apical dendrites and changed pyramidal cell behaviour from regular firing to bursting (Faas et al., 1996; Sanabria et al., 2001; Su et al., 2002; Yaari et al., 2007; Becker et al., 2008). Intriguingly, in mice with a genetic deletion of $Ca_v3.2$ not only is this pathological bursting behaviour missing but chronic SRS development was significantly reduced implying that this pathological activity is critical for epileptogenesis (Becker et al., 2008). ZNS has been found to reduce T-type Ca^{2+} channel currents in a concentration-dependent manner (Suzuki et al., 1992; Kito et al., 1996). In this study ZNS (in combination with CBZ), was significantly more effective in AMC than SE animals. This could be due to enhanced expression of T-type Ca^{2+} channels in SE animals leading to an increase in the dose required to achieve the same level of inhibition. The $Ca_v3.2$ channel is significantly upregulated at 2 and 3 days post induction and returns to normal 10 days following induction accounting for the effect of ZNS + CBZ at 24 hours post induction only (Becker et al., 2008). VPA has also been reported to block T-type Ca^{2+} channels but no significant difference was found between SE and AMC at the early time points (24 hours and 1 week). However, this is likely explained by higher concentrations than used in this study being required for T-type Ca^{2+} channel blockade (Kelly et al., 1990).

6.3.2 Alterations in sensitivity to antiepileptic drug treatment during the mid-latent period

The mid latent period (~4 weeks) of the RISE model is characterised by a reduction in gamma power in the hippocampus and progressive changes in rodent behaviour (Modebadze et al., 2016). 3/6 and 4/6 single AEDs tested in this study significantly reduced the frequency of SLEs in slices prepared from AMC and SE animals respectively. When single AEDs were applied, resistance was found in ~45 % AMC and ~20 % slices prepared from SE animals, although this difference was not significant. Resistance was ~10 % for AMC and ~6 % in slices prepared from SE animals when AEDs were applied in combination. This was the only time point in which differences between SE and AMC sensitivity was seen across multiple single and double AED combinations.

When used alone, CBZ, LTG and VPA were found to be more effective at reducing SLEs in slices prepared from SE than AMC animals. All three of these AEDs modulate Na^+ channels. The 4 week time point was also the only time point in which significant differences were found between all properties (IEI, frequency and latency to first SLE) of $0[Mg]^{2+}$ induced SLEs between slices prepared from SE and AMC animals (chapter 5) indicating PC SE slices at this time point are likely to be significantly more excitable than AMC. This increased excitatory activity could mean the Na^+ channel modulators, which are known to selectively target pathological activity, had more of an opportunity to bind to, and modulate Na^+ channels. This was supported by the observation that all three Na^+ channel modulators tested, were significantly more effective at reducing SLEs in SE compared to AMC slices at 4 weeks post induction. At this time point, the Na^+ channel modulators (CBZ, LTG and VPA) were also significantly more effective when applied alone compared to the new AED CBD and the GAT-1 inhibitor, TGB. This is a trend not seen at any other age group indicating there may be changes in the Na^+ channel sensitivity to AEDs in the mid latent period which resolves before the start of the chronic period. The latent period is characterised by the development of enhanced neuronal excitability and a reduction in seizure threshold (Pitkänen and Lukasiuk, 2009; Rattka et al., 2011). An increase in the Na^+ channel window current has been observed in the chronic stage of epilepsy following a short (2 - 4 week) latent period (Ellerkmann et al., 2003). This shifts the Na^+ channel inactivation towards more depolarising potentials and voltage-dependent activation towards more hyperpolarised potentials. When the membrane potential was within this window (-60 to -20 mV) activation could occur without inactivation thereby creating a persistent Na^+ influx. This effect is also seen following kindling and is thought to be due to a down-regulation of the $Na_v1.2$, $Na_v1.6$ and β1 subunits (Vreugdenhil et al., 1998a; Ketelaars et al., 2001; Ellerkmann et al., 2003). Downregulation of these subunits begins to occur during the latent period in the hippocampus, but differences in the electrophysiology of the persistent Na^+ channel were not assessed. In the EC, no differences were observed in the early latent period, but in the chronic period the persistent Na^+ current was enhanced (Agrawal et al., 2003). Assessment of the effect of Na^+ channel

modulators VPA, CBZ and LTG has only been performed previously in neurons taken from chronic SE rats not during the latent period (Schwarz and Grigat, 1989; Van den Berg et al., 1993; Vreugdenhil and Wadman, 1999; Remy et al., 2003; Cappaert et al., 2016) . However, as the PC is activated before the hippocampus in both the pilocarpine and kindling models of epilepsy, these changes might occur earlier in the PC which may explain why differences are seen between SE and AMC at the 4 week post-SE time point (Wall et al., 2000; André et al., 2007; Sinel'nikova et al., 2013). In contrast to our results, CBZ has been previously found to be less effective in altering the Na^+ channel window current and VPA and LTG's efficacy was unaltered in the chronic pilocarpine and kindling models of epilepsy compared to AMCs (Vreugdenhil and Wadman, 1999; Remy et al., 2003). Both LTG and VPA have also been found to exert a tonic blockade of Na^+ channels at rest in control neurons. This effect was significantly reduced in neurons from chronic SE animals compared to control with application of LTG but not VPA (Remy et al., 2003). These results are different to our data in which we have found the Na^+ channel modulators were more effective in slices prepared from SE compared to AMC. This could be due to variations between brain areas (PC compared to hippocampus) or differences between epilepsy models.

If this difference in responsiveness to AEDs between slices prepared from SE compared to AMCs was a Na^+ channel specific effect, we would expect SE and AMC slices to remain significantly different following the addition of a second Na^+ channel modulator. As expected, the addition of CBZ to VPA maintained the significant difference between SE and AMC slices. The addition of ZNS or GBP, AEDs not thought to modulate Na^+ channels, to CBZ abolished this significant difference between SE and AMC. However, the addition of GBP to LTG maintained the significant difference. This is probably due to GBP's poor efficacy and narrow spectrum of action.

There was no significant difference between SE and AMC slices after the addition of TGB, however when TGB and CBZ were applied together, the combination was significantly less effective in SE slices compared to AMCs. This was unexpected, however, when applied alone there was a trend towards an enhanced effect in AMC compared to SE and although this did not reach significance, it does indicate the effect seen is likely due to TGB not CBZ. TGB inhibits GAT-1 thereby allowing more GABA to build up in the synaptic cleft (During et al., 1992; Fink-Jensen et al., 1992; Sills et al., 1999). Alterations in $GABA_A$ receptor subunits occurs during the latent period before SRS develops (Brooks-Kayal 1998). In the RISE model, gamma oscillatory power in CA3 is reduced in the latent period and recovers in the chronic period, possibly indicating a reduction in the inhibitory network required for oscillation generation (Modebadze et al., 2016). GAT-1 transporters have been found to be reduced in epileptic animals and man which may confer resistance to TGB treatment, however, studies have only assessed the chronic, not the latent period (Patrylo et al., 2001). *In vitro*, SLEs induced by $0[Mg]^{2+}$ in the entorhinal cortex have been found to be sensitive to AEDs

(including TGB), however, a reduction in synaptically available GABA leads to a transition to LRDs and insensitivity to AEDs including TGB (Pfeiffer et al., 1996). Therefore, the decreased efficacy of TGB in slices prepared from the RISE model of SE might reflect a reduction in synaptically available GABA compared to AMC. If this was the case, application of $GABA_A$ receptor positive modulators would be expected to have no effect, whilst supplementing synaptically available GABA, by blocking the breakdown, directly applying GABA or applying a $GABA_A$ receptor agonist would be expected to abolish epileptiform activity (Heinemann et al., 1994; Mody et al., 1994; Pfeiffer et al., 1996). Blockade of GABA transporters via application of nipecotic acid or β-alanine has been previously found to block all epileptiform activity whilst TGB application failed to block drug resistant LRDs (Pfeiffer et al., 1996).

6.3.3 Pharmacosensitivity during the chronic period

Development of chronic SRS was detected following four consecutively high (≥10) PSBB scores. The increased aggressive behaviour, indicative of SRSs, exhibited by SE rats was detected with PSBB. The average time for SRS development was 20 weeks however it varied considerably between batches therefore AMC animals were carefully selected to reflect the age of animals used in SE experiments. Neuronal network oscillations recorded in the hippocampus of chronic SE rats *in vitro* have previously been found to be higher than any other age point (Modebadze et al., 2016). Resistance was lowest in this age group with 16 - 22 % of slices displaying resistance to single AED and <2 % slices displaying resistance to AEDs used in combination.

Sensitivity to CBZ has been found in the pilocarpine model *in vivo*, with CBZ application able to reduce the frequency and severity of seizures when given during the latent period, however it did not prevent epileptogenesis (Capella and Lemos, 2002). When given during SRS CBZ has been found to effectively reduce the number of spontaneous seizures (Leite and Cavalheiro, 1995). In our study, application of CBZ significantly reduced SLE frequency equally in slices prepared from AMC and SE animals and resistance to CBZ was found in a low percentage of slices from both groups. Differences in Na^+ channel sensitivity to CBZ has been found between brain slices prepared from kindling compared to control animals when stage 5 seizures were induced the day before, however, following a five week recovery this difference disappeared (Vreugdenhil and Wadman, 1999). Differences in responsiveness to CBZ have been found in slices prepared from drug resistant compared to drug sensitive human patients (Remy et al., 2003). In CBZ sensitive patients, CBZ induced a use-dependent enhancement of the inactivation of Na^+ channels and a complete block of high K^+ induced seizure activity. In contrast, CBZ application in tissue from CBZ insensitive patients and pilocarpine induced chronic SE rats, was completely ineffective on Na^+ channel inactivation and high K^+ induced seizure activity (Remy et al., 2003). Another mechanism of AED resistance is overexpression of P-glycoproteins which has been previously found in

drug resistant patients (Tishler et al., 1995; Sisodiya et al., 2002; Aronica et al., 2003). These ATP-dependent efflux transporters protect the brain at the blood brain barrier by pumping drugs back into capillaries (Tishler et al., 1995; Sisodiya et al., 2002; Aronica et al., 2003). However, this is unlikely to explain drug resistance to CBZ as it has been found to not be transported by P-glycoproteins (Baltes et al., 2007). Taken together, the reduction in sensitivity of Na^+ channels to CBZ is the likely mechanism for CBZ resistance implying that if resistance was present in the new RISE model of epilepsy, it should be reliably identified *in vitro* (Baltes et al., 2007). However, more recent research found no difference in sensitivity to CBZ between neuronal tissue removed from CBZ resistant patients and rodent control slices (Cappaert et al., 2016). Given that CBZ significantly reduced the frequency of SLEs in both SE and AMCs it is unlikely that resistance to CBZ exists in this age group.

VPA has various mechanisms of action and has a broader spectrum of use compared to CBZ. VPA did effectively reduce SLE frequency both alone and in combination with CBZ at 3 months+ post induction with no differences found between SE and AMC. Previous research also found VPA had a similar effect on both Na^+ channel inactivation and voltage-dependence in slices prepared from kindled and chronic (pilocarpine) animals compared to control animals (Vreugdenhil and Wadman, 1999; Remy et al., 2003). This was further confirmed in tissue removed from patients with drug resistant epilepsy in which VPA still induced a strong shift in the voltage-dependence of steady state inactivation (Vreugdenhil et al., 1998b). However, VPA is also known to influence T-type Ca^+ channels and increase available GABA which may be more important for its antiepileptic properties (Rogawski and Löscher, 2004). In this study, VPA applied alone was found to be less effective than TGB, whereas combined VPA and CBZ was less effective than CBD and CBZ at 3 months+ post induction. The reverse was found in previous studies in which VPA application was explored in slices prepared from young and older animals. VPA was found to be completely effective against 0$[Mg]^{2+}$ induced SLEs in slices prepared from young (postnatal day 7 – 9) in temporal lobe slices whereas TGB was ineffective (Quilichini et al., 2003). In slices prepared from older animals (6 – 8 weeks) VPA has been found to be ineffective (Dreier and Heinemann, 1990).

LTG has a very similar mechanism of action as CBZ but is associated with fewer side effects and a slightly lower efficacy (Patsalos and Bourgeois, 2010). No differences were found between SE and AMC at 3 months+ when used alone or in combination with GBP. This is in contrast with previous research which demonstrated LTG was less effective at tonic blockade of Na^+ channels at rest in hippocampal slices prepared from chronic pilocarpine rats compared to controls (Remy et al., 2003).

GBP was used in combination with Na^+ channel blockers CBZ and LTG. Both of these combinations effectively reduced the frequency of SLEs at 3 months+ post induction but

there were no significant differences in efficacy between SE and AMC. GBP is not a particularly well used drug, owing to its relative narrow spectrum and low efficacy (Rogawski and Löscher, 2004; Patsalos and Bourgeois, 2010). GBP has been previously found to be ineffective at reducing acetylcholinesterase inhibition induced SLEs prepared from guinea-pig brain slices *in vitro* (Harrison et al., 2005).

ZNS was used in combination with CBZ. Application of both CBZ and ZNS reduced the frequency of SLEs in slices prepared from AMC and SE slices with no difference observed between the two at 3 months+ post SE. ZNS reduces seizure activity via blockade of the T-type Ca^{2+} channels. Upregulation of $Ca_v3.2$ and increased T-type Ca^{2+} current has been found in the days following pilocarpine induced SE (see section 6.3.1). However, this effect was reversed one month post induction accounting for the lack of significant difference between SE and AMC at 4 weeks and 3 months+ post induction (Sanabria et al., 2001; Su et al., 2002; Yaari et al., 2007; Becker et al., 2008).

CBD and CBZ used in combination were found to be more effective at reducing the frequency of SLEs than VPA and CBZ, a pattern which is not found in any other age group. Given that CBZ is present in both combinations, this effect is likely due to differences in the efficacy of CBD and VPA. CBD has been found to reduce epileptiform activity induced by 4-AP and $0[Mg]^{2+}$ application in culture (postnatal 1 - 3) and brain slices from young animals (Drysdale et al., 2006; Jones et al., 2010). To our knowledge CBD has not been tested in slices prepared from older animals.

TGB inhibits GABA uptake transporter GAT-1 thereby increasing the GABA available in the synaptic cleft. During the chronic stage of epilepsy, application of TGB decreased SLE frequency to the same degree in SE and AMC. There is evidence that GABA transporters are reduced in TLE patients and rodent models which could result in resistance to TGB (Patrylo et al., 2001). However, more recent evidence found TGB potentiates GABA induced currents and prolongs IPSCs with the same efficacy in slices prepared from both control and chronic (pilocarpine) SE rats (Frahm et al., 2003; Stief et al., 2005).

6.3.4 Age-dependent alterations in pharmacoresistance and sensitivity to antiepileptic drug treatment

All single (except CBZ) and double drug (except LTG + GBP) combinations were found to be significantly more effective in the older age groups (4 weeks and 3 months+) compared to at least one younger age group. Resistance was found to be very high for single (50 – 60 %) and double (30 – 50 %) AEDs in younger age groups (24 hours and 1 week) and was significantly higher than resistance found at 4 weeks and 3 months+. The proportion of slices that were resistant to single and double AEDs in young animals is very similar to that found in human patients (Kwan and Brodie, 2000). PC slices prepared from young animals are therefore the best time point in which to test new AEDs in a model with similar levels of

resistance to that found clinically. At these time points there were few differences between SE and AMCs in slice excitability, assessed via response to 0[Mg]$^{2+}$ application or sensitivity to AEDs, indicating either could be used for AED screening. Despite being associated with significantly less mortality and morbidity than traditional models, the RISE protocol still elicits significant stress to the animals and therefore screening of AEDs is better carried out in the PC prepared from normal, young rats (Modebadze et al., 2016). This increase in sensitivity to AEDs is likely to be due to a global change in slices prepared from older animals rather than drug-specific alterations as significant differences were found for most drug(s) tested. However, it is first worth considering if there are any drug-specific mechanism that may account for this.

CBZ was the only single drug which did not display any statistical significance between age groups. This likely reflects its high degree of efficacy compared to other Na^+ channel AEDs (e.g LTG) (Patsalos and Bourgeois, 2010). When used in combination, there were age-dependent differences for every combination. Given that there were not any age-dependent differences for CBZ alone; these differences were likely to be due to the other drugs used in the combination rather than the action of CBZ. When the other Na^+ channels are considered, an age-dependent increase in efficacy was found for VPA alone and in combination with CBZ. There was also an increase in efficacy of LTG alone but not when used in combination with GBP, although there was a trend towards significance. As there was no increased efficacy for CBZ, the age-dependent increase in efficacy could be via a Na^+ channel independent mechanism not shared with VPA or LTG or it may be due to CBZ being more effective than other, newer AEDs. LTG in particular has a similar mechanism of action to CBZ but a lower efficacy (Patsalos and Bourgeois, 2010). CBZ might therefore, be equally as effective at all ages whereas VPA and LTG are only effective in reducing SLEs in slices that are less excitable.

There was an age-dependent enhancement in the efficacy of CBZ + ZNS. An age-dependent reduction in T-type Ca^{2+} channels has been reported in humans and mice (Rice et al., 2014), although this study is based on much older animals than the rats used in this study. If a reduction was present in the experimental rats used in this study, ZNS might be expected to more effectively block T-type Ca^{2+} channel currents in older animals which may explain the greater effect of ZNS (and CBZ) in the older age groups.

An age-dependent increase in efficacy was found for both CBD alone and in combination. CBD's mechanism of action is not well understood, however it is thought to modulate intracellular Ca^{2+} homeostasis which may explain the age-dependent changes. Intracellular Ca^{2+} homeostasis is thought to decline in slices prepared from aged animals which may explain why CBD is more effective in older animals and more effective than other AEDs (considered further below) (Drysdale et al., 2006; Ryan et al., 2009).

The effect of TGB alone and in combination with CBZ was age-dependent with a greater effect of TGB on SLEs found in the older age group (3 months+). An age-dependent reduction in TGB binding and GAT-1 expression has been previously reported in humans and rats respectively (Sundman-Eriksson and Allard, 2006; Bañuelos et al., 2014). However, this expression was compared at 6 months (young) and 22 months (aged) in rats, and as the maximum age for the rats used in this study was 7 months it is difficult to make generalisations between the data in this thesis and previous reports. TGB has been found to be ineffective on 0$[Mg]^{2+}$ induced SLEs in young animals, and its efficacy has not been assessed in older animals (Quilichini et al., 2003). Alterations in GABA inhibition found in older animals may instead decrease a slices ability to produce SLEs and make them more sensitive to AED treatment.

The majority of the single (except CBZ) and double (except LTG + GBP) drugs tested showed some form of increased pharmacosensitivity in older age groups. Although it was worthwhile considering each of these drugs separately, this increase in sensitivity to treatment is more likely to be a global phenomenon that affects all the AEDs rather than an effect of each individual receptor targeted. Given that the 0$[Mg]^{2+}$ model induces SLEs via relieving NMDA receptors of their voltage-dependent Mg^{2+} block, alterations in NMDA receptors with age must be considered (Mayer et al., 1984; Traub et al., 1994; Heinemann et al., 2006; Ghasemi and Schachter, 2011). Loss of NMDA receptor binding has been reported in aged rats and monkeys (Bonhaus et al., 1990; Miyoshi et al., 1991; Wenk et al., 1991; Castorina et al., 1993; Castorina et al., 1994). Removal of the NMDA receptor Mg^{2+} block is less effective at inducing SLEs in the older age groups with IEI, frequency and latency to first SLE modulated by age (chapter 5). This reduction in excitability could be due to a reduction in NMDA receptor function with age which may also affect AED efficacy.

Changes in GABA availability in slices may also contribute to the age-dependent increase in AED sensitivity. In younger animals, pharmacoresistance was found to depend on the availability of GABA. Early SLEs were found to be pharmacosensitive to a range of AEDs, however when these SLEs transformed into LRDs they became pharmacoresistant (Heinemann et al., 1994; Mody et al., 1994; Pfeiffer et al., 1996). This transition coincided with a reduction in synaptically available GABA. There is some evidence that GAT-1 GABA transporters are downregulated and GAD67, a GABA synthesising enzyme, is upregulated in aged humans and rats (Sundman-Eriksson and Allard, 2006; Bañuelos et al., 2014). However, others have reported an age-related downregulation of GAD67 and a decline in GABA levels (Gutierrez et al., 1994; Stanley and Shetty, 2004; Gao et al., 2013). Conversely, as the SLEs induced in younger animals are of a higher frequency, the synaptically available GABA may be utilised quicker than in older animals. In brain slices, the transition from SLEs to LRDs has also been found to occur concurrently with a failure of cellular energy metabolism (Schuchmann et al., 1999). This might mean that younger animals transition into

a pharmacoresistant form of epileptiform events whilst older animals with a lower frequency of SLEs stay pharmacosensitive. However, in the EC this transition from pharmacosensitive to pharmacoresistant is associated with a change in epileptiform pattern not found in the PC (Heinemann et al., 1994; Mody et al., 1994; Pfeiffer et al., 1996).

Alterations in propagation of epileptiform activity in older slices should also be considered. The elderly are one of the most seizure susceptible populations, however seizures in this age group are much less likely to generalise to other brain regions (DeToledo, 1999). Slices prepared from aged compared to young animals have been found have a reduced ability to spread between brain regions and a smaller increase in extracellular K^+ (Holtkamp et al., 2003). As many AEDs, including those used in this study, are thought to reduce propagation of seizures, their effect may be enhanced in a model in which propagation is minimal (Rogawski and Löscher, 2004).

A final consideration is the age-dependent decline in slice viability. Alterations in Ca^{2+} homeostasis have been reported in brain slices prepared from older animals. Age-dependent elevation in intracellular Ca^{2+} via increased Ca^{2+} influx and afterhyperpolarisation, mitochondrial disruption and oxidative stress leads to increased excitotoxicity (Landfield and Pitler, 1984; Pitler and Landfield, 1990; Moyer et al., 1992; Moyer and Disterhoft, 1994; Joseph et al., 2000; Xiong et al., 2002). Excitotoxicity damages or kills neurons and is likely to affect slice viability. To avoid this, a choline based cutting solution was used to prepare slices (Hoffman and Johnston, 1998; van Praag et al., 2002; Momiyama, 2003; Tanaka et al., 2008). However, the difficulty in obtaining patch clamp or oscillatory recordings in the older slices even when prepared using a choline based cutting solution (see chapter 3) suggests that an age-dependent decline in slice viability in the PC is still present. This might also explain why CBD (and CBZ) is more effective than VPA + CBZ in older animals as CBD alters Ca^{2+} homeostasis (Ryan et al., 2009). A decline in slice viability is likely to influence slice excitability and response to AEDs.

6.3.5 Comparison to parallel study conducted in the entorhinal cortex

This experimental work was conducted in parallel with a study by Darshna Shah. The six combinations of AEDs were tested on 0$[Mg]^{2+}$ induced SLEs in entorhinal cortex (EC) slices prepared at the same four stages of SE. AMC slices were not tested owing to the EC's insensitivity to SLE induction in AMC slices *in vitro* (see chapter 5). The highest level of resistance was observed at 1 week post SE for the EC and the lowest in 3 months+ post SE (table 6.8). An age-dependent reduction in resistance to AED treatment was observed in the EC, however, it was not as prominent as that observed in the PC. For example at 3 months+ post SE, single AED resistance was observed in 41 % compared to 23 % in the EC and PC respectively (Shah, 2017). Resistance was almost completely abolished in the PC (~2 %) when double AED combinations were applied to this age group, whereas resistance was still

found in 21 % of EC slices. In the youngest age group (24 hours post SE), resistance was higher in the PC than the EC (table 6.8). In summary, although AED resistance was also reduced with age in the EC, the reduction in resistance found in the PC was more obvious. It is not known if the change in resistance in the EC was dependent on age or epileptic state as slices prepared from AMC animals were not tested. As SLEs were more readily induced in the PC than the EC and resistance was found to be similar to that found clinically, 0$[Mg]^{2+}$ induced SLEs in PC slices prepared from young adult rats are the best *in vitro* model of drug resistant epilepsy discussed in this study.

	EC		PC	
time point	single drug (%)	double drug (%)	single drug (%)	double drug (%)
24 hrs	51.7 ± 9.4	31.0 ± 8.7	68.8 ± 4.3	50.0 ± 9.1
1 wk	83.3 ± 6.9	40.0 ± 9.1	55.4 ± 12.4	29.2 ± 4.2
4 wks	70.0 ± 8.5	30.0 ± 8.5	20.8 ± 10.5	6.3 ± 4.3
3 mnths+	41.4 ± 9.3	20.7 ± 7.7	22.9 ± 9.9	2.1 ± 2.1

Table 6.8 Mean pooled percentage of slices that display resistance at 4 time points during epileptogenesis in the entorhinal and piriform cortex

Mean ± SEM percentage of slices that displayed resistance pooled for all the single and double drugs. N = 48 for piriform cortex, n = 29 for entorhinal cortex. Entorhinal cortex data collected by Darshna Shah (Shah, 2017).

6.3.6 Final conclusions

In conclusion, the sensitivity and resistance of the PC *in vitro* to AED treatment was assessed at several time points across epileptogenesis in the new RISE model of TLE and compared to AMCs. Significant differences between SE and AMC animals were principally found at 4 weeks post induction, with AEDs primarily found to be more effective in slices prepared from SE compared to AMC animals. Pharmacoresistance was found in a high proportion of slices prepared from younger (24 hours and 1 week) age groups in both SE and AMC animals, which transitioned to pharmacosensitivity in the older age groups (4 weeks and 3 months+). A lower proportion of slices displayed AED resistance when AEDs were used in combination. In slices prepared from younger animals, resistance to single and double AEDs was very similar to that found in human patients. Clinically, two or more AEDs are used either separately or in combination before the epilepsy is confirmed as pharmacoresistant, reinforcing the need to test AEDs in combination to assess pharmacoresistance. Most single and double drug combinations showed an age-dependent increase in AED efficacy. When taken with the observation that slice excitability is reduced with age (chapter 5) a global mechanism is expected to be responsible for increased AED efficacy. Alterations in NMDA receptor binding, GABA availability and slice viability are the possible candidates for this observed difference.

Chapter 7 General discussion and further work

The main objective of this thesis was to explore the neuronal network behaviour of the piriform cortex (PC) in the rodent brain *in vitro* and explore alterations that occurred in this brain area during epileptogenesis. The PC was chosen as despite being identified as being more sensitive to chemical and electrical kindling than other areas of the brain more commonly associated with epilepsy (Piredda and Gale, 1985b; McIntyre and Gilby, 2008), it is relatively underexplored.

The experimental work in this project was initially conducted to induce and characterise the mechanisms underlying neuronal network oscillations in the PC. The study of neuronal network oscillations is a tool often utilised to uncover alterations in network activity in neurological disorders, for review see (Traub and Whittington, 2010). Odour evoked gamma oscillations in the hedgehog PC and olfactory bulb (OB) constitute the earliest experimental investigation of sensory induced neuronal rhythms (Adrian, 1942, 1950). Despite this, gamma oscillations had never been explored in the PC in an *in vitro* slice preparation and as such the cellular and synaptic mechanisms underlying their generation was not understood.

Application of kainic acid and carbachol reliably induced persistent gamma frequency oscillations in the PC in brain slices prepared from young, adult rats *in vitro* (chapter 3). These oscillations were similar to those previously found in the hippocampus and entorhinal cortex (Fisahn et al., 1998; Cunningham et al., 2003). Blockade of gap junctions abolished the oscillations indicating electrical connections between neurons were critical for oscillation generation. The kinetics of $GABA_A$ receptor mediated IPSCs were found to set the frequency of the rhythm (Segal and Barker, 1984; Traub et al., 1996b; Fisahn et al., 2004). AMPA mediated EPSCs were also found to be necessary for oscillation generation, indicating a close mechanistic resemblance to the PING model of oscillations, which depend on a mutually connected pyramidal cell-interneuron network (Cobb et al., 1995; Traub et al., 1996b; Whittington et al., 2000).

Epilepsy is a disorder characterised by abnormal synchronous network activity in the brain leading to seizures (Fisher et al., 2005; WHO, 2012). Following the characterisation of the mechanisms of PC gamma oscillations in control animals, we intended on using this as a tool to investigate changes in network activity in the PC over the course of epileptogenesis. However, induction of oscillations in slices prepared from older animals was considerably less reliable (<1 slice per animal displayed oscillatory activity) than in young adult rats. Switching to a choline based cutting solution increased the reliability, but it still remained too low to commence an analysis of network activity in the PC in aged animals during epileptogenesis (see appendix 1).

In parallel with the experimental work conducted in the rodent PC, we also induced and characterised neuronal network oscillations in slices prepared from human neuronal tissue (chapter 4). We utilised brain tissue removed from paediatric patients undergoing surgery to

treat drug resistant epilepsy. Application of similar concentrations of kainic acid and carbachol used in the rodent PC (chapter 3) induced persistent oscillatory activity in human neocortical slices. In contrast to PC oscillations, these oscillations were slower, falling within the beta frequency band. Nevertheless, the beta oscillations were mechanistically more closely related to PING-type oscillations (and PC gamma) than previously found persistent beta oscillations in the motor and somatosensory cortices (Roopun et al., 2006; Yamawaki et al., 2008). The human beta oscillations were found to depend on mACh M1, $GABA_A$ and AMPA receptors and gap junctions for oscillation generation. Fast, phasic IPSCs were found to pace the rhythm. Differences in brain area used or between human and rodent tissue, or control and epileptic tissue could account for why these oscillations fall within the beta frequency range yet pharmacologically resemble PING-type oscillations.

In vitro models of epileptiform activity have been used extensively to explore seizure mechanisms and screen antiepileptic drugs (AEDs) in both rodent and human tissue, for reviews see (Heinemann et al., 2006; Jones et al., 2015). Altering the ionic composition (high K^+, low Mg^{2+}) of the aCSF perfusate reliably induced both seizure-like events (SLEs) and inter-ictal bursts (IIBs) in human brain slices. Given that tissue was prepared from patients with drug resistant epilepsy, we speculated that this could be used as a model of drug resistant epilepsy *in vitro*. These events were found to be sensitive to the newly licenced AED perampanel (Rogawski and Hanada, 2013). In patients, perampanel has been found to be effective as an adjunct therapy in patients with drug resistant partial seizures (Rogawski and Hanada, 2013). Further evaluation of the pharmacoresistance of this induced epileptiform activity to more commonly used AEDs would be required to assess if this tissue could be used as a model of pharmacoresistant seizures.

The susceptibility of rodent brain slices to induction of epileptiform activity was also explored in the PC, and compared to the hippocampus and lateral entorhinal cortex (LEC); areas of the brain more commonly associated with epilepsy (chapter 5). The properties of these SLEs were similar between the brain areas, however in the majority of recordings SLEs were observed first in the PC. Electrodes inserted into the PC were also more likely to display SLEs than the LEC. This further confirmed the enhanced seizure susceptibility of this brain area (Piredda and Gale, 1985b; McIntyre and Gilby, 2008).

Following this, the sensitivity of the PC to seizure induction was then explored in the new RISE model of epilepsy (post SE) and compared to age-matched controls (AMCs). This modified lithium-pilocarpine model was previously developed by our research group to reduce the significant mortality and morbidity associated with traditional models (Sloviter, 2005; Modebadze et al., 2016). Spontaneous SLEs were found, however these were unreliable and did not persist, therefore the excitability of the slices was increased via application of a modified aCSF ($0[Mg]^{2+}$) solution (Mayer et al., 1984; Anderson et al., 1986;

Walther et al., 1986). Application of 0$[Mg]^{2+}$ induced SLEs in a similar proportion of slices prepared from SE compared to AMC slices. However, a reduction in excitability of the brain slices, observed as an increase in latency to first SLE and decrease in the frequency of SLEs, was noted in slices prepared from aged (AMC of 4 weeks and 3 months+) compared to young slices (AMC of 24 hours and 1 week). These alterations were absent in slices prepared from SE animals over the course of epileptogenesis, indicating they maintained the level of hyperexcitability found in slices prepared from young AMCs. We postulated that as there were changes in the excitability of PC brain slices during epileptogenesis, the sensitivity (or resistance) to AEDs might also be altered.

The need to develop new models to screen AEDs remains clear as a significant proportion of epilepsy patients remain resistant to currently available AED treatment. The drug resistance of the RISE model was assessed in the PC specifically by applying modified aCSF (0$[Mg]^{2+}$) and testing a range of AEDs on induced SLEs both alone and in combination (chapter 6). AED resistance in patients is usually defined as not obtaining adequate seizure control following a trial of two or more AEDs either separately or in combination (Bourgeois, 2008). Despite this, the majority of studies cite drug resistant *in vitro* when testing a range of single AEDs (Zhang et al., 1995; Dreier et al., 1998; Quilichini et al., 2003). In order to more accurately assess the AED resistance in the PC, we applied AEDs alone and in combination to investigate sensitivity and resistance (defined as <50 % reduction in seizure frequency) to AEDs. At 24 hours, no differences in sensitivity to AEDs was found between SE and AMC except when carbamazepine and zonisamide were applied in combination; this combination was more effective at reducing SLEs in slices prepared from AMC compared to SE animals. This likely reflected a previously found upregulation of T-type Ca^{2+} channels in the few days following SE (Becker et al., 2008). This difference disappeared at 1 week post SE with no differences in any AEDs tested found between slices prepared from SE and AMC, fitting with previous data in which upregulation of T-type Ca^{2+} channels was found to be transient and resolved within 10 days (Becker et al., 2008). In the mid latent period (4 weeks post SE), the AEDs that targeted Na^{+} channels were found to be significantly more effective at reducing seizure frequency in SE compared to AMC animals. These alterations may reflect enhanced excitability of slices (as found in chapter 5) or alterations in Na^{+} channel kinetics which resolved before the start of the chronic phase. In the chronic stage, no differences were observed in AED sensitivity between slices prepared from SE and AMC animals.

No significant difference in pharmacoresistance between SE and AMC was found, however, the pharmacoresistance was found to be significantly lower in aged (SE and AMC 4 weeks and 3 months+) compared to young animals (SE and AMC, 24 hours and 1 week). In slices prepared from young animals (SE and AMC, 24 hours and 1 week), pharmacoresistance was found in 50 - 80 % and 29 - 50 % of slices when challenged with single and double AEDs respectively. This was similar to that found clinically in TLE patients; therefore young AMC

slices could be used as a reliable *in vitro* model of drug resistant epilepsy without needing to induce epilepsy (Semah et al., 1998; Kwan and Brodie, 2000; Rogawski and Löscher, 2004). The chronic age group (SE and AMC) group displayed the least pharmacoresistance, with resistance found in 16 - 23 % and 0 - 2 % of slices in response to a single and double AED challenge respectively. The reduction in pharmacoresistance is likely to reflect global changes related to ageing, particularly as a reduction in AED resistance with age was also found in a parallel study conducted in the EC (Shah, 2017). Alterations in NMDA or $GABA_A$ receptors or a reduction in slice viability are possible explanations for the observed decline in AED resistance. Further experimental work would be required understand the mechanisms underlying the alterations in pharmacoresistance with age.

In conclusion, PC slices prepared from young animals are an excellent model of drug resistant seizure activity. This is due to the high level of sensitivity to seizure induction compared to other areas of the brain more commonly associated with epilepsy (chapter 5), the similarity in ratio between slices displaying pharmacoresistance and TLE patients reporting AED resistance (Semah et al., 1998; Kwan and Brodie, 2000; Rogawski and Löscher, 2004) and the relative ease and cost-effectiveness of using a brain slice preparation compared to an *in vivo* animal model.

Future work is required to fully characterise the PC gamma and human beta oscillations. Dual intra- and extracellular recordings combined with mathematical modelling and knock-out mouse studies are required to further uncover the cellular and synaptic mechanism generating these rhythms. To understand how network activity is altered in epilepsy, further studies of PC gamma and human beta oscillations in slices prepared from epileptic animals and human controls are required. At present is not known if the differences found between PC gamma and human beta are due to differences in animal or human tissue or control and epileptic tissue.

Further work is required to characterise the AED resistance of high K^+, low Mg^{2+} induced SLEs in resistant human tissue *in vitro*. However, if resistance to commonly used AEDs was found, this model could be used as a clinically relevant *in vitro* model of drug resistant seizures.

The clear difference in seizure susceptibility of the PC in slices prepared from SE compared to AMC slices also warrants further investigation. Alterations in NMDA receptor subunits are a possible explanation for alterations in the SLE properties. The developmental reduction in the NR2B NMDA receptor subunit has been found to be reversed in the entorhinal cortex in chronic SE rats (Yang et al., 2006). Increased expression of NR2B could increase excitability due to the role NR2B subunits have been found to play in AMPA receptor endocytosis (Tigaret et al., 2006).

Finally, the AED drug resistance in PC slices in chapter 6 focused on changes in the frequency of seizures in one fixed area; however the propagation of seizures to other brain regions is likely to be an important factor in seizure severity. Future studies should investigate how AEDs affect propagation of seizures as if there is no change in seizure incidence but a reduction in propagation to other brain regions seizure severity is likely to be significantly reduced. A multielectrode array in a slice preparation in which seizures are known to propagate between regions, such as in the hippocampal region or anterior and posterior PC, could be utilised for this purpose.

References

Acharya V, Acharya J, Lüders H (1998) Olfactory epileptic auras. *Neurology* **51**:56-61.
Adamchik Y, Baskys A (2000) Glutamate-mediated neuroprotection against N-methyl-D-aspartate toxicity: a role for metabotropic glutamate receptors. *Neuroscience* **99**:731-736.
Adrian ED (1942) Olfactory reactions in the brain of the hedgehog. *J Physiol (Lond)* **100**:459-473.
Adrian ED (1950) The electrical activity of the mammalian olfactory bulb. *Electroencephalogr Clin Neurophysiol* **2**:377-388.
Aghajanian GK, Rasmussen K (1989) Intracellular studies in the facial nucleus illustrating a simple new method for obtaining viable motoneurons in adult-rat brain-slices. *Synapse* **3**:331-338.
Agrawal N, Alonso A, Ragsdale DS (2003) Increased persistent sodium currents in rat entorhinal cortex layer V neurons in a post–status epilepticus model of temporal lobe epilepsy. *Epilepsia* **44**:1601-1604.
Albus H, Williamson R (1998) Electrophysiologic analysis of the actions of valproate on pyramidal neurons in the rat hippocampal slice. *Epilepsia* **39**:124-139.
Ambrósio AF, Soares-da-Silva P, Carvalho CM, Carvalho AP (2002) Mechanisms of action of carbamazepine and its derivatives, oxcarbazepine, BIA 2-093, and BIA 2-024. *Neurochem Res* **27**:121-130.
Amunts K, Lepage C, Borgeat L, Mohlberg H, Dickscheid T, Rousseau M-É, Bludau S, Bazin P-L, Lewis LB, Oros-Peusquens A-M (2013) BigBrain: an ultrahigh-resolution 3D human brain model. *Science* **340**:1472-1475.
Anderson WW, Lewis DV, Swartzwelder HS, Wilson WA (1986) Magnesium-free medium activates seizure-like events in the rat hippocampal slice. *Brain Res* **398**:215-219.
André V, Dubé C, François J, Leroy C, Rigoulot MA, Roch C, Namer IJ, Nehlig A (2007) Pathogenesis and Pharmacology of Epilepsy in the Lithium-pilocarpine Model. *Epilepsia* **48**:41-47.
Arai J, Natsume K (2006) The properties of carbachol-induced beta oscillation in rat hippocampal slices. *Neurosci Re* **54**:95-103.
Arnold J, Oldfield R, Pollard A, Silink M (1983) Primary hypomagnesaemia: case report. *J Paediatr Child H* **19**:45-46.
Aronica E, Gorter J, Jansen G, Van Veelen C, Van Rijen P, Leenstra S, Ramkema M, Scheffer G, Scheper R, Troost D (2003) Expression and cellular distribution of multidrug transporter proteins in two major causes of medically intractable epilepsy: focal cortical dysplasia and glioneuronal tumors. *Neuroscience* **118**:417-429.
Arroyo S, Uematsu S (1992) High-frequency EEG activity at the start of seizures. *J Clin Neurophysiol* **9**:441-448.
Azouz R, Jensen MS, Yaari Y (1996) Ionic basis of spike after-depolarization and burst generation in adult rat hippocampal CA1 pyramidal cells. *J Physiol* **492**:211.
Babb T, Kupfer W, Pretorius J, Crandall P, Levesque M (1991) Synaptic reorganization by mossy fibers in human epileptic fascia dentata. *Neuroscience* **42**:351-363.
Babb TL, Pretorius J, Kupfer W, Crandall P (1989) Glutamate decarboxylase-immunoreactive neurons are preserved in human epileptic hippocampus. *J Neurosci* **9**:2562-2574.
Babb TL, Brown WJ, Pretorius J, Davenport C, Lieb JP, Crandall PH (1984) Temporal lobe volumetric cell densities in temporal lobe epilepsy. *Epilepsia* **25**:729-740.
Bains JS, Longacher JM, Staley KJ (1999) Reciprocal interactions between CA3 network activity and strength of recurrent collateral synapses. *Nature Neurosci* **2**:720-726.
Baltes S, Gastens AM, Fedrowitz M, Potschka H, Kaever V, Löscher W (2007) Differences in the transport of the antiepileptic drugs phenytoin, levetiracetam and carbamazepine by human and mouse P-glycoprotein. *Neuropharmacology* **52**:333-346.
Barkai E, Hasselmo ME (1994) Modulation of the input/output function of rat piriform cortex pyramidal cells. *J Neurophysiol* **72**:644-658.
Barnes DC, Hofacer RD, Zaman AR, Rennaker RL, Wilson DA (2008) Olfactory perceptual stability and discrimination. *Nature Neurosci* **11**:1378-1380.
Barry E, Sussman NM, Oconnor MJ, Harner RN (1992) Presurgical electroencephalographic patterns and outcome from anterior temporal lobectomy. *Arch Neurol* **49**:21-27.

Barth DS, MacDonald KD (1996) Thalamic modulation of high-frequency oscillating potentials in auditory cortex. *Nature* **383**:78-81.
Bartos M, Vida I, Jonas P (2007) Synaptic mechanisms of synchronized gamma oscillations in inhibitory interneuron networks. *Nature Rev Neurosci* **8**:45-56.
Baskys A, Bayazitov D, Fang L, Blaabjerg M, Poulsen FR, Zimmer J (2005) Group I metabotropic glutamate receptors reduce excitotoxic injury and may facilitate neurogenesis. *Neuropharmacology* **49**:146-156.
Baxter BL (1967) Comparison of the behavioral effects of electrical or chemical stimulation applied at the same brain loci. *Exp Neurol* **19**:412-432.
Bañuelos C, Beas BS, McQuail JA, Gilbert RJ, Frazier CJ, Setlow B, Bizon JL (2014) Prefrontal cortical GABAergic dysfunction contributes to age-related working memory impairment. *J Neurosci* **34**:3457-3466.
Becker AJ, Pitsch J, Sochivko D, Opitz T, Staniek M, Chen C-C, Campbell KP, Schoch S, Yaari Y, Beck H (2008) Transcriptional upregulation of Cav3. 2 mediates epileptogenesis in the pilocarpine model of epilepsy. *J Neurosci* **28**:13341-13353.
Behan M, Haberly LB (1999) Intrinsic and efferent connections of the endopiriform nucleus in rat. *J Comp Neurol* **408**:532-548.
Behrens CJ, van den Boom LP, de Hoz L, Friedman A, Heinemann U (2005) Induction of sharp wave–ripple complexes in vitro and reorganization of hippocampal networks. *Nature Neurosci* **8**:1560-1567.
Behrens E, Schramm J, Zentner J, König R (1997) Surgical and neurological complications in a series of 708 epilepsy surgery procedures. *Neurosurgery* **41**:1-9; discussion 9-10.
Bekkers JM, Suzuki N (2013) Neurons and circuits for odor processing in the piriform cortex. *Trends Neurosci* **36**:429-438.
Bell GS, Sander JW (2001) The epidemiology of epilepsy: the size of the problem. *Seizure* **10**:306-316.
Belmaker R, Bersudsky Y (2007) Lithium–pilocarpine seizures as a model for lithium action in mania. *Neurosci Biobehav Rev* **31**:843-849.
Ben-Ari Y (1985) Limbic seizure and brain-damage produced by kainic acid - mechanisms and relevance to human temporal-lobe epilepsy. *Neuroscience* **14**:375-403.
Ben-Ari Y, Cossart R (2000) Kainate, a double agent that generates seizures: two decades of progress. *Trends Neurosci* **23**:580-587.
Ben-Ari Y, Tremblay E, Ottersen O (1980) Injections of kainic acid into the amygdaloid complex of the rat: an electrographic, clinical and histological study in relation to the pathology of epilepsy. *Neuroscience* **5**:515-528.
Ben-Ari Y, Lagowska J, Tremblay E, La Salle GLG (1979) A new model of focal status epilepticus: intra-amygdaloid application of kainic acid elicits repetitive secondarily generalized convulsive seizures. *Brain Res* **163**:176-179.
Bennett MVL, Zukin RS (2004) Electrical coupling and neuronal synchronization in the mammalian brain. *Neuron* **41**:495-511.
Ben-Ari Y, Dudek FE (2010) Primary and secondary mechanisms of epileptogenesis in the temporal lobe: there is a before and an after. *Epilepsy Currents* **10**:118-125.
Berger H (1929) Uber das Elektrenkephalogramm des Menschen. *Archiv für Psychiatrie und Nervenkrankheiten* **87**:527-570.
Bernard C, Esclapez M, Hirsch J, Ben-Ari Y (1998) Interneurones are not so dormant in temporal lobe epilepsy: a critical reappraisal of the dormant basket cell hypothesis. *Epilepsy Res* **32**:93-103.
Berretta N, Jones RSG (1996) Tonic facilitation of glutamate release by presynaptic N-methyl-D-aspartate autoreceptors in the entorhinal cortex. *Neuroscience* **75**:339-344.
Beyenburg S, Stavem K, Schmidt D (2010) Placebo-corrected efficacy of modern antiepileptic drugs for refractory epilepsy: Systematic review and meta-analysis. *Epilepsia* **51**:7-26.
Bibbig A, Middleton S, Racca C, Gillies MJ, Garner H, LeBeau FEN, Davies CH, Whittington MA (2007) Beta rhythms (15-20 Hz) generated by nonreciprocal communication in hippocampus. *J Neurophys* **97**:2812-2823.

Biber K, Fiebich BL, Gebicke-Harter P, van Calker D (1999) Carbamazepine-induced upregulation of adenosine A(1)-receptors in astrocyte cultures affects coupling to the phosphoinositol signaling pathway. *Neuropsychopharmacol* **20**:271-278.
Bih CI, Chen T, Nunn AV, Bazelot M, Dallas M, Whalley BJ (2015) Molecular targets of cannabidiol in neurological disorders. *Neurotherapeutics* **12**:699-730.
Blaabjerg M, Fang L, Zimmer J, Baskys A (2003) Neuroprotection against NMDA excitotoxicity by group I metabotropic glutamate receptors is associated with reduction of NMDA stimulated currents. *Exp Neurol* **183**:573-580.
Bliss TV, Collingridge GL (1993) A synaptic model of memory: long-term potentiation in the hippocampus. *Nature* **361**:31-39.
Bluemcke I et al. (2011) The clinicopathologic spectrum of focal cortical dysplasias: A consensus classification proposed by an ad hoc Task Force of the ILAE Diagnostic Methods Commission. *Epilepsia* **52**:158-174.
Blümcke I, Suter B, Behle K, Kuhn R, Schramm J, Elger C, Wiestler O (2000) Loss of hilar mossy cells in Ammon's horn sclerosis. *Epilepsia* **41**:S174-S180.
Boddeke H, Best R, Boeijinga P (1997) Synchronous 20 Hz rhythmic activity in hippocampal networks induced by activation of metabotropic glutamate receptors in vitro. *Neuroscience* **76**:653-658.
Boeijinga PH, Dasilva FHL (1988) Differential distribution of beta-EEG and theta-EEG activity in the entorhinal cortex of the cat. *Brain Res* **448**:272-286.
Boison D (2005) Adenosine and epilepsy: from therapeutic rationale to new therapeutic strategies. *Neuroscientist* **11**:25-36.
Boison D (2006) Adenosine kinase, epilepsy and stroke: mechanisms and therapies. *Trends Pharmacol Sci* **27**:652-658.
Bonati LH, Naegelin Y, Wieser HG, Fuhr P, Ruegg S (2006) Beta activity in status epilepticus. *Epilepsia*Epilepsia **47**47:207-210.
Bonhaus DW, Perry WB, McNamara JO (1990) Decreased density, but not number, N-methyl-D-aspartate, glycine and phencyclidine binding sites in hippocampus of senescent rats. *Brain Res* **532**:82-86.
Borden LA, Dhar TM, Smith KE, Weinshank RL, Branchek TA, Gluchowski C (1994) Tiagabine, SK&F 89976-A, CI-966, and NNC-711 are selective for the cloned GABA transporter GAT-1. *EJ Pharmacol* **269**:219-224.
Borges LF, Giicer G (1978) Effect of magnesium on epileptic foci. *Epilepsia* **19**:81-91.
Bourgeois BFD (2008) General concepts of medical intractability in HO Luders, Epilepsy surgery (2nd edition), informa healthcare pp. 63-68: informa healthcare.
Brandt C, Potschka H, Loscher W, Ebert U (2003) N-methyl-D-aspartate receptor blockade after status epilepticus protects against limbic brain damage but not against epilepsy in the kainate model of temporal lobe epilepsy. *Neuroscience* **118**:727-740.
Bressler SL, Freeman WJ (1980) frequency-analysis of olfactory system EEG in cat, rabbit, and rat. *Electroencephalogr Clin Neurophysiol* **50**:19-24.
Brown P (2003) Oscillatory nature of human basal ganglia activity: Relationship to the pathophysiology of Parkinson's disease. *Movement Disorders* **18**:357-363.
Buchheim K, Schuchmann S, Siegmund H, Gabriel HJ, Heinemann U, Meierkord H (1999) Intrinsic optical signal measurements reveal characteristic features during different forms of spontaneous neuronal hyperactivity associated with ECS shrinkage in vitro. *EJ Neurosci* **11**:1877-1882.
Buck DR, Mahoney AW, Hendricks DG (1979) Effects of cerebral intraventricular magnesium injections and a low magnesium diet on nonspecific excitability level, audiogenic seizure susceptibility and serotonin. *Pharmacol Biochem Be* **10**:487-491.
Buckle P, Haas H (1982) Enhancement of synaptic transmission by 4-aminopyridine in hippocampal slices of the rat. *J Physiol* **326**:109-122.
Buckley NJ, Bonner TI, Brann MR (1988) localization of a family of muscarinic receptor messenger-RNAs in rat-brain. *J Neurosci* **8**:4646-4652.
Buckmaster PS, Zhang GF, Yamawaki R (2002) Axon sprouting in a model of temporal lobe epilepsy creates a predominantly excitatory feedback circuit. *J Neurosci* 22:6650-6658.

Buhl DL, Harris KD, Hormuzdi SG, Monyer H, Buzsáki G (2003) Selective impairment of hippocampal gamma oscillations in connexin-36 knock-out mouse in vivo. *J Neurosci* **23**:1013-1018.
Buhl EH, Tamas G, Fisahn A (1998) Cholinergic activation and tonic excitation induce persistent gamma oscillations in mouse somatosensory cortex in vitro. *J Physiol (Lond)* **513**:117-126.
Buhl EH, Han ZS, Lorinczi Z, Stezhka VV, Karnup SV, Somogyi P (1994) Physiological-properties of anatomically identified axo-axonic cells in the rat hippocampus. *J Neurophysiol* **71**:1289-1307.
Buzsaki G (2006) Rhythms of the Brain: *Oxford University Press*.
Buzsaki G, Wang X-J (2012) Mechanisms of Gamma Oscillations. *Ann Rev Neurosci* **35**:203-225.
Buzsaki G, Traub RD, Pedley T (2003) The cellular synaptic generation of EEG activity. *Curr Practice Clin Encephalogr* **3**:1-11.
Buzsaki G, Anastassiou CA, Koch C (2012) The origin of extracellular fields and currents - EEG, ECoG, LFP and spikes. *Nature Rev Neurosci* **13**:407-420.
Buzsáki G, Draguhn A (2004) Neuronal oscillations in cortical networks. *Science* **304**:1926-1929.
Bymaster FP, Carter PA, Yamada M, Gomeza J, Wess J, Hamilton SE, Nathanson NM, McKinzie DL, Felder CC (2003) Role of specific muscarinic receptor subtypes in cholinergic parasympathomimetic responses, in vivo phosphoinositide hydrolysis, and pilocarpine-induced seizure activity. *EJ Neurosci* **17**:1403-1410.
Cai K, Nanga RP, Lamprou L, Schinstine C, Elliott M, Hariharan H, Reddy R, Epperson CN (2012) The impact of gabapentin administration on brain GABA and glutamate concentrations: a 7T 1H-MRS study. *Neuropsychopharmacol* **37**:2764-2771.
Cain DP (1981) Transfer of pentylenetetrazol sensitization to amygdaloid kindling. *Pharmacol Biochem Behav* **15**:533-536.
Cain DP (1982) Bidirectional transfer of intracerebrally administered pentylenetetrazol and electrical kindling. *Pharmacol Biochem Behav* **17**:1111-1113.
Cain DP, Corcoran ME, Desborough KA, McKitrick DJ (1988) Kindling in the deep prepyriform cortex of the rat. *Exp Neurol* **100**:203-209.
Candelario-Jalil E, Al-Dalain SM, Castillo R, Martínez G, León Fernández OS (2001) Selective vulnerability to kainate-induced oxidative damage in different rat brain regions. *J Appl Toxicol* **21**:403-407.
Cang J, Isaacson JS (2003) In vivo whole-cell recording of odor-evoked synaptic transmission in the rat olfactory bulb. *J Neurosci* **23**:4108-4116.
Capella H, Lemos T (2002) Effect on epileptogenesis of carbamazepine treatment during the silent period of the pilocarpine model of epilepsy. *Epilepsia* **43**:110-111.
Cappaert NL, Werkman TR, Benito N, Witter MP, Baayen JC, Wadman WJ (2016) Carbamazepine modulates the spatiotemporal activity in the dentate gyrus of rats and pharmacoresistant humans in vitro. *Brain Behav*.
Carmichael S, Price J (1994) Architectonic subdivision of the orbital and medial prefrontal cortex in the macaque monkey. *J Comp Neurol* **346**:366-402.
Carrier EJ, Auchampach JA, Hillard CJ (2006) Inhibition of an equilibrative nucleoside transporter by cannabidiol: a mechanism of cannabinoid immunosuppression. *P Natl Acad Sci* **103**:7895-7900.
Carriero G, Uva L, Gnatkovsky V, Avoli M, de Curtis M (2010) Independent Epileptiform Discharge Patterns in the Olfactory and Limbic Areas of the In Vitro Isolated Guinea Pig Brain During 4-Aminopyridine Treatment. *J Neurophysiology* **103**:2728-2736.
Castillo PE, Malenka RC, Nicoll RA (1997) Kainate receptors mediate a slow postsynaptic current in hippocampal CA3 neurons. *Nature* **388**:182-186.
Castorina M, Ambrosini A, Pacifici L, Ramacci M, Angelucci L (1994) Age-dependent loss of NMDA receptors in hippocampus, striatum, and frontal cortex of the rat: prevention by acetyl-L-carnitine. *Neurochem Res* **19**:795-798.
Castorina M, Ambrosini AM, Giuliani A, Pacifici L, Ramacci MT, Angelucci L (1993) A cluster analysis study of acetyl-L-carnitine effect on NMDA receptors in aging. *Exp gerontol* **28**:537-548.

Catterall WA (1980) Neurotoxins that act on voltage-sensitive sodium channels in excitable membranes. *Ann Rev Pharmacol Toxicol* **20**:15-43.
Cavalheiro E, Riche D, La Salle GLG (1982) Long-term effects of intrahippocampal kainic acid injection in rats: a method for inducing spontaneous recurrent seizures. *Electroen Clin Neuro* **53**:581-589.
Cavalheiro EA, Silva DF, Turski WA, Calderazzo-Filho LS, Bortolotto ZA, Turski L (1987) The susceptibility of rats to pilocarpine-induced seizures is age-dependent. *Dev Brain Res* **37**:43-58.
Cavalheuro E, Naffah-Mazzacoratti M, Mello L, Leite J (2006) Chapter 35 - The Pilocarpine Model of Seizures: Elsevier Academic Press.
Cavanagh J, Meyer A (1956) Aetiological aspects of Ammon's horn sclerosis associated with temporal lobe epilepsy. *Brit Med J* **2**:1403.
Cendes F, Andermann F, Carpenter S, Zatorre RJ, Cashman NR (1995) Temporal lobe epilepsy caused by domoic acid intoxication: evidence for glutamate receptor–mediated excitotoxicity in humans. *Ann Neurol* **37**:123-126.
Centeno M, Vollmar C, Stretton J, Symms MR, Thompson PJ, Richardson MP, O'Muircheartaigh J, Duncan JS, Koepp MJ (2014) Structural changes in the temporal lobe and piriform cortex in frontal lobe epilepsy. *Epilepsy Res* **108**:978-981.
Chamberlain S, Yang J, Jones R (2008) The Role of NMDA Receptor Subtypes in Short-Term Plasticity in the Rat Entorhinal Cortex. *Neural Plasticity* **2008**.
Chen ACN, Herrmann CS (2001) Perception of pain coincides with the spatial expansion of electroencephalographic dynamics in human subjects. *Neurosci Letters* **297**:183-186.
Chen C, Shih YH, Yen DJ, Lirng JF, Guo YC, Yu HY, Yiu CH (2003) Olfactory auras in patients with temporal lobe epilepsy. *Epilepsia* **44**:257-260.
Chen J, Naylor D, Wasterlain C (2007a) Advances in the pathophysiology of status epilepticus. *Acta Neurol Scand* **115**:7-15.
Chen S, Kobayashi M, Honda Y, Kakuta S, Sato F, Kishi K (2007b) Preferential neuron loss in the rat piriform cortex following pilocarpine-induced status epilepticus. *Epilepsy Res* **74**:1-18.
Chen Z, Duan RS, Quezada HC, Mix E, Nennesmo I, Adem A, Winblad B, Zhu J (2005) Increased microglial activation and astrogliosis after intranasal administration of kainic acid in C57BL/6 mice. *J Neurobiol* **62**:207-218.
Chittajallu R, Vignes M, Dev KK, Barnes JM, Collingridge GL, Henley JM (1996) Regulation of glutamate release by presynaptic kainate receptors in the hippocampus. *Nature* **379**:78-81.
Choy JMC, Suzuki N, Shima Y, Budisantoso T, Nelson SB, Bekkers JM (2015) Optogenetic Mapping of Intracortical Circuits Originating from Semilunar Cells in the Piriform Cortex. *Cerebral Cortex*.
Ciumas C, Lindström P, Aoun B, Savic I (2008) Imaging of odor perception delineates functional disintegration of the limbic circuits in mesial temporal lobe epilepsy. *Neuroimage* **39**:578-592.
Clark M, Post RM, Weiss SR, Cain CJ, Nakajima T (1991) Regional expression of c-fos mRNA in rat brain during the evolution of amygdala kindled seizures. *Mol Brain Res* **11**:55-64.
Clarke VRJ, Ballyk BA, Hoo KH, Mandelzys A, Pellizzari A, Bath CP, Thomas J, Sharpe EF, Davies CH, Ornstein PL, Schoepp DD, Kamboj RK, Collingridge GL, Lodge D, Bleakman D (1997) A hippocampal GluR5 kainate receptor regulating inhibitory synaptic transmission. *Nature* **389**:599-603.
Clementz BA, Blumenfeld LD, Cobb S (1997) The gamma band response may account for poor P50 suppression in schizophrenia. *Neuroreport* **8**:3889-3893.
Clifford DB, Olney JW, Maniotis A, Collins RC, Zorumski CF (1987) The functional anatomy and pathology of lithium pilocarpine and high-dose pilocarpine seizures. *Neuroscience* **23**:953-968.
Cobb SR, Buhl EH, Halasy K, Paulsen O, Somogyi P (1995) Synchronization of neuronal-activity in hippocampus by individual GABAergic interneurons. *Nature* **378**:75-78.
Cockerell O, Sander J, Hart Y, Shorvon S, Johnson A (1995) Remission of epilepsy: results from the National General Practice Study of Epilepsy. *Lancet* **346**:140-144.

Collins GGS (1993) Actions of agonists of metabotropic glutamate receptors on synaptic transmission and transmitter release in the olfactory cortex. *Brit J Pharmacol* **108**:422-430.
Colombo N, Tassi L, Galli C, Citterio A, Russo GL, Scialfa G, Spreafico R (2003) Focal cortical dysplasias: MR imaging, histopathologic, and clinical correlations in surgically treated patients with epilepsy. *Am J Neuroradiol* **24**:724-733.
Connors BW (2012) Tales of a dirty drug: carbenoxolone, gap junctions, and seizures. *Epilepsy Curr* **12**:66-68.
Constanti A, Bagetta G, Libri V (1993) Persistent muscarinic excitation in guinea-pig olfactory cortex neurons - involvement of a slow poststimulus after depolarizing current. *Neuroscience* **56**:887-904.
Cossart R, Dinocourt C, Hirsch J, Merchan-Perez A, De Felipe J, Ben-Ari Y, Esclapez M, Bernard C (2001) Dendritic but not somatic GABAergic inhibition is decreased in experimental epilepsy. *Nature Neurosci* **4**:52-62.
Coulter DA, Lee C-J (1993) Thalamocortical rhythm generation in vitro: extra-and intracellular recordings in mouse thalamocortical slices perfused with low Mg 2+ medium. *Brain Res* **631**:137-142.
Courtemanche R, Lamarre Y (2005) Local field potential oscillations in primate cerebellar cortex: Synchronization with cerebral cortex during active and passive expectancy. *J Neurophys* **93**:2039-2052.
Courtney KR, Etter EF (1983) Modulated anti-convulsant block of sodium-channels in nerve and muscle. *EJ Pharmacol* **88**:1-9.
Covolan L, Mello L (2000) Temporal profile of neuronal injury following pilocarpine or kainic acid-induced status epilepticus. *Epilepsy Res* **39**:133-152.
Croucher MJ, Bradford HF, Sunter DC, Watkins JC (1988) Inhibition of the development of electrical kindling of the prepyriform cortex by daily focal injections of excitatory amino-acid antagonists. *Eur J Pharmacol* **152**:29-38.
Cruikshank SJ, Lewis TJ, Connors BW (2007) Synaptic basis for intense thalamocortical activation of feedforward inhibitory cells in neocortex. *Nature Neurosci* **10**:462-468.
Cull CA, Fowler M, Brown SW (1996) Perceived self-control of seizures in young people with epilepsy. *Seizure* **5**:131-138.
Cunha J, Carlini E, Pereira AE, Ramos OL, Pimentel C, Gagliardi R, Sanvito W, Lander N, Mechoulam R (1980) Chronic administration of cannabidiol to healthy volunteers and epileptic patients. *Pharmacology* **21**:175-185.
Cunningham MO, Jones RS (2000) The anticonvulsant, lamotrigine decreases spontaneous glutamate release but increases spontaneous GABA release in the rat entorhinal cortex in vitro. *Neuropharmacology* **39**:2139-2146.
Cunningham MO, Davies CH, Buhl EH, Kopell N, Whittington MA (2003) Gamma oscillations induced by kainate receptor activation in the entorhinal cortex in vitro. *J Neurosci* **23**:9761-9769.
Cunningham MO, Roopun A, Schofield IS, Whittaker RG, Duncan R, Russell A, Jenkins A, Nicholson C, Whittington MA, Traub RD (2012) Glissandi: transient fast electrocorticographic oscillations of steadily increasing frequency, explained by temporally increasing gap junction conductance. *Epilepsia* **53**:1205-1214.
Curia G, Longo D, Biagini G, Jones RSG, Avoli M (2008) The pilocarpine model of temporal lobe epilepsy. *J Neurosci Meth* **172**:143-157.
Daval JL, Deckert J, Weiss SRB, Post RM, Marangos PJ (1989) Upregulation of adenosine-a1 receptors and forskolin binding-sites following chronic treatment with caffeine or carbamazepine - a quantitative autoradiographic study. *Epilepsia* **30**:26-33.
De Curtis M, Biella G, Forti M, Panzica F (1994) Multifocal spontaneous epileptic activity-induced by restricted bicuculline ejection in the piriform cortex of the isolated guinea-pig brain. *J Neurophysiol* **71**:2463-2476.
De Lanerolle N, Kim J, Robbins RJ, Spencer D (1989) Hippocampal interneuron loss and plasticity in human temporal lobe epilepsy. *Brain Res* **495**:387-395.
De Olmos J, Hardy H, Heimer L (1978) Afferent connections of main and accessory olfactory-bulb formations in rat - experimental hrp-study. *J Comp Neurol* **181**:213-244.

Deans MR, Gibson JR, Sellitto C, Connors BW, Paul DL (2001) Synchronous activity of inhibitory networks in neocortex requires electrical synapses containing Connexin36. *Neuron* **31**:477-485.
Debanne D, Thompson SM, Gähwiler BH (2006) A brief period of epileptiform activity strengthens excitatory synapses in the rat hippocampus in vitro. *Epilepsia* **47**:247-256.
DeLorenzo RJ, Sun DA, Deshpande LS (2005) Cellular mechanisms underlying acquired epilepsy: The calcium hypothesis of the induction and maintainance of epilepsy. *Pharmacol Ther* **105**:229-266.
Demir R, Haberly LB, Jackson MB (1998) Voltage imaging of epileptiform activity in slices from rat piriform cortex: Onset and propagation. *J Neurophysiol* **80**:2727-2742.
Demir R, Haberly LB, Jackson MB (1999) Sustained and accelerating activity at two discrete sites generate epileptiform discharges in slices of piriform cortex. *J Neurosci* **19**:1294-1306.
Demir R, Haberly LB, Jackson MB (2001) Epileptiform discharges with in-vivo-like features in slices of rat piriform cortex with longitudinal association fibers. *J Neurophysiol* **86**:2445-2460.
DeToledo JC (1999) Changing presentation of seizures with aging: clinical and etiological factors. *Gerontology* **45**:329-335.
Devinsky O, Cilio MR, Cross H, Fernandez-Ruiz J, French J, Hill C, Katz R, Di Marzo V, Jutras-Aswad D, Notcutt WG (2014) Cannabidiol: pharmacology and potential therapeutic role in epilepsy and other neuropsychiatric disorders. *Epilepsia* **55**:791-802.
Devinsky O, Marsh E, Friedman D, Thiele E, Laux L, Sullivan J, Miller I, Flamini R, Wilfong A, Filloux F (2016) Cannabidiol in patients with treatment-resistant epilepsy: an open-label interventional trial. *Lancet Neurology* **15**:270-278.
Devor M (1976) Fiber trajectories of olfactory bulb efferents in hamster. *J Comp Neurol* **166**:31-48.
Dichter M, Spencer WA (1969) Penicillin-induced interictal discharges from the cat hippocampus. II. Mechanisms underlying origin and restriction. *J Neurophysiol* **32**:663-687.
Dinocourt C, Petanjek Z, Freund TF, Ben-Ari Y, Esclapez M (2003) Loss of interneurons innervating pyramidal cell dendrites and axon initial segments in the CA1 region of the hippocampus following pilocarpine-induced seizures. *J Comp Neurol* **459**:407-425.
Dodge HW, Jr., Holman CB, Jacks QD, Lazarte JA, Petersen MC, Sem-Jacobsen CW (1956) Electric activity of the olfactory bulb in man. *AM J Med Sci* **232**:243-251.
Dragunow M, Goddard GV, Laverty R (1985) Is adenosine an endogenous anticonvulsant? *Epilepsia* **26**:480-487.
Dreier J, Heinemann U (1990) Late low magnesium-induced epileptiform activity in rat entorhinal cortex slices becomes insensitive to the anticonvulsant valproic acid. *Neurosci Letters* **119**:68-70.
Dreier J, Heinemann U (1991) Regional and time dependent variations of low Mg2+ induced epileptiform activity in rat temporal cortex slices. *Exp Brain Res* **87**:581-596.
Dreier J, Zhang CL, Heinemann U (1998) Phenytoin, phenobarbital, and midazolam fail to stop status epilepticus-like activity induced by low magnesium in rat entorhinal slices, but can prevent its development. *Acta neurologica scandinavica* **98**:154-160.
Dreixler JC, Bian JT, Cao YJ, Roberts MT, Roizen JD, Houamed KM (2000) Block of rat brain recombinant SK channels by tricyclic antidepressants and related compounds. *EJ Pharmacol* **401**:1-7.
Drexel M, Preidt AP, Sperk G (2012) Sequel of spontaneous seizures after kainic acid-induced status epilepticus and associated neuropathological changes in the subiculum and entorhinal cortex. *Neuropharmacology* **63**:806-817.
Druga R, Kubova H, Suchomelova L, Haugvicova R (2003) Lithium/pilocarpine status epilepticus-induced neuropathology of piriform cortex and adjoining structures in rats is age-dependent. *Physiol Res* **52**:251-264.
Drysdale AJ, Ryan D, Pertwee RG, Platt B (2006) Cannabidiol-induced intracellular Ca 2+ elevations in hippocampal cells. *Neuropharmacology* **50**:621-631.

Dudek E, Clark S, Williams P, Grabenstatter H (2006) Chapter 34 - Kainate-Induced Status Epilepticus: A chronic Model of Acquired Epilepsy: Elsevier Academic Press.
Dudek FE, Shao LR (2004) Mossy fiber sprouting and recurrent excitation: direct electrophysiologic evidence and potential implications. *Epilepsy Currents* **4**:184-187.
Dugladze T, Maziashvili N, Boergers C, Gurgenidze S, Haeussler U, Winkelmann A, Haas CA, Meier JC, Vida I, Kopell NJ, Gloveli T (2013) GABA(B) autoreceptor-mediated cell type-specific reduction of inhibition in epileptic mice. *Proc Natl Acad Sci USA* **110**:15073-15078.
Duley L, Henderson-Smart DJ, Walker GJ, Chou D (2010) Magnesium sulphate versus diazepam for eclampsia. *Cochrane Library*.
Dunlap K, Fischbach GD (1981) Neurotransmitters decrease the calcium conductance activated by depolarization of embryonic chick sensory neurons. *J Physiol (Lond)* **317**:519-535.
During M, Mattson R, Scheyer R, Rask C, Pierce M, McKelvy J, Thomas V (1992) The effect of tiagabine HCl on extracellular GABA levels in the human hippocampus. *Epilepsia* **33**:83.
During MJ, Spencer DD (1992) Adenosine: a potential mediator of seizure arrest and postictal refractoriness. *Ann Neurol* **32**:618-624.
Eckhorn R, Bauer R, Jordan W, Brosch M, Kruse W, Munk M, Reitboeck HJ (1988) Coherent oscillations - a mechanism of feature linking in the visual-cortex - multiple electrode and correlation analyses in the cat. *Bio Cybernetics*Bio Cybernetics **60**60:121-130.
Efron R (1956) The effect of olfactory stimuli in arresting uncinate fits. *Brain* **79**:267-281.
Efron R (1957) The conditioned inhibition of uncinate fits. *Brain* **80**:251-262.
Einevoll GT, Pettersen KH, Devor A, Ulbert I, Halgren E, Dale AM (2007) Laminar population analysis: Estimating firing rates and evoked synaptic activity from multielectrode recordings in rat barrel cortex. *J Neurophys* **97**:2174-2190.
Ellerkmann R, Remy S, Chen J, Sochivko D, Elger C, Urban B, Becker A, Beck H (2003) Molecular and functional changes in voltage-dependent Na+ channels following pilocarpine-induced status epilepticus in rat dentate granule cells. *Neuroscience* **119**:323-333.
Elliott P (1990) Action of antiepileptic and anesthetic drugs on na-spikes and ca-spikes in mammalian non-myelinated axons. *EJ Pharmacol* **175**:155-163.
Engel J, Wolfson L, Brown L (1978) Anatomical correlates of electrical and behavioral events related to amygdaloid kindling. *Annals of Neurology* **3**:538-544.
Engel J, Wiebe S, French J, Sperling M, Williamson P, Spencer D, Gumnit R, Zahn C, Westbrook E, Enos B (2003) Practice parameter: Temporal lobe and localized neocortical resections for epilepsy - Report of the quality standards subcommittee of the American Academy of Neurology, in association with the American Epilepsy Society and the American Association of Neurological Surgeons. *Neurol* **60**:538-547.
Errante LD, Williamson A, Spencer DD, Petroff OA (2002) Gabapentin and vigabatrin increase GABA in the human neocortical slice. *Epilepsy Res* **49**:203-210.
Eulitz C, Maess B, Pantev C, Friederici AD, Feige B, Elbert T (1996) Oscillatory neuromagnetic activity induced by language and non-language stimuli. *Cogn Brain Res* **4**:121-132.
Faas G, Vreugdenhil M, Wadman W (1996) Calcium currents in pyramidal CA1 neurons in vitro after kindling epileptogenesis in the hippocampus of the rat. *Neuroscience* **75**:57-67.
Farrant M, Nusser Z (2005) Variations on an inhibitory theme: phasic and tonic activation of the GABA(A) receptors. *Nature Rev Neurosci* **6**:215-229.
Farrar SJ, Whiting PJ, Bonnert TP, McKernan RM (1999) Stoichiometry of a ligand-gated ion channel determined by fluorescence energy transfer. *J Biol Chem* **274**:10100-10104.
Fauser S, Huppertz H-J, Bast T, Strobl K, Pantazis G, Altenmueller D-M, Feil B, Rona S, Kurth C, Korinthenberg R (2006) Clinical characteristics in focal cortical dysplasia: a retrospective evaluation in a series of 120 patients. *Brain* **129**:1907-1916.
Felder CC (1995) Muscarinic acetylcholine receptors: signal transduction through multiple effectors. *FASEB J* **9**:619-625.

Fink-Jensen A, Suzdak P, Swedberg M, Judge M, Hansen L, Nielsen P (1992) The γ-aminobutyric acid (GABA) uptake inhibitor, tiagabine, increases extracellular brain levels of GABA in awake rats. *EJ Pharmacol* **220**:197-201.
Fisahn A (2005) Kainate receptors and rhythmic activity in neuronal networks: hippocampal gamma oscillations as a tool. *J Physio* **562**:65-72.
Fisahn A, Pike FG, Buhl EH, Paulsen O (1998) Cholinergic induction of network oscillations at 40 Hz in the hippocampus in vitro. *Nature* **394**:186-189.
Fisahn A, Contractor A, Traub RD, Buhl EH, Heinemann SF, McBain CJ (2004) Distinct roles for the kainate receptor subunits GluR5 and GluR6 in kainate-induced hippocampal gamma oscillations. *J Neurosci* **24**:9658-9668.
Fisahn A, Yamada M, Duttaroy A, Gan JW, Deng CX, McBain CJ, Wess J (2002) Muscarinic induction of hippocampal gamma oscillations requires coupling of the M1 receptor to two mixed cation currents. *Neuron* **33**:615-624.
Fisher RS, Schachter SC (2000) The postictal state: a neglected entity in the management of epilepsy. *Epilepsy & Behavior* **1**:52-59.
Fisher RS, Boas WV, Blume W, Elger C, Genton P, Lee P, Engel J (2005) Epileptic seizures and epilepsy: Definitions proposed by the International League against Epilepsy (ILAE) and the International Bureau for Epilepsy (IBE). *Epilepsia* **46**:470-472.
Fisher RS, Acevedo C, Arzimanoglou A, Bogacz A, Cross JH, Elger CE, Engel J, Forsgren L, French JA, Glynn M, Hesdorffer DC, Lee BI, Mathern GW, Moshe SL, Perucca E, Scheffer IE, Tomson T, Watanabe M, Wiebe S (2014) ILAE Official Report: A practical clinical definition of epilepsy. *Epilepsia* **55**:475-482.
Flanagan D, Badawy RAB, Jackson GD (2014) EEG-fMRI in focal epilepsy: Local activation and regional networks. *Clin Neurophysiol* **125**:21-31.
Florez C, McGinn R, Lukankin V, Marwa I, Sugumar S, Dian J, Hazrati L-N, Carlen P, Zhang L, Valiante T (2015) In vitro recordings of human neocortical oscillations. *Cereb Cortex* **25**:578-597.
Frahm C, Stief F, Zuschratter W, Draguhn A (2003) Unaltered control of extracellular GABA-concentration through GAT-1 in the hippocampus of rats after pilocarpine-induced status epilepticus. *Epilepsy Res* **52**:243-252.
Franks KM, Isaacson JS (2005) Synapse-specific downregulation of NMDA receptors by early experience: A critical period for plasticity of sensory input to olfactory cortex. *Neuron* **47**:101-114.
Freeman WJ (1959) Distribution in time and space of prepyriform electrical activity. *J Neurophysiol* **22**:644-665.
Freeman WJ (1968a) Effects of surgical isolation and tetanization on prepyriform cortex in cats. *J Neurophysiol* **31**:349-357.
Freeman WJ (1968b) Relations between unit activity and evoked potentials in prepyriform cortex of cats. *J Neurophysiol* **31**:337-348.
Freeman WJ (1978) Spatial properties of an EEG event in olfactory-bulb and cortex. *Electroencephalogr Clin Neurophysiol* **44**:586-605.
Freichel C, Potschka H, Ebert U, Brandt C, Loescher W (2006) Acute changes in the neuronal expression of GABA and glutamate decarboxylase isoforms in the rat piriform cortex following status epilepticus. *Neurosci* **141**:2177-2194.
Freiman TM, Eismann-Schweimler J, Frotscher M (2011) Granule cell dispersion in temporal lobe epilepsy is associated with changes in dendritic orientation and spine distribution. *Exp neurol* **229**:332-338.
French C, Sah P, Buckett K, Gage P (1990) A voltage-dependent persistent sodium current in mammalian hippocampal neurons. *J Gen Physiol* **95**:1139-1157.
Frenk H, Engel J, Ackermann RF, Shavit Y, Liebeskind JC (1979) Endogenous opiods may mediate post-ictal behavioral depression in amygdaloid-kindled rats. *Brain Res* **167**:435-440.
Frerking M, Ohligre-Frerking P (2002) AMPA receptors and kainate receptors encode different features of afferent activity. *J Neurosci* **22**:7434-7443.
Freund TF, Buzsaki G (1996) Interneurons of the hippocampus. *Hippocampus* **6**:347-470.
Frien A, Eckhorn R (2000) Functional coupling shows stronger stimulus dependency for fast oscillations than for low-frequency components in striate cortex of awake monkey. *EJ Neurosci* **12**:1466-1478.

Fuchs EC, Zivkovic AR, Cunningham MO, Middleton S, LeBeau FEN, Bannerman DM, Rozov A, Whittington MA, Traub RD, Rawlins JNP, Monyer H (2007) Recruitment of parvalbumin-positive interneurons determines hippocampal function and associated behavior. *Neuron* **53**:591-604.
Fujikawa DG, Itabashi HH, Wu A, Shinmei SS (2000) Status epilepticus-induced neuronal loss in humans without systemic complications or epilepsy. *Epilepsia* **41**:981-991.
Gao F, Edden RA, Li M, Puts NA, Wang G, Liu C, Zhao B, Wang H, Bai X, Zhao C (2013) Edited magnetic resonance spectroscopy detects an age-related decline in brain GABA levels. *Neuroimage* **78**:75-82.
Gasser T, Reddington M, Schubert P (1988) Effect of carbamazepine on stimulus-evoked ca-2+ fluxes in rat hippocampal slices and its interaction with a1-adenosine receptors. *Neurosci Letters* **91**:189-193.
Gavrilovici C, D'Alfonso S, Dann M, Poulter MO (2006) Kindling-induced alterations in GABA(A) receptor-mediated inhibition and neurosteroid activity in the rat piriform cortex. *EJ Neurosci* **24**:1373-1384.
Gavrilovici C, Pollock E, Everest M, Poulter MO (2012) The loss of interneuron functional diversity in the piriform cortex after induction of experimental epilepsy. *Neurobiol Disease* **48**:317-328.
Geyer J, Payne T, Faught E, Drury I (1999) Postictal nose-rubbing in the diagnosis, lateralization, and localization of seizures. *Neurology* **52**:743-743.
Ghasemi M, Schachter SC (2011) The NMDA receptor complex as a therapeutic target in epilepsy: a review. *Epilepsy & Behavior* **22**:617-640.
Gilbert M, Goodman J (2006) Chapter 31 - Chemical Kindling: Elsevier Academic Press.
Gillies MJ, Traub RD, LeBeau FEN, Davies CH, Gloveli T, Buhl EH, Whittington MA (2002) A model of atropine-resistant theta oscillations in rat hippocampal area CA1. *J Phsiol (Lond)* 543:779-793.
Glass M, Faull R, Bullock J, Jansen K, Mee E, Walker E, Synek B, Dragunow M (1996) Loss of A1 adenosine receptors in human temporal lobe epilepsy. *Brain Res* **710**:56-68.
Glien M, Brandt C, Potschka H, Voigt H, Ebert U, Loscher W (2001) Repeated low-dose treatment of rats with pilocarpine: low mortality but high proportion of rats developing epilepsy. *Epilepsy Res* **46**:111-119.
Gloveli T, Albrecht D, Heinemann U (1995) Properties of low Mg 2+ induced epileptiform activity in rat hippocampal and entorhinal cortex slices during adolescence. *Dev Brain Res* **87**:145-152.
Gloveli T, Dugladze T, Saha S, Monyer H, Heinemann U, Traub RD, Whittington MA, Buhl EH (2005) Differential involvement of oriens/pyramidale interneurones in hippocampal network oscillations in vitro. *J Physiol (Lond)* **562**:131-147.
Goddard GV (1967) Development of epileptic seizures through brain stimulation at low intensity. *Nature* **214**:1020-1021.
Goddard GV, McIntyre DC, Leech CK (1969) A permanent change in brain function resulting from daily electrical stimulation rat cat monkey. *Exp Neurol* **25**:295-330.
Godin Y, Heiner L, Mark J, Mandel P (1969) Effects of di-n-propylacetate, an anticonvulsive compound, on gaba metabolism. *J Neurochem* **16**:869-873.
Goldin M, Epsztein J, Jorquera I, Represa A, Ben-Ari Y, Crepel V, Cossart R (2007) Synaptic kainate receptors tune oriens-lacunosum moleculare interneurons to operate at theta frequency. *J Neurosci* **27**:9560-9572.
Goncalves Pereira PM, Insausti R, Artacho-Perula E, Salmenpera T, Kalviainen R, Pitkanen A (2005) MR volumetric analysis of the piriform cortex and cortical amygdala in drug-refractory temporal lobe epilepsy. *AM J Neuroradiol* **26**:319-332.
Goodkin HP, Sun C, Yeh JL, Mangan PS, Kapur J (2007) GABAA receptor internalization during seizures. *Epilepsia* **48**:109-113.
Gottfried JA, Winston JS, Dolan RJ (2006) Dissociable codes of odor quality and odorant structure in human piriform cortex. *Neuron* **49**:467-479.
Gray CM, Singer W (1989) Stimulus-specific neuronal oscillations in orientation columns of cat visual-cortex. *Proc Natl Acad Sci USA* **86**:1698-1702.
Gray CM, DiPrisco GV (1997) Stimulus-dependent neuronal oscillations and local synchronization in striate cortex of the alert cat. *J Neurosci* **17**:3239-3253.

Greenberg DM, Tufts EV (1935) Effect of a Diet Low in Magnesium on the Rat. *P Soc Exp Biol Med* **32**:674-675.
Guekht A (2011) Debate: A 50% reduction in seizure frequency is a useful measure to assess treatment response in epilepsy. Yes. In. The 5th World Congress on Controversies in Neurology.
Gulyas AI, Megias M, Emri Z, Freund TF (1999) Total number and ratio of excitatory and inhibitory synapses converging onto single interneurons of different types in the CA1 area of the rat hippocampus. *J Neurosci* **19**:10082-10097.
Gupta A, Jeavons P, Hughes R, Covanis A (1983) Aura in temporal lobe epilepsy: clinical and electroencephalographic correlation. *J Neurol Neurosurgery Psychiatry* **46**:1079-1083.
Gutierrez A, Khan ZU, De Blas AL (1994) Immunocytochemical localization of gamma 2 short and gamma 2 long subunits of the GABAA receptor in the rat brain. *J Neurosci* **14**:7168-7179.
Götz E, Feuerstein T, Lais A, Meyer D (1993) Effects of gabapentin on release of gamma-aminobutyric acid from slices of rat neostriatum. *Arzneimittel-Forschung* **43**:636-638.
Haberly L, Behan M (1983) Structure of the piriform cortex of the opossum .3. ultrastructural characterization of synaptic terminals of association and olfactory-bulb afferent-fibers. *J Comp Neurol* **219**:448-460.
Haberly LB, Price JL (1978a) Association and commissural fiber systems of olfactory cortex of rat .2. systems originating in olfactory peduncle. *J Comp Neurol* **181**:781-807.
Haberly LB, Price JL (1978b) Association and commissural fiber systems of olfactory cortex of rat .1. systems originating in piriform cortex and adjacent areas. *J Compar Neurol* **178**:711-740.
Haberly LB, Feig SL (1983) Structure of the piriform cortex of the opossum .2. fine-structure of cell-bodies and neuropil. *J Comp Neurol* **216**:69-88.
Hajos N, Palhalmi J, Mann EO, Nemeth B, Paulsen O, Freund TF (2004) Spike timing of distinct types of GABAergic interneuron during hippocampal gamma oscillations in vitro. *J Neurosci* **24**:9127-9137.
Hall SD, Barnes GR, Hillebrand A, Furlong PL, Singh KD, Holliday IE (2004) Spatio-temporal imaging of cortical desynchronization in migraine visual aura: A magnetoencephalography case study. *Headache* **44**:204-208.
Hamed SA, Elserogy YB, Abdou MA, Abdellah MM (2012) Risks of suicidality in adult patients with epilepsy. *World J psychiatry* **2**:33.
Hamilton SE, Loose MD, Qi M, Levey AI, Hille B, McKnight GS, Idzerda RL, Nathanson NM (1997) Disruption of the m1 receptor gene ablates muscarinic receptor-dependent M current regulation and seizure activity in mice. *Proc Natl Acad Sci USA* **94**:13311-13316.
Hammers A, Asselin M-C, Hinz R, Kitchen I, Brooks DJ, Duncan JS, Koepp MJ (2007) Upregulation of opioid receptor binding following spontaneous epileptic seizures. *Brain* **130**:1009-1016.
Hampson DR, Huang X-p, Wells JW, Walter JA, Wright JL (1992) Interaction of domoic acid and several derivatives with kainic acid and AMPA binding sites in rat brain. *EJ Pharmacol* **218**:1-8.
Hanada T, Hashizume Y, Tokuhara N, Takenaka O, Kohmura N, Ogasawara A, Hatakeyama S, Ohgoh M, Ueno M, Nishizawa Y (2011) Perampanel: A novel, orally active, noncompetitive AMPA-receptor antagonist that reduces seizure activity in rodent models of epilepsy. *Epilepsia* **52**:1331-1340.
Hanna N, Black M, Sander J, Smithson W, Appleton R, Brown S, Fish D (2002) National Sentinel clinical audit of epilepsy-related death: report 2002. Epilepsy-death in the shadows. In.
Harrison PK, Sheridan RD, Green AC, Tattersall JE (2005) Effects of anticonvulsants on soman-induced epileptiform activity in the guinea-pig in vitro hippocampus. *EJ Pharmacol* **518**:123-132.
Harvey AS, Cross JH, Shinnar S, Mathern GW, Mathern BW, Taskforce IPESS (2008) Defining the spectrum of international practice in pediatric epilepsy surgery patients. *Epilepsia* **49**:146-155.

Haut SR, Hall CB, Masur J, Lipton RB (2007) Seizure occurrence - Precipitants and prediction. *Neurology* **69**:1905-1910.
Hebeisen S, Pires N, Loureiro AI, Bonifacio MJ, Palma N, Whyment A, Spanswick D, Soares-da-Silva P (2015) Eslicarbazepine and the enhancement of slow inactivation of voltage-gated sodium channels: A comparison with carbamazepine, oxcarbazepine and lacosamide. *Neuropharm* **89**:122-135.
Heinemann U, Staley KJ (2014) What is the clinical relevance of in vitro epileptiform activity? In: Issues in Clinical Epileptology: A View from the Bench, pp 25-41: Springer.
Heinemann U, Kann O, Schuchmann S (2006) Chapter 4 - An Overview of In Vitro Seizure Models in Acute and Organotypic Slices: Elsevier Academic Press.
Heinemann U, Dreier J, Leschinger A, Stabel J, Draguhn A, Zhang C (1994) Effects of anticonvulsant drugs on hippocampal neurons. *Hippocampus* **4**:291-296.
Hendrich J, Van Minh AT, Heblich F, Nieto-Rostro M, Watschinger K, Striessnig J, Wratten J, Davies A, Dolphin AC (2008) Pharmacological disruption of calcium channel trafficking by the α2δ ligand gabapentin. *P Natl Acad Sci* **105**:3628-3633.
Hensch TK (2005) Critical period plasticity in local cortical circuits. *Nature Rev Neurosci* **6**:877-888.
Hermanns G, Noachtar S, Tuxhorn I, Holthausen H, Ebner A, Wolf P (1996) Systematic testing of medical intractability for carbamazepine, phenytoin, and phenobarbital or primidone in monotherapy for patients considered for epilepsy surgery. *Epilepsia* **37**:675-679.
Hill DR (1985) GABAB receptor modulation of adenylate-cyclase activity in rat-brain slices. *BJ Pharmacol* **84**:249-257.
Hillert MH, Imran I, Zimmermann M, Lau H, Weinfurter S, Klein J (2014) Dynamics of hippocampal acetylcholine release during lithium-pilocarpine-induced status epilepticus in rats. *J Neurochem* **131**:42-52.
Hirsch E, Jansen FE, Lagae L, Moshé SL, Peltola J, Perez10 ER, Scheffer11 IE, Zuberi12 SM, Rohmer UF, Fisher RS (2016) Operational Classification of Seizure Types by the International League Against Epilepsy.
Hirsch LJ, Lain AH, Walczak TS (1998) Postictal nosewiping lateralizes and localizes to the ipsilateral temporal lobe. *Epilepsia* **39**:991-997.
Hitiris N, Mohanraj R, Norrie J, Brodie MJ (2007) Mortality in epilepsy. *Epilep Behav* **10**:363-376.
Hoffman DA, Johnston D (1998) Downregulation of transient K+ channels in dendrites of hippocampal CA1 pyramidal neurons by activation of PKA and PKC. *J Neurosci* **18**:3521-3528.
Hoffman W, Haberly L (1991a) Epileptiform potentials in slices of piriform cortex from kindled rats originate in deep structures. In: *Soc Neurosci Abstr*, p 511.
Hoffman WH, Haberly LB (1989) Bursting induces persistent all-or-none EPSPs by an NMDA-dependent process in piriform cortex. *J Neurosci* **9**:206-215.
Hoffman WH, Haberly LB (1991b) Bursting-induced epileptiform EPSPs in slices of piriform cortex are generated by deep cells. *J Neurosci* **11**:2021-2031.
Hollmann M, Hartley M, Heinemann S (1991) Ca2+ permeability of ka-ampa gated glutamate receptor channels depends on subunit composition. *Science* **252**:851-853.
Holmes KH, Bilkey DK, Laverty R (1992) The infusion of an NMDA antagonist into perirhinal cortex suppresses amygdala-kindled seizures. *Brain Res* **587**:285-290.
Holtkamp M, Buchheim K, Siegmund H, Meierkord H (2003) Optical imaging reveals reduced seizure spread and propagation velocities in aged rat brain in vitro. *Neurobiol Aging* **24**:345-353.
Holtkamp M, Matzen J, Van Landeghem F, Buchheim K, Meierkord H (2005) Transient loss of inhibition precedes spontaneous seizures after experimental status epilepticus. *Neurobiol Dis* **19**:162-170.
Holtkamp M, Buchheim K, Elsner M, Matzen J, Weissinger F, Meierkord H (2011) Status epilepticus induces increasing neuronal excitability and hypersynchrony as revealed by optical imaging. *Neurobiol Dis* **43**:220-227.
Honack D, Wahnschaffe U, Loscher W (1991) Kindling from stimulation of a highly sensitive locus in the posterior part of the piriform cortex - comparison with amygdala kindling and effects of antiepileptic drugs. *Brain Res* **538**:196-202.

Honchar MP, Olney JW, Sherman WR (1983) Systemic cholinergic agents induce seizures and brain-damage in lithium-treated rats. *Science* **220**:323-325.
Hormuzdi SG, Pais I, LeBeau FEN, Towers SK, Rozov A, Buhl EH, Whittington MA, Monyer H (2001) Impaired electrical signaling disrupts gamma frequency oscillations in connexin 36-deficient mice. *Neuron* **31**:487-495.
Houser CR (1990) Granule cell dispersion in the dentate gyrus of humans with temporal lobe epilepsy. *Brain Res* **535**:195-204.
Howe J, Gibson J (1982) Uncinate seizures and tumors, a myth reexamined. *Ann Neurol* **12**:227-227.
Huberfeld G, de La Prida LM, Pallud J, Cohen I, Le Van Quyen M, Adam C, Clemenceau S, Baulac M, Miles R (2011) Glutamatergic pre-ictal discharges emerge at the transition to seizure in human epilepsy. *Nature Neurosci* **14**:627-634.
Huettner JE (2003) Kainate receptors and synaptic transmission. *Prog Neurobiol* **70**:387-407.
Hufnagel A, Dumpelmann M, Zentner J, Schijns O, Elger CE (2000) Clinical relevance of quantified intracranial interictal spike activity in presurgical evaluation of epilepsy. *Epilepsia* **41**:467-478.
Hughes JR, Andy OJ (1979) The human amygdala. I. Electrophysiological responses to odorants. *Electroen Clin Neuro* **46**:428-443.
Huguenard J (1996) Low-threshold calcium currents in central nervous system neurons. *Ann Rev Physiol* **58**:329-348.
Hummel T, Pauli E, Schüler P, Kettenmann B, Stefan H, Kobal G (1995) Chemosensory Event-Related Potentials in Patients with Temporal Lobe Epilepsy. *Epilepsia* **36**:79-85.
Hummel T, Henkel S, Negoias S, Galván JR, Bogdanov V, Hopp P, Hallmeyer-Elgner S, Gerber J, Reuner U, Haehner A (2013) Olfactory bulb volume in patients with temporal lobe epilepsy. *J Neurol* **260**:1004-1008.
Igelström KM, Shirley CH, Heyward PM (2011) Low-magnesium medium induces epileptiform activity in mouse olfactory bulb slices. *J Neurophysiol* **106**:2593-2605.
Ikeda A, Yazawa S, Kunieda T, Araki K, Aoki T, Hattori H, Taki W, Shibasaki H (1997) Scalp-Recorded, Ictal Focal DC Shift in a Patient with Tonic Seizure. *Epilepsia* **38**:1350-1354.
Isaev D, Ivanchick G, Khmyz V, Isaeva E, Savrasova A, Krishtal O, Holmes GL, Maximyuk O (2012) Surface charge impact in low-magnesium model of seizure in rat hippocampus. *J Neurophysiol* **107**:417-423.
Ishibashi H, Simos PG, Wheless JW, Baumgartner JE, Kim HL, Castillo EM, Davis RN, Papanicolaou AC (2002) Localization of ictal and interictal bursting epileptogenic activity in focal cortical dysplasia: Agreement of magnetoencephalography and electrocorticography. *Neurol Res* **24**:525-530.
Isojarvi JIT, Tokola RA (1998) Benzodiazepines in the treatment of epilepsy in people with intellectual disability. *J Intellectual Disability Res* **42**:80-92.
Jackson JH, Beevor C (1889) Case of tumour of the right temporosphenoidal lobe bearing on the localisation of the sense of smell and on the interpretation of a particular variety of epilepsy. *Brain* **12**:346-349.
Jackson JH, Stewart P (1899) Epileptic attacks with a warning of a crude sensation of smell and with the intellectual aura (dreamy state) in a patient who had symptoms pointing to gross organic disease of the right temporo-sphenoidal lobe. *Brain* **22**:534-549.
Jacobs J, Zelmann R, Jirsch J, Chander R, Dubeau CÉCF, Gotman J (2009) High frequency oscillations (80–500 Hz) in the preictal period in patients with focal seizures. *Epilepsia* **50**:1780-1792.
Jan M, Sadler M, Rahey SR (2001) Lateralized postictal EEG delta predicts the side of seizure surgery in temporal lobe epilepsy. *Epilepsia* **42**:402-405.
Janszky J, Janszky I, Schulz R, Hoppe M, Behne F, Pannek HW, Ebner A (2005) Temporal lobe epilepsy with hippocampal sclerosis: predictors for long-term surgical outcome. *Brain* **128**:395-404.
Jaseja H (2008) Scientific basis behind traditional practice of application of “shoe-smell” in controlling epileptic seizures in the eastern countries. *Clin Neurol Neurosur* **110**:535-538.
Jasper HH (2012) Jasper's basic mechanisms of the epilepsies: OUP USA.

Jefferys J, Haas H (1982) Synchronized bursting of CA1 hippocampal pyramidal cells in the absence of synaptic transmission. *Nature* **300**:448-450.
Jensen MS, Yaari Y (1988) The relationship between interictal and ictal paroxysms in an in vitro model of focal hippocampal epilepsy. *Ann Neurol* **24**:591-598.
Jensen MS, Yaari Y (1997) Role of intrinsic burst firing, potassium accumulation, and electrical coupling in the elevated potassium model of hippocampal epilepsy. *J Neurophysiol* **77**:1224-1233.
Jensen MS, Azouz R, Yaari Y (1996) Spike after-depolarization and burst generation in adult rat hippocampal CA1 pyramidal cells. *J Physiol* **492**:199.
Jiang L, Xu J, Nedergaard M, Kang J (2001) A Kainate receptor increases the efficacy of GABAergic synapses. *Neuron* **30**:503-513.
Jirsch J, Urrestarazu E, LeVan P, Olivier A, Dubeau F, Gotman J (2006) High-frequency oscillations during human focal seizures. *Brain* **129**:1593-1608.
Johnson N (2016) Mechanistic Insights into Neuronal Oscillatory Activity in the Intact and Dopamine-depleted Primary Motor Cortex. In: Aston University.
Jones NA, Hill AJ, Smith I, Bevan SA, Williams CM, Whalley BJ, Stephens GJ (2010) Cannabidiol displays antiepileptiform and antiseizure properties in vitro and in vivo. *J Pharmacol Exp Ther* **332**:569-577.
Jones NA, Glyn SE, Akiyama S, Hill TD, Hill AJ, Weston SE, Burnett MD, Yamasaki Y, Stephens GJ, Whalley BJ (2012) Cannabidiol exerts anti-convulsant effects in animal models of temporal lobe and partial seizures. *Seizure* **21**:344-352.
Jones RS, da Silva AB, Whittaker RG, Woodhall GL, Cunningham MO (2015) Human brain slices for epilepsy research: Pitfalls, solutions and future challenges. *J Neurosci Meth* **260** 221-232.
Jope RS, Morrisett RA, Snead OC (1986) Characterization of lithium potentiation of pilocarpine-induced status epilepticus in rats. *Exp Neurol* **91**:471-480.
Joseph J, Denisova N, Bielinski D, Fisher D, Shukitt-Hale B (2000) Oxidative stress protection and vulnerability in aging: putative nutritional implications for intervention. *Mech Ageing Dev* **116**:141-153.
Jung MW, Larson J, Lynch G (1990) role of NMDA and non-NMDA receptors in synaptic transmission in rat piriform cortex. *Exp Brain Res* **82**:451-455.
Kabat J, Król P (2012) Focal cortical dysplasia-review. Pol J Radiol 77:35-43.
Kadohisa M, Wilson DA (2006) Separate encoding of identity and similarity of complex familiar odors in piriform cortex. *Proc Natl Acad Sci* **103**:15206-15211.
Kaibara M, Blume WT (1988) The postictal electroencephalogram. *Electroen Clin Neuro* **70**:99-104.
Kairiss EW, Racine RJ, Smith GK (1984) The development of the interictal spike during kindling in the rat. *Brain Res* **322**:101-110.
Kaneda M, Farrant M, Cullcandy SG (1995) Whole-cell and single-channel currents activated by GABA and glycine in granule cells of the rat cerebellum. *J Physiol (Lond)* **485**:419-435.
Kanter ED, Haberly LB (1990) NMDA-dependent induction of long-term potentiation in afferent and association fiber systems of piriform cortex *in vitro*. *Brain Res* **525**:175-179.
Kapur A, Pearce RA, Lytton WW, Haberly LB (1997) GABA(A)-mediated IPSCs in piriform cortex have fast and slow components with different properties and locations on pyramidal cells. *J Neurophysiol* **78**:2531-2545.
Kashiwadani H, Sasaki YF, Uchida N, Mori K (1999) Synchronized oscillatory discharges of mitral/tufted cells with different molecular receptive ranges in the rabbit olfactory bulb. *J Neurophysiol* **82**:1786-1792.
Katzner S, Nauhaus I, Benucci A, Bonin V, Ringach DL, Carandini M (2009) Local Origin of Field Potentials in Visual Cortex. *Neuron* **61**:35-41.
Kay LM (2014) Circuit oscillations in odor perception and memory. *Prog Brain Res* **208**:223-251.
Kay LM, Freeman WJ (1998) Bidirectional processing in the olfactory-limbic axis during olfactory behavior. *Behav Neurosci* **112**:541-553.
Kay LM, Stopfer M (2006) Information processing in the olfactory systems of insects and vertebrates. *Seminars in Cell & Dev Biol* **17**:433-442.

Keil A, Muller MM, Ray WJ, Gruber T, Elbert T (1999) Human gamma band activity and perception of a gestalt. *J Neurosci* **19**:7152-7161.
Kelley MS, Steward O (1997) Injury-induced physiological events that may modulate gene expression in neurons and glia. *Rev Neuroscience* **8**:147-178.
Kelly KM, Gross RA, Macdonald RL (1990) Valproic acid selectively reduces the low-threshold (T) calcium current in rat nodose neurons. *Neurosci Letters* **116**:233-238.
Kelsey JE, Belluzzi JD (1982) Endorphin mediation of post-ictal effects of kindled seizures in rats. *Brain Res* **253**:337-340.
Kerr DIB, Ong J (1995) GABA(B) receptors. *Parmacol Ther* **67**:187-246.
Ketelaars S, Gorter J, Van Vliet E, da Silva FL, Wadman W (2001) Sodium currents in isolated rat CA1 pyramidal and dentate granule neurones in the post-status epilepticus model of epilepsy. *Neuroscience* **105**:109-120.
Khosravani H, Mehrotra N, Rigby M, Hader WJ, Pinnegar CR, Pillay N, Wiebe S, Federico P (2009) Spatial localization and time-dependant changes of electrographic high frequency oscillations in human temporal lobe epilepsy. *Epilepsia* **50**:605-616.
Kia A, Ribeiro F, Nelson R, Gavrilovici C, Ferguson SSG, Poulter MO (2011) Kindling alters neurosteroid-induced modulation of phasic and tonic GABA(A) receptor-mediated currents: role of phosphorylation. *J Neurochem* **116**:1043-1056.
Kim J-E, Yeo S-I, Ryu HJ, Kim M-J, Kim D-S, Jo S-M, Kang T-C (2010) Astroglial Loss and Edema Formation in the Rat Piriform Cortex and Hippocampus Following Pilocarpine-Induced Status Epilepticus. *J Compar Neurol* **518**:4612-4628.
King DW, Marsan CA (1977) Clinical features and ictal patterns in epileptic patients with EEG temporal lobe foci. *Ann Neurol* **2**:138-147.
Kito M, Maehara M, Watanabe K (1996) Mechanisms of T-type calcium channel blockade by zonisamide. *Seizure* **5**:115-119.
Kobayashi M, Buckmaster PS (2003) Reduced inhibition of dentate granule cells in a model of temporal lobe epilepsy. *J Neurosci* **23**:2440-2452.
Kochanek PM, Vagni VA, Janesko KL, Washington CB, Crumrine PK, Garman RH, Jenkins LW, Clark RS, Homanics GE, Dixon CE (2006) Adenosine A1 receptor knockout mice develop lethal status epilepticus after experimental traumatic brain injury. *J Cerebral Blood F Met* **26**:565-575.
Koehling R, Avoli M (2006) Methodological approaches to exploring epileptic disorders in the human brain in vitro. *J Neurosci Meth* **155**:1-19.
Koepp MJ, Diehl B, Woermann FG (2010) Functional neuroimaging in the postictal state. *Epilepsy & Behavior* **19**:127-130.
Konnerth A, Heinemann U, Yaari Y (1986) Nonsynaptic epileptogenesis in the mammalian hippocampus in vitro. I. Development of seizurelike activity in low extracellular calcium. *J Neurophysiol* **56**:409-423.
Konopacki J, Kowalczyk T, Gołębiewski H (2004) Electrical coupling underlies theta oscillations recorded in hippocampal formation slices. *Brain Res* **1019**:270-274.
Kopell N, Ermentrout B (2004) Chemical and electrical synapses perform complementary roles in the synchronization of interneuronal networks. *Proc Natl Acad Sci USA* **101**:15482-15487.
Kostopoulos G, Drapeau C, Avoli M, Olivier A, Villemeure JG (1989) Endogenous adenosine can reduce epileptiform activity in the human epileptogenic cortex maintained in vitro. *Neurosci letters* **106**:119-124.
Kreiman G, Hung CP, Kraskov A, Quiroga RQ, Poggio T, DiCarlo JJ (2006) Object selectivity of local field potentials and spikes in the macaque inferior temporal cortex. *Neuron* **49**:433-445.
Kreiter AK, Engel AK, Singer W (1992) Stimulus-dependent synchronization of oscillatory neuronal-activity in the superior temporal sulcus of the macaque monkey. *EJ Neurosci*:20-20.
Krishek BJ, Moss SJ, Smart TG (1996) A functional comparison of the antagonists bicuculline and picrotoxin at recombinant GABA(A) receptors. *Neuropharmacology* **35**:1289-1298.
Kukino K, Deguchi T (1978) Anticonvulsant activity and effects of sodium dipropylacetate on cerebral 5-hydroxytryptamine and. GAMMA.-aminobutyric acid in reserpinized mice. *Chem Pharm Bull* **26**:3551-3555.

Kuo CC, Chen RS, Lu L, Chen RC (1997) Carbamazepine inhibition of neuronal Na+ currents: Quantitative distinction from phenytoin and possible therapeutic implications. *Mol Pharmacol* **51**:1077-1083.
Kuzniecky R, Ho S, Pan J, Martin R, Gilliam F, Faught E, Hetherington H (2002) Modulation of cerebral GABA by topiramate, lamotrigine, and gabapentin in healthy adults. *Neurology* **58**:368-372.
Kwan P, Brodie MJ (2000) Early identification of refractory epilepsy. *New Engl J Med* **342**:314-319.
Kwan P, Sperling MR (2009) Refractory seizures: try additional antiepileptic drugs (after two have failed) or go directly to early surgery evaluation? *Epilepsia* **50**:57-62.
Kwan P, Sills GJ, Brodie MJ (2001) The mechanisms of action of commonly used antiepileptic drugs. *Pharmacol Therapeut* **90**:21-34.
Kwan P, Schachter SC, Brodie MJ (2011) Drug-resistant epilepsy. *New Engl J Med* **365**:919-926.
Lacey MG, Gooding-Williams G, Prokic EJ, Yamawaki N, Hall SD, Stanford IM, Woodhall GL (2014) Spike Firing and IPSPs in Layer V Pyramidal Neurons during Beta Oscillations in Rat Primary Motor Cortex (M1) In Vitro. *Plos One* **9**.
Lachaux JP, Rodriguez E, Martinerie J, Adam C, Hasboun D, Varela FJ (2000) A quantitative study of gamma-band activity in human intracranial recordings triggered by visual stimuli. *EJ Neurosci* **12**:2608-2622.
Lado FA, Moshé SL (2008) How do seizures stop? *Epilepsia* **49**:1651-1664.
Lancaster B, Wheal HV (1982) A comparative histological and electrophysiological study of some neurotoxins in the rat hippocampus. *J Comp Neurol* **211**:105-114.
Landfield PW, Pitler TA (1984) Prolonged Ca2+-dependent afterhyperpolarizations in hippocampal neurons of aged rats. *Science* **226**:1089-1092.
Lang DG, Wang CM, Cooper B (1993) Lamotrigine, phenytoin and carbamazepine interactions on the sodium current present in N4TG1 mouse neuroblastoma cells. *J Pharmacol Exp Ther* **266**:829-835.
Laufs H, Richardson MP, Salek-Haddadi A, Vollmar C, Duncan JS, Gale K, Lemieux L, Loescher W, Koepp MJ (2011) Converging PET and fMRI evidence for a common area involved in human focal epilepsies. *Neurol* **77**:904-910.
Le Van Quyen M, Soss J, Navarro V, Robertson R, Chavez M, Baulac M, Martinerie J (2005) Preictal state identification by synchronization changes in long-term intracranial EEG recordings. *Clin Neurophysiol* **116**:559-568.
Leach JP, Sills GJ, Butler E, Forrest G, Thompson GG, Brodie MJ (1997) Neurochemical actions of gabapentin in mouse brain. *Epilepsy Res* **27**:175-180.
Leach MJ, Marden CM, Miller AA (1986) Pharmacological studies on lamotrigine, a novel potential antiepileptic drug. *Epilepsia* **27**:490-497.
LeBeau FE, Towers SK, Traub RD, Whittington MA, Buhl EH (2002) Fast network oscillations induced by potassium transients in the rat hippocampus in vitro. *J Physiol* **542**:167-179.
Lee D (2003) Coherent oscillations in neuronal activity of the supplementary motor area during a visuomotor task. *J Neurosci* **23**:6798-6809.
Lee K, McKenna F, Rowe ICM, Ashford MLJ (1997) The effects of neuroleptic and tricyclic compounds on BKCa channel activity in rat isolated cortical neurones. *BJ Pharmacol* **121**:1810-1816.
Lehmann H, Ebert U, Loscher W (1998) Amygdala-kindling induces a lasting reduction of GABA-immunoreactive neurons in a discrete area of the ipsilateral piriform cortex. *Synapse* **29**:299-309.
Lehrner J, Baumgartner C, Serles W, Olbrich A, Pataraia E, Bacher J, Aull S, Deecke L (1997) Olfactory prodromal symptoms and unilateral olfactory dysfunction are associated in patients with right mesial temporal lobe epilepsy. *Epilepsia* **38**:1042-1044.
Leite J, Cavalheiro E (1995) Effects of conventional antiepileptic drugs in a model of spontaneous recurrent seizures in rats. *Epilepsy Res* **20**:93-104.
Leite JP, Bortolotto ZA, Cavalheiro EA (1990) Spontaneous recurrent seizures in rats - an experimental-model of partial epilepsy. *Neurosci Biobehav Rev* **14**:511-517.

Leppik IE (2004) Zonisamide: chemistry, mechanism of action, and pharmacokinetics. *Seizure* **13**:S5-S9.
Leschinger A, Stabel J, Igelmund P, Heinemann U (1993) Pharmacological and electrographic properties of epileptiform activity induced by elevated K2+ and lowered Ca2+ and Mg2+ concentration in rat hippocampal slices. *Exp Brain Res* **96**:230-240.
Leski S, Linden H, Tetzlaff T, Pettersen KH, Einevoll GT (2013) Frequency Dependence of Signal Power and Spatial Reach of the Local Field Potential. *Plos Comp Bio* **9**.
Leung LS (1992) Fast (beta) rhythms in the hippocampus: a review. *Hippocampus* **2**:93-98.
Leung S (2010) Field Potential Generation and Current Source Density Analysis: Humana Press.
Leutmezer F, Serles W, Lehrner J, Pataraia E, Zeiler K, Baumgartner C (1998) Postictal nose wiping: a lateralizing sign in temporal lobe complex partial seizures. *Neurology* **51**:1175-1177.
Levey AI, Edmunds SM, Koliatsos V, Wiley RG, Heilman CJ (1995) Expression of M1-M4 muscarinic acetylcholine-receptor proteins in rat hippocampus and regulation by cholinergic innervation. *J Neurosci* **15**:4077-4092.
Lewis DV, Jones LS, Mott DD (1990) Hippocampal epileptiform activity induced by magnesium-free medium: differences between areas CA1 and CA2–3. *Epilepsy Res* **6**:95-101.
Libri V, Constanti A, Calaminici M, Nistico G (1994) A comparison of the muscarinic response and morphological properties of identified cells in the guinea-pig olfactory cortex in-vitro. *Neuroscience* **59**:331-347.
Libri V, Constanti A, Zibetti M, Nistico S (1996) Effects of felbamate on muscarinic and metabotropic-glutamate agonist-mediated responses and magnesium-free or 4-aminopyridine-induced epileptiform activity in guinea pig olfactory cortex neurons in vitro. *J Pharmacol Exp Ther* **277**:1759-1769.
Librizzi L, de Curtis M (2003) Epileptiform ictal discharges are prevented by periodic interictal spiking in the olfactory cortex. *Ann Neurol* **53**:382-389.
Lim C, Blume HW, Madsen JR, Saper CB (1997) Connections of the hippocampal formation in humans: I. The mossy fiber pathway. *J Comp Neurol* **385**:325-351.
Linden H, Pettersen KH, Einevoll GT (2010) Intrinsic dendritic filtering gives low-pass power spectra of local field potentials. *J Comp Neurosci* **29**:423-444.
Linden H, Tetzlaff T, Potjans TC, Pettersen KH, Gruen S, Diesmann M, Einevoll GT (2011) Modeling the Spatial Reach of the LFP. *Neuron* **72**:859-872.
Loscher W, Ebert U (1996) The role of the piriform cortex in kindling. *Prog Neurobiol* **50**:427.
Loscher W, Lehmann H, Ebert U (1998) Differences in the distribution of GABA- and GAD-immunoreactive neurons in the anterior and posterior piriform cortex of rats. *Brain Res* **800**:21-31.
Lu CB, Jefferys JGR, Toescu EC, Vreugdenhil M (2011) In vitro hippocampal gamma oscillation power as an index of in vivo CA3 gamma oscillation strength and spatial reference memory. *Neurobiol Learn Mem* **95**:221-230.
Ludvig N, Moshe SL (1988) Deep prepiriform cortex lesion and development of amygdala kindling. *Epilepsia* 29:401-403.
Luna VM, Pettit DL (2010) Asymmetric rostro-caudal inhibition in the primary olfactory cortex. *Nature Neurosci* **13**:533-535.
Luskin MB, Price JL (1983) The laminar distribution of intracortical fibers originating in the olfactory cortex of the rat. *J Comp Neurol* **216**:292-302.
Lux H, Heinemann U, Dietzel I (1985) Ionic changes and alterations in the size of the extracellular space during epileptic activity. *Adv Neurol* **44**:619-639.
Lévesque M, Avoli M (2013) The kainic acid model of temporal lobe epilepsy. *Neurosci Biobehav Rev* **37**:2887-2899.
Löscher W (1999) Valproate: a reappraisal of its pharmacodynamic properties and mechanisms of action. *Prog Neurobiol* **58**:31-59.
Löscher W, Schmidt D (1980) Increase of human plasma GABA by sodium valproate. *Epilepsia* **21**:611-615.
Löscher W, Ebert U, Wahnschaffe U, Rundfeldt C (1995) Susceptibility of different cell layers of the anterior and posterior part of the piriform cortex to electrical stimulation and

kindling: comparison with the basolateral amygdala and “area tempestas”. *Neuroscience* **66**:265-276.
Löscher W, Hörstermann D, Hönack D, Rundfeldt C, Wahnschaffe U (1993) Transmitter amino acid levels in rat brain regions after amygdala-kindling or chronic electrode implantation without kindling: evidence for a pro-kindling effect of prolonged electrode implantation. *Neurochem Res* **18**:775-781.
Macdonald RL (1989) Antiepileptic drug actions. *Epilepsia* **30**:S19-S28.
Maggio R, Gale K (1989) Seizures evoked from area tempestas are subject to control by GABA and glutamate receptors in substantia nigra. *Exp Neurol* **105**:184-188.
Mai JK, Majtanik M, Paxinos G (2015) Atlas of the human brain: Academic Press.
Mangan PS, Kapur J (2004) Factors underlying bursting behavior in a network of cultured hippocampal neurons exposed to zero magnesium. *J Neurophysiol* **91**:946-957.
Mann EO, Suckling JM, Hajos N, Greenfield SA, Paulsen O (2005) Perisomatic feedback inhibition underlies cholinergically induced fast network oscillations in the rat hippocampus in vitro. *Neuron* **45**:105-117.
Margineanu DG (2012) Systems biology impact on antiepileptic drug discovery. *Epilepsy Res* **98**:104-115.
Martin C, Gervais R, Messaoudi B, Ravel N (2006) Learning-induced oscillatory activities correlated to odour recognition: a network activity. *EJ Neurosci* **23**:1801-1810.
Martin C, Gervais R, Chabaud P, Messaoudi B, Ravel N (2004a) Learning-induced modulation of oscillatory activities in the mammalian olfactory system: The role of the centrifugal fibres. *J Physiol* **98**:467-478.
Martin C, Gervais R, Hugues E, Messaoudi B, Ravel N (2004b) Learning modulation of odor-induced oscillatory responses in the rat olfactory bulb: A correlate of odor recognition? *J Neurosci* **24**:389-397.
Martin G, Nie Z, Siggins GR (1997) μ-Opioid receptors modulate NMDA receptor-mediated responses in nucleus accumbens neurons. *J Neurosci* **17**:11-22.
Martinez BA, Cain WS, de Wijk RA, Spencer DD, Novelly RA, Sass KJ (1993) Olfactory functioning before and after temporal lobe resection for intractable seizures. *Neuropsychology* **7**:351.
Mathern GW, Adelson PD, Cahan LD, Leite JP (2002) Hippocampal neuron damage in human epilepsy: Meyer's hypothesis revisited. *Prog brain res* **135**:237-251.
Mathern GW, Babb TL, Pretorius JK, Melendez M, Lévesque MF (1995) The pathophysiologic relationships between lesion pathology, intracranial ictal EEG onsets, and hippocampal neuron losses in temporal lobe epilepsy. *Epilepsy Res* **21**:133-147.
Matsumoto H, Marsan CA (1964) Cortical cellular phenomena in experimental epilepsy: interictal manifestations. *Exp Neurol* **9**:286-304.
Matsumoto Y, Enomoto K, Moritake K, Maeno T (1998) Effects of carbamazepine on nerve activity and transmitter release in neuroblastoma-glioma hybrid cells and the frog neuromuscular junction. *Cell Bio Toxicol* **14**:191-198.
Matsuo F (1999) Lamotrigine. *Epilepsia* **40**:s30-s36.
Mayer M, Westbrook G (1985) The action of N-methyl-D-aspartic acid on mouse spinal neurones in culture. *J Physiol* **361**:65.
Mayer ML, Westbrook GL, Guthrie PB (1984) Voltage-dependent block by Mg-2+ of NMDA responses in spinal-cord neurons. *Nature* **309**:261-263.
McBain CJ, Dichiara TJ, Kauer JA (1994) Activation of metabotropic glutamate receptors differentially affects 2 classes of hippocampal interneurons and potentiates excitatory synaptic transmission. *J Neurosci* **14**:4433-4445.
McCormick DA, Contreras D (2001) On the cellular and network bases of epileptic seizures. *Annu Rev Physiol* **63**:815-846.
McGaraughty S, Cowart M, Jarvis MF, Berman RF (2005) Anticonvulsant and antinociceptive actions of novel adenosine kinase inhibitors. *Curr Top Med Chem* **5**:43-58.
Mcintyre D (2006) Chapter 28 - The Kindling Phenomenon: Elsevier Academic Press.
McIntyre DC (1970) Differential amnestic effect of cortical vs. amygdaloid elicited convulsions in rats. *Physiol Behav* **5**:747-753.

McIntyre DC, Plant JR (1993) Long-lasting changes in the origin of spontaneous discharges from amygdala-kindled rats: piriform vs. perirhinal cortex in vitro. *Brain Res* **624**:268-276.
McIntyre DC, Gilby KL (2008) Mapping seizure pathways in the temporal lobe. *Epilepsia* **49**:23-30.
McLennan H, Lodge D (1979) Antagonism of amino acid-induced excitation of spinal neurons in the cat. *Brain Res* **169**:83-90.
McNamara JO (1994) Cellular and molecular basis of epilepsy. *J Neurosci* **14**:3413-3425.
Meyer M, Westbrook G, Guthrie P (1984) Voltage-dependent block by Mg2+ of NMDA responses in spinal cord neurons. *Nature* **309**:261-263.
Michael M, Holsinger D, Ikeda-Douglas C, Cammisuli S, Ferbinteanu J, DeSouza C, DeSouza S, Fecteau J, Racine RJ, Milgram NW (1998) Development of spontaneous seizures over extended electrical kindling - I. Electrographic, behavioral, and transfer kindling correlates. *Brain Res* **793**:197-211.
Michaloudi H, Grivas I, Batzios C, Chiotelli M, Papadopoulos GC (2005) Areal and laminar variations in the vascularity of the visual, auditory, and entorhinal cortices of the developing rat brain. *Develop Brain Res* **155**:60-70.
Middleton SJ, Racca C, Cunningham MO, Traub RD, Monyer H, Knopfel T, Schofield IS, Jenkins A, Whittington MA (2008) High-frequency network oscillations in cerebellar cortex. *Neuron* **58**:763-774.
Miyoshi R, Kito S, Doudou N, Nomoto T (1991) Influence of age on N-methyl-D-aspartate antagonist binding sites in the rat brain studied by in vitro autoradiography. *Synapse* **8**:212-217.
Modebadze T (2014) Neuronal network dynamics during epileptogenesis in the medial temporal lobe. In, pp 0-249: Aston University.
Modebadze T, Morgan NH, Pérès IA, Hadid RD, Amada N, Hill C, Williams C, Stanford IM, Morris CM, Jones RS (2016) A Low Mortality, High Morbidity Reduced Intensity Status Epilepticus (RISE) Model of Epilepsy and Epileptogenesis in the Rat. *PloS one* **11**:e0147265.
Mody I, Lambert J, Heinemann U (1987) Low extracellular magnesium induces epileptiform activity and spreading depression in rat hippocampal slices. *J Neurophysiol* **57**:869-888.
Mody I, De Koninck Y, Otis TS, Soltesz I (1994) Bridging the cleft at GABA synapses in the brain. *Trends Neurosci* **17**:517-525.
Molaie M, Kadzielawa K (1989) Effect of naloxone infusion on the rate of epileptiform discharges in patients with complex partial seizures. *Epilepsia* **30**:194-200.
Molnar M, Gacs G, Ujvari G, Skinner JE, Karmos G (1997) Dimensional complexity of the EEG in subcortical stroke - A case study. *Int J Psychophysiol* **25**:193-199.
Momiyama T (2003) Parallel decrease in ω-conotoxin-sensitive transmission and dopamine-induced inhibition at the striatal synapse of developing rats. *J Physiol* **546**:483-490.
Mori K, Mataga N, Imamura K (1992) Differential specificities of single mitral cells in rabbit olfactory-bulb for a homologous series of fatty-acid odor molecules. *J Neurophysiol* **67**:786-789.
Morimoto K, Dragunow M, Goddard GV (1986) Deep prepyriform cortex kindling and its relation to amygdala kindling in the rat. *Exp Neurol* **94**:637-648.
Morimoto K, Fahnestock M, Racine RJ (2004) Kindling and status epilepticus models of epilepsy: rewiring the brain. *Prog Neurobiol* **73**:1-60.
Morrisett RA, Jope RS, Snead OC (1987) Effects of drugs on the initiation and maintenance of status epilepticus induced by administration of pilocarpine to lithium-pretreated rats. *Exp Neurol* **97**:193-200.
Moyer J, Thompson LT, Black JP, Disterhoft JF (1992) Nimodipine increases excitability of rabbit CA1 pyramidal neurons in an age-and concentration-dependent manner. *J Neurophysiol* **68**:2100-2109.
Moyer JR, Disterhoft JF (1994) Nimodipine decreases calcium action potentials in rabbit hippocampal CA1 neurons in an age-dependent and concentration-dependent manner. *Hippocampus* **4**:11-17.
Muller RU, Finkelstein A (1974) The electrostatic basis of Mg++ inhibition of transmitter release. *P Natl Acad Sci* **71**:923-926.

Murthy VN, Fetz EE (1996) Oscillatory activity in sensorimotor cortex of awake monkeys: Synchronization of local field potentials and relation to behavior. *J Neurophys* **76**:3949-3967.
Myhrer T, Enger S, Aas P (2008) Anticonvulsant impact of lesions in the ventrolateral forebrain of rats challenged with soman. *Brain Res* **1226**:241-247.
Nadler JV (2003) The recurrent mossy fiber pathway of the epileptic brain. *Neurochem Res* **28**:1649-1658.
Nadler JV, Perry BW, Cotman CW (1978) Preferential vulnerability of hippocampus to intra ventricular kainic-acid.
Nagao T, Alonso A, Avoli M (1996) Epileptiform activity induced by pilocarpine in the rat hippocampal-entorhinal slice preparation. *Neuroscience* **72**:399-408.
Nairismagi J, Grohn OHJ, Kettunen MI, Nissinen J, Kauppinen RA, Pitkanen A (2004) Progression of brain damage after status epilepticus and its association with epileptogenesis: A quantitative MRI study in a rat model of temporal lobe epilepsy. *Epilepsia* **45**:1024-1034.
Nakasu Y, Nakasu S, Morikawa S, Uemura S, Inubushi T, Handa J (1995a) diffusion-weighted MR in experimental sustained seizures elicited with kainic acid. *Am J Neuroradiol* **16**:1185-1192.
Nakasu Y, Nakasu S, Kizuki H, Uemura S, Morikawa S, Inubushi T, Handa J (1995b) Changes in water diffusion of rat limbic system during status epilepticus elicited by kainate. *Psychiat Clin Neuros* **49**:S228-S230.
Neville KR, Haberly LB (2003) Beta and gamma oscillations in the olfactory system of the urethane-anesthetized rat. *J Neurophysiol* **90**:3921-3930.
Neville KR, Haberly LB (2004) Olfactory cortex in G.M. Shepherd (Ed.), The Synaptic Organization of the Brain (5th edn), Oxford University Press pp. 415–454. In.
Newberry NR, Nicoll RA (1985) Comparison of the action of baclofen with gamma-aminobutyric acid on rat hippocampal pyramidal cells-*in vitro*. *J Physiol (Lond)* **360**:161-185.
Niswender CM, Conn PJ (2010) Metabotropic Glutamate Receptors: Physiology, Pharmacology, and Disease. *Annu Rev Pharmacol*Annu Rev Pharmacol 50:295-322.
Noachtar S, Borggraefe I (2009) Epilepsy surgery: A critical review. *Epilepsy & Behavior* **15**:66-72.
Nuytten D, Van Hees J, Meulemans A, Carton H (1991) Magnesium deficiency as a cause of acute intractable seizures. *J Neurol* **238**:262-264.
Obenaus A, Esclapez M, Houser C (1993) Loss of glutamate decarboxylase mRNA-containing neurons in the rat dentate gyrus following pilocarpine-induced seizures. *J Neurosci* **13**:4470-4485.
Okada M, Zhu G, Yoshida S, Kanai K, Hirose S, Kaneko S (2002) Exocytosis mechanism as a new targeting site for mechanisms of action of antiepileptic drugs. *Life Sci* **72**:465-473.
Okada M, Hirano T, Mizuno K, Chiba T, Kawata Y, Kiryu K, Wada K, Tasaki H, Kaneko S (1997) Biphasic effects of carbamazepine on the dopaminergic system in rat striatum and hippocampus. *Epilepsy Res* **28**:143-153.
Olsen RW, Sieghart W (2009) GABA(A) receptors: Subtypes provide diversity of function and pharmacology. *Neuropharmacology* **56**:141-148.
Ormandy GC, Song L, Jope RS (1991) Analysis of the convulsant-potentiating effects of lithium in rats. *Expl Neurol* **111**:356-361.
Pack AM (2013) Zonisamide Should Be Considered a First-Line Antiepileptic Drug for Patients with Newly Diagnosed Partial Epilepsy. *Epilepsy Currents* **13**:22-23.
Pais I, Hormuzdi SG, Monyer H, Traub RD, Wood IC, Buhl EH, Whittington MA, LeBeau FEN (2003) Sharp wave-like activity in the hippocampus in vitro in mice lacking the gap junction protein connexin 36. *J Neurophysiol* **89**:2046-2054.
Palmini A, Najm I, Avanzini G, Babb T, Guerrini R, Foldvary-Schaefer N, Jackson G, Lüders H, Prayson R, Spreafico R (2004) Terminology and classification of the cortical dysplasias. *Neurology* **62**:S2-S8.
Pandolfo P, Silveirinha V, dos Santos-Rodrigues A, Venance L, Ledent C, Takahashi RN, Cunha RA, Köfalvi A (2011) Cannabinoids inhibit the synaptic uptake of adenosine and dopamine in the rat and mouse striatum. *EJ Pharmacol* **655**:38-45.

Pantev C, Makeig S, Hoke M, Galambos R, Hampson S, Gallen C (1991) Human auditory evoked gamma-band magnetic-fields. *P Natl Acad Sci USA* **88**:8996-9000.
Panuccio G, Sanchez G, Levesque M, Salami P, de Curtis M, Avoli M (2012) On the ictogenic properties of the piriform cortex in vitro. *Epilepsia* **53**:459-468.
Patrylo PR, Spencer DD, Williamson A (2001) GABA uptake and heterotransport are impaired in the dentate gyrus of epileptic rats and humans with temporal lobe sclerosis. *J Neurophysiol* **85**:1533-1542.
Patsalos P, Bourgeois B (2010) The epilepsy prescribers guide to antiepileptic drugs: *Cambridge medicine*.
Penttonen M, Kamondi A, Acsady L, Buzsaki G (1998) Gamma frequency oscillation in the hippocampus of the rat: intracellular analysis in vivo. *EJ Neurosci* **10**:718-728.
Perez-Reyes E (2003) Molecular physiology of low-voltage-activated t-type calcium channels. *Physiol Rev* **83**:117-161.
Perreault P, Avoli M (1991) Physiology and pharmacology of epileptiform activity induced by 4-aminopyridine in rat hippocampal slices. *J Neurophysiol* **65**:771-785.
Petitmengin C, Baulac M, Navarro V (2006) Seizure anticipation: Are neurophenomenological approaches able to detect preictal symptoms? *Epilepsy & Behavior* **9**:298-306.
Petroff O, Rothman D, Behar K, Lamoureux D, Mattson R (1995) Gabapentin increases brain gamma-aminobutyric-acid levels in patients with epilepsy. In: *Ann Neurol*, pp 295-296.
Pettersen KH, Hagen E, Einevoll GT (2008) Estimation of population firing rates and current source densities from laminar electrode recordings. *J Comp Neurosci* **24**:291-313.
Pfeiffer M, Draguhn A, Meierkord H, Heinemann U (1996) Effects of γ-aminobutyric acid (GABA) agonists and GABA uptake inhibitors on pharmacosensitive and pharmacoresistant epileptiform activity in vitro. *Brit J Pharmacol* **119**:569-577.
Pinel JPJ, Rovner LI (1978) Experimental epileptogenesis - kindling-induced epilepsy in rats. *Exp Neurol* **58**:190-202.
Pinel JPJ, Mucha RF, Phillips AG (1975) Spontaneous seizures generated in rats by kindling - preliminary report. *Physiol Psychol* **3**:127-129.
Pinel JPJ, Treit D, Rovner LI (1977) Temporal-lobe aggression in rats. *Science* **197**:1088-1089.
Piredda S, Gale K (1985a) A crucial epileptogenic site in the deep prepiriform cortex. *Nature* **317**:623-625.
Piredda S, Gale K (1985b) Evidence that the deep prepiriform cortex contains a crucial epileptogenic site. *Nature* **317**:623-625.
Piredda S, Gale K (1986) Anticonvulsant action of 2-amino-7-phosphonoheptanoic acid and muscimol in the deep prepiriform cortex. *EJ Pharmacol* **120**:115-118.
Pitkänen A, Lukasiuk K (2009) Molecular and cellular basis of epileptogenesis in symptomatic epilepsy. *Epilepsy Behav* **14**:16-25.
Pitler TA, Landfield PW (1990) Aging-related prolongation of calcium spike duration in rat hippocampal slice neurons. *Brain Res* **508**:1-6.
Platt SR (2007) The role of glutamate in central nervous system health and disease - A review. *Vet J* **173**:278-286.
Pollock E, Everest M, Brown A, Poulter MO (2014) Metalloproteinase inhibition prevents inhibitory synapse reorganization and seizure genesis. *Neurobiol Disease* **70**:21-31.
Postlethwaite M, Constanti A, Libri V (1998) Muscarinic Agonist–Induced Burst Firing in Immature Rat Olfactory Cortex Neurons In Vitro. *J Neurophysiol* **79**:2003-2012.
Pothmann L, Mueller C, Averkin RG, Bellistri E, Miklitz C, Uebachs M, Remy S, Menendez de la Prida L, Beck H (2014) Function of Inhibitory Micronetworks Is Spared by Na+ Channel-Acting Anticonvulsant Drugs. *J Neurosci* **34**:9720-9735.
Price JL (1973) Autoradiographic study of complementary laminar patterns of termination of afferent fibers to olfactory cortex. *J Comp Neurol* **150**:87-108.
Price JL (1985) Beyond the primary olfactory cortex - olfactory-related areas in the neocortex, thalamus and hypothalamus. *Chem Senses* **10**:239-258.
Priel MR, Albuquerque EX (2002) Short-term effects of pilocarpine on rat hippocampal neurons in culture. *Epilepsia* **43**:40-46.

Prince D, Connors BW (1985) Mechanisms of interictal epileptogenesis. *Adv Neurol* **44**:275-299.
Prince DA, Futamachi KJ (1968) Intracellular recordings in chronic focal epilepsy. *Brain Res* **11**:681-684.
Prokic E (2011) Modulation of neuronal network activity in the primary motor cortex. In: Aston University.
Prokic EJ, Weston C, Yamawaki N, Hall SD, Jones RSG, Stanford IM, Ladds G, Woodhall GL (2015) Cortical oscillatory dynamics and benzodiazepine-site modulation of tonic inhibition in fast spiking interneurons. *Neuropharmacology* **95**:192-205.
Pulvermuller F, Lutzenberger W, Preissl H, Birbaumer N (1995) Spectral responses in the gamma-band - physiological signs of higher cognitive-processes. *Neuroreport* **6**:2059-2064.
Qian A, Johnson JW (2002) Channel gating of NMDA receptors. *Physiol Behav* **77**:577-582.
Quilichini PP, Diabira D, Chiron C, Milh M, Ben-Ari Y, Gozlan H (2003) Effects of antiepileptic drugs on refractory seizures in the intact immature corticohippocampal formation in vitro. *Epilepsia* **44**:1365-1374.
Racine R, Chipashv.S, Okujava V (1972) Modification of seizure activity by electrical stimulation .3. mechanisms. *Electroencephalogr Clin Neurophysiol* **32**:295.
Racine RJ (1972) Modification of seizure activity by electrical stimulation .2. motor seizure. *Electroencephalogr Clin Neurophysiol* **32**:281.
Racine RJ, Mosher M, Kairiss EW (1988a) The role of the pyriform cortex in the generation of interictal spikes in the kindled preparation. Brain Res 454:251-263.
Racine RJ, Paxinos G, Mosher JM, Kairiss EW (1988b) The effects of various lesions and knife-cuts on septal and amygdala kindling in the rat. *Brain Res* **454**:264-274.
Rattka M, Brandt C, Bankstahl M, Bröer S, Löscher W (2011) Enhanced susceptibility to the GABA antagonist pentylenetetrazole during the latent period following a pilocarpine-induced status epilepticus in rats. *Neuropharmacology* **60**:505-512.
Ravel N, Chabaud P, Martin C, Gaveau V, Hugues E, Tallon-Baudry C, Bertrand O, Gervais R (2003) Olfactory learning modifies the expression of odour-induced oscillatory responses in the gamma (60-90 Hz) and beta (15-40 Hz) bands in the rat olfactory bulb. *EJ Neurosci* **17**:350-358.
Reddy DS, Kuruba R (2013) Experimental models of status epilepticus and neuronal injury for evaluation of therapeutic interventions. *Int J Mol Sci* **14**:18284-18318.
Remy S, Gabriel S, Urban BW, Dietrich D, Lehmann TN, Elger CE, Heinemann U, Beck H (2003) A novel mechanism underlying drug resistance in chronic epilepsy. *Ann Neurol* **53**:469-479.
Ribak CE, Bradburne RM, Harris AB (1982) A preferential loss of GABAergic, symmetric synapses in epileptic foci: a quantitative ultrastructural analysis of monkey neocortex. *J Neurosci* **2**:1725-1735.
Rice RA, Berchtold NC, Cotman CW, Green KN (2014) Age-related downregulation of the CaV 3.1 T-type calcium channel as a mediator of amyloid beta production. *Neurobiol Aging* **35**:1002-1011.
Rigas P, Castro-Alamancos M (2004) Leading role of the piriform cortex over the neocortex in the generation of spontaneous interictal spikes during block of GABA A receptors. *Neuroscience* **124**:953-961.
Rigau V, Morin M, Rousset M-C, de Bock F, Lebrun A, Coubes P, Picot M-C, Baldy-Moulinier M, Bockaert J, Crespel A, Lerner-Natoli M (2007) Angiogenesis is associated with blood-brain barrier permeability in temporal lobe epilepsy. *Brain* **130**:1942-1956.
Righini A, Pierpaoli C, Alger JR, Dichiro G (1994) Brain parenchyma apparent diffusion-coefficient alterations associated with experimental complex partial status epilepticus. *Magn Res Imaging* **12**:865-871.
Rock DM, Macdonald RL, Taylor CP (1989) Blockade of sustained repetitive action potentials in cultured spinal cord neurons by zonisamide (AD 810, CI 912), a novel anticonvulsant. *Epilepsy Res* **3**:138-143.
Rodin E, Modur P (2008) Ictal intracranial infraslow EEG activity. *Clinical Neurophysiol* **119**:2188-2200.
Rodriguez-Moreno A, Herreras O, Lerma J (1997) Kainate receptors presynaptically downregulate GABAergic inhibition in the rat hippocampus. *Neuron* **19**:893-901.

Roepstorff A, Lambert JD (1992) Comparison of the effect of the GABA uptake blockers, tiagabine and nipecotic acid, on inhibitory synaptic efficacy in hippocampal CA1 neurones. *Neurosci letters* **146**:131-134.
Rogawski MA, Löscher W (2004) The neurobiology of antiepileptic drugs. *Nature Rev Neurosci* **5**:553-564.
Rogawski MA, Hanada T (2013) Preclinical pharmacology of perampanel, a selective non-competitive AMPA receptor antagonist. *Acta Neurologica Scandinavica* **127**:19-24.
Rojas-Libano D, Frederick DE, Egana JI, Kay LM (2014) The olfactory bulb theta rhythm follows all frequencies of diaphragmatic respiration in the freely behaving rat. *Front Behav Neurosci* **8**.
Roman F, Staubli U, Lynch G (1987) Evidence for synaptic potentiation in a cortical network during learning. *Brain Res* **418**:221-226.
Roopun AK, Cunningham MO, Racca C, Alter K, Traub RD, Whittington MA (2008) Region-specific changes in gamma and beta2 rhythms in NMDA receptor dysfunction models of schizophrenia. *Schizophrenia Bulletin* **34**:962-973.
Roopun AK, Middleton SJ, Cunningham MO, LeBeau FEN, Bibbig A, Whittington MA, Traub RD (2006) A beta2-frequency (20-30 Hz) oscillation in nonsynaptic networks of somatosensory cortex. *Proc Natl Acad Sci USA* **103**:15646-15650.
Roopun AK, Simonotto JD, Pierce ML, Jenkins A, Nicholson C, Schofield IS, Whittaker RG, Kaiser M, Whittington MA, Traub RD (2010) A nonsynaptic mechanism underlying interictal discharges in human epileptic neocortex. *Proc Natl Acad Sci* **107**:338-343.
Ross HR, Napier I, Connor M (2008) Inhibition of recombinant human T-type calcium channels by Δ9-tetrahydrocannabinol and cannabidiol. *J Biol Chem* **283**:16124-16134.
Rouse ST, Hamilton SE, Potter LT, Nathanson NM, Conn PJ (2000) Muscarinic-induced modulation of potassium conductances is unchanged in mouse hippocampal pyramidal cells that lack functional M 1 receptors. *Neurosci Letters* **278**:61-64.
Rowley HL, Marsden CA, Martin KF (1995) Differential effects of phenytoin and sodium valproate on seizure-induced changes in γ-aminobutyric acid and glutamate release in vivo. *EJ Pharmacol* **294**:541-546.
Rudolph U, Crestani F, Benke D, Brunig I, Benson JA, Fritschy JM, Martin JR, Bluethmann H, Mohler H (1999) Benzodiazepine actions mediated by specific gamma-aminobutyric acid(A) receptor subtypes. *Nature* **401**:796-800.
Rundfeldt C (1997) The new anticonvulsant retigabine (D-23129) acts as an opener of K+ channels in neuronal cells. *EJ Pharmacol* **336**:243-249.
Russo EB, Burnett A, Hall B, Parker KK (2005) Agonistic properties of cannabidiol at 5-HT1a receptors. *Neurochem Res* **30**:1037-1043.
Ryan D, Drysdale AJ, Lafourcade C, Pertwee RG, Platt B (2009) Cannabidiol targets mitochondria to regulate intracellular Ca2+ levels. *J Neurosci* **29**:2053-2063.
Sachidhanandam S, Blanchet C, Jeantet Y, Cho YH, Mulle C (2009) Kainate Receptors Act as Conditional Amplifiers of Spike Transmission at Hippocampal Mossy Fiber Synapses. *J Neurosci* **29**:5000-5008.
Sanabria ER, Su H, Yaari Y (2001) Initiation of network bursts by Ca2+-dependent intrinsic bursting in the rat pilocarpine model of temporal lobe epilepsy. *J Physiol* **532**:205-216.
Sanes JN, Donoghue JP (1993) Oscillations in local-field potentials of the primate motor cortex during voluntary movement. *Proc Natl Acad Sci U S A* **90**:4470-4474.
Sato T, Yamada N, Morimoto K, Uemura S, Kuroda S (1998) A behavioral and immunohistochemical study on the development of perirhinal cortical kindling: a comparison with other types of limbic kindling. *Brain Res* **811**:122-132.
Savic I, Bookheimer SY, Fried I, Engel J (1997) Olfactory bedside test: a simple approach to identify temporo-orbitofrontal dysfunction. *Arch Neurol* **54**:162-168.
Sayer RJ, Brown AM, Schwindt PC, Crill WE (1993) calcium currents in acutely isolated human neocortical neurons. *J Neurophysiol* **69**:1596-1606.
Scaramelli A, Braga P, Avellanal A, Bogacz A, Camejo C, Rega I, Messano T, Arciere B (2009) Prodromal symptoms in epileptic patients: Clinical characterization of the pre-ictal phase. *Seizure- EJ Epilepsy* **18**:246-250.

Schauf C (1987) Zonisamide enhances slow sodium inactivation inMyxicola. *Brain Res* **413**:185-188.
Schechter P, Tranier Y, Grove J (1978) Effect of n-dipropylacetate on amino acid concentrations in mouse brain: correlations with anti-convulsant activity. *J Neurochem* **31**:1325-1327.
Schirrmacher K, Mayer A, Walden J, Dusing R, Bingmann D (1993) Effects of carbamazepine on action-potentials and calcium currents in rat spinal ganglion-cells in-vitro. *Neuropsychobiol* **27**:176-179.
Schirrmacher K, Mayer A, Walden J, Dusing R, Bingmann D (1995) Effects of carbamazepine on membrane properties of rat sensory spinal ganglion cells in vitro. *European Neuropsychopharmaco* **5**:501-507.
Schmitz D, Schuchmann S, Fisahn A, Draguhn A, Buhl EH, Petrasch-Parwez E, Dermietzel R, Heinemann U, Traub RD (2001) Axo-axonal coupling: A novel mechanism for ultrafast neuronal communication. *Neuron* **31**:831-840.
Scholl EA, Dudek FE, Ekstrand JJ (2013) Neuronal degeneration is observed in multiple regions outside the hippocampus after lithium pilocarpine-induced status epilepticus in the immature rat. *Neuroscience* **252**:45-59.
Schuchmann S, Buchheim K, Meierkord H, Heinemann U (1999) A relative energy failure is associated with low-Mg2+ but not with 4-aminopyridine induced seizure-like events in entorhinal cortex. *J Neurophysiol* **81**:399-403.
Schwarcz R, Zaczek R, Coyle JT (1978) Microinjection of kainic acid into the rat hippocampus. *EJ Pharmacol* **50**:209-220.
Schwarz JR, Grigat G (1989) Phenytoin and carbamazepine: potential-and frequency-dependent block of Na currents in mammalian myelinated nerve fibers. *Epilepsia* **30**:286-294.
Segal M, Barker JL (1984) Rat hippocampal-neurons in culture - voltage-clamp analysis of inhibitory synaptic connections. *J Neurophysiol* **52**:469-487.
Semah F, Picot MC, Adam C, Broglin D, Arzimanoglou A, Bazin B, Cavalcanti D, Baulac M (1998) Is the underlying cause of epilepsy a major prognostic factor for recurrence? *Neurology* **51**:1256-1262.
Semyanov A, Kullmann DM (2001) Kainate receptor-dependent axonal depolarization and action potential initiation in interneurons. *Nature Neurosci* **4**:718-723.
Shah D (2017) Mechanisms of hyperexcitability and efficacy of antiepileptic drugs in hippocampal-entorhinal networks in the Reduced Intensity Status Epilepticus (RISE) model of chronic epilepsy. In: Aston University.
Shaheen U, Akka J, Hinore JS, Girdhar A, Bandaru S, Sumithnath TG, Nayarisseri A, Munshi A (2015) Computer aided identification of sodium channel blockers in the clinical treatment of epilepsy using molecular docking tools. *Bioinfo* **11**:131-137.
Shimono K, Brucher F, Granger R, Lynch G, Taketani M (2000) Origins and distribution of cholinergically induced beta rhythms in hippocampal slices. *J Neurosci* **20**:8462-8473.
Shuai J, Bikson M, Hahn PJ, Lian J, Durand DM (2003) Ionic mechanisms underlying spontaneous CA1 neuronal firing in Ca 2+-free solution. *Biophys J* **84**:2099-2111.
Sik A, Penttonen M, Ylinen A, Buzsaki G (1995) Hippocampal ca1 interneurons - an in-vivo intracellular labeling study. *J Neurosci* **15**:6651-6665.
Sills G, Leach J, Butler E, Carswell A, Thompson G, Brodie M (1996) Antiepileptic drug action in primary cultures of rat cortical astrocytes. *Epilepsia* **37**:116.
Sills GJ, Butler E, Thompson GG, Brodie MJ (1999) Vigabatrin and tiagabine are pharmacologically different drugs. A pre-clinical study. *Seizure* 8:404-411.
Simon A, Traub RD, Vladimirov N, Jenkins A, Nicholson C, Whittaker RG, Schofield I, Clowry GJ, Cunningham MO, Whittington MA (2014) Gap junction networks can generate both ripple-like and fast ripple-like oscillations. *EJ Neurosci* **39**:46-60.
Sinel'nikova V, Shubina L, Gol'tyaev M, Loseva E, Kichigina V (2013) Detection of c-fos expression in the brains of animals with a pilocarpine model of temporal lobe epilepsy. *Neurosci Behav Physiol* **43**:1084-1091.
Sinfield JL, Collins DR (2006) Induction of synchronous oscillatory activity in the rat lateral arnygdala in vitro is dependent on gap junction activity. *EJ Neurosci* **24**:3091-3095.

Sisodiya S, Lin WR, Harding B, Squier M, Thom M (2002) Drug resistance in epilepsy: expression of drug resistance proteins in common causes of refractory epilepsy. *Brain* **125**:22-31.
Sitges M, Chiu LM, Guarneros A, Nekrassov V (2007) Effects of carbamazepine, phenytoin, lamotrigine, oxcarbazepine, topiramate and vinpocetine on Na+ channel-mediated release of [3 H] glutamate in hippocampal nerve endings. *Neuropharmacology* **52**:598-605.
Skerritt JH, Davies LP, Johnston GAR (1983) Interactions of the anti-convulsant carbamazepine with adenosine receptors .1. neurochemical studies. *Epilepsia* **24**:634-642.
Sloviter RS (1987) Decreased hippocampal inhibition and a selective loss of interneurons in experimental epilepsy. *Science* **235**:73-76.
Sloviter RS (1991) Permanently altered hippocampal structure, excitability, and inhibition after experimental status epilepticus in the rat: the “dormant basket cell” hypothesis and its possible relevance to temporal lobe epilepsy. *Hippocampus* **1**:41-66.
Sloviter RS (2005) The neurobiology of temporal lobe epilepsy: too much information, not enough knowledge. *Comptes Rendus Biologies* **328**:143-153.
Sloviter RS, Zappone CA, Harvey BD, Bumanglag AV, Bender RA, Frotscher M (2003) “Dormant basket cell” hypothesis revisited: relative vulnerabilities of dentate gyrus mossy cells and inhibitory interneurons after hippocampal status epilepticus in the rat. *J Comp Neurol* **459**:44-76.
Sombati S, Delorenzo RJ (1995) Recurrent spontaneous seizure activity in hippocampal neuronal networks in culture. *J Neurophysiol* **73**:1706-1711.
Sommer B, Kohler M, Sprengel R, Seeburg PH (1991) RNA editing in brain controls a determinant of ion flow in glutamate-gated channels. *Cell* **67**:11-19.
Spector S, Cull C, Goldstein LH (2000) Seizure precipitants and perceived self-control of seizures in adults with poorly-controlled epilepsy. *Epilepsy Res* **38**:207-216.
Sperling MR, Feldman H, Kinman J, Liporace JD, O'Connor MJ (1999) Seizure control and mortality in epilepsy. *Ann Neurol* **46**:45-50.
Sperling MR, Harris A, Nei M, Liporace JD, O'Connor MJ (2005) Mortality after epilepsy surgery. *Epilepsia* **46**:49-53.
Stafstrom CE (2007) Persistent sodium current and its role in epilepsy. *Epilepsy Currents* **7**:15-22.
Stafstrom CE (2011) Distinct Mechanisms Mediate Interictal and Pre-Ictal Discharges in Human Temporal Lobe Epilepsy. *Epilepsy Currents* **11**:200-202.
Staley K, Hellier JL, Dudek FE (2005) Do interictal spikes drive epileptogenesis? *The Neuroscientist* **11**:272-276.
Staley KJ, Dudek FE (2006) Interictal spikes and epileptogenesis. *Epilepsy Currents* **6**:199-202.
Stam CJ, van Walsum AMV, Pijnenburg YAL, Berendse HW, de Munck JC, Scheltens P, van Dijk BW (2002) Generalized synchronization of MEG recordings in Alzheimer's disease: Evidence for involvement of the gamma band. *J Clin Neurophysiol* **19**:562-574.
Stanley DP, Shetty AK (2004) Aging in the rat hippocampus is associated with widespread reductions in the number of glutamate decarboxylase-67 positive interneurons but not interneuron degeneration. *J Neurochem* **89**:204-216.
Stanton P, Jones R, Mody I, Heinemann U (1987) Epileptiform activity induced by lowering extracellular [Mg2+] in combined hippocampal-entorhinal cortex slices: modulation by receptors for norepinephrine and N-methyl-D-aspartate. *Epilepsy Res* **1**:53-62.
Staubli U, Thibault O, Dilorenzo M, Lynch G (1989) Antagonism of NMDA receptors impairs acquisition but not retention of olfactory memory. *Behav Neurosci* **103**:54-60.
Stavem K, Guldvog B (2005) Long-term survival after epilepsy surgery compared with matched epilepsy controls and the general population. *Epilepsy Res* **63**:67-75.
Stefani A, Spadoni F, Siniscalchi A, Bernardi G (1996) Lamotrigine inhibits Ca 2+ currents in cortical neurons: functional implications. *EJ Pharmacol* **307**:113-116.
Stell BM, Mody I (2002) Receptors with different affinities mediate phasic and tonic GABA(A) conductances in hippocampal neurons. *J Neurosci* **22**.

Stevens JR, Phillips I, Debeaurepaire R (1988) Gamma-vinyl gaba in endopiriform area suppresses kindled amygdala seizures. *Epilepsia* **29**:404-411.
Stief F, Piechotta A, Gabriel S, Schmitz D, Draguhn A (2005) Functional GABA uptake at inhibitory synapses in CA1 of chronically epileptic rats. *Epilepsy Res* **66**:199-202.
Stoop R, Conquet F, Zuber B, Voronin LL, Pralong E (2003) Activation of metabotropic glutamate 5 and NMDA receptors underlies the induction of persistent bursting and associated long-lasting changes in CA3 recurrent connections. *J Neurosci* **23**:5634-5644.
Struber D, Basar-Eroglu C, Hoff E, Stadler M (2000) Reversal-rate dependent differences in the EEG gamma-band during multistable visual perception. *Int J Psychophysiol* **38**:243-252.
Su H, Sochivko D, Becker A, Chen J, Jiang Y, Yaari Y, Beck H (2002) Upregulation of a T-type Ca2+ channel causes a long-lasting modification of neuronal firing mode after status epilepticus. *J Neurosci* **22**:3645-3655.
Su TZ, Lunney E, Campbell G, Oxender DL (1995) Transport of Gabapentin, a γ-Amino Acid Drug, by System L α-Amino Acid Transporters: A Comparative Study in Astrocytes, Synaptosomes, and CHO Cells. *J Neurochem* **64**:2125-2131.
Sukov W, Barth DS (2001) Cellular mechanisms of thalamically evoked gamma oscillations in auditory cortex. *J Neurophysiol* **85**:1235-1245.
Sundman-Eriksson I, Allard P (2006) Age-correlated decline in [3H] tiagabine binding to GAT-1 in human frontal cortex. *Aging Clin Exp Res* **18**:257-260.
Sutula T (2002) Seizure-Induced Axonal Sprouting: Assessing Connections Between Injury, Local Circuits, and Epileptogenesis. *Epilepsy Currents* **2**:86-91.
Suzuki N, Bekkers JM (2006) Neural coding by two classes of principal cells in the mouse piriform cortex. *J Neurosci* **26**:11938-11947.
Suzuki N, Bekkers JM (2007) Inhibitory interneurons in the piriform cortex. *Clin Exp Pharm Physiol* **34**:1064-1069.
Suzuki N, Bekkers JM (2010a) Distinctive Classes of GABAergic Interneurons Provide Layer-Specific Phasic Inhibition in the Anterior Piriform Cortex. *Cereb Cortex* **20**:2971-2984.
Suzuki N, Bekkers JM (2010b) Inhibitory Neurons in the Anterior Piriform Cortex of the Mouse: Classification Using Molecular Markers. *J Comp Neurol* **518**:1670-1687.
Suzuki N, Bekkers JM (2011) Two Layers of Synaptic Processing by Principal Neurons in Piriform Cortex. *J Neurosci* **31**:2156-2166.
Suzuki N, Bekkers JM (2012) Microcircuits Mediating Feedforward and Feedback Synaptic Inhibition in the Piriform Cortex. *J Neurosci* **32**:919-931.
Suzuki S, Rogawski MA (1989) T-type calcium channels mediate the transition between tonic and phasic firing in thalamic neurons. *P Natl Acad Sci* **86**:7228-7232.
Suzuki S, Kawakami K, Nishimura S, Watanabe Y, Yagi K, Scino M, Miyamoto K (1992) Zonisamide blocks T-type calcium channel in cultured neurons of rat cerebral cortex. *Epilepsy Res* **12**:21-27.
Takagi SF (1986) Studies on the olfactory nervous-system of the old-world monkey. *Prog Neurobiol* **27**:195.
Tallis R, Hall G, Craig I, Dean A (1991) How common are epileptic seizures in old age? *Age Ageing* **20**:442-448.
Tanabe T, Yarita H, Iino M, Ooshima Y, Takagi SF (1975) Olfactory projection area in orbitofrontal cortex of monkey. *J Neurophysiol* **38**:1269-1283.
Tanaka Y, Tanaka Y, Furuta T, Yanagawa Y, Kaneko T (2008) The effects of cutting solutions on the viability of GABAergic interneurons in cerebral cortical slices of adult mice. *J Neurosci Meth* **171**:118-125.
Tang AC, Hasselmo ME (1994) Selective suppression of intrinsic but not afferent fiber synaptic transmission by baclofen in the piriform (olfactory) cortex. *Brain Res* **659**:75-81.
Tang FR, Chen PM, Tang YC, Tsai MC, Lee WL (2007) Two-methyl-6-phenylethynyl-pyridine (MPEP), a metabotropic glutamate receptor 5 antagonist, with low doses of MK801 and diazepam: A novel approach for controlling status epilepticus. *Neuropharmacology* **53**:821-831.

Tassi L, Colombo N, Garbelli R, Francione S, Russo GL, Mai R, Cardinale F, Cossu M, Ferrario A, Galli C (2002) Focal cortical dysplasia: neuropathological subtypes, EEG, neuroimaging and surgical outcome. *Brain* **125**:1719-1732.

Taverna S, Mantegazza M, Franceschetti S, Avanzini G (1998) Valproate selectively reduces the persistent fraction of Na+ current in neocortical neurons. *Epilepsy Res* **32**:304-308.

Taylor CP, Gee NS, Su T-Z, Kocsis JD, Welty DF, Brown JP, Dooley DJ, Boden P, Singh L (1998) A summary of mechanistic hypotheses of gabapentin pharmacology. *Epilepsy Res* **29**:233-249.

Taylor DC, Falconer MA, Bruton CJ, Corselli.Ja (1971) Focal dysplasia of cerebral cortex in epilepsy. *J Neurol Neurosurgery Psychiatry* **34**:369-&.

Teitelbaum JS, Zatorre RJ, Carpenter S, Gendron D, Evans AC, Gjedde A, Cashman NR (1990a) Neurologic sequelae of domoic acid intoxication due to the ingestion of contaminated mussels. *New England J Med*New England J Med 322:1781-1787.

Teitelbaum JS, Zatorre RJ, Carpenter S, Gendron D, Evans AC, Gjedde A, Cashman NR (1990b) Neurologic sequelae of domoic acid intoxication due to the ingestion of contaminated mussels. New England J Med 322:1781-1787.

Teoh H, Fowler L, Bowery N (1995) Effect of lamotrigine on the electrically-evoked release of endogenous amino acids from slices of dorsal horn of the rat spinal cord. *Neuropharmacology* **34**:1273-1278.

Thom M (2009) Hippocampal sclerosis: progress since Sommer. *Brain Pathol* **19**:565-572.

Thom M, Zhou J, Martinian L, Sisodiya S (2005) Quantitative post-mortem study of the hippocampus in chronic epilepsy: seizures do not inevitably cause neuronal loss. *Brain* **128**:1344-1357.

Thom M, Sisodiya SM, Beckett A, Martinian L, Lin W-R, Harkness W, Mitchell TN, Craig J, Duncan J, Scaravilli F (2002) Cytoarchitectural abnormalities in hippocampal sclerosis. *J Neuropathol Exp Neurol* **61**:510-519.

Tigaret CM, Thalhammer A, Rast GF, Specht CG, Auberson YP, Stewart MG, Schoepfer R (2006) Subunit dependencies of NMDA receptor-induced AMPA receptor internalization. *Mol Pharmacol*.

Tiitinen H, Sinkkonen J, Reinikainen K, Alho K, Lavikainen J, Naatanen R (1993) Selective attention enhances the auditory 40-Hz transient-response in humans. *Nature* **364**:59-60.

Tishler DM, Weinberg KI, Hinton DR, Barbaro N, Annett GM, Raffel C (1995) MDR1 gene expression in brain of patients with medically intractable epilepsy. *Epilepsia* **36**:1-6.

Tkach D, Reimer J, Hatsopoulos NG (2007) Congruent activity during action and action observation in motor cortex. *J Neurosci* **27**:13241-13250.

Toth Z, Yan X-X, Haftoglou S, Ribak CE, Baram TZ (1998) Seizure-induced neuronal injury: vulnerability to febrile seizures in an immature rat model. *J Neurosci* **18**:4285-4294.

Traub RD, Bibbig A (2000) A model of high-frequency ripples in the hippocampus based on synaptic coupling plus axon-axon gap junctions between pyramidal neurons. *J Neurosci* **20**:2086-2093.

Traub RD, Whittington MA (2010) Cortical oscillations in health and disease: Oxford University Press.

Traub RD, Jefferys J, Whittington MA (1994) Enhanced NMDA conductance can account for epileptiform activity induced by low Mg2+ in the rat hippocampal slice. *J Physiol* **478**:379.

Traub RD, Whittington MA, Stanford IM, Jefferys JGR (1996a) A mechanism for generation of long-range synchronous fast oscillations in the cortex. *Nature* **383**:621-624.

Traub RD, Whittington MA, Colling SB, Buzsaki G, Jefferys JGR (1996b) Analysis of gamma rhythms in the rat hippocampus in vitro and in vivo. *J Physiol (Lond)* **493**:471-484.

Traub RD, Whittington MA, Buhl EH, Jefferys JGR, Faulkner HJ (1999) On the mechanism of the gamma ->beta frequency shift in neuronal oscillations induced in rat hippocampal slices by tetanic stimulation. *J Neurosci* **19**:1088-1105.

Traub RD, Bibbig A, Fisahn A, LeBeau FEN, Whittington MA, Buhl EH (2000) A model of gamma-frequency network oscillations induced in the rat CA3 region by carbachol in vitro. *EJ Neurosci* **12**:4093-4106.

Traub RD, Kopell N, Bibbig A, Buhl EH, LeBeau FE, Whittington MA (2001a) Gap junctions between interneuron dendrites can enhance synchrony of gamma oscillations in distributed networks. *J Neurosci* **21**:9478-9486.
Traub RD, Whittington MA, Buhl EH, LeBeau FE, Bibbig A, Boyd S, Cross H, Baldeweg T (2001b) A possible role for gap junctions in generation of very fast EEG oscillations preceding the onset of, and perhaps initiating, seizures. *Epilepsia* **42**:153-170.
Traub RD, Pais I, Bibbig A, LeBeau FEN, Buhl EH, Hormuzdi SG, Monyer H, Whittington MA (2003) Contrasting roles of axonal (pyramidal cell) and dendritic (interneuron) electrical coupling in the generation of neuronal network oscillations. *Proc Natl Acad Sci USA* **100**:1370-1374.
Traynelis SF, Dingledine R (1988) Potassium-induced spontaneous electrographic seizures in the rat hippocampal slice. *J Neurophysiol* **59**:259-276.
Trevelyan AJ, Sussillo D, Yuste R (2007) Feedforward inhibition contributes to the control of epileptiform propagation speed. *J Neurosci* **27**:3383-3387.
Trimble MR (1991) Epilepsy and behavior. *Epilepsy Res* **10**:71-79.
Tseng GF, Haberly LB (1989a) Deep neurons in piriform cortex .2. membrane-properties that underlie unusual synaptic responses. *J Neurophysiol* **62**:386-400.
Tseng GF, Haberly LB (1989b) Deep neurons in piriform cortex .1. morphology and synaptically evoked-responses including a unique high-amplitude paired shock facilitation. *J Neurophysiol* **62**:369-385.
Turski WA, Czuczwar SJ, Kleinrok Z, Turski L (1983a) Cholinomimetics produce seizures and brain-damage in rats. *Experientia* **39**:1408-1411.
Turski WA, Cavalheiro EA, Schwarz M, Czuczwar SJ, Kleinrok Z, Turski L (1983b) Limbic seizures produced by pilocarpine in rats - behavioral, electroencephalographic and neuropathological study. *Beh Brain Res* **9**:315-335.
Turski WA, Cavalheiro EA, Coimbra C, da Penha Berzaghi M, Ikonomidou-Turski C, Turski L (1987) Only certain antiepileptic drugs prevent seizures induced by pilocarpine. *Brain Res Rev* **12**:281-305.
Tzschentke TM (2002) Glutamatergic mechanisms in different disease states: overview and therapeutical implications - An introduction. *Amino Acids* **23**:147-152.
Uhlhaas PJ, Linden DEJ, Singer W, Haenschel C, Lindner M, Maurer K, Rodriguez E (2006) Dysfunctional long-range coordination of neural activity during Gestalt perception in schizophrenia. *J Neurosci* **26**:8168-8175.
Uva L, Librizzi L, Wendling F, De Curtis M (2005) Propagation dynamics of epileptiform activity acutely induced by bicuculline in the hippocampal–parahippocampal region of the isolated guinea pig brain. *Epilepsia* **46**:1914-1925.
Van den Berg R, Kok P, Voskuyl R (1993) Valproate and sodium currents in cultured hippocampal neurons. *Exp Brain Res* **93**:279-287.
Van Hooft JA, Giuffrida R, Blatow M, Monyer H (2000) Differential expression of group I metabotropic glutamate receptors in functionally distinct hippocampal interneurons. *J Neurosci* **20**:3544-3551.
van Praag H, Schinder AF, Christie BR, Toni N, Palmer TD, Gage FH (2002) Functional neurogenesis in the adult hippocampus. *Nature* **415**:1030-1034.
Van Vliet EA, Araujo SdC, Redeker S, Van Schaik R, Aronica E, Gorter JA (2007) Blood-brain barrier leakage may lead to progression of temporal lobe epilepsy. *Brain* **130**:521-534.
Vancalker D, Steber R, Klotz KN, Greil W (1991) Carbamazepine distinguishes between adenosine receptors that mediate different 2nd messenger responses. *EJ Pharmacol* **206**:285-290.
Vaughan DN, Jackson GD (2014) The piriform cortex and human focal epilepsy. *Frontiers Neurol* **5**:259.
Veening JG (1978) Sub-cortical afferents of amygdaloid complex in rat - hrp study. *Neurosci Letters* **8**:197-202.
Vignes M, Collingridge GL (1997) The synaptic activation of kainate receptors. *Nature* **388**:179-182.
Vosu H, Wise RA (1975) Cholinergic seizure kindling in the rat: comparison of caudate, amygdala and hippocampus. *Behav Biol* **13**:491-495.

Vreugdenhil M, Wadman WJ (1999) Modulation of sodium currents in rat CA1 neurons by carbamazepine and valproate after kindling epileptogenesis. *Epilepsia* **40**:1512-1522.
Vreugdenhil M, Faas G, Wadman W (1998a) Sodium currents in isolated rat CA1 neurons after kindling epileptogenesis. *Neuroscience* **86**:99-107.
Vreugdenhil M, van Veelen CW, van Rijen PC, da Silva FHL, Wadman WJ (1998b) Effect of valproic acid on sodium currents in cortical neurons from patients with pharmaco-resistant temporal lobe epilepsy. *Epilepsy Res* **32**:309-320.
Wahnschaffe U, Ebert U, Loscher W (1993) The effects of lesions of the posterior piriform cortex on amygdala kindling in the rat. *Brain Res* **615**:295-303.
Wall CJ, Kendall EJ, Obenaus A (2000) Rapid alterations in diffusion-weighted images with anatomic correlates in a rodent model of status epilepticus. *Am J Neuroradiol* **21**:1841-1852.
Walther H, Lambert J, Jones R, Heinemann U, Hamon B (1986) Epileptiform activity in combined slices of the hippocampus, subiculum and entorhinal cortex during perfusion with low magnesium medium. *Neurosci Letters* **69**:156-161.
Wang S-J, Huang C-C, Hsu K-S, Tsai J-J, Gean P-W (1996a) Inhibition of N-type calcium currents by lamotrigine in rat amygdalar neurones. *Neuroreport* **7**:3037-3040.
Wang Y, Majors A, Najm I, Xue M, Comair Y, Modic M, Ng TC (1996b) Postictal alteration of sodium content and apparent diffusion coefficient in epileptic rat brain induced by kainic acid. *Epilepsia*Epilepsia 37:1000-1006.
Wardas J, Graham J, Gale K (1990) Evidence for a role of glycine in area tempestas for triggering convulsive seizures. *EJ pharmacol* **187**:59-66.
Wass CT, Rajala MM, Hughes JM, Sharbrough FW, Offord KP, Rademacher DM, Lanier WL (1996) Long-term follow-up of patients treated surgically for medically intractable epilepsy: results in 291 patients treated at Mayo Clinic Rochester between July 1972 and March 1985. In: *Mayo Clinic Proceedings*, pp 1105-1113: Elsevier.
Wasterlain CG, Jonec V (1983) Chemical kindling by muscarinic amygdaloid stimulation in the rat. *Brain Res* **271**:311-323.
Weinand ME, Carter LP, Patton DD, Oommen KJ, Labiner DM, Talwar D (1994) Long-term surface cortical cerebral blood-flow monitoring in temporal-lobe epilepsy. *Neurosurgery* **35**:657-664.
Weinand ME, Carter P, ElSaadany WF, Sioutos PJ, Labiner DM, Oommen KJ (1997) Cerebral blood flow and temporal lobe epileptogenicity. *J Neurosurgery* **86**:226-232.
Weir RL, Anderson SM, Daly JW (1990) Inhibition of n6- h-3 cyclohexyladenosine binding by carbamazepine. *Epilepsia* **31**:503-512.
Wenk GL, Walker LC, Price DL, Cork LC (1991) Loss of NMDA, but not GABA-A, binding in the brains of aged rats and monkeys. *Neurobiol Aging* **12**:93-98.
Wennberg R, Quesney F, Olivier A, Rasmussen T (1998) Electrocorticography and outcome in frontal lobe epilepsy. *Electroen Clin Neuro* **106**:357-368.
West SE, Doty RL (1995) Influence of epilepsy and temporal lobe resection on olfactory function. *Epilepsia* **36**:531-542.
Westbrook G, Lothman E (1983) Cellular and synaptic basis of kainic acid-induced hippocampal epileptiform activity. *Brain Res* **273**:97-109.
Whalley BJ, Postlethwaite M, Constanti A (2005) Further characterization of muscarinic agonist-induced epileptiform bursting activity in immature rat piriform cortex, in vitro. *Neuroscience* **134**:549-566.
Whalley BJ, Stephens GJ, Constanti A (2009) Investigation of the effects of the novel anticonvulsant compound carisbamate (RWJ-333369) on rat piriform cortical neurones in vitro. *BJ Pharmacol* **156**:994-1008.
Whittington MA, Traub RD, Jefferys JGR (1995) Synchronized oscillations in interneuron networks driven by metabotropic glutamate-receptor activation. *Nature* **373**:612-615.
Whittington MA, Traub RD, Faulkner HJ, Stanford IM, Jefferys JGR (1997) Recurrent excitatory postsynaptic potentials induced by synchronized fast cortical oscillations. *P Natl Acad Sci USA* **94**:12198-12203.
Whittington MA, Traub RD, Kopell N, Ermentrout B, Buhl EH (2000) Inhibition-based rhythms: experimental and mathematical observations on network dynamics. *Int J Psychophysiol* **38**:315-336.

WHO (2012) Epilepsy fact sheet. In, p Fact sheet number 999. World Health Organisation website.
WHO (2015) WHO list of essential medicines. In. http://www.who.int/medicines/publications/essentialmedicines/en/.
Wiebe S, Blume WT, Girvin JP, Eliasziw M, Effectiveness Efficiency Surgery T (2001) A randomized, controlled trial of surgery for temporal-lobe epilepsy. *New England J Med* 345:311-318.
Wieser H-G (2004) ILAE Commission Report. Mesial temporal lobe epilepsy with hippocampal sclerosis. *Epilepsia* **45**:695-714.
Williams R, Rosen G (2003) Mouse Brain Atlas: C57BL/6J Horizontal. In: Mouse Brain Atlas.
Willoughby JO, Fitzgibbon SP, Pope KJ, Mackenzie L, Medvedev AV, Clark CR, Davey MP, Wilcox RA (2003) Persistent abnormality detected in the non-ictal electroencephalogram in primary generalised epilepsy. *J Neurol Neurosur Ps* **74**:51-55.
Willow M, Catterall WA (1982) Inhibition of binding of h-3 -labeled batrachotoxinin-a 20-alpha-benzoate to sodium-channels by the anticonvulsant drugs diphenylhydantoin and carbamazepine. *Molecular Pharmacol* **22**:627-635.
Willow M, Kuenzel EA, Catterall WA (1984) Inhibition of voltage-sensitive sodium-channels in neuro-blastoma cells and synaptosomes by the anticonvulsant drugs diphenylhydantoin and carbamazepine. *Molecular Pharmacol* **25**:228-234.
Willow M, Gonoi T, Catterall WA (1985) Voltage clamp analysis of the inhibitory actions of diphenylhydantoin and carbamazepine on voltage-sensitive sodium-channels in neuro-blastoma cells. *Molecular Pharmacol* **27**:549-558.
Wilson DA (2001) Receptive fields in the rat piriform cortex. *Chem senses* **26**:577-584.
Wisden W, Seeburg PH (1993) A complex mosaic of high-affinity kainate receptors in rat-brain. *J Neurosci* **13**:3582-3598.
Wittner L, Maglóczky Z, Borhegyi Z, Halasz P, Tóth S, Erőss L, Szabo Z, Freund T (2001) Preservation of perisomatic inhibitory input of granule cells in the epileptic human dentate gyrus. *Neuroscience* 108:587-600.
Wittner L, Huberfeld G, Clémenceau S, Erőss L, Dezamis E, Entz L, Ulbert I, Baulac M, Freund TF, Maglóczky Z (2009) The epileptic human hippocampal cornu ammonis 2 region generates spontaneous interictal-like activity in vitro. *Brain* **132**:3032-3046.
Woeffler-Maucler C, Beghin A, Ressnikoff D, bezin L, Marinesco S (2014) Automated Immunohistochemical method to quantify neuronal density in brain sections: application to neuronal loss after *status epilepticus*. *J Neurosci Meth* **225**:32-41.
Woodhall G, Evans DI, Cunningham MO, Jones RSG (2001) NR2B-containing NMDA autoreceptors at synapses on entorhinal cortical neurons. *J Neurophysiol* **86**:1644-1651.
Wooltorton JRA, Mathie A (1993) Block of potassium currents in rat isolated sympathetic neurons by tricyclic antidepressants and structurally related-compounds. *BJ Pharmacol* **110**:1126-1132.
Xie X, Lancaster B, Peakman T, Garthwaite J (1995) Interaction of the antiepileptic drug lamotrigine with recombinant rat brain type IIA Na+ channels and with native Na+ channels in rat hippocampal neurones. *Pfluegers Archiv* **430**:437-446.
Xing D, Yeh C-I, Shapley RM (2009) Spatial Spread of the Local Field Potential and its Laminar Variation in Visual Cortex. *J Neurosci* **29**:11540-11549.
Xiong J, Verkhratsky A, Toescu EC (2002) Changes in mitochondrial status associated with altered Ca2+ homeostasis in aged cerebellar granule neurons in brain slices. *J Neurosci* **22**:10761-10771.
Yaari Y, Konnerth A, Heinemann U (1983) Spontaneous epileptiform activity of CA1 hippocampal neurons in low extracellular calcium solutions. *Exp Brain Res* **51**:153-156.
Yaari Y, Yue C, Su H (2007) Recruitment of apical dendritic T-type Ca2+ channels by backpropagating spikes underlies de novo intrinsic bursting in hippocampal epileptogenesis. *J Physiol* **580**:435-450.
Yamamura S, Ohoyama K, Nagase H, Okada M (2009) Zonisamide enhances delta receptor-associated neurotransmitter release in striato-pallidal pathway. *Neuropharmacology* **57**:322-331.

Yamawaki N, Stanford IM, Hall SD, Woodhall GL (2008) Pharmacologically induced and stimulus evoked rhythmic neuronal oscillatory activity in the primary motor cortex in vitro. *Neurosci* **151**:386-395.

Yang J, Woodhall GL, Jones RS (2006) Tonic facilitation of glutamate release by presynaptic NR2B-containing NMDA receptors is increased in the entorhinal cortex of chronically epileptic rats. *J Neurosci* **26**:406-410.

Yo Ko D (2015) Generalized Tonic-Clonic Seizures. In: Medscape.

Yordanova J, Banaschewski T, Kolev V, Woerner W, Rothenberger A (2001) Abnormal early stages of task stimulus processing in children with attention-deficit hyperactivity disorder - evidence from event-related gamma oscillations. *Clin Neurophysiol* **112**:1096-1108.

Yoshida S, Okada M, Zhu G, Kaneko S (2005) Effects of zonisamide on neurotransmitter exocytosis associated with ryanodine receptors. *Epilepsy Res* **67**:153-162.

Yoshimura R, Yanagihara N, Terao T, Minami K, Abe K, Izumi F (1995) Inhibition by carbamazepine of various ion channels mediated catecholamine secretion in cultured bovine adrenal-medullary cells. *Naunyn-Schmiedebergs Archives of Pharmacology* **352**:297-303.

Young D, Dragunow M (1994) Status epilepticus may be caused by loss of adenosine anticonvulsant mechanisms. *Neuroscience* 58:245-261.

Yu F, Zhong P, Liu X, Sun D, Gao H-q, Liu Q-s (2013) Metabotropic glutamate receptor I (mGluR1) antagonism impairs cocaine-induced conditioned place preference via inhibition of protein synthesis. *Neuropsychopharmacology* **38**:1308-1321.

Zelano C, Mohanty A, Gottfried JA (2011) Olfactory Predictive Codes and Stimulus Templates in Piriform Cortex. *Neuron* **72**:178-187.

Zhang CL, Dreier JP, Heinemann U (1995) Paroxysmal epileptiform discharges in temporal lobe slices after prolonged exposure to low magnesium are resistant to clinically used anticonvulsants. *Epilepsy Res* **20**:105-111.

Zona C, Tancredi V, Palma E, Pirrone GC, Avoli M (1990) potassium currents in rat cortical-neurons in culture are enhanced by the antiepileptic drug carbamazepine. *CJ Physiol and Pharmacol* **68**:545-547.

Zwart R, Sher E, Ping X, Jin X, Sims J, Chappell A, Gleason S, Hahn P, Gardinier K, Gernert D (2014) Perampanel, an antagonist of α-amino-3-hydroxy-5-methyl-4-isoxazolepropionic acid receptors, for the treatment of epilepsy: studies in human epileptic brain and nonepileptic brain and in rodent models. *J Pharmacol Exp Ther* **351**:124-133.

Appendix

Appendix one

A1.1 Oscillatory activity in the piriform cortex over the course of epileptogenesis

The pharmacological mechanisms of gamma oscillations in PC slices prepared from young adult controls were outlined in chapter 3 of this thesis. Following on from this, experiments were conducted to evaluate differences in network activity in the PC throughout epileptogenesis. However, difficulty obtaining oscillations in slices prepared from older animals (<1 slice per animal) prevented a thorough analysis. Switching to a choline based cutting solution improved the number of slices which oscillated (~1 slice per animal), however oscillations were still too rare to justify using animals for the experiments in line with the 3Rs (the National Centre for Refinement, Replacement and Reduction in animal research). The power and frequency of these oscillations when the PC was prepared in choline based cutting solution is presented in figure A1.1. Further studies would be required to investigate if other cutting solutions could better preserve PC slices prepared from older animals.

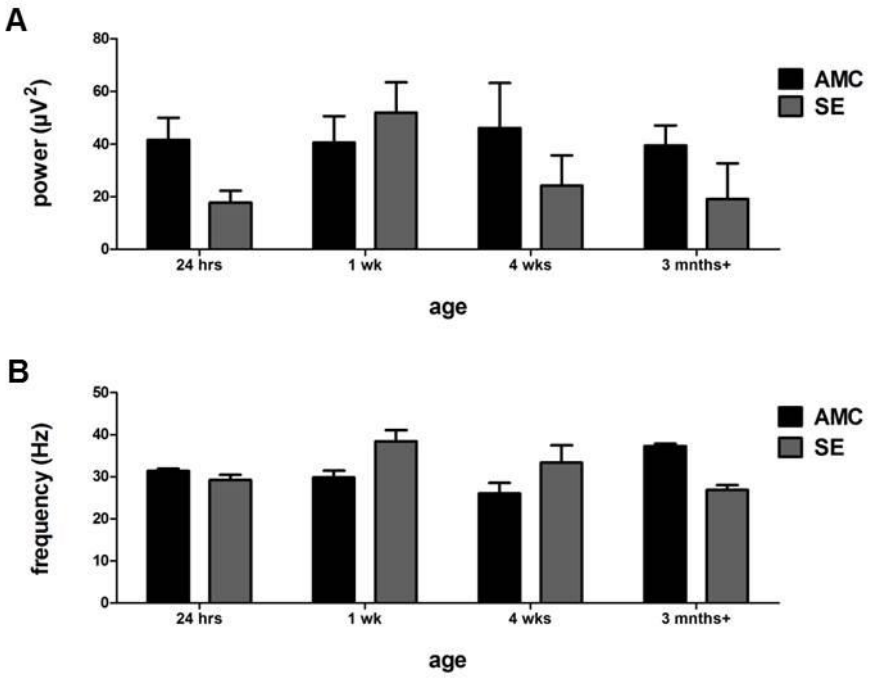

Figure A1.1 Oscillatory activity in the piriform cortex over the course of epileptogenesis
A) Power of oscillations recorded in layer II of PC at four stages of epileptogenesis (SE) compared to age-matched controls (AMCs). B) Frequency of oscillations recorded in layer II of PC at four stages of post SE compared AMC. Variable n numbers (2-25 for each condition).

Appendix two

A2.1 Raw data from ranked graphs (chapter 6)

Multiple comparisons were made between groups in chapter 6, the data was ranked to make it normally distributed in order to not violate the conditions of the between subjects ANOVA. The raw data is presented in this appendix. A comparison between different drugs is presented for 24 hours (figure A2.1), 1 week (figure A2.2), 4 weeks (figure A2.3) and 3 months+ (figure A2.4) post SE and AMCs. A comparison between ages for each single and double AED for the four stages of epileptogenesis and AMCs is presented in figure A2.5 and figure A2.6 respectively.

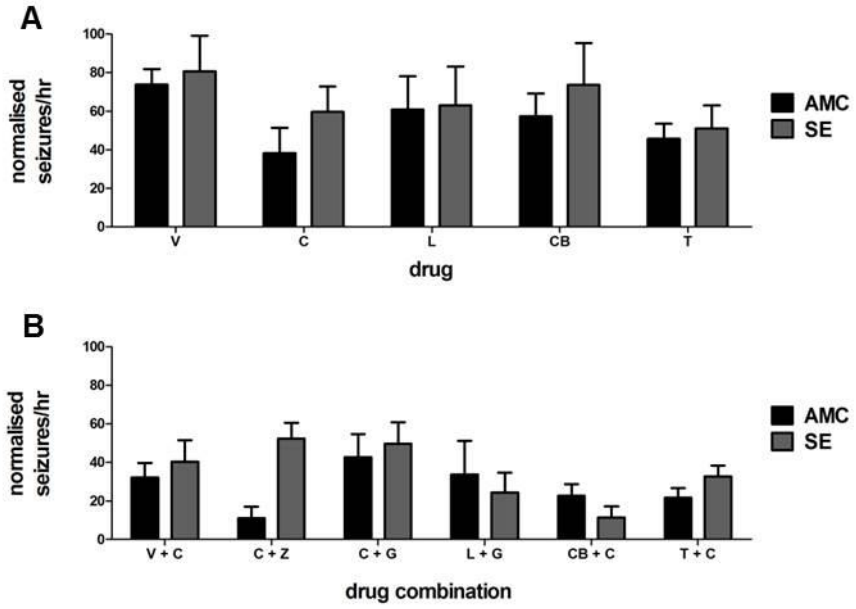

Figure A2.1 Comparison of different drugs on SLEs in slices prepared from animals 24 hours post SE and AMCs.

Raw mean SLE per hour (normalised to 0$[Mg]^{2+}$) after single (A) and double (B) drug application. N = 8 for all conditions. V – valproic acid, C – carbamazepine, L – lamotrigine, CB – cannabidiol, T – tiagabine.

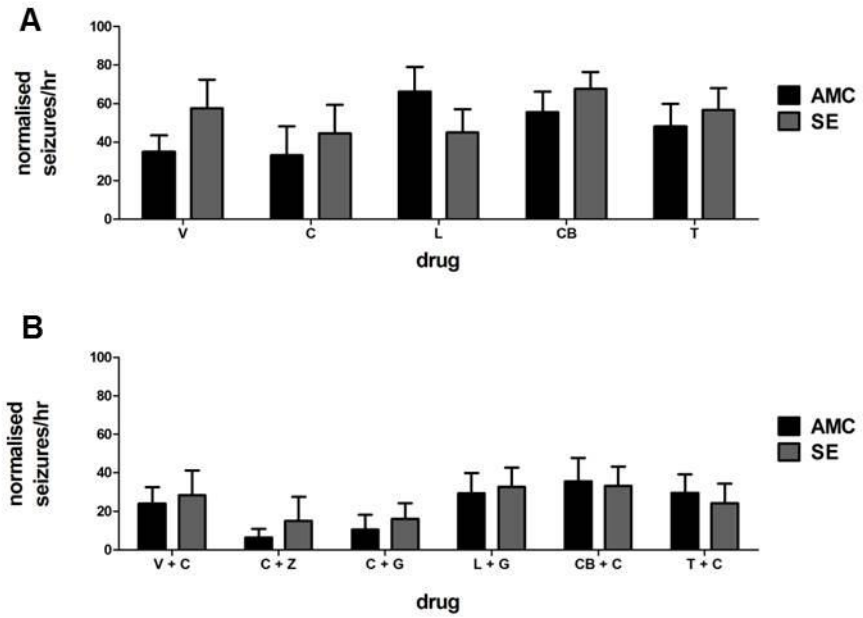

Figure A2.2 Comparison of different drugs on SLEs in slices prepared from animals 1 week post SE and AMCs.

Raw mean SLE per hour (normalised to 0$[Mg]^{2+}$) after single (A) and double (B) drug application. N = 8 for all conditions. V – valproic acid, C – carbamazepine, L – lamotrigine, CB – cannabidiol, T – tiagabine.

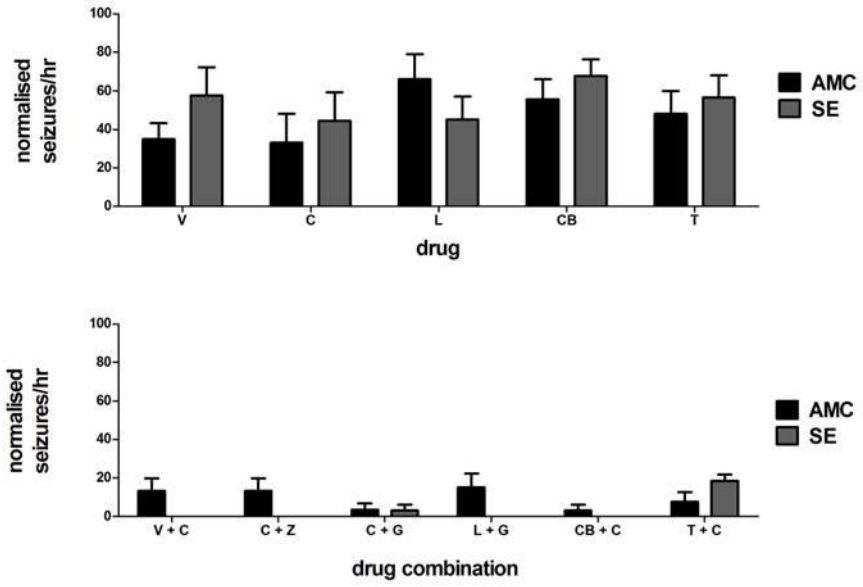

Figure A2.3 Comparison of different drugs on SLEs in slices prepared from animals 4 weeks post SE and AMCs.

Raw mean SLE per hour (normalised to 0$[Mg]^{2+}$) after single (A) and double (B) drug application. N = 8 for all conditions. V – valproic acid, C – carbamazepine, L – lamotrigine, CB – cannabidiol, T – tiagabine.

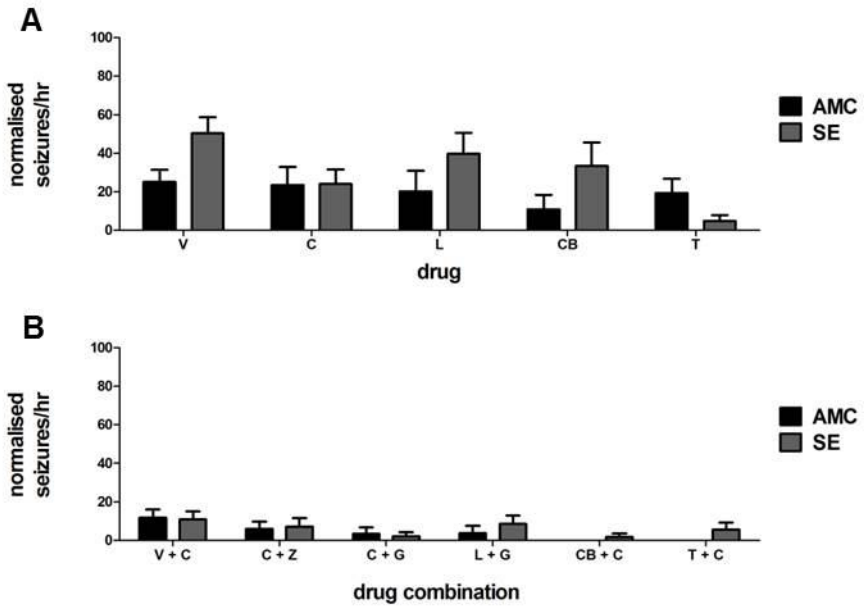

Figure A2.4 Comparison of different drugs on SLEs in slices prepared from animals 3 months+ post SE and AMCs.

Raw mean SLE per hour (normalised to 0$[Mg]^{2+}$) after single (A) and double (B) drug application. N = 8 for all conditions. V – valproic acid, C – carbamazepine, L – lamotrigine, CB – cannabidiol, T – tiagabine.

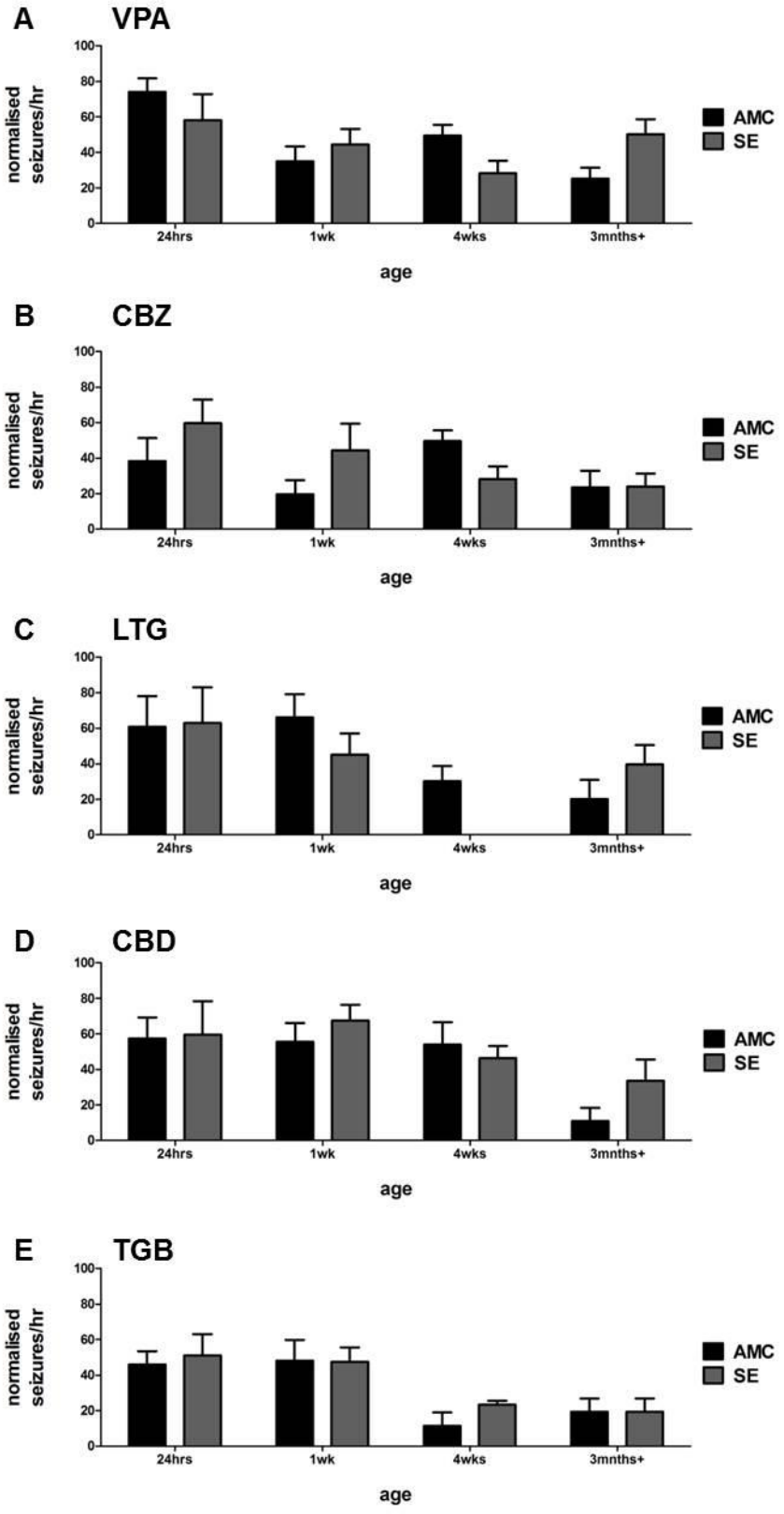

Figure A2.5 Comparison of the effect of 5 single AEDs at 4 stages post SE compared to AMC
Raw mean SLEs per hour (normalised to 0$[Mg]^{2+}$) after double drug application at 24 hours, 1 week, 4 weeks and 3 months + post epilepsy induction (SE – grey) and age-matched controls (AMC - black). N = 8 for all conditions.

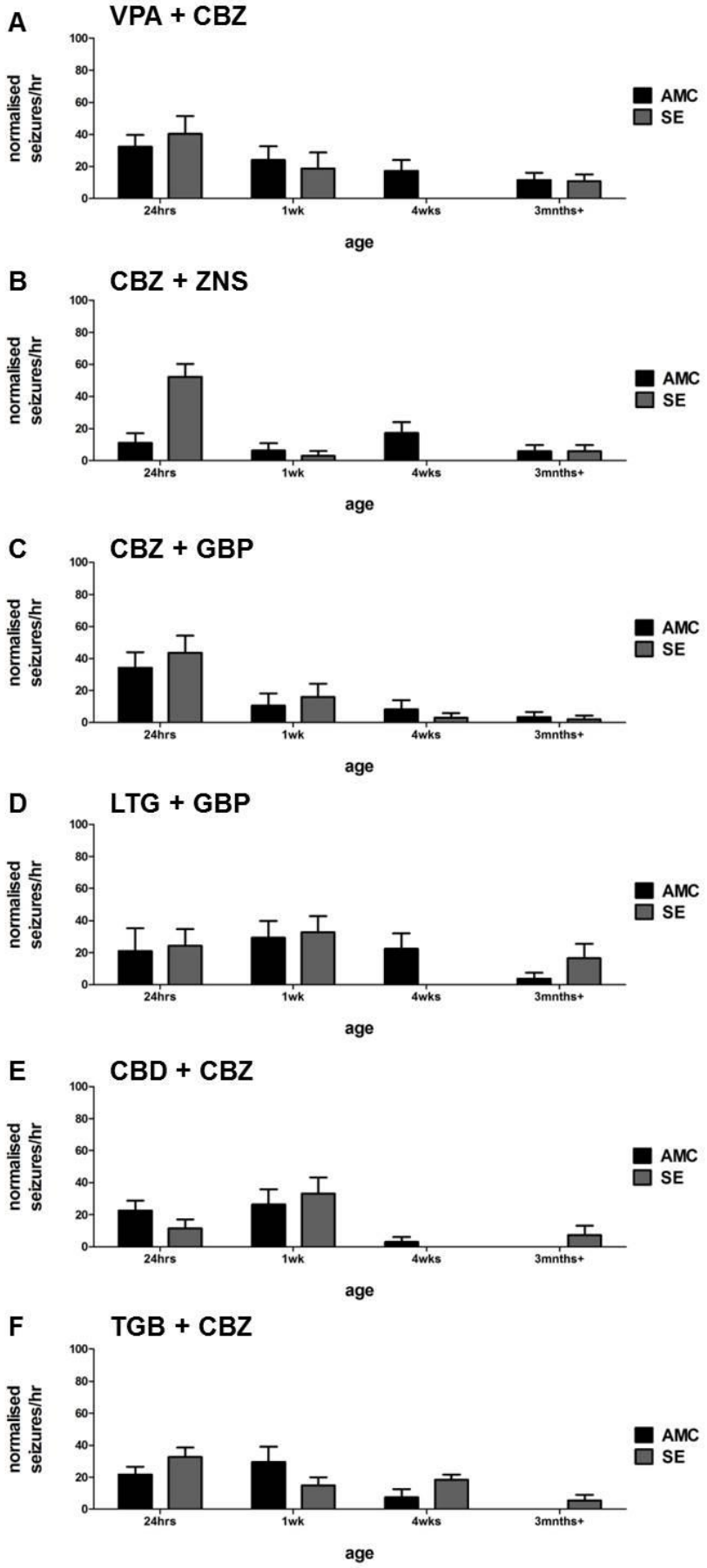

Figure A2.6 Comparison of the effect of 5 single AEDs at 4 stages post SE compared to AMC
Raw mean SLEs per hour (normalised to 0$[Mg]^{2+}$) after double drug application at 24 hours, 1 week, 4 weeks and 3 months+ post epilepsy induction (SE – grey) and age-matched controls (AMC - black). N = 8 for all conditions.